Coordination Chemistry Reviews 255 (2011) 485–546

Contents lists available at ScienceDirect

Coordination Chemistry Reviews

journal homepage: www.elsevier.com/locate/ccr

Review

Triazoles and tetrazoles: Prime ligands to generate remarkable coordination materials

Guillem Aromí[a], Leoní A. Barrios[a], Olivier Roubeau[b], Patrick Gamez[a,c,*]

[a] Departament de Química Inorgànica, Universitat de Barcelona, Martí i Franquès 1-11, 08028 Barcelona, Spain
[b] Instituto de Ciencia de Materiales de Aragón, CSIC and Universidad de Zaragoza, Plaza San Francisco, s/n 50009 Zaragoza, Spain
[c] ICREA, Spain

Contents

1. Introduction 486
2. Coordination polymers 487
   2.1. 1,2,3-Triazole-containing ligands 487
   2.2. 1,2,4-Triazole-containing ligands 400
   2.3. Tetrazole-containing ligands 491
3. Metal complexes 493
   3.1. Dinuclear complexes 493
      3.1.1. Dinuclear complexes with triple [–N–N–] bridge 493
      3.1.2. Dinuclear complexes with double [–N–N–] bridge 494
      3.1.3. Dinuclear complexes with single [–N–N–] bridge 501
      3.1.4. Dinuclear complexes with other bridges 501
   3.2. Trinuclear complexes 502
      3.2.1. Linear trinuclear complexes with triple [–N–N–] ($\mu_{1,2}$) bridges 503
      3.2.2. Linear trinuclear complexes with double [–N–N–] and a mono-atomic bridge 507
      3.2.3. Trinuclear complexes with a triangular geometry 508
   3.3. Tetranuclear complexes 509
      3.3.1. Tetrahedral complexes 509
      3.3.2. Rectangular complexes 510
      3.3.3. Other tetranuclear topologies 511
   3.4. Pentanuclear complexes 511
   3.5. Higher nuclearities 512
      3.5.1. Complexes with six to nine metals 512
      3.5.2. Fluoride-bridged manganese complexes 513
      3.5.3. A family of [M_{14}] complexes 514
      3.5.4. Other complexes with more than nine metals 514
4. Coordination compounds with spin-crossover properties 515
   4.1. Complexes of 1,2,3-triazole ligands 516
      4.1.1. Monomers 516
      4.1.2. Extended systems (2D) 522
   4.2. Complexes of 1,2,4-triazoles 523
      4.2.1. Monomers 523
      4.2.2. Dimers 527
      4.2.3. Trimers 528
      4.2.4. 1D compounds 529
      4.2.5. 2D compounds 530
      4.2.6. 3D compounds 531

* Corresponding author at: Departament de Química Inorgànica, Universitat de Barcelona, Martí i Franquès 1-11, Diagonal 467, 08028 Barcelona, Spain.
E-mail addresses: guillem.aromi@qi.ub.es (G. Aromí), roubeau@unizar.es (O. Roubeau), patrick.gamez@qi.ub.es (P. Gamez).

0010-8545/$ – see front matter
doi:10.1016/j.ccr.2010.10.038

4.3. Tetrazole compounds 532
4.3.1. Monomers 532
4.3.2. 1D compounds 535
4.3.3. 2D compounds 536
4.3.4. 3D compounds 537
5. Conclusions 538
Acknowledgements 538
Appendix A. Supplementary data 538
References 538

ARTICLE INFO

Article history:
Received 24 August 2010
Accepted 26 October 2010
Available online 4 November 2010

Keywords:
Triazole ligands
Tetrazole ligands
MOFs
Magnetic clusters
Spin crossover

ABSTRACT

The current great interest in preparing functional metal-organic materials is inevitably associated with tremendous research efforts dedicated to the design and synthesis of new families of sophisticated multinucleating ligands. In this context, the N-donor triazole and tetrazole rings represent two categories of ligands that are increasingly used, most likely as the result of the recent dramatic development of "click chemistry" and Zeolitic Imidazolate Frameworks (ZIFs). Thus, azole-based complexes have found numerous applications in coordination chemistry.

In the present review, we focus on the utilization of 1,2,3-triazole, 1,2,4-triazole and tetrazole ligands to create coordination polymers, metal complexes and spin-crossover compounds, reported to the end of 2009. In the first instance, we present a compendium of all the relevant ligands that have been employed to generate coordination polymers and Metal-Organic Frameworks (MOFs). Due to the huge amount of reported MOFs and coordination polymers bearing these azole rings, three representative examples for each category (therefore nine in total) are described in detail. The second section is devoted to the use of the bridging abilities of these azole ligands to prepare metal complexes (containing at least two metal centers). Given the large number and the great structural diversity of the polynuclear compounds found in the literature, these have been grouped according to their nuclearity. Finally, in the last section, the triazole- and tetrazole-containing coordination compounds exhibiting spin-crossover properties are presented.

1. Introduction

Triazoles and tetrazoles are aromatic five-membered heterocycles containing respectively three and four nitrogen atoms. 1,2,3-Triazoles have been known since the end of the 19th century, when Werner and Stiasny described 2-phenylbenzotriazole 1-oxide [1]. In 1937, the binding ability of the triazole ring was noted [2], and the first crystallographically characterized coordination compound was reported in 1976 [3]. The isomeric 1,2,4-triazole ring was first mentioned by Bladin as early as 1885 [4,5]. The aptitude of the 1,2,4-triazole ring to bind metal ions was established a few decades later [6], and the first crystal structure of one of the resulting adducts was published in 1962 [7]. In 1886, Bladin proposed the term tetrazole for a five-membered heteroarene including four nitrogens [8], and in 1910, the potential binding of this heterocycle to metal ions was shown [9]. The first tetrazole complex characterized by X-ray diffraction was described in 1971 by Mason [10]. It can be noticed that although the chemistry of these three azole rings is known since about a century, their coordination behaviour has not been extensively investigated [6]. Actually, structural reports of triazole- and tetrazole-based coordination compounds have become increasingly common in the literature only since the early 1980s [11], and the present review will tend to demonstrate the growing importance of these families of nitrogen-donor ligands in topical fields of Inorganic Chemistry.

1,2,3-Triazole derivatives are typically prepared by a 1,3-dipolar cycloaddition reaction between an alkyne and an azide [12]. This cyclization reaction, also known as the azide alkyne Huisgen cycloaddition [13,14], was developed in the early 1960s by Huisgen [15]. This reaction became highly popular when Sharpless and Meldal separately reported its Cu(I)-catalyzed version, allowing a dramatic improvement of both the rate and regioselectivity of the process, yielding 1,4-disubstituted 1,2,3-triazoles under mild reaction conditions (Scheme 1) [16,17]. This copper-catalyzed reaction, commonly named "click reaction" [18], has found many applications in various areas of chemistry [19–22].

1,2,4-Triazoles are usually prepared using either of two reactions, *i.e.* the Einhorn–Brunner reaction (Scheme 2)[23] and the Pellizzari reaction (Scheme 3) [24]. The Einhorn–Brunner reaction occurs between an alkyl hydrazine and an imide. This cyclization reaction is catalyzed by an organic acid, such as acetic acid (Scheme 2) [25].

In the Pellizzari reaction, an acyl hydrazide is condensed with an amide at high temperature (Scheme 3) [26].

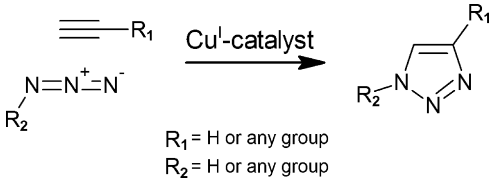

Scheme 1. Preparation of 1,2,3-triazoles via the copper(I)-catalyzed azide alkyne Huisgen cycloaddition reaction [12,15,770].

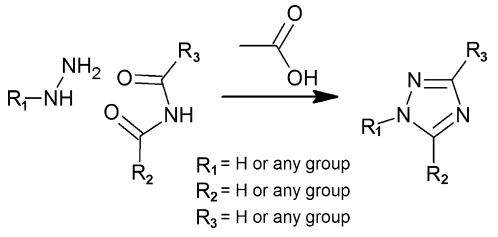

Scheme 2. Preparation of 1,2,4-triazoles via the Einhorn–Brunner cyclization reaction [4].

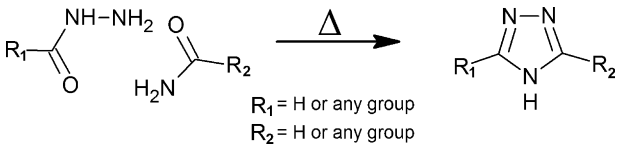

Scheme 3. Preparation of 1,2,4-triazoles via the Pellizzari cyclization reaction [4].

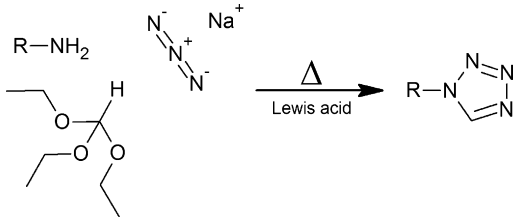

Scheme 4. Preparation of tetrazoles using a three-component reaction.

Tetrazoles can be prepared through a cyclization process involving three reactant partners, namely an amine, triethyl orthoformate and sodium azide (Scheme 4). This three-component reaction may be carried out at high temperature [27], and can be catalyzed by a Lewis acid like ytterbium(III) cations [28].

These three simple azole rings may act as polydentate ligands since they exhibit potentially three or four nitrogen-donor atoms. In addition, these small heterocycles may function as bridging ligands, therefore allowing the preparation of (polymeric) coordination compounds with potentially interesting physicochemical properties resulting from interactions between metal ions. This will be illustrated extensively in the following sections.

The scope of the present review encompasses the utilization up to the year 2009, of 1,2,3-triazole-, 1,2,4-triazole- and tetrazole-containing ligands to prepare (porous) polymeric coordination materials, metal coordination complexes and spin-crossover complexes.

2. Coordination polymers

Coordination polymers are hybrid inorganic/organic structures formed by metal cation centers that are linked by organic ligands, in form of one-, two- or three-dimensional architectures [29]. For the past fifteen years, this area of chemistry has received a great deal of attention from the scientific community [30,31], especially after the development of the so-called Metal-Organic Frameworks (MOFs) [32], which are composed of two major components, namely a cluster of metal ions or secondary building unit (SBU), connected by an organic linker [33]. Typically, MOFs are built from O-donor ligands [32,34], but the use of N-donor linkers, such as azole-based ligands, is increasingly reported [35,36], most likely because they allow the preparation of inorganic/organic materials, like the Zeolitic Imidazolate Frameworks (ZIFs) [37], with exceptional chemical and thermal stability [38]. Thus, triazole- and tetrazole-based coordination polymers have been exponentially described in the literature since the early 2000s, as is demonstrated in Fig. 1. More than 950 crystal structures (end 2009) are found in the Cambridge Structural Database (CSD version 5.30; November 2008 + 4 updates)[39] for coordination polymers with these three families of ligands (*i.e.* 1,2,3-triazoles, 1,2,4-triazoles and tetrazoles). Therefore, in the following three sub-sections, three representative examples for each category will be presented in detail.

2.1. 1,2,3-Triazole-containing ligands

The 1,2,3-triazole ring can bridge metal ions in five different coordination modes, which are depicted in Scheme 5. In its protonated form, this heteroarene can act as a dinucleating ligand ($\mu_{2,3}$- and $\mu_{1,3}$-binding modes; Scheme 5A). The deprotonated ring may function as a dinucleating ($\mu_{1,2}$- and $\mu_{1,3}$-binding modes; Scheme 5B) or a trinucleating ligand ($\mu_{1,2,3}$-binding mode; Scheme 5B), thus providing for a high versatility in the preparation of coordination materials.

By the end of 2009, more than fifty papers describing the single-crystal X-ray structures of 1,2,3-triazole-containing coordination polymers were published (CSD version 5.30; November 2008 + 4 updates) [39], involving twenty different ligands (Fig. 2 and Table 1). For instance, the first X-ray structure of a coordination polymer bearing this heteroaromatic ring was reported in 1981 [40], with the utilization of 1,2,3-benzotriazole (HL3; Table 1 and Fig. 2) to prepare $[Zn_2(L3)_4]_n$ exhibiting a three-dimensional (3D) architecture.

The twenty 1,2,3-triazole-based ligands so far employed to generate coordination networks have been roughly classified in three categories, namely the ligands containing a sole coordinative ring (**HL1**–**L6** in Fig. 2), the bridged ligands (**L7**–**L16** in Fig. 2), characterized by the presence of two or more coordinative rings linked by a spacer, and the mixed ligands (**H_3L17**–**L20** in Fig. 2), having two or more donor groups (for example a triazole ring and a carboxylic acid function). The names of all twenty ligands are given in Table S1 (see Supporting Information). Table 1 summarizes the metals with which the ligands depicted in Fig. 2 have formed structurally characterized coordination polymers described until the end of 2009.

As is demonstrated in Table 1, the number of polymeric coordination compounds including 1,2,3-triazole moieties is huge; therefore, a representative example for each type of ligands will be presented below.

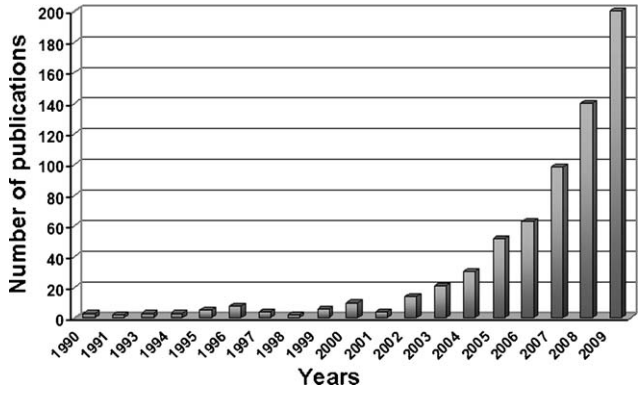

Fig. 1. Annual progression of crystal structures of triazole- and tetrazole-based coordination polymers found in the Cambridge Structural Database (CSD version 5.30; November 2008 + 4 updates) from 1990 to 2009.

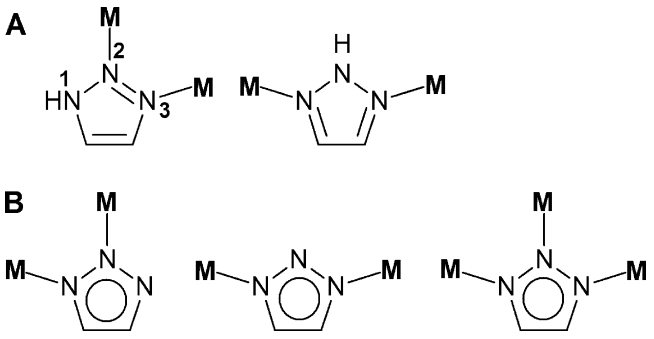

Scheme 5. Bridging coordination modes of (A) 1,2,3-triazole ($\mu_{2,3}$ and $\mu_{1,3}$) and (B) 1,2,3-triazolate ($\mu_{1,2}$, $\mu_{1,3}$ and $\mu_{1,2,3}$). **M** symbolizes a metal ion.

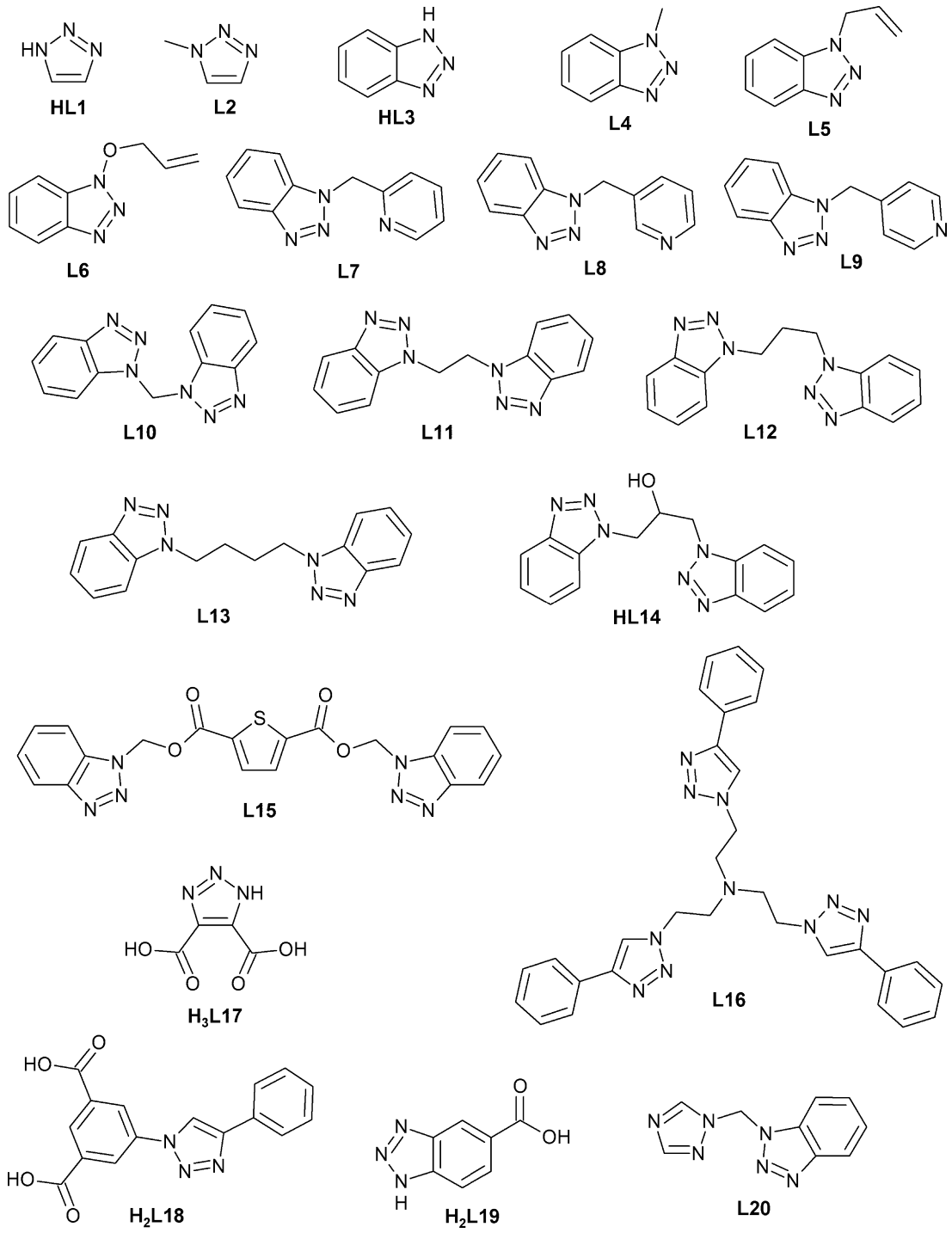

Fig. 2. Non-exhaustive list of 1,2,3-triazole ligands (**HL1**–**L20**) used to prepare coordination polymers.

The hydrothermal reaction of $Zn(OAc)_2{\cdot}2H_2O$ with 1,2,3-benzotriazole (**HL3**) in water (pH 5), at 170 °C under autogenous pressure for five days, yields the compound $[Zn(\mathbf{L3})_2]_n$, which exhibits a 2D layer structure (Fig. 3) [41]. This 2D network is constituted of dizinc(II) units bridged by two deprotonated $\mu_{1,2}$-benzotriazolato ligands, that are linked to each other through four deprotonated $\mu_{1,3}$-benzotriazolato ligands. $[Zn(\mathbf{L3})_2]_n$ displays a strong fluorescence emission in the blue region, which is ascribed to the $\pi \rightarrow \pi^*$ transition of the $\mathbf{L3}^-$ ligand [41].

The category of bridged 1,2,3-triazole ligands is nicely represented by the molecule 1,3-bis(1,2,3-benzotriazol-1-yl)propane (**L12**). Indeed, the equimolar reaction of $CuCl_2{\cdot}2H_2O$ with **L12** in methanol at room temperature produces single crystals of $[Cu(\mathbf{L12})Cl_2]_n$ [42]. Fig. 4 shows a perspective view of the crystal packing of this compound. The compound is formed by dicopper(II) units doubly bridged by μ-chlorido ligands. These dinuclear metal moieties are connected to each other via four bridging **L12** ligands, generating a complicated two-dimensional network that exhibits large 44-membered fused metallacyclic ring-systems as $Cu_6(\mathbf{L12})_4$

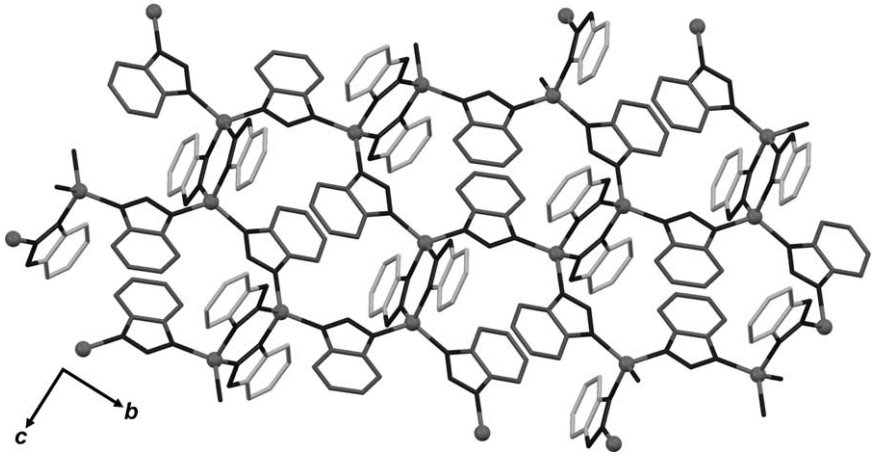

Fig. 3. Representation of the crystal packing of $[Zn(\mathbf{L3})_2]_n$ [41], illustrating the 2D-layered framework along the *bc* plane, formed by zinc(II) ions coordinated to $\mu_{1,2}$-benzotriazolato (light grey) and $\mu_{1,3}$-benzotriazolato (dark grey) ligands. The zinc(II) ions are symbolized by dark-grey balls.

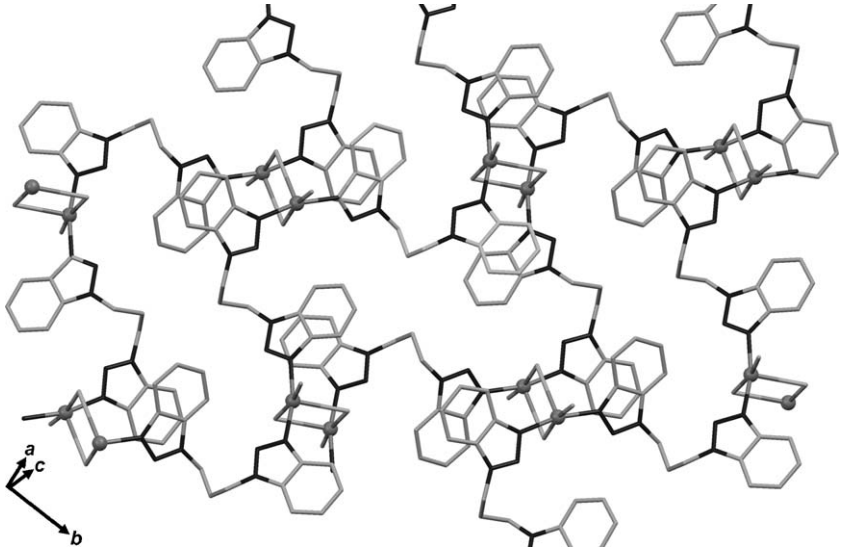

Fig. 4. Representation of the crystal packing of $[Cu(\mathbf{L12})Cl_2]_n$ [42], illustrating its extended two-dimensional polymeric structure. The copper(II) ions are symbolized by grey balls.

Table 1
Metal ions coordinated by the 1,2,3-triazole-based ligands presented in Fig. 1 to generate polymeric networks. See Table S1 for the names of the ligands.

Ligand	Metals [Refs.]
HL1	Ag [280], Cu/Mo[281]
L2	Cu [282]
HL3	Zn [40,41,283–290], Cd [291,292], Mn [291,293], Cu [282,294], Ce [295], Ho [295], Nd [295], Pr [295], Co [143,296,297], Pb [298], Ag [299], Li [300], La [301,302], Ni [143]
L4	Mn [303], Fe [303], Cu [94,95,303]
L5	Cu [304,305]
L6	Cu [306]
L7	Hg [307]
L8	Cd [308]
L9	Ag [309]
L10	Cu [54], Ag [54]
L11	Co [310], Ag [311], Cd [312]
L12	Cu [303,313], Zn [314], Co [303,315], Ni [315]
L13	Zn [314], Co [316], Mn [316], Cd [316], Cu [317]
HL14	Cu [318]
L15	Co [319]
L16	Ag [320]
H_3L17	Gd [321], Mn [321–323], Cd [324]
H_2L18	Co [325]
H_2L19	Co [43]
L20	Ag [326,327]

entities (Fig. 4). This framework appears to be stabilised by π–π stacking interactions between the benzotriazole rings separated by the Cu_2Cl_2 units (Fig. 4) [42].

The final group of 1,2,3-triazole ligands is beautifully illustrated by a remarkable MOF obtained from 1,2,3-benzotriazole-5-carboxylic acid (**H_2L19**). Actually, the solvothermal reaction of $Co(NO_3)_2{\cdot}6H_2O$ with **H_2L19** in acetonitrile/water at 150 °C yields the hydrated MOF $[Co_3(\mathbf{L19})_2(OH)_2]{\cdot}3.7H_2O$ [43]. Fig. 5A shows the coordination mode adopted by the doubly deprotonated ligand **L19**$^-$ in this compound. The carboxylic part of **L19**$^-$ acts as a bridging dinucleating ligand and the triazolate moiety binds three cobalt(II) ions in a $\mu_{1,2,3}$-fashion (Scheme 5B). The metal centers are further bridged by μ-hydroxido groups, forming $Co_3(OH)_2$ chains. The interconnection of these chains via **L19**$^-$ linkers creates a neutral 3D framework, featuring 1D nanosized rhombic channels along the crystallographic *c* axis (Fig. 5B).

Interestingly, this porous homometallic MOF material can be easily dehydrated at 95 °C and the resulting water-free nanoporous MOF is stable up to 310 °C. Furthermore, the original hydrated phase shows ferrimagnetism (through its ferrimagnetic cobalt hydroxide chains) and single-chain-magnet like behaviour while the dehydrated MOF exhibits field-induced metamagnetism from antiferromagnetism to ferrimagnetism [43]. This host material

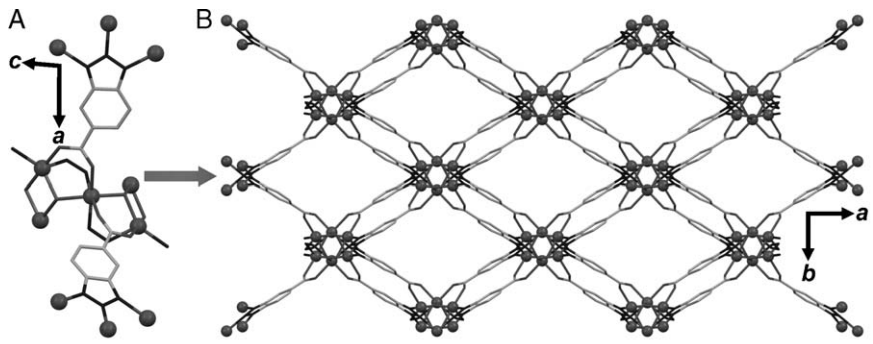

Fig. 5. (A) Illustration of the binding mode observed for the ligand **L19** in $[Co_3(\mathbf{L19})_2(OH)_2]_n{\cdot}3.7nH_2O$ [43]; (B) representation of the crystal packing of $[Co_3(\mathbf{L19})_2(OH)_2]_n{\cdot}3.7nH_2O$ showing the 1D nanosized rhombic channels along the crystallographic *c* axis [43]. The cobalt(II) ions are symbolized by dark-grey balls.

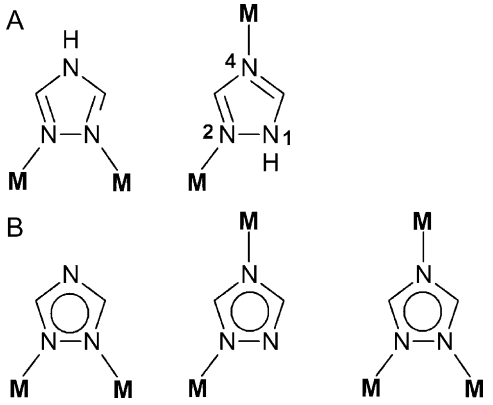

Scheme 6. Bridging coordination modes of (A) 1,2,4-triazole ($\mu_{1,2}$ and $\mu_{2,4}$) and (B) 1,2,4-triazolate ($\mu_{1,2}$ and $\mu_{1,4}$ and $\mu_{1,2,4}$). **M** symbolizes a metal ion.

represents an outstanding case of guest-induced switching of (magnetic) properties, which is one of the potential, promising developments of MOF chemistry.

2.2. 1,2,4-Triazole-containing ligands

Compared to 1,2,3-triazoles, a significantly larger variety of 1,2,4-triazole-based ligands have been used so far to prepare polymeric coordination networks. Similarly to 1,2,3-triazole, the 1,2,4-triazole ring can bridge metal ions through five different coordination modes, as is demonstrated in Scheme 6. Thus, protonated 1,2,4-triazole may function as a dinucleating ligand ($\mu_{1,2}$- and $\mu_{2,4}$-binding modes; Scheme 6A) while deprotonated 1,2,4-triazolate can coordinate two or three metal ions ($\mu_{1,2}$- and $\mu_{1,4}$- and $\mu_{1,2,4}$-binding modes; Scheme 6B).

All these bridging coordination types provide infinite possibilities for the design and preparation of hybrid inorganic/organic architectures. Coordination polymers presenting 1,2,4-triazole units were initially reported in 1979 by Engelfriet and co-workers, who described the first crystal structures of the isomorphous 2D compounds $[Cu(\mathbf{HL21})(NCS)_2]_n$, $[Zn(\mathbf{HL21})(NCS)_2]_n$ and $[Co(\mathbf{HL21})(NCS)_2]_n$ [44]. Since then, 82 distinct 1,2,4-triazole-containing ligands (whose names are listed in Table S2; see Supporting Information) have been employed to synthesize polymeric coordination frameworks, giving rise to the publication of about 300 articles by the end of 2009 (Table 2).

As for the 1,2,3-triazole ligands, the 1,2,4-triazole-based ligands have been organized in three categories, namely those containing a sole coordinative ring (**HL21**–**L39**), the bridged ligands (**L40**–**L62**), possessing two or more coordinative rings linked by a spacer, and the mixed ligands (**L63**–**HL102**), having two or more functional groups. Table 2 summarizes the metals with which the 1,2,4-triazole ligands reported until 2009 have formed structurally characterized coordination polymers.

The 1,2,4-triazole ligands of the first group (**HL21**–**L39**) are depicted in Fig. 6.

An illustrative example for the first group of ligands (depicted in Fig. 6) is obtained by reaction of the simple 1,2,4-triazole ring (**HL21**) with $CuSO_4{\cdot}5H_2O$ in water, at 200 °C for two days [45]. This hydrothermal reaction leads to the formation of $[Cu_3(\mu_3\text{-}OH)(\mathbf{L21})_3(OH)_2(H_2O)_4]_n{\cdot}4.5n(H_2O)$, featuring a triangular Cu^{II} complex (Fig. 7A) acting as the building block of a 3D framework (Fig. 7B). This microporous MOF encompasses a considerable solvent accessible volume in its channels along the crystallographic *a* axis (Fig. 7B), and exhibits host–guest properties [45]. In addition, this material shows unusual magnetic behaviour, with the presence of both intra- and intercluster antiferromagnetic interactions.

The second group of 1,2,4-triazole-based ligands (**L40**–**L62**) is shown in Fig. 8. A remarkable coordination material exemplifying this category is achieved by reaction of $Cu(NO_3)_2{\cdot}2.5H_2O$ with the ligand 1,4-bis(1,2,4-triazol-4-yl)benzene (**L51**) in water at 130 °C [46].

The resulting porous coordination polymer, *i.e.* $[Cu_2(\mu\text{-}\mathbf{L51})_4(\mu_4\text{-}\mathbf{L51})]_n(NO_3)_{4n}{\cdot}2nH_2O$, shows a crystal arrangement driven by the intercalating packing principle (Fig. 9). The **L51** ligands display two distinct coordination modes, namely a tetradentate (μ_4-**L51**; light grey ligands in Fig. 9A and B) and a N1,N2-bidentate (μ-**L51**; dark grey ligands in Fig. 9A and B) coordination fashion with a ratio of 1: 4, respectively. The η_2-triazole (η_2-trz) units self-assemble with copper(II) ions to generate 1D $[Cu_2(\eta_2\text{-trz})_3]_n$ infinite chains along the crystallographic *c* axis (Fig. 9B). In the perpendicular direction (*i.e.* along the crystallographic *b* axis), the coordination chains are connected by means of μ_4-**L51** ligands leading to 2D zigzag sheets (Fig. 9B) [46]. These 2D layers are linked to each other through noncovalent π–π interactions (see rectangle in Fig. 9C; the closest intermolecular contact is 3.455 Å) between the intercalated uncoordinated trz-C_6H_4 arms (dark grey **L51** ligands in Fig. 9A and 9B). This structural organization results in a framework in which each Cu-axis is surrounded by six triangular channels of two kinds, whose corresponding edge distances between the copper vertices are $15.8 \times 16.1 \times 16.1$ Å^3 and $13.2 \times 13.2 \times 15.8$ Å^3 (Fig. 9C). The voids between the layers are filled by uncoordinated nitrate anions and water molecules. Interestingly, one half of the NO_3^- ions, occupying the smaller channels, are located above and below the phenylene rings of the tetradentate **L51** ligands (circles in Fig. 9C), forming anion–pi–anion[47,48] double-stacks (nitrate···arene contact distance of 3.46 Å).

Fourty ligands compose the last category, namely the mixed 1,2,4-triazole ligands (**L63**–**HL102**; Fig. 10).

This category of ligands is well represented by 4-(3-pyridinyl)-1,2,4-triazole (**L64**). Actually, the reaction between $Cu(BF_4)_2{\cdot}6H_2O$, **L64** and excess $NaClO_4{\cdot}2H_2O$ in water/ethanol/acetonitrile for

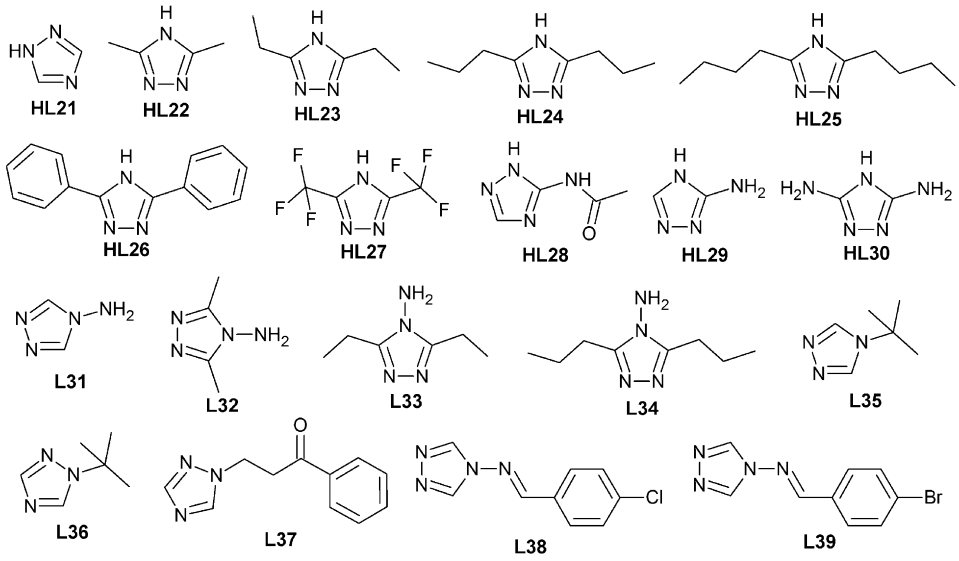

Fig. 6. Non-exhaustive list of 1,2,4-triazole ligands (**HL21**–**L39**) containing a sole coordinative ring used to prepare coordination polymers.

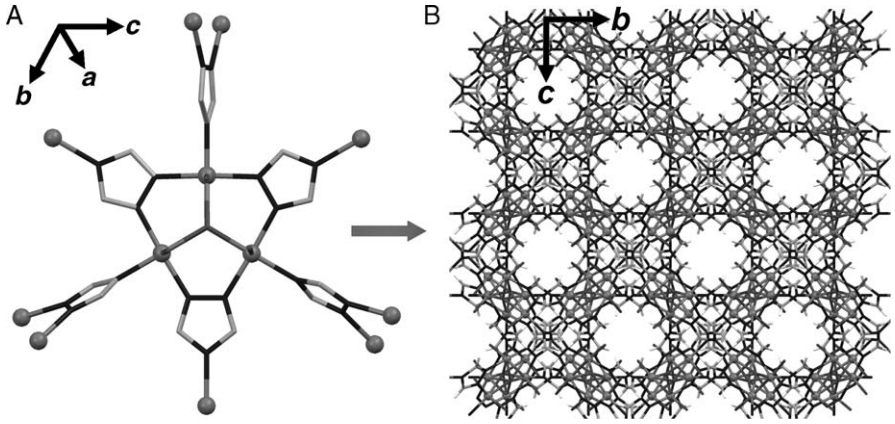

Fig. 7. (A) Trinuclear triangular building block constructing the framework of $[Cu_3(\mu_3\text{-}OH)(\mathbf{L21})_3(OH)_2(H_2O)_4]_n{\cdot}4.5n(H_2O)$ [45]; (B) representation of the crystal packing of $[Cu_3(\mu_3\text{-}OH)(\mathbf{L21})_3(OH)_2(H_2O)_4]_n{\cdot}4.5n(H_2O)$ emphasizing the 1D channels along the crystallographic *a* axis [45]. The copper(II) ions are symbolized by grey balls.

6 h produces the coordination polymer $\{[Cu_3(\mu_3\text{-}\mathbf{L64})_3(\mu_3\text{-}O)(H_2O)_3](ClO_4)_4{\cdot}4.5H_2O\}_n$ (Fig. 11) [49]. The self-assembly of the bifunctional ligand and copper(II) ions leads to the formation of $Cu_{24}(\mathbf{L64})_{12}$ cages (Fig. 11B and C). This framework is built from trinuclear $Cu_3(\mu_3\text{-}O)(\mathbf{L64})_6$ units with three-fold symmetry. These tricopper(II) complexes, bridged by the μ-triazole rings of three **L64** ligands, are connected to each other through the pyridyl donor group of the **L64** ligands (Fig. 11A).

The $M_{24}L_{12}$ cage building units are linked by extra ligands to yield an extended 3D framework with formula $Cu_{24}(\mathbf{L64})_{24}$ that exhibits a CaB_6 topology (Fig. 12A) [49]. The volume of the cavity is about 1.6 nm^3; this nano-sized $M_{24}L_{12}$ cage hosts 16 large anions (ClO_4^-). Interestingly, this material possesses remarkable anion-exchange properties ($BF_4^- \leftrightarrow ClO_4^-$, Fig. 12B) [49], which is one of the very interesting, potential applications of coordination polymers.

2.3. Tetrazole-containing ligands

The last family of azole ligands described in the present review, namely the tetrazoles, hold an additional nitrogen atom. Consequently, compared to the triazole rings, the tetrazole unit exhibits more bridging coordination possibilities, *i.e.* 10 different coordination modes (Scheme 7). Thus, neutral tetrazole may function both as a dinucleating ligand ($\mu_{2,3}$-, $\mu_{2,4}$-, and $\mu_{3,4}$-binding modes; Scheme 7A) and a trinucleating ligand ($\mu_{2,3,4}$-binding mode; Scheme 7A). Deprotonated tetrazolate can bridge two, three and up to four metal ions (dinucleating $\mu_{1,2}$-, $\mu_{2,3}$- and $\mu_{1,3}$-, trinucleating $\mu_{1,2,3}$- and $\mu_{1,2,4}$-, and tetranucleating $\mu_{1,2,3,4}$-binding modes; Scheme 7B).

These numerous bridging coordination modes afford great synthetic possibilities for the design and preparation of hybrid inorganic/organic architectures. In fact, by the end of 2009, no less than 90 tetrazole-based ligands have been described in more than 160 publications. Table 3 summarizes the metals with which these tetrazole ligands (whose names are listed in Table S3) have formed structurally characterized coordination polymers. The first X-ray structures of coordination polymers obtained from tetrazole ligands were reported in 1982. Thus, Yu and co-workers described the solid-state structure of the 3D framework $[Hg(\mathbf{L122})_2]_n$. The same year, Pierce-butler reported the crystal structure of $[Pb_2(\mathbf{L141})(\mu\text{-}OH)_2]_n$, which reveals a 2D sheet network [50].

As done earlier for the triazole-based ligands, the tetrazoles have been classified in three categories, namely those containing a sole coordinative ring (**HL103**–**L124**), the bridged ligands (**H_2L125**–**H_4L147**), possessing two or more coordinative rings linked by a spacer, and the mixed ligands (**HL148**–**L192**), having two or more functional groups.

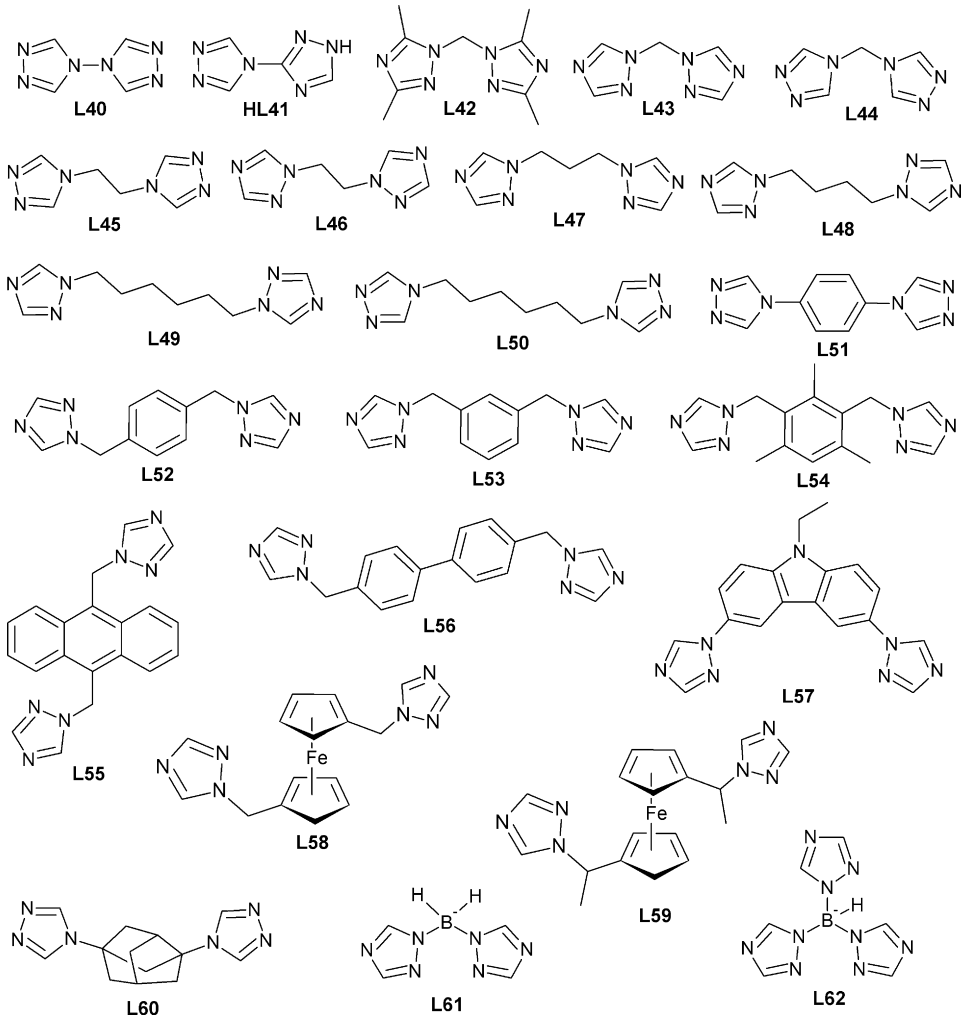

Fig. 8. Non-exhaustive list of bridged 1,2,4-triazole ligands (**L40**–**L62**) used to prepare coordination polymers.

The tetrazole ligands of the first group (**HL103**–**L124**) are depicted in Fig. 13. An excellent example for this first category of ligands is provided by the layering reaction of an ethanolic solution of the simple tetrazole ring (**HL103**) with an aqueous solution of silver(I) nitrate (1.5 equiv.), at room temperature for 2 h [51]. A double salt, namely Ag(**L103**)·$AgNO_3$, is obtained that consists of a non-interpenetrated 3D cationic framework with large channels. This structural architecture contains triconnected and biconnected silver centers (Fig. 14A) in a 2:1 ratio. The metal ions are linked by exo-tetradentate **L103**$^-$ anions, generating single undulated layers of ($4{\cdot}8^2$) topology, which are connected through N–Ag–N bridges to produce a 3D network with large channels along the crystallographic *c* axis, containing nitrate anions (Fig. 14B). This hybrid organic/inorganic material is stable up to 248 °C, thus demonstrating that tetrazoles can be used to prepare robust interesting polymeric networks, which may be used as anion exchangers.

The bridged tetrazole-containing ligands (**H_2L125**–**H_4L147**) used to prepare coordination polymers are shown in Fig. 15.

A beautiful example for this category of ligands is achieved with the ligand 1,4-bis(tetrazol-5-yl) benzene (**H_2L137**). Thus, Long and co-workers have used this bis-tetrazole ligand to synthesize a series of remarkable porous MOFs with BET surface areas in the range 200–640 $m^2\,g^{-1}$ [52]. For instance, the reaction of $Zn(NO_3)_2{\cdot}6H_2O$ with **H_2L137** in methanol/dimethylformamide (1/1; vol/vol), at room temperature for 4 days, produces large, colorless crystals of $[Zn_3(\mathbf{L137})_3(DMF)_4(H_2O)_2]_n{\cdot}3.5nCH_3OH$ [52]. Its single-crystal structure contains linear Zn_3 units linked via **L137**$^{2-}$ bridges to form a neutral, 3D architecture (Fig. 16). The Zn_3 complex consists of a central, octahedral Zn^{2+} ion coordinated by six tetrazolate nitrogen atoms ($\mu_{2,3}$-binding mode) and two outer Zn^{2+} ions, each octahedrally coordinated by three tetrazolate nitrogen atoms, two dimethylformamide molecules, and one water molecule (Fig. 16A). The trizinc(II) moieties and the linear **L137**$^{2-}$ ligands self-assemble to generate a 4,6 3D net, defining infinite 1D channels (Fig. 16B), which are occupied by dimethylformamide, water, and disordered methanol molecules [52].

$[Zn_3(\mathbf{L137})_3(DMF)_4(H_2O)_2]_n{\cdot}3.5nCH_3OH$ exhibits an estimated surface area of 640 $m^2\,g^{-1}$. Once degassed under mild conditions, this material with permanent porosity can uptake 1.46 wt% of H_2. These results clearly demonstrate the utility of tetrazoles for producing robust MOFs with permanent porosity, and with topologies and gas adsorption properties comparable to those of the pioneering, carboxylate-based MOF materials.

The last category, *i.e.* the mixed ligands (Fig. 17), is elegantly represented by the trifunctional ligand 5-(tetrazol-5-yl)isophthalic acid (**H_3L187**).

The solvothermal reaction between $Cu(NO_3)_2{\cdot}2.5H_2O$ and **H_3L187** in dimethylformamide/ethanol at 85 °C for 12 h, produces the 3D compound $[Cu_6O(\mathbf{L187})_3(H_2O)_9(NO_3)]_n{\cdot}15nH_2O$ [53]. The single-crystal structure of this compound reveals that both the carboxylato and tetrazolato groups of deprotonated **L187**$^{3-}$ act as bridging dinucleating ligands, thus coordinating 6 copper(II)

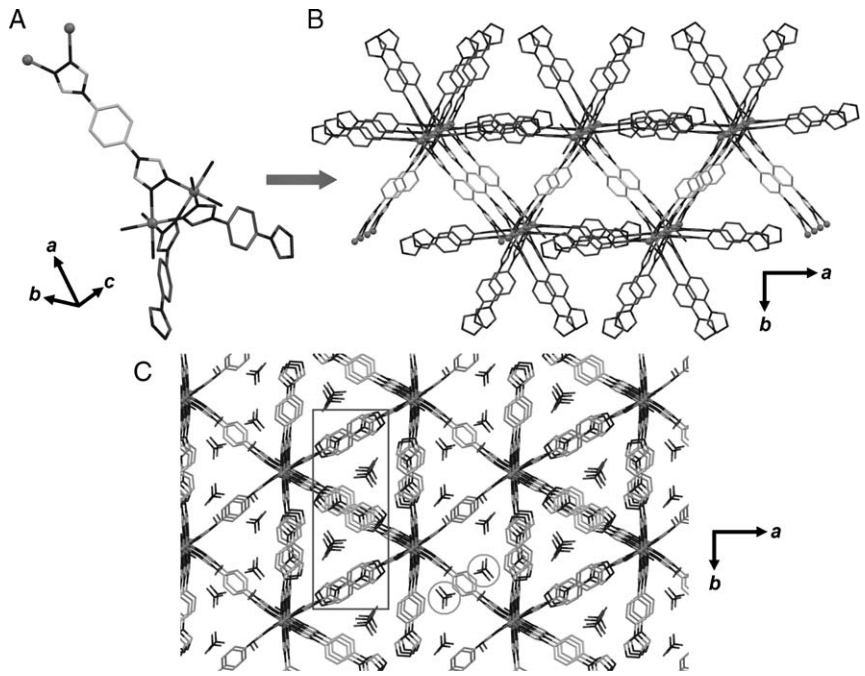

Fig. 9. (A) Building block constructing the framework of $[Cu_2(\mu\text{-}\mathbf{L51})_4(\mu_4\text{-}\mathbf{L51})]_n(NO_3)_{4n}\cdot 2nH_2O$ [46]; (B) crystal packing showing the 1D $[Cu_2(\mu_2\text{-trz})_3]_n$ infinite chains along the crystallographic *c* axis and the 2D zigzag sheets. The tetradentate μ_4-**L51** ligands are depicted in light grey and the N1,N2-bidentate μ-**L51** ligands are shown in dark grey; (C) intercalating packing of the 2D sheets by means of π–π interactions (rectangle). The nitrate ions in the grey circles are involved in anion–π interactions with phenylene rings. The copper(II) ions are symbolized by grey balls.

ions (Fig. 18A). The two carboxylato units of $\mathbf{L187}^{3-}$ generate $[Cu_2(O_2CR)_4]$ paddlewheels (Fig. 18B), and the triazolate moiety is involved in the formation of trigonal $[Cu_3O(N_4CR)_3]$ trimers (Fig. 18C).

24 Functionalized isophthalate ligands are connected by 12 copper dimer centers, *i.e.* $[Cu_2(O_2CR)_4]$ paddlewheels, to form finite truncated cuboctahedra, which are linked through the trigonal $[Cu_3O(N_4CR)_3]$ trimeric Secondary Building Blocks (SBBs). This self-assembly results in a 24-connected rhombicuboctahedral Tertiary Building Unit (TBU). Thus, the TBU are formed via the isophthalate unit, linked to 12 neighboring TBUs (Fig. 18B) through 24 3-connected trigonal SBUs (tricopper(II) complexes; Fig. 18C). The resulting MOF is a (3,24)-connected network having *rht*-like topology. This porous material is characterized by large 1D channels (along all three crystallographic axes; Fig. 19). The total solvent-accessible volume for this material was estimated to be 75% [53]. The large accessible cavities and its cationic nature make this framework a potential porous material for gas storage, like H_2. Actually, up to 2.4 wt% of H_2 can be uptaken by this compound at 77 K and atmospheric pressure.

3. Metal complexes

Ligands bearing the triazole (any of its two isomers) or the tetrazole ring have served to help stabilize molecular complexes of transition metals exhibiting a large variety of structures and nuclearities, the latter ranging from 2 to 26. We show in this section an overview of the various structural types obtained with 3*d* metals, based primarily on a search on the Cambridge Structural Database (CSD version 5.30; November 2008 + 4 updates) [39]. Together with this we include a brief discussion of the magnetic properties arisen from these compounds. We employ during this description the $H = -2JS_iS_j$ convention for the phenomenological description of the magnetic coupling. Of the *circa* 216 species examined, nearly two thirds are made with 1,2,4-triazole derivatives, whereas only about 8% involve tetrazoles. The predominant nuclearity is dinuclear (40% of compounds), followed by trinuclear (19%) and pentanuclear (6%). The analysis is organized according to the number of metal centers of the molecule, starting from the smallest systems. Many of the ligands discussed in this section have already been seen in the previous section and are represented in figures of that section. Ligands not yet shown are collected on Fig. 20.

3.1. Dinuclear complexes

The dominance of this nuclearity for the ligands reviewed here is caused by the tendency of triazole and tetrazole rings to show the [M–N–N–M] bridging moiety (see Schemes 5–7), most often in the absence of conditions that could lead to further growth of the complex. This moiety, however, is less common with 1,2,3-triazole ligands, and has been found within dinuclear systems only in the complex $[Cu_2(\mathbf{L7})_4Cl_4]$ (Fig. 21) [54], involving a 1-substituted methylpyridine benzotriazole (**L7**), which acts as bridging as well as chelating ligand. It needs to be mentioned at this point that the [M–N–N–M] fragment is extremely commonplace among discrete complexes of ligands containing a pyrazole fragment (596 hits on the CSD). This area is, however, not the topic of this review.

3.1.1. Dinuclear complexes with triple [–N–N–] bridge

A family of at least seven dinuclear complexes exhibiting a triple [–N–N–] bridge has been identified, all of them with 1,2,4-triazole. All these compounds contain a pair of six coordinate M(II) centers: we have found this structure for the case of Ni(II), $[Ni_2(\mathbf{L193})_4(NCS)_4(H_2O)]$ [55] and $[Ni_2(\mathbf{L31})_3(tp)_2(H_2O)_4]$ (H_2tp = terephthalic acid) [56]; Co(II), $[Co_2(\mathbf{L194})_4(NCS)_4(H_2O)]$ [57], $[Co_2(\mathbf{L195})_5(NCS)_4]$ [58] and $[Co_2(\mathbf{L31})_6(tp)_2(H_2O)_4]$ [56]; Mn(II), $[Mn_2(\mathbf{L196})_5(NCS)_4]$ (Fig. 22) [59] and Fe(II) (see Section 4). In these complexes, the 1,2,4-triazole rings are disposed with their plane parallel to the molecular axis and with mutual

dihedral angles of approximately 120°, as in a paddlewheel (Fig. 22).

The three *fac* coordination sites remaining on the external side of each metal are occupied by anionic ligands (compensating the charge of the metals), solvent molecules and/or the corresponding triazole acting as a monodentate ligand. The μ-triazole units keep the metals separated by distances that range from 3.747 Å ([Ni_2(**L31**)$_3$(tp)$_2$(H_2O)$_4$]) [56] to 4.139 Å ([Mn_2(**L196**)$_5$(NCS)$_4$]) [59]. It is worth noting that this list of compounds is relatively small compared with the series of related trinuclear complexes comprising three metals disposed linearly, also linked to each other by triple [–N–N–] bridges (see below). The reasons for the formation of either the dinuclear or the trinuclear system are not clear. It is likely that the [M_2] and [M_3] species co-exist in solution (perhaps along with larger oligomers) while the compound finally obtained is the one that crystallizes or precipitates first or better. The magnetic properties of these complexes when the metal is cobalt, have been studied and reviewed [60]. This has allowed studying the interaction through the triple bridge independently of other influences (such as the possible coupling between both external metals in the trinuclear analogues). The coupling was always antiferromagnetic, and in general, weaker than for the pyrazole-based analogues. The reason is, presumably, the electron withdrawing effect of substituting a carbon atom in the ring by a more electronegative nitrogen atom [60].

3.1.2. Dinuclear complexes with double [–N–N–] bridge

The longest list of dinuclear compounds corresponds to complexes showing two $\mu_{1,2}$ bridging moieties (from tri- or tetrazole ligands), in most cases as the only type of bridge between metals. There are however a few complexes exhibiting a molecule of H_2O as an additional bridge. This is the case of [Cu_2(**HL30**)$_2$(SO_4)(H_2O)$_5$](SO_4) (Fig. 23) [61], [Ni_2(**L33**)$_4$(H_2O)$_5$](SO_4)$_2$ [62], [Ni_2(**L32**)$_2$(piv)$_4$(H_2O)$_3$] [63] and [Ni_2(**L33**)$_2$(piv)$_4$(H_2O)] (Hpiv = pivalic acid) [63]. The copper complex (Fig. 23) exhibits one square pyramidal and one octahedral Cu(II) center.

The magnetic coupling between both Cu(II) ions ($J = -47.2\ cm^{-1}$) results from the direct overlap between the $d_{x^2-y^2}$ magnetic orbitals of the metals and the σ-orbitals of the triazole bridges. The nickel systems show the metallic centers in the octahedral geometry, with terminal ligands (H_2O, **L33** or piv^-) completing their coordination sphere. In complex [Ni_2(**L33**)$_2$(piv)$_4$(H_2O)], two of the terminal piv^- ligands act as chelates to the Ni(II) centers. This compound and [Ni_2(**L32**)$_2$(piv)$_4$(H_2O)$_3$] exhibit similar magnetic coupling ($J = -6.88$ and $-5.63\ cm^{-1}$, respectively) and they constitute the only examples with this core where the magnetic exchange has been investigated.

When both metals are linked only by two $\mu_{1,2}$-azole bridges, these occupy almost always, two equatorial positions of each metal. The outer equatorial sites are often occupied by substituents on the

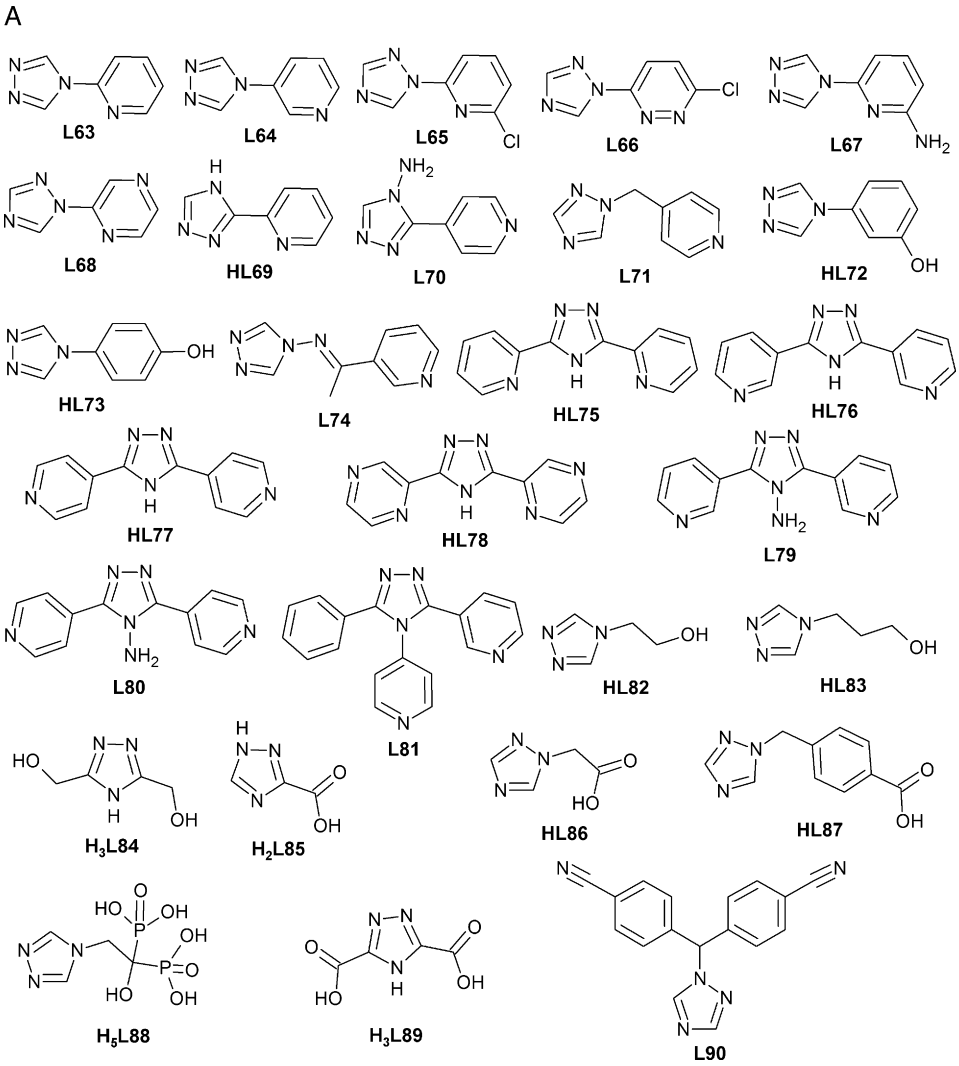

Fig. 10. Non-exhaustive list of the mixed 1,2,4-triazole ligands (**L63**–**HL102**) used to prepare coordination polymers.

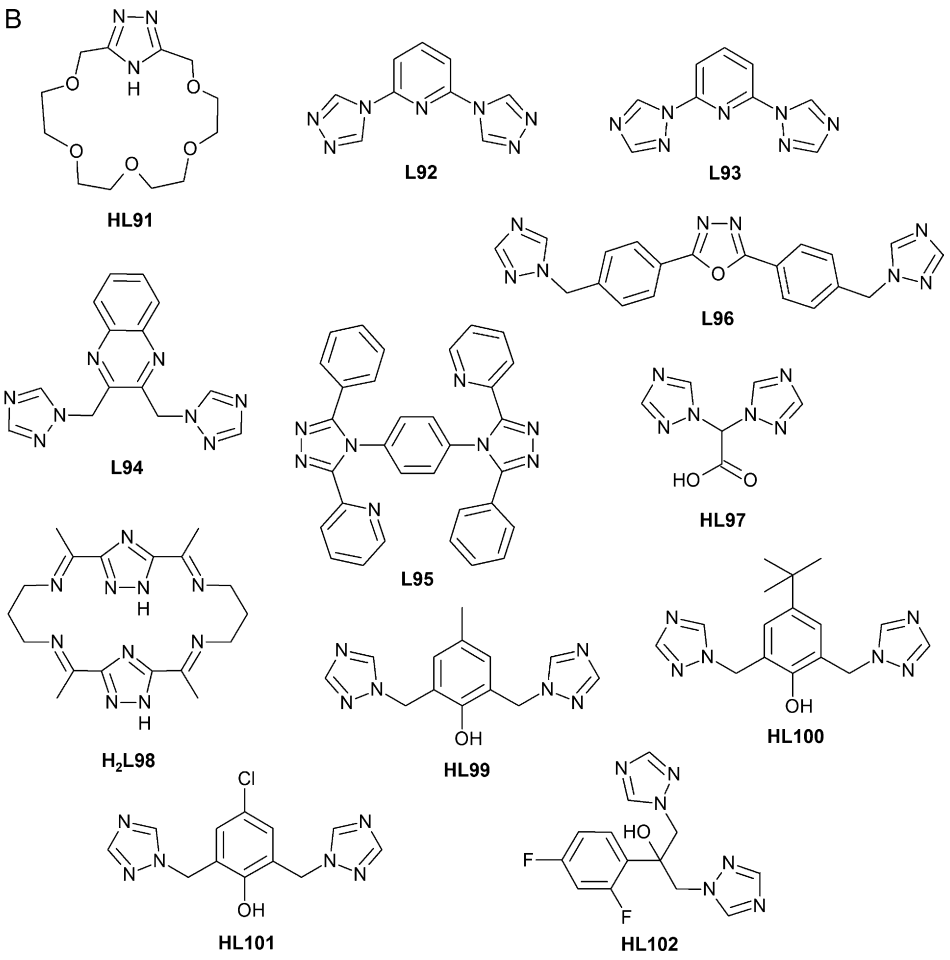

Fig. 10. (*Continued*).

heterocycles while the axial sites are usually filled by monodentate ligands (in general, anions or solvent molecules). Both azole rings are generally disposed, together with the metallic centers, approximately in a planar arrangement. Significant deviations from planarity only occur when the assembly lacks sufficient degrees of freedom and is structurally constrained. This might happen for example if the tri- or tetrazole rings are integrated within a macrocyclic structure, as observed in the complex $[Co_2(\mathbf{L98})Cl_2]$ (Fig. 24) [64].

The ligand $\mathbf{H_2L98}$ is a macrocycle containing two facially disposed 1,2,4-triazole rings, and four imine functions, suited for the encapsulation of transition metal ions. In the complex, two Co(II) ions are trapped through their coordination to this ligand. The Co–N distances however, are too long for the metals to fit perfectly within the cavities of the ligand (averages of 2.07 and 2.13 Å for distances to N_{triaz} and N_{imin}, respectively), forcing them to lie slightly away from their respective equatorial planes. A consequence of this is the bending of the bridging triazole rings with respect to one another, exhibiting an almost right dihedral angle (85.52°). By contrast, the Co(III) quasi-analogue, $[Co_2(\mathbf{L98})Cl_2(CH_2NO_2)_2]$ (Fig. 25) [64], which involves smaller metals and thus shorter Co–N distances (averages of 1.83 and 1.93 Å, respectively), has the cations perfectly accommodated within the ligand cavities, the whole assembly exhibiting a very flat configuration.

The Cu(II) complexes of $\mathbf{H_2L98}$, $[Cu_2(\mathbf{L98})(MeCN)_2](ClO_4)_2$ and $[Cu_2(\mathbf{L98})(NCS)_2]$ also display bent configurations [65]. Shorter coordination bonds (with average distances of 1.968/2.007 and 1.969/2.019 Å, respectively, in the Cu–N_{triaz}/Cu–N_{imin} notation) explain wider angles between triazole planes (110.64° and 110.89°, respectively, thus closer to planarity). Complexes of a related macrocycle with a longer aliphatic backbone (butylene fragments instead of propylene), $[Co_2(\mathbf{L197})(H_2O)_3(MeCN)](ClO_4)_2$, $[Co_2(\mathbf{L197})(NCO)_2]$ and $[Co_2(\mathbf{L197})Cl_2]$ [66], exhibit Co–N distances very similar to these in the $[Co(II)_2]$ complex but a larger dihedral angle between triazole rings because of the larger flexibility of the cyclic ligand. The ligand $\mathbf{H_2L198}$ is even larger than the two macrocycles discussed, thus furnishing a flat structure with Mn(II) in form of the complex $[Mn_2(\mathbf{L198})(H_2O)_4)]Cl_2$ [67].

A large group of dinuclear complexes exhibiting the double $\mu_{1,2}$-azoles has been described using symmetrically di-substituted 1,2,4-triazole rings, where the substituents are coordinating (a very complete review on the complexes made of this type of ligands is available) [68]. These multi-donors are suited to act as ditopic ligands, by both chelating and bridging two metals. These ligands, however, do not limit the degrees of freedom of the final assembly as do the macrocyclic donors discussed above. Usually, two di-substituted rings locate in front of each other, "sandwiching" two metals in between them, with the metals and the triazole rings sharing approximately the same plane, while additional monodentate donors occupy axial positions. The most numerous group is formed by complexes of 3,5-bis-(pyridin-2-yl)-1,2,4-triazole (**HL75**) or very close derivatives, incorporating Fe (see Section 4), Mn [69], Ni [70,71], Co [72] and Cu [73] as metals. Examples with the parent ligand **HL75** are $[Mn_2(\mathbf{L75})_2Cl_2(H_2O)_2]$ [69], $[Mn_2(\mathbf{L75})_2(NCS)_2(H_2O)_2]$ [69] and $[Ni_2(\mathbf{L75})_2(NCS)_2(H_2O)_2]$ [71]. Interestingly, this ligand is not used as a reagent in the synthesis of any of the three complexes but is formed *in situ* from solvothermal reactions. In the case of the manganese complexes, the reaction sys-

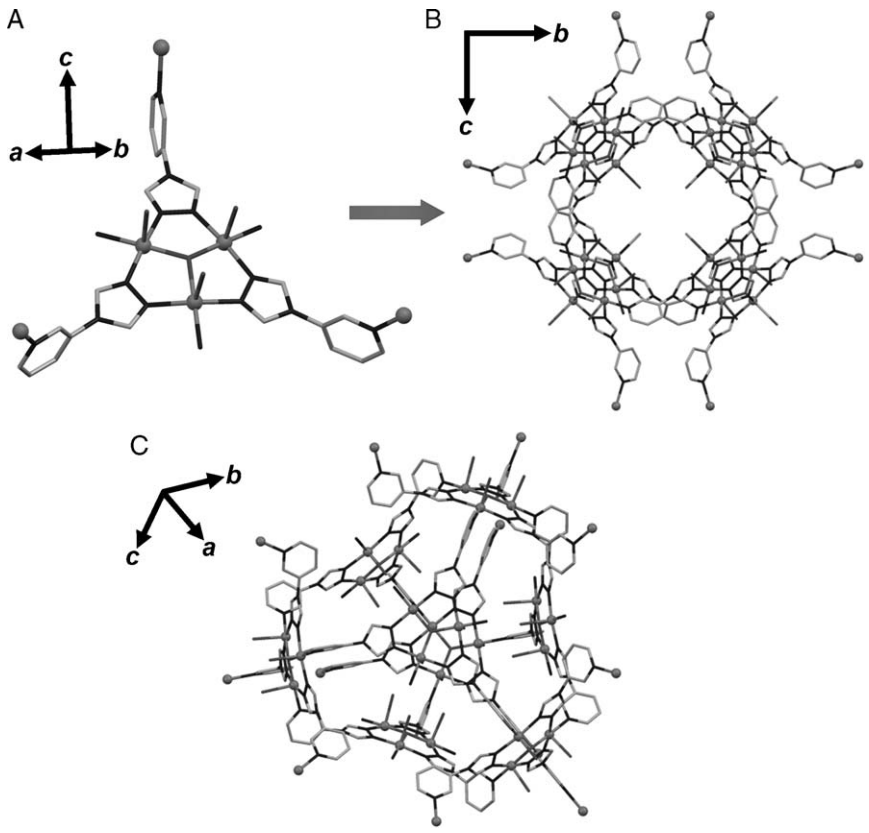

Fig. 11. (A) Coordination motif acting as building block for the generation of $\{[Cu_3(\mu_3\text{-}\mathbf{L64})_3(\mu_3\text{-}O)(H_2O)_3](ClO_4)_4{\cdot}4.5H_2O\}_n$ [49]; (B and C) two views of the (empty) $M_{24}L_{12}$ coordination cages in this compound. The copper(II) ions are symbolized by dark-grey balls.

tems are made originally of 2-cyanopyridine and hydrazine in EtOH in the presence of $MnCl_2$, or formed by 2-pyridylamidrazone (2-pa) together with $Mn(SO_4)_2$ and KSCN in ethanol. The latter reaction was in fact conducted to proof that 2-pa is a key intermediate in the formation of the ligand **HL75** from the corresponding organonitrile and hydrazine. Interestingly, $[Mn_2(\mathbf{L75})_2Cl_2(H_2O)_2]$ is present in the crystal as two topological isomers (Fig. 26) that vary in the positions of the Cl^- and H_2O ligands on the complexes. Both Mn complexes of **HL75** exhibit severely distorted six-coordinate metal centers.

The complex of Ni(II) is formed after the de-amination of the ligand 4-amino-3,5-bis-(pyridin-2-yl)-1,2,4-triazole (**L199**) during its reaction with $NiCl_2$ and KSCN in solvothermal conditions [71]. Susceptibility measurements on $[Ni_2(\mathbf{L75})_2(NCS)_2(H_2O)_2]$ revealed, as expected, an antiferromagnetic coupling of the two metals through the [N–N] bridges of $J = -17.62\,cm^{-1}$. It is interesting to note that the first example of this family of dinuclear complexes characterized structurally, $[Ni_2(\mathbf{L199})_2Cl_2(H_2O)_2]Cl_2$ [72], was made with the amino derivative **L199** and reported in 1984. In that report, evidence was provided for the preparation of the Co(II) analogue. The magnetic coupling within the Ni(II) complex was estimated to be $J = -12.5\,cm^{-1}$. Many other complexes of this type have been characterized using related ligands with other substituents on the position "4" of the tetrazole. These substituents are isobutyl, pyrrol-1-yl or *para*-methoxyphenyl. Especially interesting is the series of compounds with the pyrrolyl substituted

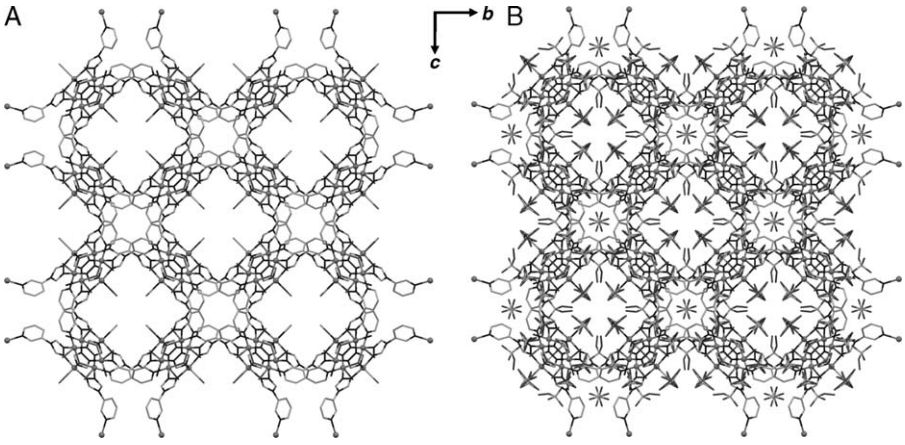

Fig. 12. 3D network of $\{[Cu_3(\mu_3\text{-}\mathbf{L64})_3(\mu_3\text{-}O)(H_2O)_3](ClO_4)_4{\cdot}4.5H_2O\}_n$ viewed along the *a* axis with A) with empty cavities; B) with the cavities containing perchlorate anions [49]. The copper(II) ions are symbolized by grey balls.

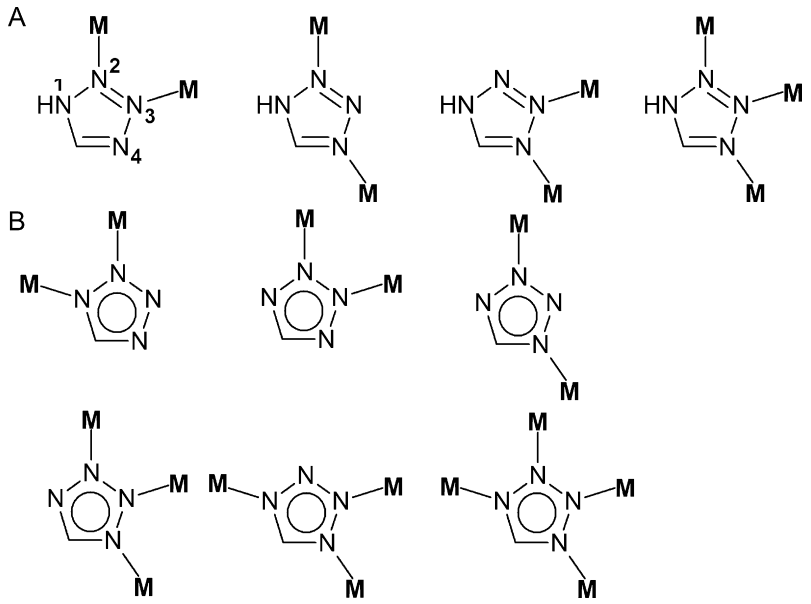

Scheme 7. Bridging coordination modes of (A) tetrazole ($\mu_{2,3}$, $\mu_{2,4}$, $\mu_{3,4}$ and $\mu_{2,3,4}$) and (B) tetrazolate ($\mu_{1,2}$, $\mu_{2,3}$, $\mu_{1,3}$, $\mu_{1,2,3}$, $\mu_{1,2,4}$, and $\mu_{1,2,3,4}$). **M** symbolizes a metal ion.

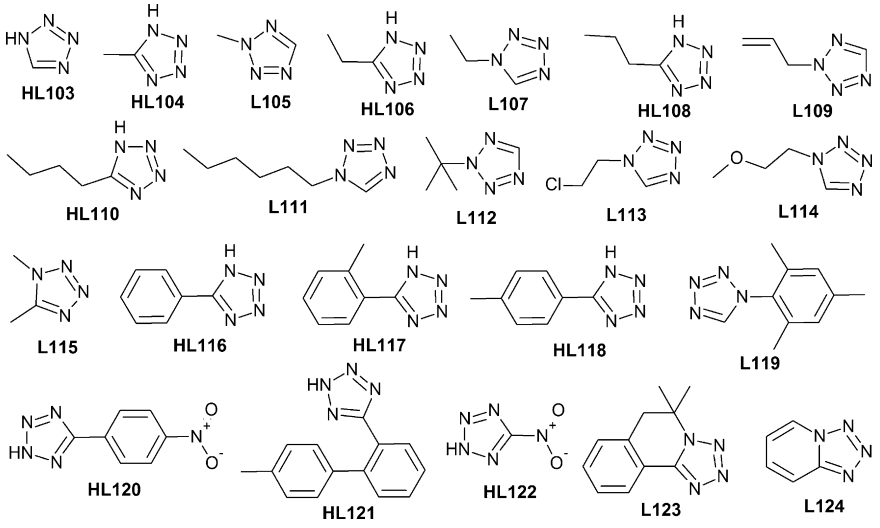

Fig. 13. Non-exhaustive list of tetrazole ligands (**HL103**–**L124**) containing a sole coordinative ring used to prepare coordination polymers.

4-(1-*H*-pyrrol-1-yl)-3,5-bis-(pyridin-2-yl)-1,2,4-triazole (**L200**), the latter prepared from the reaction of the amino derivative **L199** with 2,5-dimethoxytetrahydrofuran in AcOH/1,4-dioxane. The ligand **L200** reacts with M(II) 3*d* metals to yield either mononuclear or dinuclear complexes. The formation of one or the other type depends on small variables such as solvents, anions, or solubility differences. The following dinuclear systems have been characterized structurally [74,75]; $[Co_2(\mathbf{L200})_2(H_2O)_2(DMF)_2](ClO_4)_4$, $[Co_2(\mathbf{L200})_2(H_2O)_2(MeCN)_2](BF_4)_4$, $[Ni_2(\mathbf{L200})_2(MeCN)_4](BF_4)_4$, $[Cu_2(\mathbf{L200})_2(H_2O)_2$

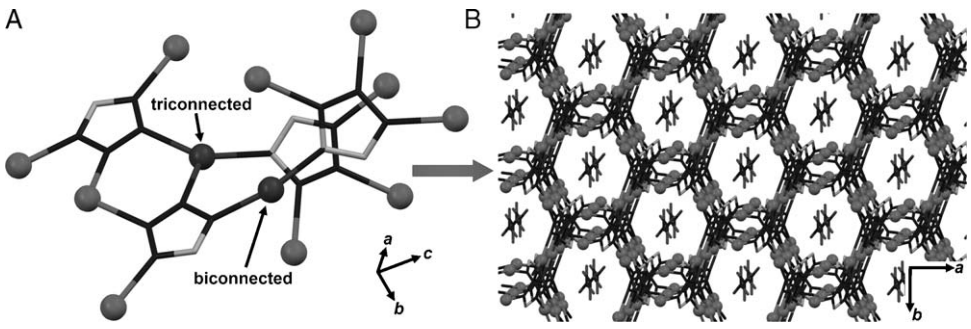

Fig. 14. (A) Triconnected and biconnected silver(I) centers, emphasized as black balls, found in the solid-state structure of $[Ag_3(\mathbf{L103})_2](NO_3)$ [51]; B) representation of the 3D network of this polymer, with the silver(I) ions symbolized by grey balls.

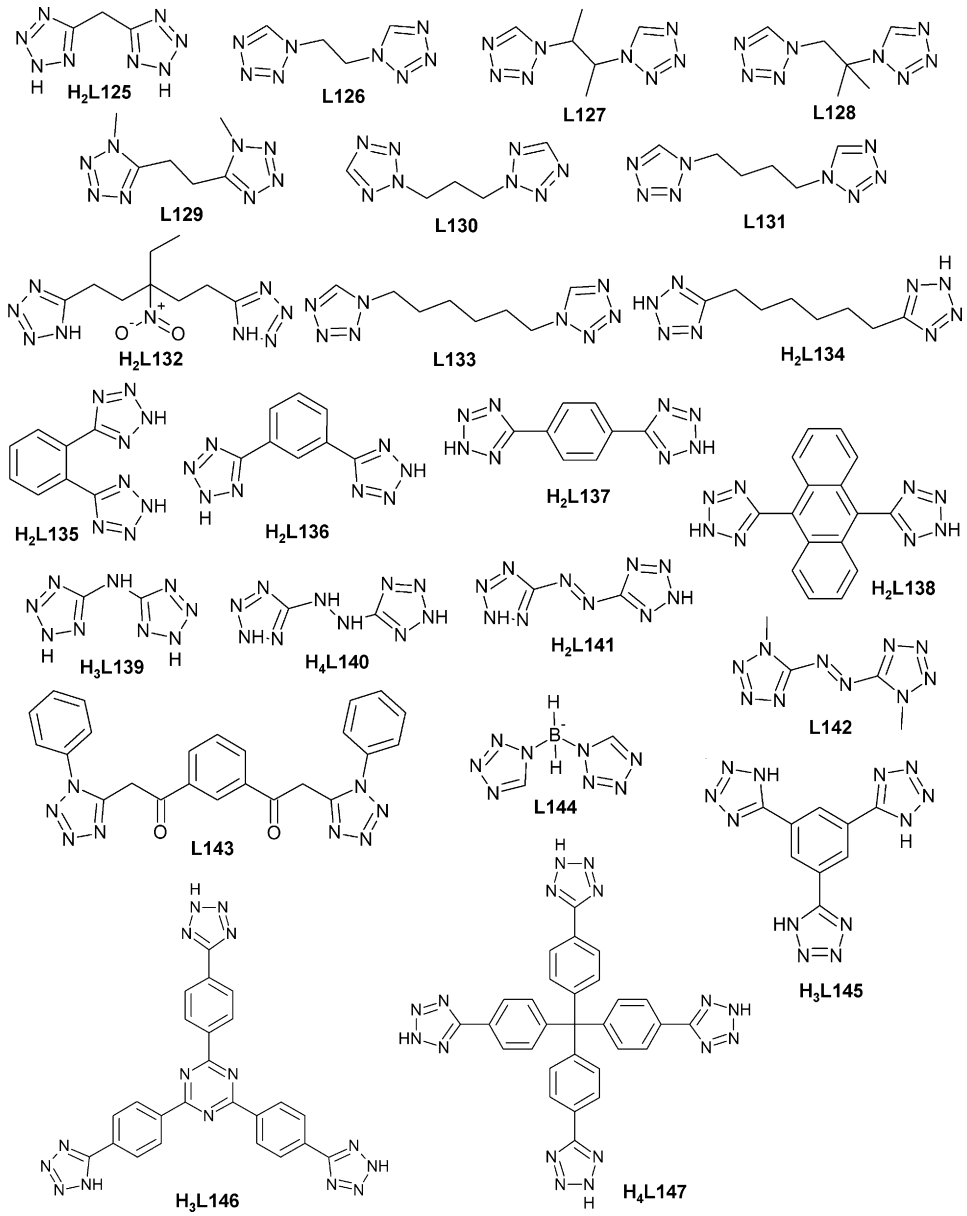

Fig. 15. Non-exhaustive list of bridged tetrazole ligands (**H_2L125**–**H_4L147**) used to prepare coordination polymers.

$(MeCN)_2](ClO_4)_4$ and $[Fe_2($**L200**$)_2(H_2O)_2(MeCN)_2](BF_4)_4$ (Fig. 27). The structures of these complexes are very similar among them and consist again of two ligands positioned in front of each other, chelating the two metals sitting in between them. This fragment lies approximately within one plane, except for the pyrrolyl substituents, which are positioned perpendicularly. In all cases, coordination number six around the metallic ions is completed by solvent ligands (Fig. 27).

As expected, weak antiferromagnetic interactions between the metals are observed within all the complexes, with *J* val-

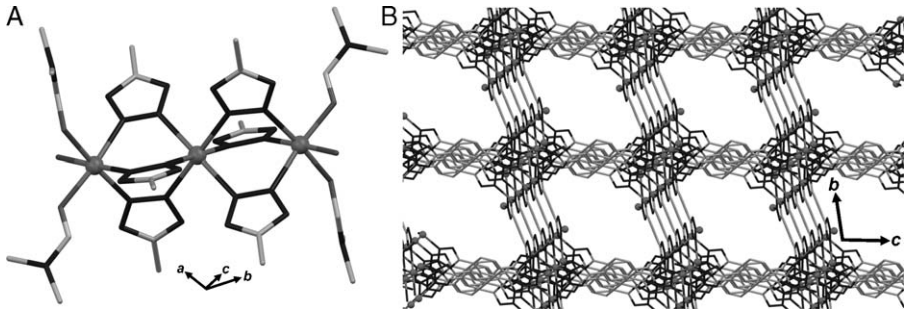

Fig. 16. (A) Trinuclear Zn_3 building units of $[Zn_3($**L137**$)_3(DMF)_4(H_2O)_2]_n \cdot 3.5n CH_3OH$ [52]; (B) crystal packing upon removing of the DMF and water ligands, showing the channels along the crystallographic *a* axis. Hydrogen atoms and solvate guest molecules are omitted for clarity. The zinc(II) ions are symbolized by dark-grey balls.

ues ranging from −0.44 to −7.8 cm^{-1}. The complexes made with ligands with other substituents on the position "4" of the triazole rings share a very similar structure to that in Fig. 26, and show antiferromagnetic interactions of the same magnitude, except for the complex $[Cu_2(\mathbf{L201})_2(ClO_4)_2(MeCN)_2](ClO_4)_2$ [76], where the magnetic exchange is significantly stronger ($J = -105\ cm^{-1}$). The magnetic properties of the **L200** analogue $[Cu_2(\mathbf{L200})_2(H_2O)_2(MeCN)_2](ClO_4)_4$ [74] were not reported. Related ligands exhibit other coordinating groups on the "3" and "5" positions of the 1,2,4-triazole ring, such as amino or diacetylamino groups, and yield the corresponding dinuclear systems, namely $[Cu(\mathbf{L202})(H_2O)_2]_2$ [77], $[Cu_2(\mathbf{L202})_2Br_2(H_2O)_2]Br_2$ [78] and $[Cu(\mathbf{L203})(NO_3)(H_2O)]_2$ (this complex prepared along with the Co and Ni analogues) [79].

The last group of dinuclear complexes with only the [M–(N–N)$_2$–M] bridging fragment is made with tri- or tetrazole rings exhibiting only one coordinating substituent or none. In these complexes, the number of degrees of freedom is even larger than for the dinucleating ligands discussed just above; thus, the ensemble of the two metals and the five membered heterocycles are also disposed approximately on one plane. Most triazole ligands with one coordinating substituent are derivatives of 3-(pyridine-2-yl)-1,2,4-triazole (**HL69**). The complexes with the parent ligand $[Cu_2(\mathbf{L69})_2(mim)_2(NO_3)_2(H_2O)_2]$ (mim = *N*-methylimidazole) [80], $[Cu_2(\mathbf{L69})_2(H_2O)_3(SO_4)]$ [81] (Fig. 28) and $[Ni_2(\mathbf{HL69})_2(H_2O)_4](NO_3)_4$ [82] have been crystallographically characterized. The second copper complex is one of the (surprisingly) very few cases in this family exhibiting square pyramidal Cu(II) ions (Fig. 28).

In addition, this complex features an interesting monocoordinated SO_4^- ligand on an equatorial site. It was found that for the case of Cu(II), the intramolecular magnetic coupling between

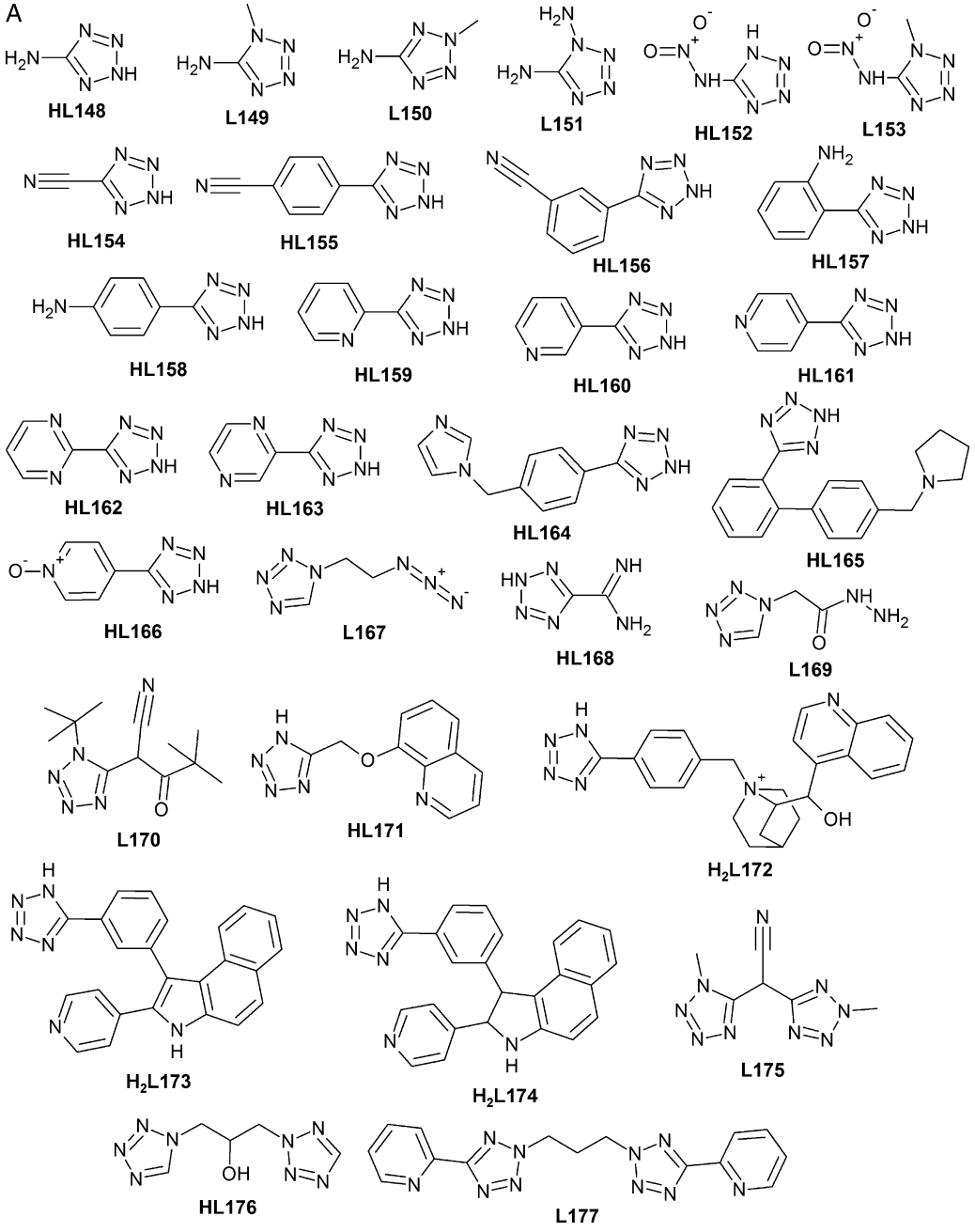

Fig. 17. Non-exhaustive list of the mixed tetrazole ligands (**HL148**–**L192**) used to prepare coordination polymers.

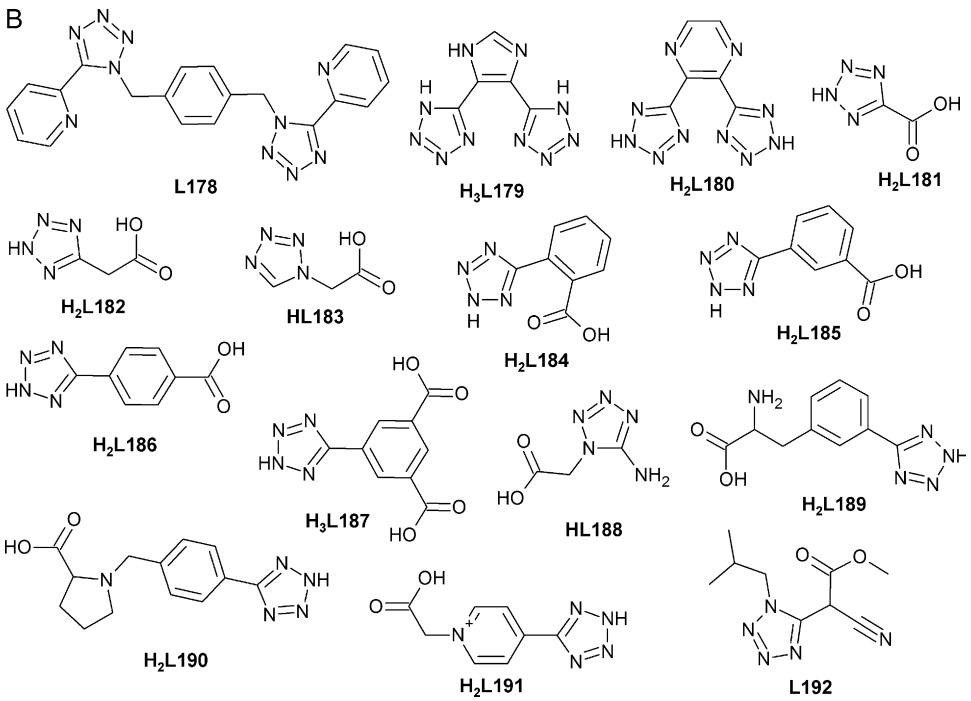

Fig. 17. (*Continued*).

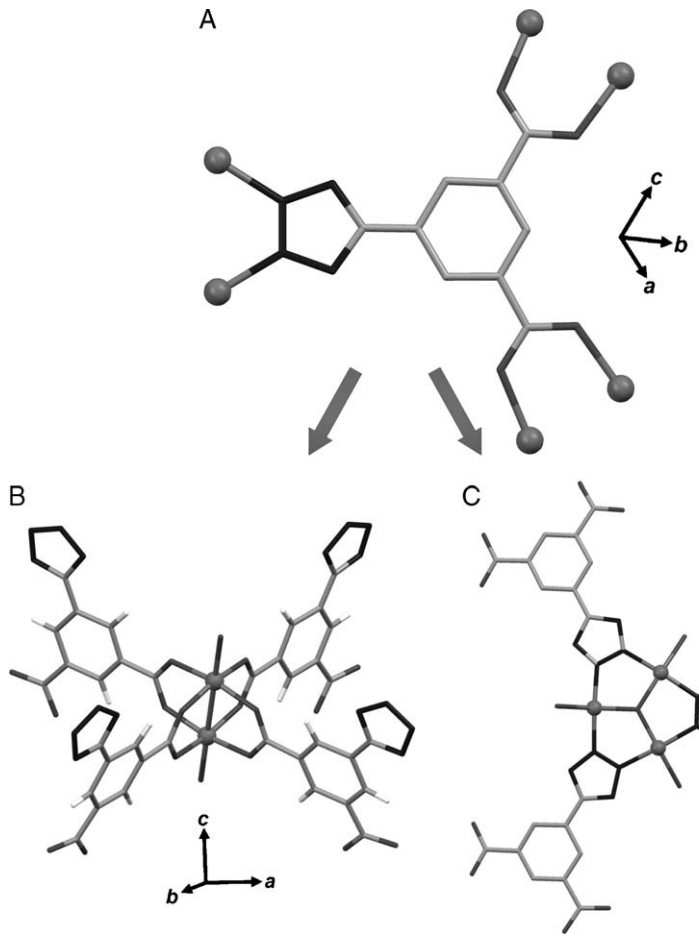

Fig. 18. (A) Coordination mode of the multifunctional ligand 5-(tetrazol-5-yl)isophthalic acid (**H_3L187**) in $[Cu_6O(\mathbf{L187})_3(H_2O)_9(NO_3)]_n \cdot 15nH_2O$ [53]; (B) $[Cu_2(O_2CR)_4]$ paddlewheel Molecular Building Block (MBB) and (C) $[Cu_3O(N_4CR)_3]$ trimeric Secondary Building Block (SBB). The copper(II) ions are symbolized by grey balls.

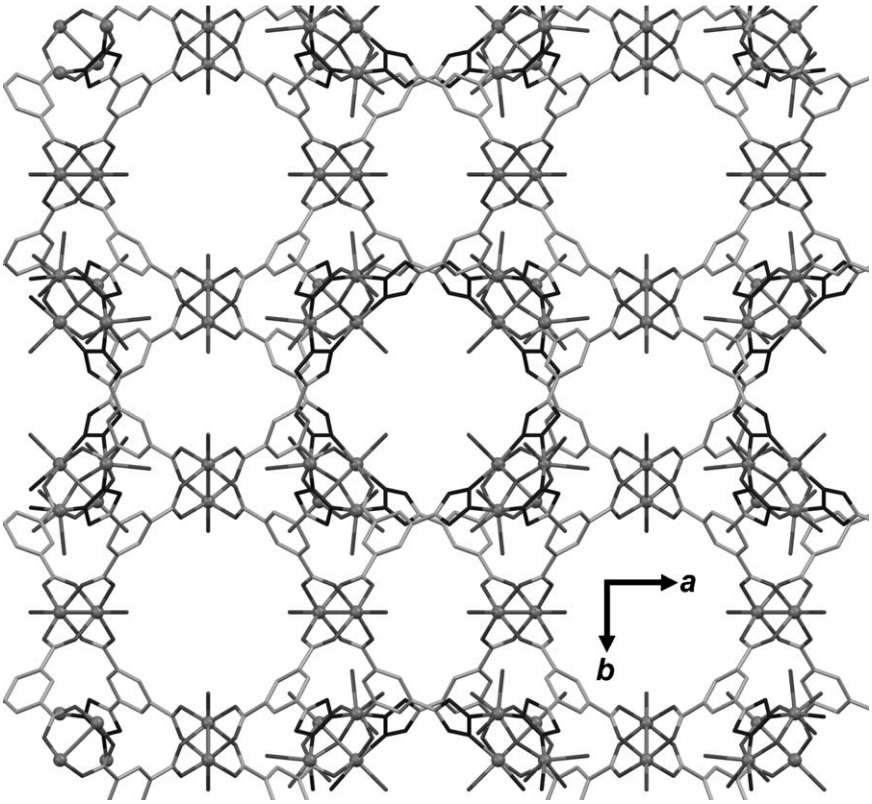

Fig. 19. Crystal packing of $[Cu_6O(\mathbf{L187})_3(H_2O)_9(NO_3)]_n \cdot 15nH_2O$ showing infinite 1D channels along the crystallographic *c* axis [53]. Hydrogen atoms, nitrate anions and solvate guest molecules are omitted for clarity. The copper(II) ions are symbolized by grey balls.

metals is significantly reduced in dinuclear systems with monosubstituted ligands with respect to the group of compounds reviewed above, involving disubstituted triazole rings. For example, the coupling featured by the complex $[Cu_2(\mathbf{L69})_2(mim)_2(NO_3)_2(H_2O)_2]$ is $J = -47\,cm^{-1}$ [80]. This has been attributed to a significant distortion to the symmetry of the [M–(N–N)$_2$–M] core resulting from the fact that each bridging ligand only chelates one of the metals, instead of both [80]. The nickel complex also exhibits antiferromagnetic interactions. A pioneering study of the dependence of the magnetic properties with external pressure was carried out on this complex, showing that the strength of the coupling increases with pressure until the latter reaches 8 Kbar, where it starts to decrease again [82]. Other 2-pyridyl substituted ligands are **L204**, **L205** and **L206**, which have lead to the related complexes $[Cu_2(\mathbf{L204})Cl_4]$ [83], $[Cu_2Cl_4(\mathbf{L205})_2]$ [83], and $[Cu_2(\mathbf{L206})_2Cl_4]$ [84]. Some tetrazole ligands also exhibit one coordinating substituent, thereby exhibiting the capacity of bridging two metals while chelating one of them. Two of the resulting dinuclear complexes are $[Cu_2(\mathbf{HL163})_2(N_3)_2(bpy)_2]$ [85] and $[Ni_2(\mathbf{L52})_2(NH_3)_6]$ [86]. The latter has been prepared in the context of an investigation of the coordination chemistry of a relatively unexplored family of ligands; organic nitramines, called by the authors "energetic" because of their capacity to undergo exothermic, autocatalytic thermal decomposition. Dinuclear complexes with a planar [M–(N–N)$_2$–M] core may be formed with bridging tri- or tetrazole ligands with no additional coordinating groups. Examples of these are $[Cu_2(\mathbf{L116})_4(bpy)_2]$ [87], $[Co_2(\mathbf{L32})_2Cl_4]$ [88], $[Cu_2(\mathbf{L38})_4](ClO_4)_2$ [89] or $[Cu_2(\mathbf{L21})_2(ox)_2(H_2O)_4]$ [90]. Particularly interesting is the series of dinuclear lanthanide complexes $[Yb_2(Cp)_4(\mathbf{L116})_2]$ (Fig. 29), $[Dy_2(Cp)_4(\mathbf{L116})_2]$ and $[Gd_2(Cp)_4(\mathbf{L116})_2]$ [91].

The three complexes feature two Ln(III) ions linked by two tetrazolate ligands in the very rare $\mu{:}\eta^2{:}\eta^1$ coordination mode. This binding mode is presumably facilitated by the fact that lanthanides establish longer bonds and larger coordination numbers than 3*d* metals. In addition to three nitrogen atoms from tetrazole, each metal binds to two η^5-methyl-cyclopentadienil ligands.

3.1.3. Dinuclear complexes with single [–N–N–] bridge

We have found two examples of dinuclear complexes exhibiting only one [–N–N–] bridge from tri- or tetrazole, and supported by other bridging ligands. One is $[Cu_2(\mathbf{L199})(SO_4)_2(H_2O)_4]$ [92], which is formed by the dinucleating ligand **L199**, with the metals further bridged by an SO_4^{2-} group, both ligands occupying equatorial positions. The other equatorial sites of the metals are filled by monodentate SO_4^{2-} and H_2O, respectively, while H_2O molecules occupy the axial sites to complete six and five coordination geometries, respectively. The other complex is $[Ni_2(L)_2(\mathbf{L103})](BPh_3)$[93] –and related derivatives–, where tetrazole completes a double thiophenolate bridge provided by a large macrocyclic ligand, L.

3.1.4. Dinuclear complexes with other bridges

Some dinuclear complexes involving tri- or tetrazoles exhibit other bridges than the ubiquitous N–N bridge. The most numerous type is that of complexes of two Cu(II) ions linked by two μ-Cl^- ligands, with 1,2,3-triazole ligands attached to metals in a monodentate fashion [54,94,95] (for example $[Cu_2(\mathbf{HL3})_4Cl_4]$) [96]. One exception is $[Mn_2(\mathbf{L206})_2(H_2O)_2Cl_4]$) [97], which features Mn(II) as metal. In these complexes, the triazole ligands are not conditioning the nuclearity of the complex, and their position could be occupied by any other terminal ligand (there are hundreds of $[M(II)_2]$ complexes bridged by two Cl^- ions reported in the literature). This is also the case of other complexes with (end-to-end) μ-SCN^- bridges[98,99] (e.g. $[Cu_2(NCS)_4(\mathbf{L207})_4]$) [100] O^{2-} units $[Fe_2OCl_2(\mathbf{L208})_4](PF_6)_2$) [101], OH^- groups (e.g. $[Yb_2(OH)_2(\mathbf{L159})_4(H_2O)_4]$) [102], and

alkoxide[103] or phenoxide bridges (e.g. $[Cu_2(\mathbf{L102})_2(MeOH)_2]$) [104].

Only one structure of a dinuclear complex has been found with a 1,2,3-triazole, exhibiting a [–N–N–N–] bridge, *i.e.* $[Cu_2(tmbma)_2(\mathbf{L3})](NO_3)_3$ (tmbma = tris-(N-methylbenzimidazol-2-ylmethyl)amine [105]. In this complex, the link between both metals seems only supported by the triazole ring; however, the multicyclic ligands also forming part of the complex reinforce the bridge through the establishment of intramolecular π–π interactions (Fig. 30).

In the complex $[Ni_2(\mathbf{L209})(en)_4](ClO_4)_3$ (en = ethylenediamine) [106], a [–N–C–N–] bridge (typical of imidazolate ligands) is observed contributing to the bridging of two Ni(II) ions, which are kept together with the help of other donors included in the ligand **HL209**. A few other complexes exhibit two metals in the molecule, well separated by multi-topic ligands containing tetrazole and other donors. A good example is the family of the ligands represented by $[Mn_2(\mathbf{L210})_2(hfac)_4]$ (hfacH = hexafluoroacetylacetone), also prepared with Co, Ni and Cu (Fig. 31) [107]. The ligand **L210** is a triazole ring attached to an N-aminoxylphenyl radical. The radical center of each ligand is directly attached to one metal of the complex, with which it establishes a very strong antiferromagnetic interaction. This leads to two non-zero spin fragments that interact weakly with each other through the conjugated π system by means of a spin polarization mechanism.

3.2. Trinuclear complexes

As mentioned above, molecules containing three metals constitute the second largest group of discrete complexes in this review. These group into three structural types; (i) linear chains with triple $\mu_{1,2}$-bridges (from tri- or tetrazole), (ii) linear molecules exhibiting a double $\mu_{1,2}$-bridge and a monodentate bridging ligand between metals, (iii) hydroxo centered triangular complexes. Many of these were reviewed about ten years ago[6] for the case of 1,2,4-triazoles (to which correspond 95% of the examples).

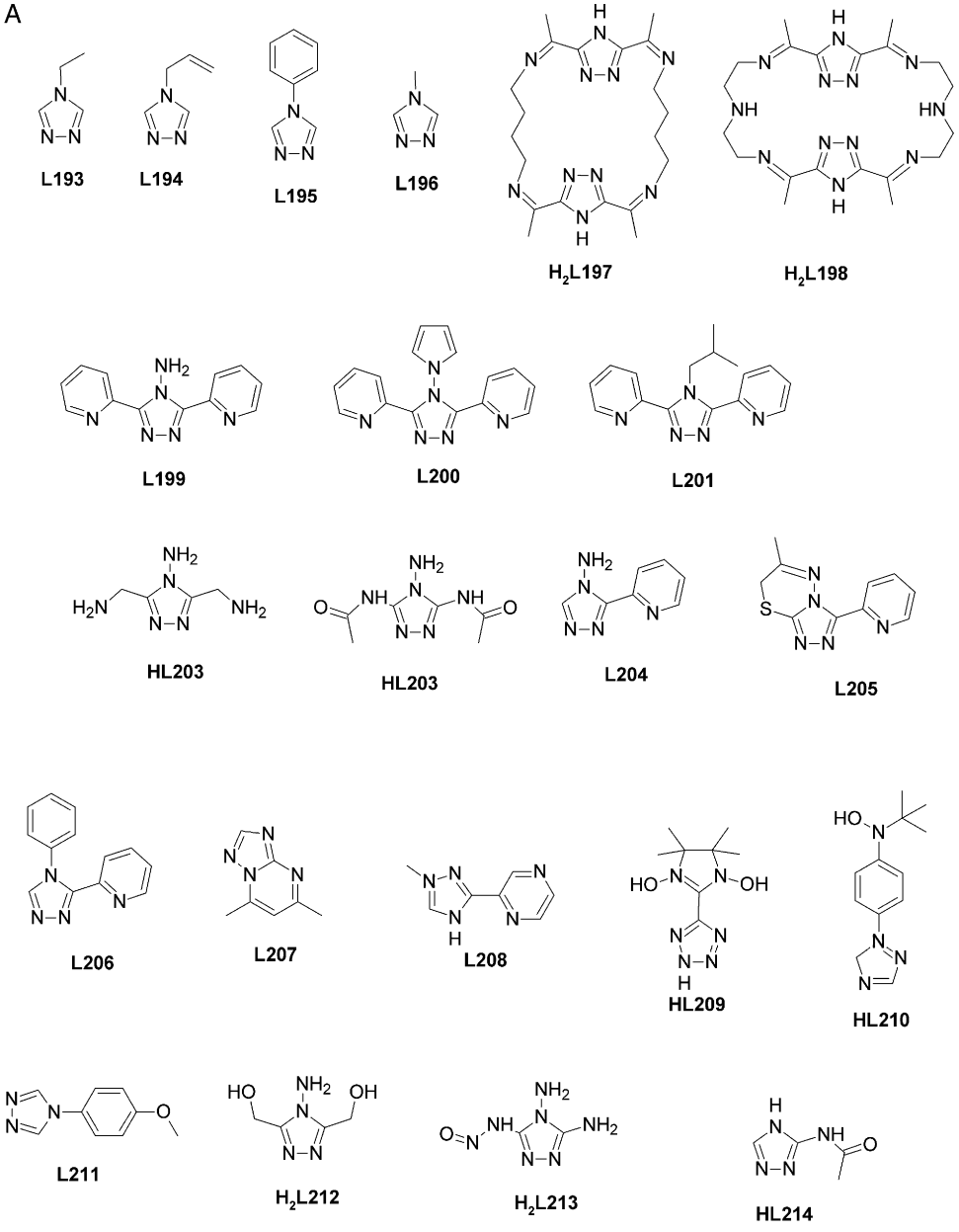

Fig. 20. List of triazole or tetrazole ligands (**L193**–**HL223**) used for the preparation of coordination complexes, not discussed in Section 2.

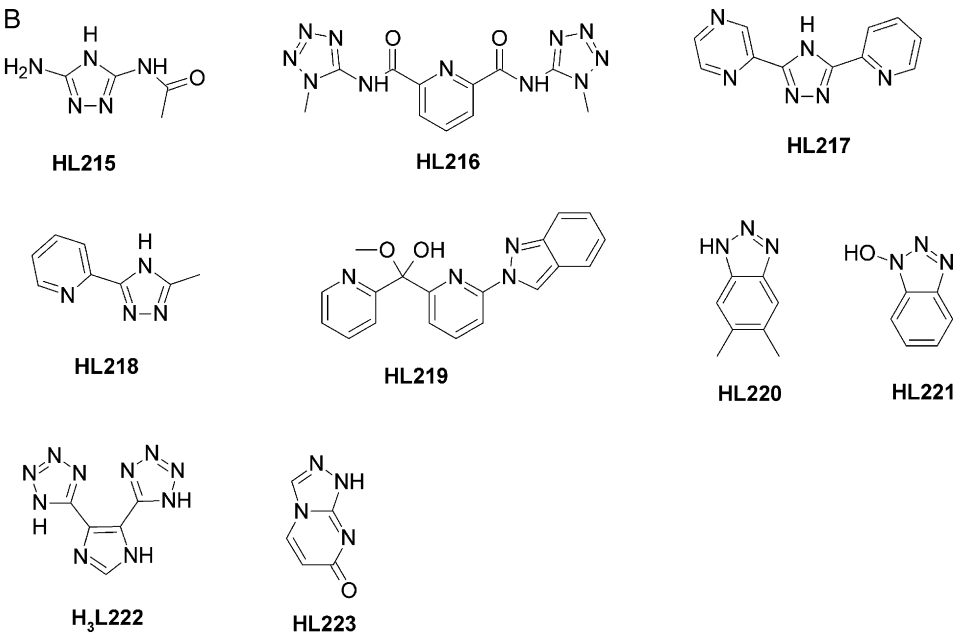

Fig. 20. (*Continued*).

3.2.1. Linear trinuclear complexes with triple [–N–N–] ($\mu_{1,2}$) bridges

There is a large list of crystallographically characterized complexes that contain the same linear trinuclear fragment as in the complex $[Ni_3(\mathbf{HL21})_6(H_2O)_6](NO_3)_6$ (Fig. 32) [108], involving the metals Cu, Co, Mn and Fe, in addition to Ni (the most frequent).

Complex $[Ni_3(\mathbf{HL21})_6(H_2O)_6](NO_3)_6$ was the first reported of any of the complexes reviewed in this manuscript and also, the simplest of the trinuclear chains of the type discussed in the current section. Its structural description will serve to characterize most aspects of the rest of the members of this family. This complex exhibits three octahedrally coordinated Ni(II) ions disposed along a perfect straight line (Ni–Ni–Ni angle of 180.0°), with pairs of adjacent metals linked by three 1,2,4-triazole rings through their [–N–N–] moiety. Within each pair, the three ligands are disposed in mutual angles of 120° in form of a paddlewheel, reproducing the topology of the [M–(N–N)$_3$–M] fragments featured by the related type of dinuclear complexes (see above and Fig. 22). Both paddlewheels present in the [Ni_3] complex are disposed in a staggered conformation, as required for steric reasons (see Fig. 32, right), which suits perfectly the octahedral geometry of the central metal in this assembly type. The external three coordination sites of each peripheral metal are occupied by molecules of water. The complex unit exhibits a total of six positive charges that are compensated by NO_3^- anions distributed within the lattice, primarily in between the sheets formed by the complexes. Each triad of ligands keeps the metals 3.737 Å apart, the distance between external Ni centers being thus exactly twice as long, *i.e.* 7.474 Å. At least seven other [Ni(II)$_3$] complexes with the same central core have been crystallographically characterized and reported since the first example was made. The differences between the various complexes lie mainly in the nature of the various substituents of the 1,2,4-triazole ligand, either on the '4*N*' position (for example, in the

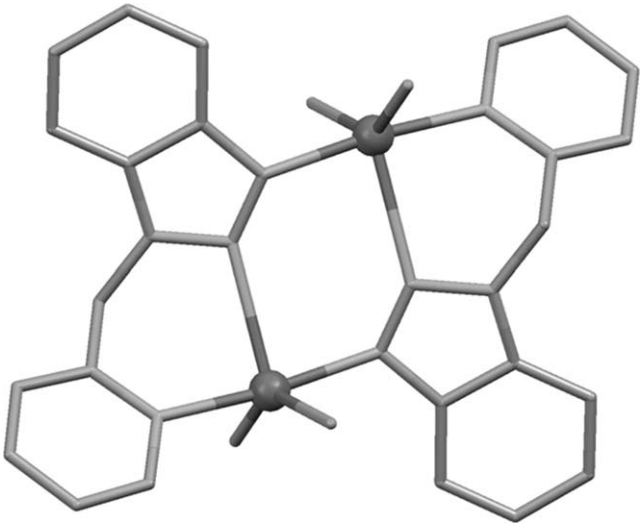

Fig. 21. Molecular representation of $[Cu_2(\mathbf{L7})_4Cl_4]$ [54]. Large balls are Cu ions, dark grey is Cl, medium grey is C and light grey is N. Hydrogen atoms not shown for clarity.

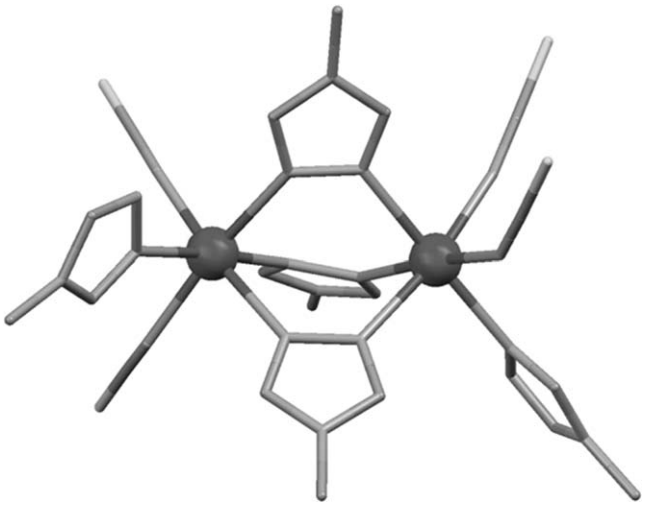

Fig. 22. Molecular representation of $[Mn_2(\mathbf{L196})_5(NCS)_4]$ [59]. Large balls are Mn ions, medium grey is C and S and light grey is N. Hydrogen atoms not shown for clarity.

Table 2
Metal ions coordinated by the 1,2,4-triazole-based ligands presented in Figs. 6, 8 and 10 to generate polymeric networks. See Table S2 for the names of the ligands.

Ligand	Metal [Refs.]
HL21	Ag [136,280,328], Cd [292,329–334], Cu [44,45,136,335–343], Eu [344], Pb [345], Co [346–349], Zn [44,212,214,215,231–241], Mo [350], Mn [351–354], Hg [355], Cu,Mo [356], Fe [354,357], Ni [354,358], Ag, Re [359], Ho [360]
HL22	Cu [136,361–364], Cd [365,366], Zn [366], Cu,Mo [367], Hg [368], Ag [369]
HL23	Cu [370]
HL24	Cu [136,361]
HL25	Cu [136]
HL26	Ag [371], Cu [136]
HL27	Ag [372]
HL28	Cu [129]
HL29	Zn [373–381], Cd [379,382,383], Co [377,384], Mn [385]
HL30	Zn [374,379,383,386,387], Cd [366,388–390], Mn [391], Ag [392], Cu [393,394], Cu,Mo [367]
L31	Cu [119,208,395–397], Cd [366,397], Ni [397], Co [397], Zn [397], Mn [398,399]
L32	Cd [365], Ag [400,401], Cu [120,339,402]
L33	Cd [365], Cu,Mo [367]
L34	Cu,Mo [367]
L35	Cd [403]
L36	Ni [404]
L37	Cd [405]
L38	Cu [406]
L39	Cu [406]
L40	Cd [407–409], Fe [229,230,232,240,410], Mn [411–414], Co [415], Cu [341,408,409,416,417], Cu,Cd [416], Cu,Hg [416]
HL41	Cu [418], Cd [404,419,420]
L42	Cu [421]
L43	Fe [422], Ag [423,424], Co [425], Sn [426], Cu [421]
L44	Mn [427]
L45	Co [428], Cu [429,430], Cd [430–432], Ni [433], Zn [430,432,433]
L46	Ni [434], Ag [434,435], Zn [431,436–439], Cu [440,441], Cd [431,442,443], Co [444–447], Mn [447,448], Cu,Mo [449,450], Cu,W [450]
L47	Cu [451], Co [452], Cd [453], Fe [454], Cu,W [455]
L48	Mn [456], Zn [457–459], Cd [458–462], Fe [454], Cu,W [450,455], Cu, Mo [449], Fe, W [463]
L49	Zn [464], Cu [465], Cd [464], Cu, W [455], Cu, Mo [449]
L50	Cd [464]
L51	Cu [46]
L52	Ni [466,467], Cd [468–472], Co [473–475], Cu [476–480], Ag [481,482], Zn [483], Pb [483], Cu, Mo [484], Ni, Mo [485]
L53	Mn [486], Cd [487,488]
L54	Zn [489], Cu [489]
L55	Cu [490], Ag [490], Zn [490], Cd [490], Hg [490]
L56	Cu, Mo [491]
L57	Co [492]
L58	Ag [493], Cd [493], Zn [493], Co [494]
L59	Zn [495], Cd [495]
L60	Cu [496]
L61	Cu, Ru [497], Ag [498,499], Mn [500], Cu [500]
L62	Fe, Mn [501], Fe, Rh [502], Zn [503], Cu [504], Ag [505], Pb [506], Mn [507]
L63	Ag [508], Cd [509], Cu [402]
L64	Ag [508], Cu [49], Cd [509]
L65	Cd [510]
L66	Cd [327]
L67	Cu [511], Ag [512]
L68	Cd [513]
HL69	Ag [514]
L70	Ag [515]
L71	Cd [308]
HL72	Zn [516], Hg [516], Cu [516]
HL73	Cu [150]
L74	Zn [517]
HL75	Mn [518–520], Cu [69,137,521], Cu, V [522]
HL76	Cu [136]
HL77	Cu [136,523], Ag [524,525]
HL78	Cd [526]
L79	Cd [495], Ag [527], Ni [528]
L80	Ag [527]
L81	Cu [529]
HL82	Cu [207,209]
HL83	Cu [530]
H_3L84	Cu [531]
H2L85	Pb [532,533]
HL86	Ag [534], Cu [535], Gd [536], Nd [536]
HL87	Co [537], Zn [537]
H_5L88	Mn [538], Cu [538], Co [538], Ni [538]
H_3L89	Cu [539], Mn [540], Zn [541]
L90	Cu [542]
HL91	Ag [543]
L92	Ag [508], Zn [544,545], Cd [545,546], Cu [547,548]
L93	Cu [549–552], Fe [553], Ag [554], Cd [555], Rh [556], Zn [557,558]
L94	Zn [559], Mn [559], Cd [559], Ag [559]
L95	Cu [560]
L96	Cd [537], Cu [537]
HL97	Mn [561], Zn [561], Cu [561], Cd [561], Ag [561]
H_2L98	Cu [65]
HL99	Cu [562], Cd [563]
HL100	Zn [564], Fe [564], Co [564,565], Cu [564], Ni [564], Mn [564], Cd [563,566]
HL101	Zn [567], Mn [567], Cd [563]
HL102	Zn [568–572], Ni, Mo [467,572], Cu [569,570,572–576], Ag [577], Ni [578], Co, Mo [579], Zn, Mo [579,580], Cu, Mo [104,579,581,582], Ag, Mo [579,580], Mn [569], Fe [569,575], Co [569,570], Cd [569,570], Co, W [580], Ni, W [580], Cu, W [582]

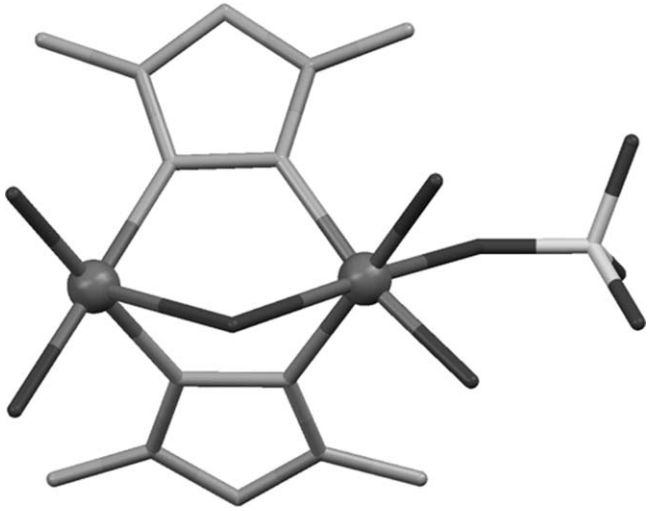

Fig. 23. Molecular representation of the cation of $[Cu_2(\mathbf{HL30})_2(SO_4)(H_2O)_5](SO_4)$ [61]. Large balls are Cu ions, dark grey is O, medium grey is C and Cl and light grey is N. Hydrogen atoms not shown for clarity.

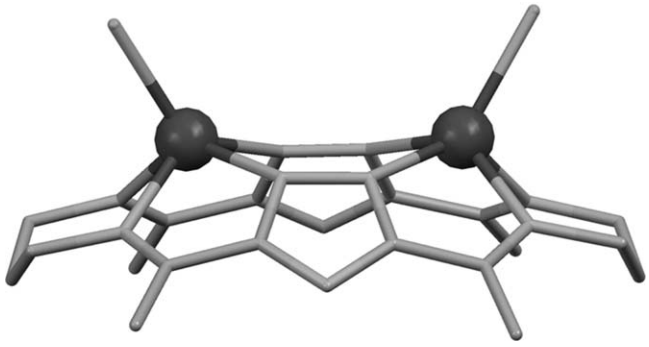

Fig. 24. Molecular representation of $[Co_2(\mathbf{L98})Cl_2]$ [64]. Large balls are Co ions, dark grey is Cl, medium grey is C and light grey is N. Hydrogen atoms not shown for clarity.

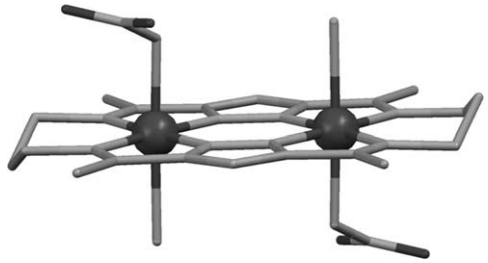

Fig. 25. Molecular representation of $[Co_2(\mathbf{L98})Cl_2(CH_2NO_2)_2]$ [64]. Large balls are Co ions, dark grey is Cl and O, medium grey is C and light grey is N. Hydrogen atoms not shown for clarity.

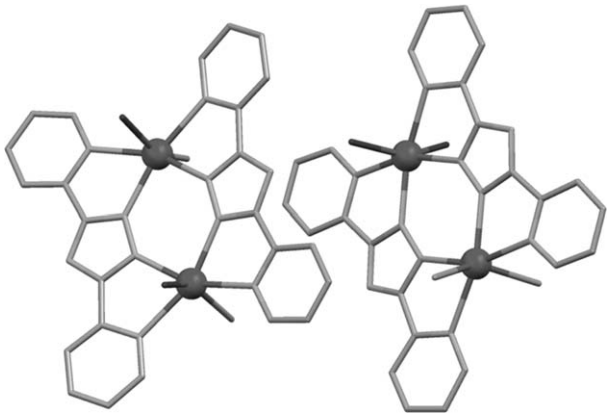

Fig. 26. Molecular representation of both isomers of the compound $[Mn_2(\mathbf{L75})_2Cl_2(H_2O)_2]$ [69]. Large balls are Mn ions, dark grey is Cl and O, medium grey is C and light grey is N. Hydrogen atoms not shown for clarity.

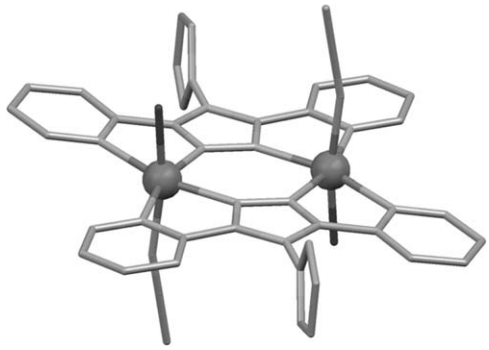

Fig. 27. Molecular representation of the cation of $[Fe_2(\mathbf{L200})_2(H_2O)_2(MeCN)_2](BF_4)_4$ [74,75]. Large balls are Fe ions, dark grey is O, medium grey is C and light grey is N. Hydrogen atoms not shown for clarity.

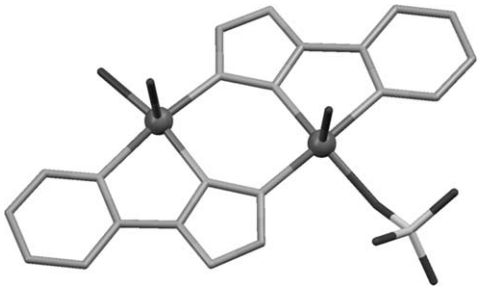

Fig. 28. Molecular representation of $[Cu_2(\mathbf{L69})_2(H_2O)_3(SO_4)]$ [81]. Large balls are Cu ions, dark grey is O, medium grey is S and C and light grey is N. Hydrogen atoms not shown for clarity.

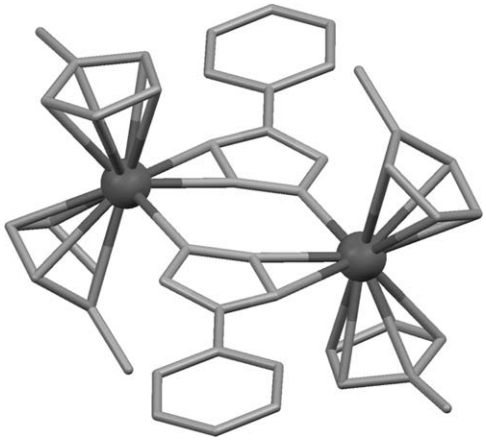

Fig. 29. Molecular representation of $[Yb_2(Cp)_4(\mathbf{L116})_2]$ [91]. Large balls are Yb ions, medium grey is C and light grey is N. Hydrogen atoms not shown for clarity.

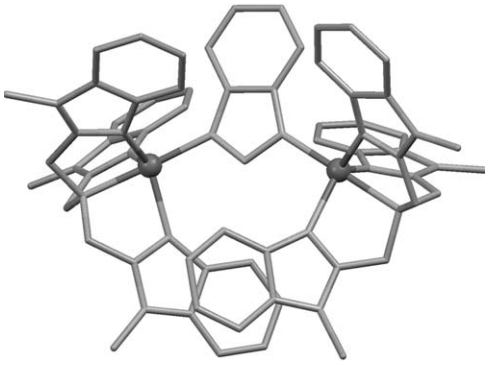

Fig. 30. Molecular representation of $[Cu_2(tmbma)_2(\mathbf{L3})](NO_3)_3$ [105]. Large balls are Cu ions, medium grey is C and light grey is N. Hydrogen atoms not shown for clarity.

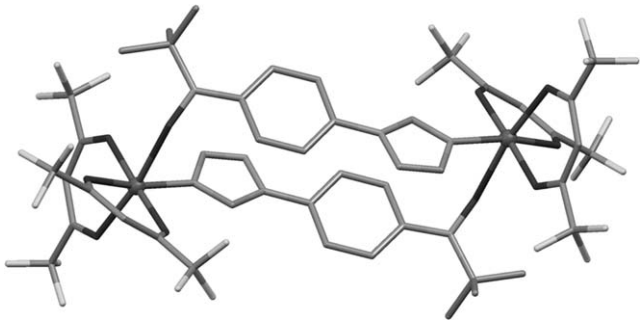

Fig. 31. Molecular representation of $[Cu_2(\mathbf{L210})_2(hfac)_4]$ [107]. Large balls are Cu ions, dark grey is O and F, medium grey is C and light grey is N. Hydrogen atoms not shown for clarity.

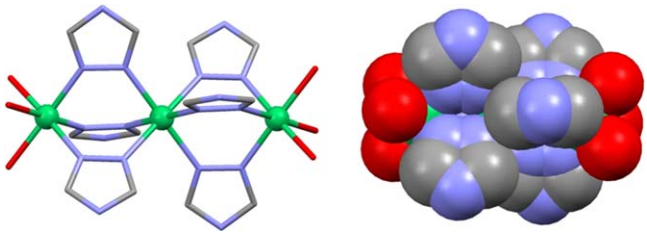

Fig. 32. (left) Molecular representation of $[Ni_3(\mathbf{HL21})_6(H_2O)_6](NO_3)_6$ [108]. Green balls are Ni ions, blue is N, red is O and grey is C. (right) Space-filling diagram of the same complex, using the same code for colors. Hydrogen atoms not shown for clarity.

Table 3
Metal ions coordinated by the tetrazole-based ligands presented in Figs. 13, 15 and 17 to generate polymeric coordination networks. See Table S3 for the names of the ligands.

Ligand	Metal [Refs.]
HL103	Ag [51,583], Cu [584–586], Cd [586,587], Zn [588]
HL104	Cu [585,589–593], Ag [585,594], Cd [595,596], Co [597]
L105	Cu [598–600], Cd [601]
HL106	Ag [594]
L107	Cu [602–604]
HL108	Ag [585]
L109	Cu [605,606], Co [607]
HL110	Zn [608]
L111	Cu [602]
L112	Cu [609]
L113	Cu [610]
L114	Cu [611]
L115	Co [612]
HL116	Cu [339], Zn [613], Ag [614,615]
HL117	Sn [616]
HL118	Zn [588]
L119	Cu [617]
HL120	Zn [618]
HL121	Zn [619]
HL122	Hg [620]
L123	Cu [621]
L124	Zn [622]
H_2L125	Zn[623]
L126	Fe [264], Cu [624,625], Zn [271], Cd [626], Ni [625,626], Co [627–629]
L127	Fe [266]
L128	Fe [267], Zn [630,631]
L129	Cu [632]
L130	Cu [272,633], Zn [272], Fe [244,270]
L131	Fe [275], Cu [273,624,626], Tl [634], Cd [626], Ni [626], Co [626,629]
H_2L132	Sn [635]
L133	Co [627]
H_2L134	Sn [636]
H_2L135	Sn [637]
H_2L136	Zn [638], Cd [638], Cu [639]
H_2L137	Cd [640], Zn [52], Mn [52], Cu [46,52]
H_2L138	Zn [641]
H_3L139	Zn [642–645], Cd [643,644], Cu [646,647], Mn [644,647–649], Er [650], Gd [650], Yb [650], Dy [650], Eu [650], Pr [650], Tb [650]
H_4L140	Sr [651]
H_2L141	Pb [50], Mn [652]
L142	Cu [653]
L143	Zn [654]
L144	Co [177], Zn [177], Cd [177], Ni [507]
H_3L145	Mn [655], Sn [635]
H_3L146	Mn [656]
H_4L147	Cu [657]
HL148	Zn [631,658], Cd [587]
L149	Ag [659]
L150	Ag [659]
L151	Cu [660]
HL152	Hg [661], Sr [662]
L153	Cu [663], Ag [664], Sr [662]
HL154	Co [665]
HL155	Cu [666]
HL156	Cu [592]
HL157	Cd [667], Zn [668]
HL158	Cd [669], Zn [613]
HL159	Cu [670], Pb [671]
HL160	Ag [585,672], Zn [673], Cd [673,674], Zn [675], Cu [674], Co [676], Mn [676]
HL161	Cu [658,677–679], Cd [680], Sn [681], Zn [673,675,682], Ag [615]
HL162	Zn [683], Ni [684,685], Co [686], Fe [686], Cd [687–689], Zn [690], Cu [691]
HL163	Cd [692], Ag [692], Hg [693]
HL164	Zn [694]
HL165	Zn [695,696]
HL166	Co [697]
L167	Cu [698]
HL168	Co [665]
L169	Cu [699]
L170	Cu [700]
HL171	Mn [701], Co [702]
H_2L172	Zn [703]
H_2L173	Zn [613]
H_2L174	Cd [704]
L175	Zn [705]
HL176	Fe [243]
L177	Cu [706]
L178	Cu [707]
H_3L179	Zn [708]
H_2L180	Zn [709]
H_2L181	Co [710], Mn [710]
H_2L182	Mn [711]
HL183	Fe [279], Cu [712,713], Ag [713], Cd [714], Mn [714], Zn [714], Co [714]
H_2L184	Zn [715], Cd [716,717]
H_2L185	Zn [718]
H_2L186	Cd [719,720], Zn [720–722], Mn [723], Co [724]
H_3L187	Cu [53], Gd [725]
HL188	Cd,[726], Pb [727], Cu [728]
H_2L189	Cd [729], Zn [729]
H_2L190	Cd [730]
H_2L191	Cd [678], Pb [727], Mn [731]
L192	Cu [732]

complex $[Ni_3(\mathbf{HL72})_6(H_2O)_6](BF_4)_6$) [109], on the sites '3,5' of the ring (like in the compound $[Ni_3(\mathbf{HL22})_6(H_2O)_6](SO_4)_3$) [62], or both (see for example $[Ni_3(\mathbf{L32})_6(H_2O)_6]Cl_6$) [110]. If the counter ions are coordinating, these might be found occupying external positions on the end metals instead of being in the crystal lattice (e.g. $[Ni_3(\mathbf{HL30})_6(NCS)_6]$) [111]. The reasons governing whether a trinuclear or the related dinuclear complex (see above) is the species isolated from a given reaction might have to do primarily with solubility issues. Interestingly, the nuclearity of three seems to be the upper limit in length for this category of discrete chains. The magnetic behaviour of some of the reported [Ni(II)$_3$] complexes has been investigated [110,111]. In all cases, weak antiferromagnetic interactions between adjacent Ni ions have been determined, with coupling constants J ranging from $-7.9\,cm^{-1}$ to $-23\,cm^{-1}$. The differences have not been discussed in depth, although it is clear that the electronic properties of the groups attached to the triazole rings influence the extent of the coupling, presumably through modification of the energy of the orbitals that interact with the magnetic orbitals of the metals. An exceptional complex, related to this family of trinuclear compounds is $[Ni_3(\mathbf{L3})_6(NH_3)_6]$ [112], where the bridging ligands are 1,2,3-benzotriazolate groups in the $\mu_{1,2}$ coordination mode (Fig. 33).

From the above description, it is clear that it will be possible to reach this architecture with any of the metals usually found in octahedral geometry (at least divalent). Complexes made of cobalt are especially frequent. A review from 2003 was devoted, in part, to summarize the synthesis, structure and magnetic properties of these and their related dinuclear analogues [60]. The earliest reported example was $[Co_3(\mathbf{L35})_8(NCS)_4](SCN)_2$ [113], which was also the first trinuclear Co(II) complex to be analyzed for its magnetic properties. Given the strong influence of the spin–orbit coupling in this ion, only the low temperature region (<40 K) of the variable temperature susceptibility curve was simulated, by considering isotropic metal ions with only the lowest $S = 1/2$ Kramers' doublets populated. This model provided a coupling constant of $J = -9.0\,cm^{-1}$ and a large g value as a consequence of the anisotropy of the metals, otherwise not included in the model ($g = 4.5$). Similar values have been found for related [Co(II)$_3$] complexes when using this magnetic model [114]. More recently, the bulk magnetization of the analogue $[Co_3(\mathbf{L63})_6(H_2O)_6](NO_3)_6$[115] was modeled for a larger temperature range (2–250 K) using an isotropic model where the Co(II) centers were considered to carry

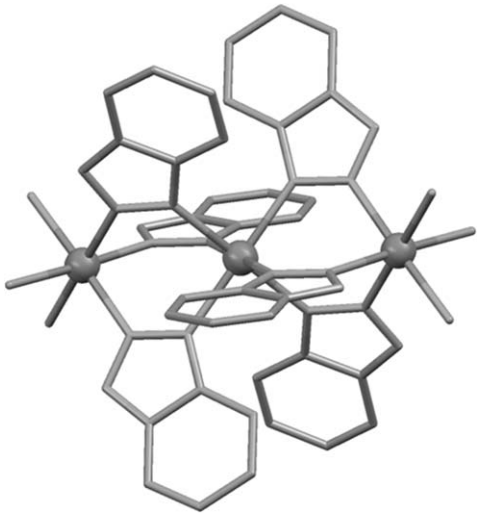

Fig. 33. Molecular representation of $[Ni_3(\mathbf{L3})_6(NH_3)_6]$ [112]. Large balls are Ni ions, medium grey is C and light grey is N. Hydrogen atoms not shown for clarity.

$S = 3/2$ spin magnetic moments. This fit provided the parameters $J = -10.54\,cm^{-1}$ and $g = 2.02$. A quite peculiar cobalt complex of this family involves metals in two different oxidation states. Thus, the metal centers in $[Co_3(\mathbf{L30})_4(\mathbf{HL30})_2(H_2O)_6]Cl_3$ [116] were identified as Co(III) (central position) and Co(II) (at both ends). This could be corroborated crystallographically (with the bond distances to Co(III) ≈5% shorter than for the more reduced centers), by means of UV–vis and EPR spectroscopy and through bulk magnetization measurements. The first related trinuclear complex made of Mn, $[Mn_3(\mathbf{L193})_9(H_2O)_3](Tf)_6$ (HTf = triflic acid) [117], which exhibits an almost negligible magnetic interaction between adjacent metals ($J = -0.6\,cm^{-1}$), was modelled using both, variable temperature magnetic susceptibility and isothermal magnetization measurements. Interestingly, the analogous complex $[Mn_3(\mathbf{HL72})_6(H_2O)_6](ClO_4)_6$, reported much more recently, displays almost exactly the same (lack of) intensity of magnetic exchange ($J = -0.65\,cm^{-1}$) [109]. The few trinuclear complexes of the kind discussed here featuring copper as metal show quite a high degree of versatility. The complex $[Cu_3(\mathbf{L63})_8(H_2O)_4](NO_3)_6$ [118] contains Cu(II) ions exhibiting the rarely found compressed Jahn–Teller distortion. Thus the axial (compressed) bond distances to Cu(II) range from 1.973 to 2.030 Å, whereas the (long) equatorial distances span the 2.178–2.195 Å range. Surprisingly, the almost exact same complex $[Cu_3(\mathbf{L63})_{10}(H_2O)_2](ClO_4)_6$ [119] exhibits Jahn–Teller elongated Cu(II) ions (with ranges from 1.995 to 2.043 Å and 2.275 to 2.535 Å for equatorial and axially elongated bonds, respectively). It is interesting to note that these two complexes share the same core. The only differences are the nature of the (non coordinated) counter anions and one terminal ligand on each metal (terminal triazole versus water). It might be expected that, these disparate types of Jahn–Teller distortion lead to differences on the magnetic exchange between metals, since the shape and orientation of the magnetic orbitals differ completely from one geometry to the other. This is indeed the case, with J values of -23.6 and $-5.41\,cm^{-1}$ for the first and second complex, respectively. A mixed valence trinuclear complex with copper has also been reported; $[Cu_3(\mathbf{L32})_6(NCS)_2](ClO_4)_2$ (Fig. 34) [120]. The core of this complex is the same as all the linear $[M_3]$ chains described above, with the difference that the end metals (Cu^I) only feature one terminal ligand, thus exhibiting tetrahedral coordination geometry.

The above complex is prepared using exactly the same procedure that leads to a $[Cu(II)_3]$ complex of the same ligand with a triangular structure. Paradoxically, the method for obtaining either one or the other was not explained by the authors of the manuscript where these compounds were reported [120]. There are also a few complexes with the chain trinuclear structure made of iron(II). One example is $[Fe_3(\mathbf{L211})_6(H_2O)_6](Tos)_6$ (HTos = paratoluensulfonic acid), which was reported together with its BF_4^- analogue [121]. The latter exhibits three high-spin Fe(II) centers in the whole range of temperatures examined (2–335 K), with antiferromagnetic coupling between the central ion and the external centers ($J = -11.4\,cm^{-1}$). Interestingly, changing just the (non coordinated) counter ion from BF_4^- to Tos^- causes the central ion to undergo thermal spin transition. This remarkable effect is attributed to the change in the dihedral angle between the aromatic cycles of the ligand **L211**, which has an electronic influence on the coordination environment around the Fe(II) ions, so as to change the spin state of the central metal. Other related $[Fe(II)_3]$ complexes show also spin transition and are discussed more in detail in Section 4 of this review.

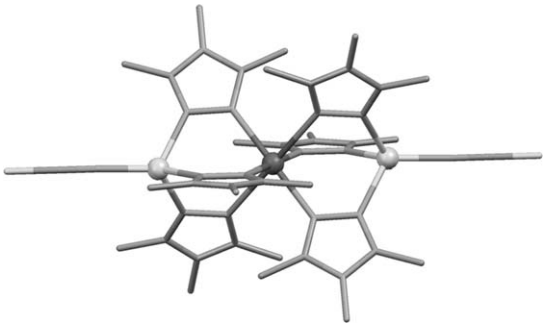

Fig. 34. Molecular representation of $[Cu_3(\mathbf{L32})_6(NCS)_2](ClO_4)_2$ [120]. Dark balls are Cu(II) ions, light balls are Cu(I) ions, medium grey is S and C and light grey is N. Hydrogen atoms not shown for clarity.

3.2.2. Linear trinuclear complexes with double [–N–N–] and a mono-atomic bridge

There is another well established family of complexes formed by three metals disposed linearly, bridged pairwise by only two 1,2,4-triazole rings in the $\mu_{1,2}$-mode, together with one bridging atom from another ligand (F^-, Cl^-, NCS^-, and OH^-). Of these, the complexes of Cu(II) constitute a representative group. Within that group, it has been observed that the intramolecular Cu···Cu coupling falls within two categories independently of the nature of the third bridging ligand; (i) couplings with J values near $-37\,cm^{-1}$, where both triazole bridges lie on equatorial positions of adjacent Cu(II) ions, such as in the complex $[Cu_3(\mathbf{HL30})_4(Cl)_2(H_2O)_4(SO_4)_2]$ (Fig. 35) [61], and (ii) couplings of approximately $J = -17\,cm^{-1}$, with one of the bridging triazole ligands binding to the apical site of one of the Cu(II) ions, like in $[Cu_3(\mathbf{H_2L212})_6Cl_4]Cl_2$ (Fig. 36, left) [122].

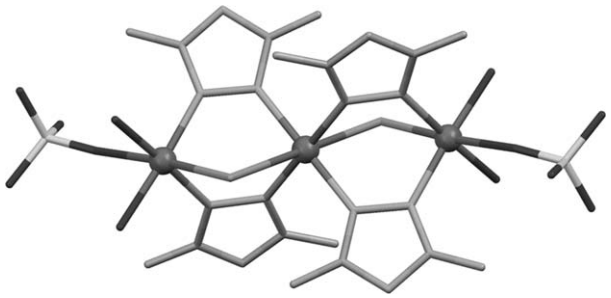

Fig. 35. Molecular representation of $[Cu_3(\mathbf{HL30})_4(Cl)_2(H_2O)_4(SO_4)_2]$ [61]. Large balls are Cu ions, dark grey is O and Cl, medium grey is S and C and light grey is N. Hydrogen atoms not shown for clarity.

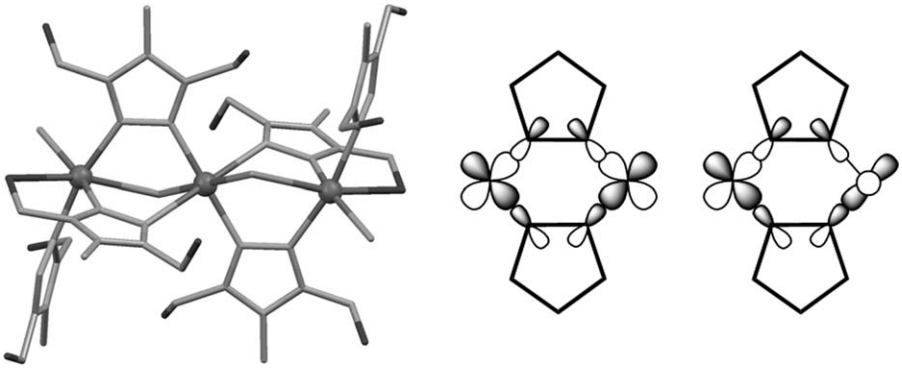

Fig. 36. (left) Molecular representation of $[Cu_3(\mathbf{H_2L212})_6Cl_4]Cl_2$ [122]. Large balls are Cu ions, dark grey is O and Cl, medium grey is C and light grey is N. Hydrogen atoms not shown for clarity. (right) Scheme of the overlap between the σ orbitals of 1,2,4-triazole ligands and the magnetic orbital ($d_{x^2-y^2}$) of Cu(II) when the former occupy all metal equatorial positions and when there is a bond to one metal apical position.

In complexes of the first kind, the magnetic orbitals of the metal ions ($d_{x^2-y^2}$) overlap directly with the σ orbitals of the triazole ligands that participate of the bond (see Fig. 36, right), thus allowing for a strong antiferromagnetic coupling [61,123]. If one of the Cu–N bonds to the bridging triazoles occurs on the metal's axial position, one of the coupling pathways is practically interrupted, since in that case the magnetic ($d_{x^2-y^2}$) orbital of that metal is oriented perpendicularly to that bond, and therefore does not overlap with the ligand's σ orbital (Fig. 36, right). The consequence is that the strength of the coupling is reduced significantly. There are also interesting complexes of this type involving other metals. The synthesis of $[Co_3(\mathbf{HL23})_6(NCS)_4F_2]$ [124], with F^- bridging ions, was preceded by the preparation of a very related complex $[Co_3(\mathbf{HL21})_6(NCS)_6]$ (not crystallographically characterized) [125], with SCN^- groups instead of F^- ions. The main synthetic difference was the addition of CoF_2 to the reaction system as part of the metal source, in the preparation of the fluoride analogue. Comparison between both compounds allowed establishing that the μ-F^- bridge facilitates stronger antiferromagnetic interactions than the μ-NCS^- pathway. The same trend was observed on the analogous pair of compounds with Ni(II), $[Ni_3(\mathbf{HL23})_6(NCS)_6(H_2O)]$ [125] and $[Ni_3(\mathbf{HL23})_6(NCS)_4F_2]$ (not crystallographically characterized) [125]. In this case, the modelling of the magnetic behaviour was more accurate than for the cobalt systems, since Ni(II) is not subject to the complicating effects of spin–orbit coupling, present in octahedral Co(II) ions. The trends observed with Ni(II) were much more pronounced; in the all SCN^- complex, a ferromagnetic Ni···Ni exchange coupling constant was observed ($J = +9.6\,cm^{-1}$), whereas for the fluoride-bridged system, an antiferromagnetic interaction was determined ($J = -11.1\,cm^{-1}$). This was ascribed to the sharper M–X–M angle in the former compound (105.5° versus an estimated value of 114.4°), together with the fact that more electronegative bridges tend to enhance the antiferromagnetic character of the coupling. The ferromagnetic character in $[Ni_3(\mathbf{HL23})_6(NCS)_6(H_2O)]$ could be corroborated with a very similar derivative, $[Ni_3(\mathbf{L32})_6(NCS)_6]$ [126], reported several years later ($J = +10.45\,cm^{-1}$).

3.2.3. Trinuclear complexes with a triangular geometry

The triangular complexes identified, relevant to this review, are of two types. The first is a series of hydroxide centered $[Cu(II)_3]$ complexes, always involving 1,2,4-triazole bridging ligands. Most of them exhibit octahedral or square pyramidal Cu(II) ions bridged pairwise through $\mu_{1,2}$-triazole groups, which bind to the metals on equatorial sites. The other two equatorial sites are occupied by the central μ_3-OH^- and by, either a terminal ligand or by another donor atom from the triazole ligand. A long list of compounds belong to the latter category, for example $[Cu_3(\mathbf{L213})_3(OH)(H_2O)_2](NO_3)_2$ [127], $[Cu_3(OH)(\mathbf{HL214})_3A(H_2O)_2]A$ ($A^- = CF_3SO_3^-$, NO_3^-, ClO_4^-; Fig. 37)[128] and $[Cu_3(OH)(\mathbf{HL215})_3(H_2O)_3](NO_3)_2$ [129].

Solvent molecules or anions usually occupy one or two axial positions of the metals. Originally, the ligand **HL214** had only produced mononuclear systems, in form of the bis-chelate. The key to synthesize the triangular system was the ability of this ligand to lose a proton and thus acquire the capacity to bind additional metals. These complexes constitute appropriate systems to investigate the magnetic phenomenon of geometrical spin frustration, since the Cu(II) ions are coupled antiferromagnetically. The magnetic properties of complex $[Cu_3(OH)(\mathbf{HL215})_3(H_2O)_3](NO_3)_2$ [129] were investigated in detail, and the data were modeled by introducing a term for the antisymmetric exchange to the spin Hamiltonian. The low temperature data, however could only by reproduced correctly by considering two different (and strongly antiferromagnetic) exchange constants within the triangle, and thus the lack of perfect trigonal symmetry. Values of $J = -156.4$ to $-191.0\,cm^{-1}$ were obtained. The triangular complex $[Cu_3(OH)(\mathbf{L33})_2(piv)_5(H_2O)]$ (Fig. 38)[130] is a singularity within this group of compounds. It is made from the corresponding triazole and the pivalate salt of Cu(II). This counter-ion is a much better ligand than the other ions employed as part of the metal salts; therefore, it has a drastic impact on the structure by acting as one of the bridging ligands between the Cu(II) ions, or by displacing one of the triazole groups from equatorial to axial positions.

The result is a highly asymmetric structure, where each copper ion displays a distinct coordination environment. In line with this

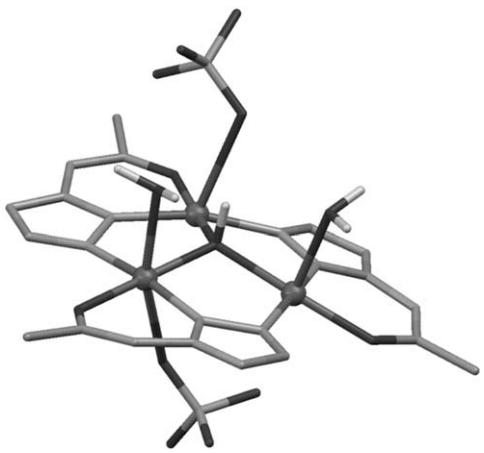

Fig. 37. Molecular representation of $[Cu_3(OH)(\mathbf{HL214})_3(ClO_4)(H_2O)_2](ClO_4)$ [128]. Large balls are Cu ions, dark grey is O, medium grey is Cl, H and C and light grey is N. Only hydrogen atoms (yellow) of H_2O or OH^- ligands are shown.

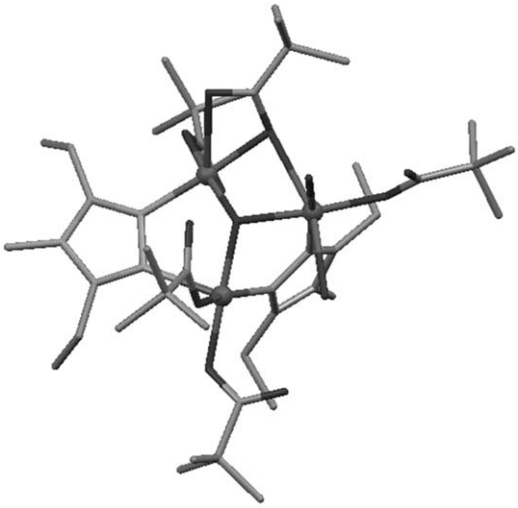

Fig. 38. Molecular representation of $[Cu_3(OH)(\mathbf{L33})_2(piv)_5(H_2O)]$ [130]. Large balls are Cu ions, dark grey is O, medium grey is C and light grey is N. Hydrogen atoms not shown for clarity.

structure, three different coupling constants were determined from modeling the variable-temperature bulk magnetization. The value involving [–N–N–] bridges *via* equatorial positions ($J = -55.6\ cm^{-1}$) is lower than the values observed for this pathway on the regular triangles. The reason is perhaps the highly distorted coordination geometries observed in this complex. The second type of triangular systems is a group of related $[Fe(III)_2M(II)]$ (M = Fe, Co, Ni, Cu) complexes with formula $[Fe_2MO(\mathbf{L216})_2]$ [131]. These heterovalent complexes are held together by the chelating and bridging capacity of three $\mathbf{L216}^{2-}$ ligands, each consisting of a central 2,6-diamidopyridine moiety and two external tetrazole groups. Thus, each metal is coordinated by the three atoms of the central pocket of one ligand and linked to the other two metals through two N-atoms of the tetrazole rings of that same ligand. As a result, each pair of metals exhibits a double [–N–C–N–] bridge. In addition, the metals are bridged by a central μ_3-O^{2-} group (Fig. 39).

The core of these complexes is equivalent to that of the well-known $[M_3O(O_2CR)_6L_3]$ basic carboxylate complexes (S = monodentate ligands, usually from solvents) [132], with the

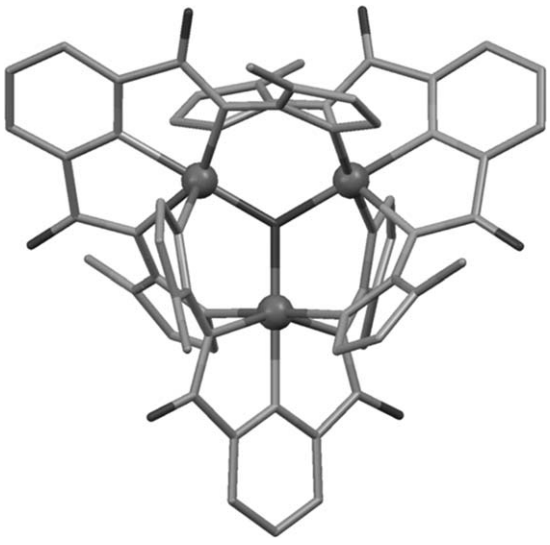

Fig. 39. Molecular representation of $[Fe_3O(\mathbf{L216})_2]$ [131]. Large balls are Fe ions, dark grey is O, medium grey is C and light grey is N. Hydrogen atoms not shown for clarity.

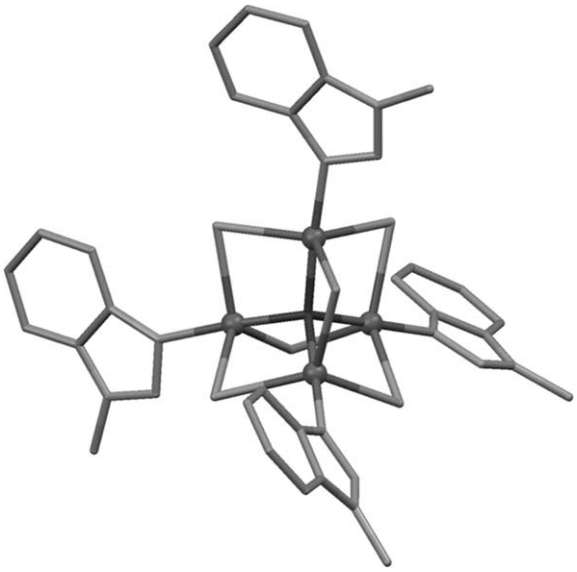

Fig. 40. Molecular representation of $[Cu_4OCl_6(\mathbf{L4})_4]$ [94]. Large balls are Cu ions, medium grey is Cl and C and light grey is N. Hydrogen atoms not shown for clarity.

advantage that all the peripheral bridging ligands bind now the three metals *via* five coordination bonds, the resulting structure being therefore much more robust. This has allowed for a very complete characterization of these complexes, especially in solution. One of the issues that have been evaluated in this manner is the important question of electron transfer. For example, in the all-iron complex, it has been established that the complex remains in a "partially valence-trapped" state up to room temperature. Another triangular complex related to both groups just described is $(NHEt_3)_2[Mn_3O(\mathbf{L3})_6F_3]$ [133]. It belongs to a series of high-nuclearity Mn(III) complexes made using MnF_3 as a source of this metal ion (see below). The complex anion contains an oxo-centered triangle of Mn(III) centers linked pairwise by double [–N–N–] bridges from $\mathbf{L3}^-$. The distorted, Jahn–Teller elongated coordination geometry is completed by one terminal F^- ligand on each metal (occupying equatorial positions).

3.3. Tetranuclear complexes

A structural search reveals a group of several complexes made of tri- or tetrazoles containing four metal atoms. These molecules occur mainly in form of tetrahedral, rectangular or "butterfly"-like topologies, in addition to other shapes, occasionally.

3.3.1. Tetrahedral complexes

Tetrahedral Cu(II) complexes with a central μ_4-O^{2-} ligand are extremely commonplace in the literature. Of these, the majority feature a $[Cu_4OX_6]$ ($X^- = Cl^-$, Br^-) neutral core while the trigonal–bipyramidal coordination geometry of each metal is completed with four terminal ligands on the axial positions. In relation with this review are the examples where these terminal ligands are monodentate 1,2,3-triazole molecules (such as in $[Cu_4OCl_6(\mathbf{L4})_4]$, Fig. 40) [94], or a terminal tetrazole ($[Cu_4OCl_6(\mathbf{L107})_4]$ [134].

The structural role played by the heterocycles in this type of complexes is clearly not very relevant. Beyond this group, one peculiar complex is $[Cu(\mathbf{HL217})(H_2O)]_4(NO_3)_4$ (Fig. 41) [135], which features the four metals at the vertices of an imaginary tetrahedron.

The formation of this complex was very surprising, since the ligand **HL217** (3-(pyridin-2-yl)-5-(pyrazin-2-yl)-1,2,4-triazole) is very similar to the symmetric ligand 3,5-bis-(pyridin-2-yl)-1,2,4-triazole (**HL75**), which generally leads to dinuclear Cu(II) complexes

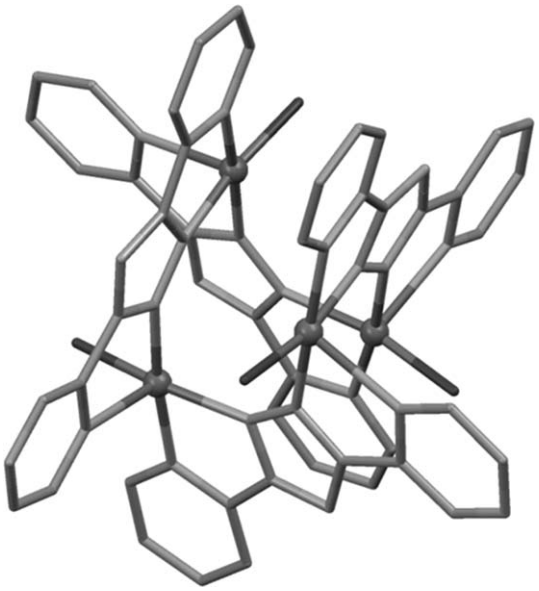

Fig. 41. Molecular representation of the cation of $[Cu(\mathbf{HL217})(H_2O)]_4(NO_3)_4$ [135]. Large balls are Cu ions, dark grey is O, medium grey is C and light grey is N. Hydrogen atoms not shown for clarity.

with two ligands bridging, chelating and "sandwiching" the metals (see above). In these adducts, the ligands occupy only the equatorial positions. By contrast, in the complex with **HL217**, the two chelating rings on each metal are in *cis* position; thus, both ligands are mutually perpendicular, each binding to a different second Cu(II) ion. In this manner, a cycle of four bridging ligands and four metals is formed with the ligands disposed as two pairs; within each pair, both are parallel and exhibit π–π stacking through one of their pyridine moieties, whereas in between pairs, the ligands are perpendicular to each other. A molecule of H_2O completes the square-pyramidal geometry around each Cu(II) ion (binding on an equatorial position). Preliminary investigations suggested antiferromagnetic interactions between the metals within the molecule.

3.3.2. Rectangular complexes

The few rectangular complexes reported are made of 1,2,4-triazole ligands and can be regarded as dimers of [–N–N–] bridged dinuclear units. In complexes $[Mn_4(H_3bpa)_2(\mathbf{HL69})_4(N_3)_2]$ (Fig. 42)[69] and $[Mn_4(H_3bpa)_2(\mathbf{HL218})_4(N_3)_2]$ [69] these units feature two Mn(II) ions bridged by two pyridyl-1,2,4-triazole ligands, which in turn are linked to each other by the polydentate ligand N,N′-bis(picolinamide)azine (H_4bpa), thereby conforming the rectangle [69].

All the ligands in these complexes are formed under solvothermal conditions from 2-pyridyl amidrazone and either manganese(II) formate or acetate in the presence of N_3^-. These studies helped to elucidate the mechanism of formation of pyridyl substituted 1,2,4-triazoles from 2-cyanopyridine and hydrazine in solvothermal conditions, either in the presence of metals or not. Magnetic susceptibility measurements on these complexes underscores the fact that the coupling between Mn(II) ions through $\mu_{1,2}$-triazoles is much weaker (of the order of $1\,cm^{-1}$) than for most Cu(II) systems. Complexes $[Cu_4(\mathbf{L75})_4(pic)_2]$ (Hpic = picolinic acid)[136] and $[Cu_4(\mathbf{L75})_4]$[137] can be regarded as two $[Cu_2]$ units held together by one $\mathbf{L75}^-$ ligand in the usual $\mu_{1,2}$ manner, and linked to each other by two additional $\mathbf{L75}^-$ ligands chelating the metals *via* their pyridine groups and $\mu_{1,4}$-triazole groups (thus adopting a *syn,anti* configuration with respect to the "N–N" moiety). In complex $[Cu_4(\mathbf{L75})_4(pic)_2]$, two metals are in the oxidation state +2 and the other two are monovalent. The octahedral coordination

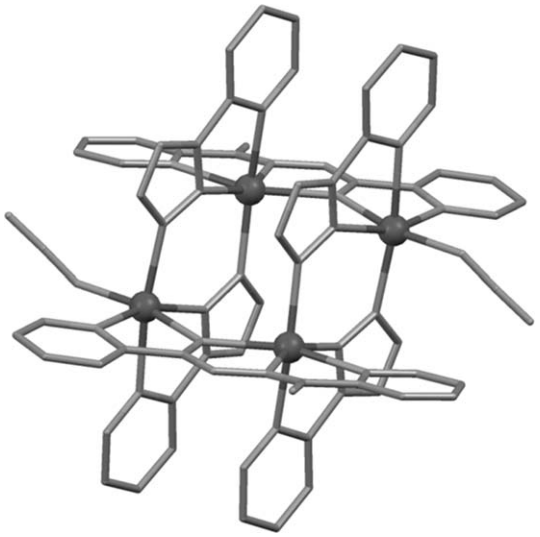

Fig. 42. Molecular representation of $[Mn_4(H_3bpa)_2(\mathbf{HL69})_4(N_3)_2]$ [69]. Large balls are Co ions, medium grey is C and light grey is N. Hydrogen atoms not shown for clarity.

geometry around the Cu(II) ions and the charges of the complex are completed through binding of one chelating picolinate ligand to each of them. Complex $[Cu_4(\mathbf{L75})_4]$ is made of four Cu(I) ions; thus, the four bridging and chelating $\mathbf{L75}^-$ ligands suffice to achieve a (distorted) tetrahedral coordination geometry, as preferred by this ion. Again, one of the important aspects in the formation of these complexes is the method of preparation; in both cases, the triazole is formed *in situ*, using 2-pyridylacetonitrile and ammonia as precursors and solvothermal conditions. The rectangular complex $[Cu_4(\mathbf{L30})_4(OH)_2(NO_3)(H_2O)_6](NO_3)$ [138] also exhibits two types of Cu···Cu bridges; one involves only the [–N–N–] moiety of a guanazole ligand (**HL30**), and the other one exhibits this motif together with a μ-OH^- bridge, all these ligands always occupying equatorial positions. In this complex, three of the Cu(II) ions are square-based pyramidal while the fourth one is square planar. The remaining equatorial sites (one per metal) are filled by water molecules, whereas the apical positions (three in total) are occupied by two molecules of H_2O and one NO_3^- ligand, respectively. The nickel(II) complex $[Ni_4(\mathbf{L199})_2(\mathbf{L199\text{-}H})(N_3)_5(AcO)_2]$ (Fig. 43)[71]

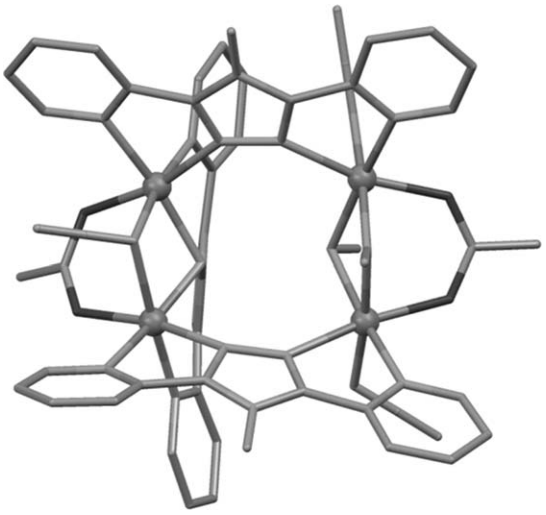

Fig. 43. Molecular representation of $[Ni_4(\mathbf{L199})_2(\mathbf{L199\text{-}H})(N_3)_5(AcO)_2]$ [71]. Large balls are Ni ions, dark grey is O, medium grey is C and light grey is N. Hydrogen atoms not shown for clarity.

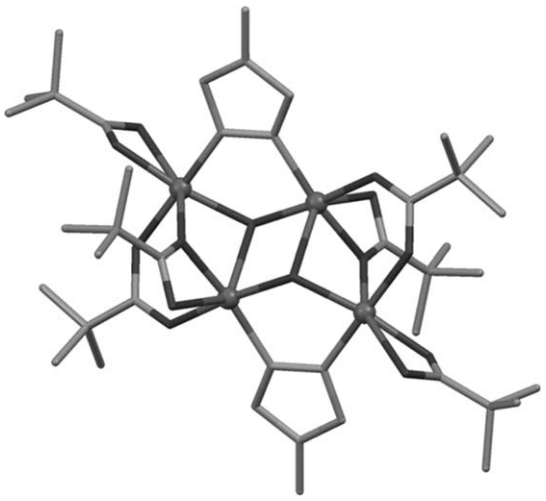

Fig. 44. Molecular representation of $[Cu_4(OH)_2(\mathbf{L31})_2(piv)_6]$ [130]. Large balls are Cu ions, dark grey is O, medium grey is C and light grey is N. Hydrogen atoms not shown for clarity.

exhibits an irregular rectangular structure. Two faces are virtually identical and feature Ni···Ni pairs connected through two 4-amino-3,5-bis(pyridin-2-yl)-1,2,4-triazole ligands in the $\mu_{1,2}$ mode, which also chelate the metals in the usual manner (see above).

The other two sides are unequal; one exhibits two end-on (EO) μ-N_3^- bridging ligands and one *syn,syn* bridging acetate, and the other side features one acetate, one azide and the deprotonated amine of one **L199** ligand, which also coordinates with its pyridyl groups to both metals, respectively. In fitting the magnetic data, these two sides were considered equal and were assigned weak ferromagnetic coupling ($J = 15.3\ cm^{-1}$), while the other two sides were attributed a coupling constant of $J = -2.2\ cm^{-1}$.

3.3.3. Other tetranuclear topologies

Among the structural types involving four metal ions can be found the so called "butterfly" arrangement. This organization consists of two fused oxo- or hydroxo-centred triangles, usually exhibiting additional bridging carboxylate ligands. The two central metal ions form the "body" of the butterfly and the remaining two external metals constitute the wings. The complexes[130] $[Cu_4(OH)_2(\mathbf{L31})_2(piv)_6]$ (Fig. 44), $[Cu_4(OH)_2(\mathbf{L35})_2(piv)_6]$ and $[Cu_4(OH)_2(\mathbf{L32})_6(piv)_4]^{2+}$ belong to this category.

The latter is in fact a complex cation that co-crystallizes with a dinuclear and dianionic complex. These three complexes exhibit bridging pivalate ligands, in addition to μ-triazolate ligands, which are a unique occurrence among "butterfly" type complexes. Both donors are also found as terminal ligands. The magnetic coupling within the first two complexes was very strongly antiferromagnetic (with J values in the -260 to $-216\ cm^{-1}$ range) and leading to ground states of $S = 0$. Such coupling occurs *via* the OH^- and triazolate bridges, linking the metals through equatorial positions (along which, lie the magnetic orbitals $d_{x^2-y^2}$).

A rare combination of alkoxide, pyridyl and triazole donors on one ligand affords the conditions for the assembly of a cubic complex, $[Cu_4(\mathbf{L219})_4](NO_3)_4$ [139], exhibiting the $[Cu_4O_4]$ core, which otherwise is extremely common in coordination chemistry. In this instance, the triazole cycle only acts as a terminal ligand, saturating one coordination site per metal. A very aesthetic cationic complex, exhibiting a centered triangular structure and formula $[Cu_4(\mathbf{L3})_3(PPh_3)_4]^+$ has been reported (Fig. 45) [140].

The core of this complex features a central ring with the sequence $(-Cu-N-N-N-)_3$, the strings of three adjacent N-atoms belonging to $\mu_{1,2,3}$-benzotriazole ligands. The mid N atoms of these are pointing towards the center of the complex and are bound to a Cu(I) ion. A PPh_3 ligand occupies the fourth coordination position on this metal to complete a tetrahedral coordination environment. The three peripheral Cu(I) ions are also bound to a PPh_3 ligand each, thereby reaching a coordination number of three. The shape of this molecular ion was described as a "reverse umbrella".

3.4. Pentanuclear complexes

The complex $[Cu_5(L)_2(\mathbf{L22})_2](ClO_4)_3$ contains two dinuclear units formed within a polyimine macrocyclic ligand (L) [141]. These units are linked by two 1,2,4-triazole ligands, each bound to both metals of one dinuclear $[Cu(I)_2]$ unit in the $\mu_{1,2}$-mode, and both attached through the 4N position to a central Cu(I) ion acting as a bridge. This complex and very close derivatives come about thanks to the formation *in situ* of the triazole bridges by the oxidative coupling of aliphatic nitriles catalyzed by the presence of the $[Cu_2]$ entities, with the concurrence of NH_3, presumably present after hydrolysis of part of the corresponding organonitrile. Besides this group of Cu aggregates, all the pentanuclear complexes in this review are made of benzotriazole (or one very close derivative in one instance) and exhibit a centered tetrahedral topology. With one exception (see below), these are regular or only slightly distorted tetrahedra. The core shared by most of these complexes is in Fig. 46, which shows six μ_3-$\mathbf{L3}^-$ ligands spanning the edges of the tetrahedron.

The earliest example is the mixed-valence complex $[Cu_5(\mathbf{L3})_6(tbi)_4]$ (tbi = *t*-butylisocyanide) [142] with a central Cu(II) ion exhibiting unusual compressed Jahn–Teller distortion, and four Cu(I) metals at the vertices of the tetrahedron. The latter are four coordinated, their tetrahedral geometry being completed by an isocyanide ligand bound through one C atom. The reaction involves partial aerobic oxidation of Cu(I) to Cu(II) and it does not proceed in the absence of air. Thus, Cu(II) is necessary for the formation of the assembly; the reduced metal would not be capable of occupying the central position, probably because of the crystal-field energy rather than for charge considerations. The tetrahedral structural motif in Fig. 46 is also stable with other metals and other oxidation states. For example, in complexes $[Co_5(\mathbf{L3})_6(NO_3)_4(H_2O)_4]$ and $[Ni_5(\mathbf{L3})_6(NO_3)_4(H_2O)_4]$ [143] the metals are all in the oxidation state +2. Coordination number six around the external M(II) ions is, in both cases completed with one bidentate NO_3^- ligand and one H_2O molecule per metal. The low coordinating ability of nitrate was exploited for the preparation of functional networks of the $[M_5]$ complexes by replacement of this ligand with bridging $TCNQ^{\cdot-}$ radicals (TCNQ = 7,7,8,8-tetracyano-*p*-quinodimethane), yielding 3D polymers with formula $[M_5(\mathbf{L3})_6(TCNQ)_4(H_2O)_4]_n$ [143]. Other complexes of this category are $[Cu_5(\mathbf{L3})_6(acac)_4]$ (Hacac = acetylacetone) [144], $[Cu_5(\mathbf{L3})_6(Hbtfam)_4]$ (Hbtfam = benzoyltrifluoroacetylmethane)[145] and $[Cu_5(\mathbf{L3})_6(trop)_4]$ (Htrop = tropolone) [145]. These three complexes are made of all Cu(II) and only differ on the nature of the chelating ligand that serves to complete the coordination number five around each metal. Several other derivatives have been made and characterized unambiguously, just by changing the terminal chelating ligands, without need of determining the molecular structure [145]. Interestingly, the central Cu(II) ion in these complexes, contrary to the mixed-valence complex (see above), exhibits Jahn–Teller elongation instead of compression. The overall magnetic coupling within the $[Cu^{II}_5]$ complexes was antiferromagnetic. Models discriminating between the central–apical interaction and the apex–apex exchange have been used to fit the data. The result is that the coupling is weak (with J values ranging from -6.5 to $-10\ cm^{-1}$). Another group of related complexes are $[Ni_5(\mathbf{L3})_5(acac)_4(OH)(H_2O)_4]$ [146], $[Ni_5(\mathbf{L220})_5(acac)_4(OH)(H_2O)_4]$ [147] and $[Cu_5(\mathbf{L3})_5Cl(PPh_3)_4]$

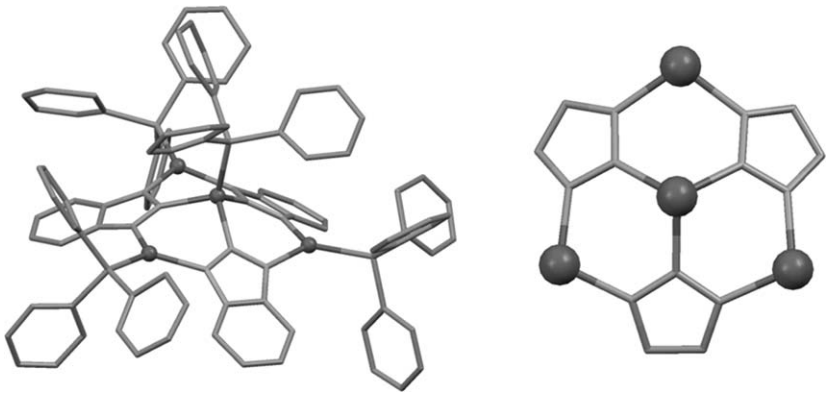

Fig. 45. (left) Molecular representation of the complex cation $[Cu_4(\mathbf{L3})_3(PPh_3)_4]^+$ [140]. Large balls are Cu ions, medium grey is P and C and light grey is N. Hydrogen atoms not shown for clarity. (right) Core of the same complex cation.

[148]. In these complexes, one of the sides of the tetrahedron is occupied by a monoatomic bridge (OH^- or Cl^-) instead of triazole. In the case of the Ni(II) complexes, this bridge originates from deprotonation of H_2O molecules by part of the $acac^-$ ligands used in the reaction, whereas for the copper complex, the authors of its preparation are not very clear about the origin of the Cl^- ligand, since the only source of this element in the reaction appears to be ClO_4^-. In any case, the formation of the asymmetric complexes could reflect the relaxation of structural strains present on the regular complexes, or an energy gain resulting from the bonds formed by the new bridging ligands.

The complex $[Fe_5O_2(OMe)_2Cl_5(\mathbf{L3})_4(\mathbf{HL3})(MeOH)_5]$ [149] is related to the family of pentanuclear compounds of this section, with significant differences. It consists of a centered tetrahedron, elongated by the insertion of a μ_3-O^{2-} ligand between the central metal and each of both pairs of apical Fe centers (Fig. 47). Besides these bridges, there is one $\mu_{1,2}$-$\mathbf{L3}^-$ connection between the central metal ion and each of the other metals, which completes the octahedral environment around the former. The pairs of metals on each side of the elongated tetrahedron are linked through their respective μ_3-O^{2-} ligands and one μ-OMe^- group. Five- or six coordination numbers around these metals are completed by terminal Cl^-, MeOH or **HL3** ligands. The magnetic coupling within this complex is dominated by the oxygen, monoatomic bridges. The central-apical interaction, occurring through wide Fe–O–Fe angles (near 129°) is reflected by an antiferromagnetic coupling constant of $J_1 = -7.3\ cm^{-1}$, while the apical pairs of metals, mediated by bridges with small Fe–O–Fe angles (<102°) exhibit ferromagnetic coupling, with $J_2 = +8.6\ cm^{-1}$. This yields a high-spin ground state of $S = 15/2$.

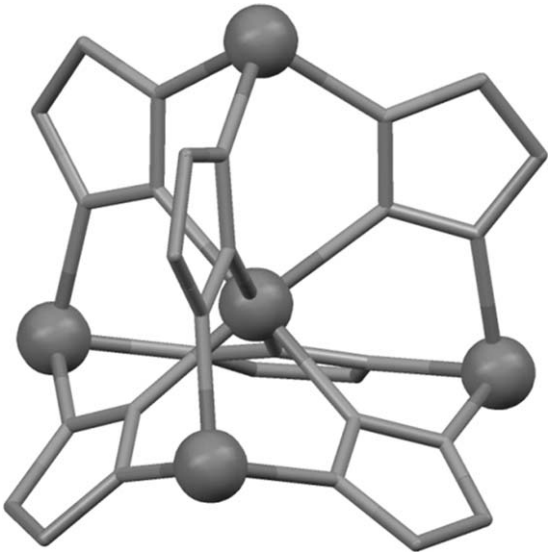

Fig. 46. Core, $[M_5(\mathbf{L3})_6]$ [141], of the family of centered tetrahedral complexes. Large balls are metal ions, medium grey is C and light grey is N. Hydrogen atoms not shown for clarity.

3.5. Higher nuclearities

3.5.1. Complexes with six to nine metals

The compound $[Cu_6Cl_{10}(OH)_2(\mathbf{HL73})_6(H_2O)_3]$ [150] is the only molecular complex with six metals found in the context of this compendium. Its molecular structure (Fig. 48) shows two hydroxo-centered triangles of distorted octahedral Cu(II) ions of the kind described above, linked by a μ_6-Cl^- ligand bound on axial positions of all the metals. Triazole ligands span each side of the triangles, bridging pairs of metals *via* the –N–N– fragment. The equatorial sites of the Cu(II) ions are occupied by terminal chloride ligands, whereas the six available axial positions are filled by three Cl^- ions and three H_2O molecules distributed statistically. The study of the magnetic properties in this complex reveals moderate antiferromagnetic interactions ($J = -17.1\ cm^{-1}$) along the edges of the triangles (through $\mu_{1,2}$-triazoles) and weak interactions between both triangles ($zJ = -2.3\ cm^{-1}$). This fit did not involve the inclusion of antisymmetric exchange terms to the Hamiltonian.

The nuclearity of seven is also represented only by one compound; $[Ni_7(OH)_2(acac)_8(\mathbf{L221})_4(H_2O)_2]$ [151]. This complex exhibits seven Ni(II) ions in form of a pentanuclear "undulated" string, linked laterally to two other metal ions (Fig. 49). There are three types of bridging ligands cementing the heptanuclear structure; two μ_3-OH^- groups, four $\mathbf{L221}^-$ ligands (two as 'μ_4' and two linking a pair of metals), and four $acac^-$ donors (two triply bridging and two μ-$acac^-$ moieties). In addition, there are four terminal (chelating) $acac^-$ ligands and two water molecules. Clearly, the additional oxygen donor of the $\mathbf{L221}^-$ ligand contributes to the complexity and higher nuclearity of this complex, as compared to the majority of complexes of 1,2,3-triazoles. A combination of ferro- and antiferromagnetic interactions leads to a total spin ground state of $S = 1$. The nature of the exchange interactions is justified in view of magnetostructural correlations, which postulate that the coupling is expected to be ferromagnetic for acute Ni–O–Ni angles and switch to antiferromagnetic for wider angles.

A beautiful representation of octanuclearity is the cage complex $(TBA)_{14}[Co_8(\mathbf{L222})_{12}]$ (TBA^+ = tetrabutylammonium, Fig. 50) [152]. The complex anion in this compound is a cubic arrangement of octahedral cobalt ions, each chelated by three ligands disposed along perpendicular directions. There are two metals in the oxidation

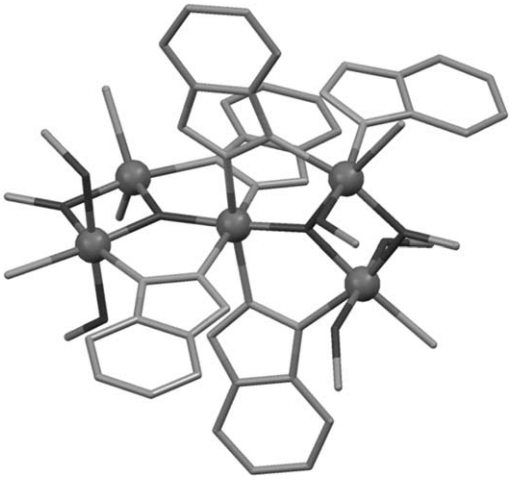

Fig. 47. (top) Molecular representation of $[Fe_5O_2(OMe)_2Cl_5(\mathbf{L3})_4(\mathbf{HL3})(MeOH)_5]$ [149]. Large balls are Fe ions, dark grey is O, medium grey is Cl and C and light grey is N. Hydrogen atoms not shown for clarity.

state +2, while the remaining metals are Co(III). This is reflected on a geometrical distortion of the cube and can be traced through magnetic susceptibility measurements. The other complexes with this nuclearity are also remarkable; these are the analogous compounds $[V_8O_4(\mathbf{L3})_8(piv)_4Cl_6]$ and $[V_8O_4(\mathbf{L3})_8(BzO)_4Cl_6]$ [153]. In fact, many of these all V(III) molecules were prepared, under solvothermal conditions, using various 1,2,3-triazole and carboxylate derivatives, with $[^nBu_4N]_3[V_2Cl_9]$ as starting material. Their structures (Fig. 51) feature one central oxo-bridged butterfly of four V(III) ions linked on each side to a further pair of metals *via* a total of eight μ_3-triazole ligands. Each of the external V_2 pairs exhibit two *syn,syn* carboxylate bridges. The strong ferromagnetic interactions exhibited by some V(III) complexes motivated attempts to prepare SMMs of this ion. In fact, the $[V_8]$ complexes exhibit $S = 4$ spin ground states, and some of the ferromagnetic coupling constants encountered are unusually strong (up to $J = +101\ cm^{-1}$).

The complex $[Ni_9(\mathbf{L223})_8(OH)_6(NH_3)_4(H_2O)_8](NO_3)_4$ contains nine Ni(II) ions held together in the molecule by the bridging action of $\mathbf{L223}^-$, with the help of six O^{2-} groups [154]. The complex exhibits a central $[Ni_3]$ string as observed with the linear trinuclear complexes with triple [–N–N–] bridges studied above. The additional donor atoms of the triazole rings allow for the growth of the complex at both ends, which are both capped by three Ni(II) ions. The ends of the complex thus constitute two open cubane units, each involving three μ-O^{2-} groups and with one vacant apex, fused with the central fragment.

3.5.2. Fluoride-bridged manganese complexes

A successful synthetic program focused on the use of F^- ions to foster the formation of novel high-nuclearity manganese aggregates. This was done in part in combination with benzotriazole as bridging co-ligand. The first complex made in this manner is the spectacular molecule (and the largest of this review) with formula $[Mn_{26}O_{16}(OH)_{10}(OMe)_6F_{10}(\mathbf{L3})_{20}(\mathbf{HL3})_2(MeOH)_{13}(H_2O)]$ (Fig. 52) [155]. It is prepared in low yield from the reaction of MnF_3 and **HL3** as a melt at 100 °C (with no solvent), followed by extraction with MeOH and diffusion of Et_2O. In fact, the F^- ligands are only found on terminal positions; therefore, they do not seem to be essential for the stabilization of the structure of the $[Mn_{26}]$ complex. It has not however, been prepared from any other starting material. The complex structure relies on the cohesive function of sixteen triply bridging oxide ligands and ten μ- or μ_3-OH^- groups. In addition there are $\mathbf{L3}^-$ ligands bound in the $\mu_{1,2}$ or $\mu_{1,2,3}$-modes. The magnetic coupling within this molecule appears to be dominated by antiferromagnetic interactions. However, a combination of experiments leads to the conclusion that the spin ground state lies in between $S = 4$ and 5. It was found that this complex behaves as a Single Molecule Magnet (SMM), and it constitutes one of the very few examples in this review presenting this behaviour.

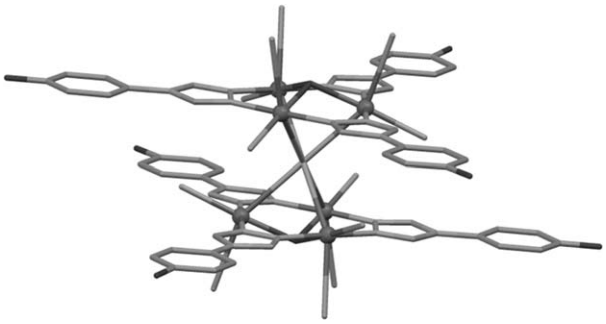

Fig. 48. Molecular representation of $[Cu_6Cl_{10}(OH)_2(\mathbf{HL73})_6(H_2O)_3]$ [150]. Large balls are Cu ions, dark grey is O, medium grey is Cl and C and light grey is N. Hydrogen atoms not shown for clarity.

The $[Mn_{26}]$ complex can be made in better yield from the same reaction using MeOH directly as a solvent. If pyridine is added to the reaction mixture, the new complex $[Mn_{10}O_6(OH)_2(\mathbf{L3})_8(py)_8F_8]$ is formed instead (Fig. 53) [155]. This molecule exhibits an irregular supertetrahedral structure, centered on the edges. The core of this structure contains six μ_3-O^{2-} and two μ_3-OH^- groups. The three metals of each edge are either linked by two $\mathbf{L3}^-$ bridges or by one μ-$\mathbf{L3}^-$ and one μ-F^- ligand. The remaining coordination sites are occupied by terminal F^- ions or pyridine ligands. This compound exhibits a diamagnetic ground state. The nature and strength of the magnetic coupling is hard to establish, presumably because there are a lot of closely spaced magnetic states. The very same reaction scheme using **HL220** in boiling MeOH produced complexes $[Mn_{13}O_{12}(\mathbf{L220})_{12}F_6(MeOH)_{10}(H_2O)_2]$ [156] and $[Mn_8O_4(\mathbf{L220})_6(OMe)_2F_8(\mathbf{HL220})(MeOH)_8]$ [156]. The former (Fig. 54) consist of an oxido-bridged, centered hexagonal dish of Mn(III) ions. Each pair on the periphery of this dish is bridged by an O^{2-} group, which links it to a further Mn(III) ion with the help of two $\mu_{1,2}$-$\mathbf{L220}^-$ ligands. Of the six external metal ions attached in this manner to the central dish, three point above the plane of the dish and three below. The F^- ions occupy again terminal positions. The octanuclear complex (Fig. 55) also exhibits a succession of fused, oxo-centered $[Mn_3]$ triangles. By contrast to the previous complex, it shows bridging F^- ligands, while it combines $\mathbf{L220}^-$

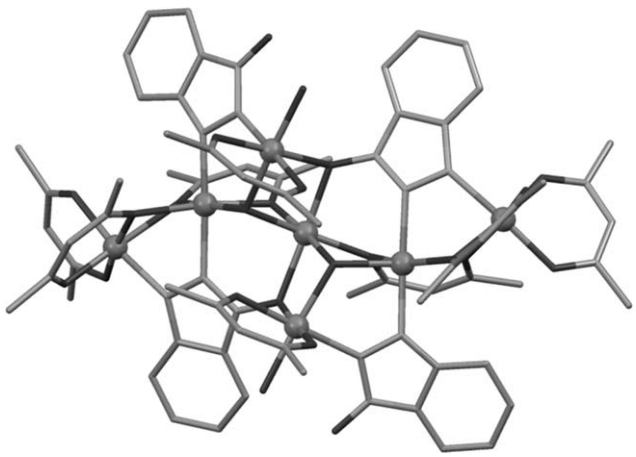

Fig. 49. Molecular representation of $[Ni_7(OH)_2(acac)_8(\mathbf{L221})_4(H_2O)_2]$ [151]. Large balls are Ni ions, dark grey is O, medium grey is C and light grey is N. Hydrogen atoms not shown for clarity.

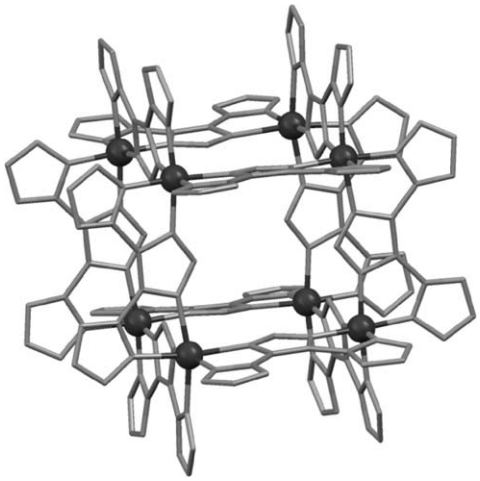

Fig. 50. Molecular representation of the anion of $(TBA)_{14}[Co_8(\mathbf{L222})_{12}]$ [152]. Large balls are Co ions, medium grey is C and light grey is N. Hydrogen atoms not shown for clarity.

ligands acting in bridging and terminal modes. The only difference in the synthesis of the $[Mn_{13}]$ and the $[Mn_8]$ complexes is that the system was boiled for 20 min to prepare the former and only for 10 min to obtain the other complex. No magnetic studies have been reported for any of these compounds.

3.5.3. A family of $[M_{14}]$ complexes

A family of remarkable $[M_{14}]$ complexes of various metals, involving benzotriazole, has been synthesized using solvothermal techniques. The first example was the all Fe(III) complex $[Fe_{14}(\mathbf{L3})_6O_6(OMe)_{18}Cl_6]$ (Fig. 56) [157], prepared in superheated MeOH (100 °C) from the complex $[Fe_3O(O_2CMe)_6(H_2O)_3]Cl$ and **HL3**.

This original molecule contains a central hexagonal bipyramid of Fe(III) ions held together by six O^{2-} and six OMe^- ligands. The oxide groups link this central cage to six additional metals (three above and three below the hexagonal plane), thereby adopting the μ_4-O^{2-} coordination mode. Additional OMe^- groups also contribute to link the peripheral metals to the central complex. Each triad of external Fe(III) ions are 'crowned' by three bridging 1,2,3-triazole ligands, which bind simultaneously to the metal conforming the apex of the 'ferric' bipyramid. Preliminary magnetic studies revealed that the spin ground state of this complex is near $S = 25$, with many other spin states in the vicinity. These properties are not ideal for SMMs but they render this complex a good candidate for magnetic refrigeration [158]. The analogous complex with 1,2,3-triazole (**HL1**), $[Fe_{14}(\mathbf{L1})_6O_6(OMe)_{18}Cl_6]$ has been prepared more recently [159]. Since the **HL1** ligand is smaller, the packing of this complex is more compact. Antiferromagnetic ordering is observed at low temperatures for both derivatives, although it is more intense in the latter $[Fe_{14}]$ complex. Other 1,2,3-triazole ligands also led to the same type of structure. In addition, the analogous arrangement could be made for other metals. Thus, solvothermal methods were used to isolate complexes $[Cr_{14}(\mathbf{L3})_6O_6(OMe)_{18}Cl_6]$ and $[V_{14}O_6(\mathbf{L220})_6(OMe)_{18}Cl_{6-x}O_x]$ [159]. In the vanadium complex, some V^{III}–Cl moieties had been replaced by V^{IV}–O fragments, presumably resulting from partial oxidation of the system during the synthesis. The samples used analyzed for $x = 2$.

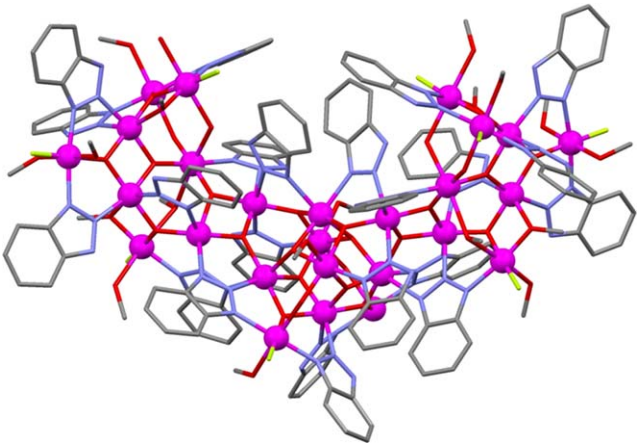

Fig. 52. Molecular representation of $[Mn_{26}O_{16}(OH)_{10}(OMe)_6F_{10}(\mathbf{L3})_{20}(\mathbf{HL3})_2(MeOH)_{13}(H_2O)]$ [155]. Pink balls are Mn ions, light green is F, blue is N, red is O and grey is C. Hydrogen atoms not shown for clarity.

3.5.4. Other complexes with more than nine metals

Most of the complexes gathering more than nine metals in their molecular structure ($[Mn_{26}]$, $[Mn_{13}]$, $[Mn_{10}]$, and $[M_{14}]$) have been grouped and featured already in previous sections. Another related high-nuclearity complex is $[(VO)_8V_2(\mathbf{L220})_8(OH)_4(OMe)_{10}]$ (Fig. 57) [160]. This molecule consists of a doubly μ-MeO^- bridged dimer of V(III) ions, encapsulated by a tetragonal rectangular prism of V=O moieties. The eight (long) edges of the squares are spanned by ($\mu_{1,3}$ or $\mu_{1,2,3}$) 1,2,3-triazole ligands, while each of the short edges are built by two μ-MeO^- groups and a μ_3-O^{2-} ligand (also

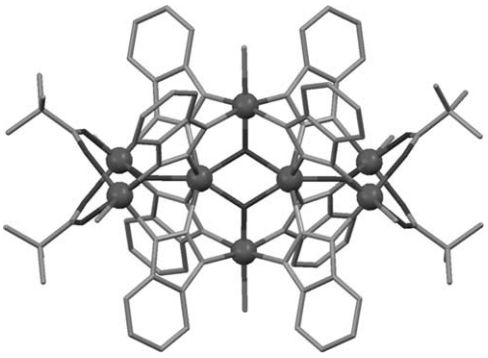

Fig. 51. Molecular representation of $[V_8O_4(\mathbf{L3})_8(piv)_4Cl_6]$ [153]. Large balls are V ions, dark grey is O, medium grey is Cl and C and light grey is N. Hydrogen atoms not shown for clarity.

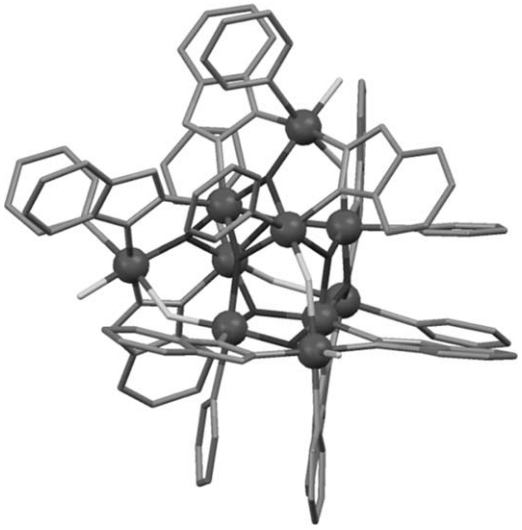

Fig. 53. Molecular representation of $[Mn_{10}O_6(OH)_2(\mathbf{L3})_8(py)_8F_8]$ [155]. Large balls are Mn ions, dark grey is F and O, medium grey is C and light grey is N. Hydrogen atoms not shown for clarity.

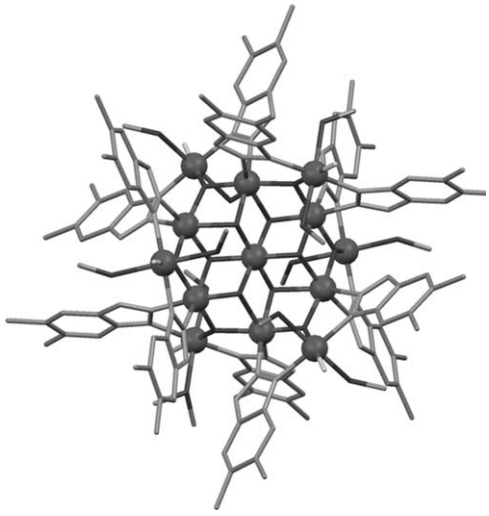

Fig. 54. Molecular representation of $[Mn_{13}O_{12}(\mathbf{L220})_{12}F_6(MeOH)_{10}(H_2O)_2]$ [156]. Large balls are Mn ions, light grey is F, dark grey is O and grey is C and N. Hydrogen atoms not shown for clarity.

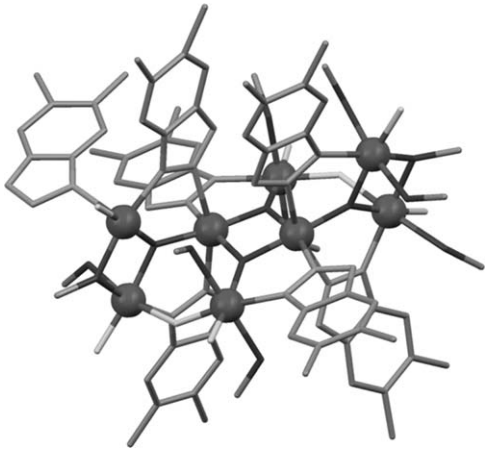

Fig. 55. Molecular representation of $[Mn_8O_4(\mathbf{L220})_6(OMe)_2F_8(\mathbf{HL220})(MeOH)_8]$ [156]. Large balls are Mn ions, dark grey is F and O, medium grey is C and light grey is N. Hydrogen atoms not shown for clarity.

bound to a central vanadium ion). The overall magnetic coupling within the complex is antiferromagnetic.

The last complex in this section is $[Ni_{13}(OH)_6(O_2CMe)_8(\mathbf{L221})_{12}(H_2O)_6(^n PrOH)_4]$ (Figs. 58 and 59) [161]. This molecule comes about as a result of the capacity of the $\mathbf{L221}^-$ ligand to bind several metals in a variety of coordination modes. In this complex, the twelve $\mathbf{L221}^-$ ligands bind to three metals, with both of their available N-donor atoms and the oxygen atom attached to one metal each. The molecule consists of a central $[Ni_3]$ moiety with triple [–N–N–] bridges, linked at each end to a "star" of three Ni(II) ions by μ_3-OH^- groups and $\mathbf{L221}^-$ ligands. Each such "star" is further bridged to another nickel center by three $\mathbf{L221}^-$ ligands. The authors of this preparation made react the $[Ni_{13}]$ complex in MeOH with an excess of N_3^- in order to replace by these ligands the μ_3-OH^- groups, as they had done before with other complexes [162]. All the indications suggest that this procedure led to the formation of the complex $[Ni_{13}(N_3)_6(O_2CMe)_8(\mathbf{L221})_{12}(MeOH)_{10}]$, although crystallographic evidence could not be obtained.

4. Coordination compounds with spin-crossover properties

The spin-crossover (SCO) phenomenon is a purely molecular property of transition metal ions related to the population of a metastable state exhibiting a higher spin than the ground state. This event basically occurs as the result of the interplay between the dependence of the ligand-field (LF) strength on the metal-to-ligand distance and the electron-electron repulsion. It has been observed in coordination complexes of 3d transition-metal ions with d^4 to d^7 electronic configurations. Nevertheless, the vast majority of SCO complexes involve iron(II), usually in a close to octahedral FeN_6 environment. As depicted in Fig. 60, iron(II) systems are more interesting since the SCO occurs between a diamagnetic low-spin (LS) $S = 0$ ground state and a high-spin (HS) paramagnetic $S = 2$ metastable state. In addition, a thermochromic effect is often accompanying the SCO in compounds of this metal ion. Thermal SCO occurs quantitatively as a result of the higher entropy of the HS state and follows a Boltzmann's population law for complexes in solution. In the solid state, secondary effects such as packing or cooperative interactions are responsible for the observation a different types of SCO behaviour. In particular, cooperative effects [163–165] may lead to extremely abrupt thermal spin changes, that may occur with hysteretic loops, therefore giving a bistable character to the transition. A schematic representation of an ideal thermal SCO curve with a cooperative behaviour, a crucial feature for potential applications in information storage or optical devices [166], is shown in Fig. 60, right. In the absence of cooperativity, the SCO occurs in one sole step; however, the presence of different SCO centers or competing interactions in the solid may result in two-step SCO. The HS state can be trapped either through thermal quenching or by irradiation with an adequate wavelength, the lat-

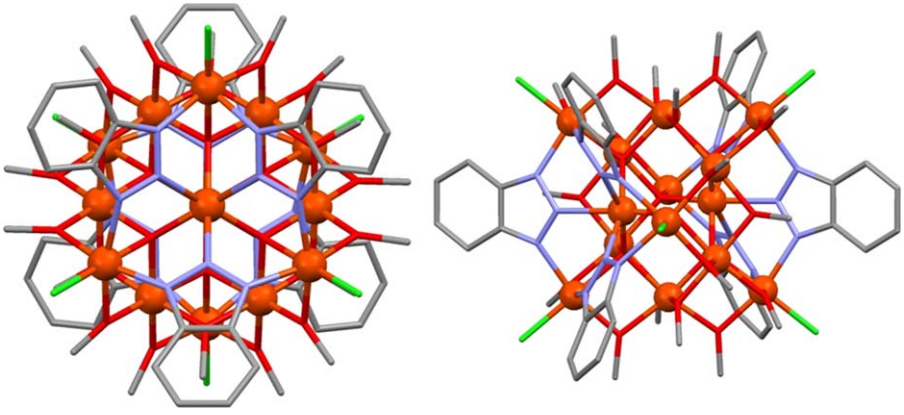

Fig. 56. Two views of the structure of $[Fe_{14}(\mathbf{L3})_6O_6(OMe)_{18}Cl_6]$ [157]. Orange balls are Fe ions, green is Cl, blue is N, red is O and grey is C. Hydrogen atoms not shown for clarity.

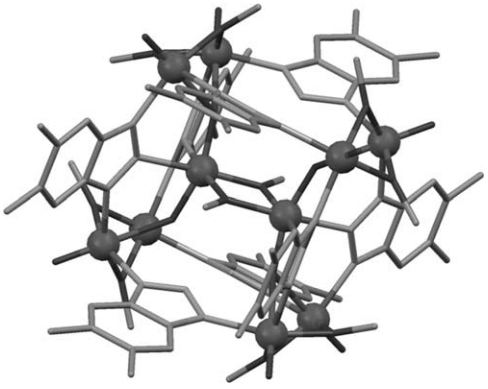

Fig. 57. Structure representation of $[(VO)_8V_2(\mathbf{L220})_8(OH)_4(OMe)_{10}]$ [160]. Large balls are V ions, dark grey is O, medium grey is C and light grey is N. Hydrogen atoms not shown for clarity.

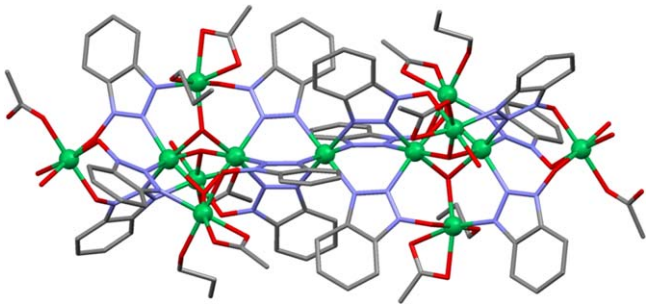

Fig. 58. Structure representation of $[Ni_{13}(OH)_6(O_2CMe)_8(\mathbf{L221})_{12}(H_2O)_6(^n PrOH)_4]$ [161]. Green balls are Ni ions, blue is N, red is O and grey is C. Hydrogen atoms not shown for clarity.

ter being the most interesting photophysical effect for iron(II). This light-induced effect or LIESST (Light-Induced Excited Spin-State Trapping) has been widely studied and is reversible in some compounds (reverse-LIESST) [167]. The SCO phenomenon is now well understood, and the reader is referred to a number of recognized references compiling these investigations [168,169].

Although triazoles and tetrazoles possess a rich variety of binding and bridging modes (see Schemes 5–7), their most relevant advantage here is their particular donor strength as ligands in iron(II) complexes. Indeed, triazoles and tetrazoles are well suited to produce the above-mentioned FeN_6 octahedral environment around iron(II). Actually, the LF strengths provided by these azole rings are in the ideal range for the occurrence of SCO with this metal ion. Thus, some of the most studied SCO compounds are triazole or tetrazole-containing monomers, and have been obtained only with iron(II). This section covers the whole family of iron(II) coordination compounds containing at least one triazole or tetrazole ring. It is first organized by azole type, and then by nuclearity/dimensionality of the SCO compounds. A succinct description of the structure and SCO properties is given for an ample selection of these. All compounds described in the literature are listed in Tables 4 (triazoles) and 5 (tetrazoles), together with the corresponding references. In addition, the structural information and the SCO properties (temperature range, type of SCO, and techniques used) are summarized. When relevant, the description focuses on structural aspects influencing the SCO. The importance of packing interactions will be highlighted. Selected experimental (mostly magnetic) data describing the SCO phenomenon in the featured examples are given as found in the literature, either for their originality, interest or typical character. We have used χT as a unifying presentation of the bulk, variable temperature magnetization data, the original data being reported either in HS fraction, χ, χT, μ_{eff} or μ^2_{eff}. SCO triazole and tetrazole compounds have been previously partially reviewed [170,171], especially for monomers [172]. The 1,2,3- and 1,2,4-triazole ligands involved in SCO complexes are shown in Fig. 61 and the tetrazole ones in Fig. 82.

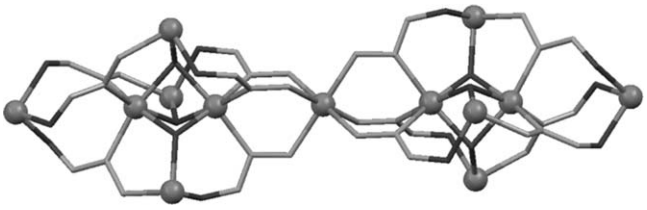

Fig. 59. Core of $[Ni_{13}(OH)_6(O_2CMe)_8(\mathbf{L221})_{12}(H_2O)_6(^n PrOH)_4]$ [161].

4.1. Complexes of 1,2,3-triazole ligands

The 1,2,3-triazole ring is by far the least used for the generation of SCO coordination compounds. This is in part due to the relatively little abundance of coordination complexes with this type of ligand. Because of their scarcity, 1,2,3-triazole-based SCO compounds will be described here in greater detail compared to those obtained from 1,2,4-triazole and tetrazole ligands.

4.1.1. Monomers

There is only one family of monomeric SCO complexes bearing a 1,2,3-triazole ligand, *i.e.* solvated and unsolvated complexes with formula *trans*-$[Fe(\mathbf{L224})_2(NCX)_2]$, where **L224** = 3-(2-pyridyl)[1,2,3]triazolo[1,5-a]pyridine and X = S or Se. The bidentate ligand **L224** contains a 1,2,3-triazole ring and a pyridyl group, and is chelating like 2,2'-bipyridine (Fig. 62). The X = S complex was first reported as di-chloroform (SCO1) and water (SCO2) solvates [173]; however, only the triclinic crystal struc-

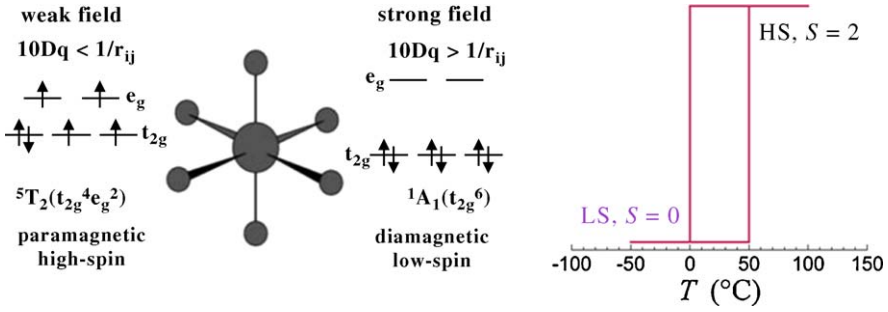

Fig. 60. (left) Electronic configurations of the two possible ground states of an iron(II) ion in an octahedral environment. Intermediate fields may favor a LS ground state with a metastable HS state populated at temperatures close to ambient temperature. (right) Schematic representation of an abrupt SCO behaviour of an iron(II) compound with a large hysteresis centered at room temperature, considered ideal for potential applications. The *Y* axis is typically the HS fraction.

Table 4
Triazole-containing SCO compounds.

Complex	Reference(s)	Structure	Nuclearity/ dimensionality	SCO type	Techniques used	$T_{1/2}$ (K)
[Fe(**L224**)$_2$(NCS)$_2$]·2CHCl$_3$	[173]	HS	Monomer	Gradual only 20%	Mag	90
[Fe(**L224**)$_2$(NCS)$_2$]·H$_2$O	[173]		Monomer	Gradual	Mag, LIESST, relax	118
[Fe(**L224**)$_2$(NCS)$_2$] A and B	[174]	HS, LS and LIESST (A), only HS (B)	Monomer	2-step (A) + impurity abrupt (B)	Mag, XANES, IR, LIESST, relax	100–200 (A) 102 (B)
[Fe(**L224**)$_2$(NCSe)$_2$]	[173]		Monomer	Gradual	Mag, Cal,	251
[Fe(**L225**)$_3$](ClO$_4$)$_2$	[175]	HS	2D	Abrupt, asymmetric hysteresis	Mag, Cal	101/109
[Fe(**L62**)$_2$]·xH$_2$O	[177,178,507]	LS	Monomer	Abrupt	Mag, Cal, solution studies (NMR)	335
[Fe(**HL69**)$_3$]A$_2$·nH$_2$O (A$^-$ = Cl$^-$,ClO$_4^-$, PF$_6^-$, 1/2SO$_4^{2-}$)	[180,184,185]		Monomer	Gradual	Mag, Möss	140–210
mer-[Fe(**HL69**)$_3$](BF$_4$)$_2$·2H$_2$O	[179,180,184,185]	HS	Monomer	Gradual/incomplete (30%)	Mag, Möss	135
[Fe(**HL69**)$_3$](SO$_4$)$_{0.4}$(BF$_4$)$_{1.2}$·3H$_2$O	[180]		Monomer	Gradual	Mag, Cal, LIESST, Quen, relax	170
[Fe(**L226**)$_3$]A$_2$·nH$_2$O (A$^-$ = BF$_4^-$, ClO$_4^-$, PF$_6^-$)	[183,185]		Monomer	Gradual (sample-dependent)	Mag, Möss	HS or <89–250
[Fe(**HL218**)$_3$](PF$_6$)$_2$·H$_2$O	[183]		Monomer	Gradual (incomplete)	Mag, Möss	250
mer-[Fe(**L227**)$_3$]A$_2$ (A$^-$ = BF$_4^-$, ClO$_4^-$, PF$_6^-$)	[185]	HS (BF$_4$)	Monomer	Gradual	Mag, Möss	160 (BF$_4$)
[Fe(**HL228**)$_3$](ClO$_4$)$_2$	[101]		Monomer	Gradual (32% res. HS)	Mag	277
[Fe(**L208**)$_3$]A$_2$·nH$_2$O (A$^-$ = BF$_4^-$, ClO$_4^-$, PF$_6^-$, $_{1/2}$ SO$_4^{2-}$)	[101]	<50%HS, LS (ClO$_4$)	Monomer	Gradual	Mag	HS or 182–350
trans-[Fe(**L199**)$_2$(TCNQ)]	[189]	50% HS–LS	Monomer	Gradual	Mag, Möss, IR, EPR	280
trans-[Fe(**L199**)$_2$(NCS)$_2$] 4 phases (A, B, C, D)	[190,191,733,734]	HS, LS, LIESST, Quen	Monomer	Gradual	Mag, Cal, LIESST, Quen, Relax, Press	180 (A)/HS (B, 65–179 under pressure)/86 (C, partial)/162 (D, partial)
trans-[Fe(**L199**)$_2$(NCSe)$_2$]	[191,733,734]	HS	Monomer	Gradual	LIESST, relax, Cal	224
trans-[Fe(**L199**)$_2$(N(CN)$_2$)$_2$]	[735]	HS	Monomer	Gradual incomplete (complete after Quen) 2 step	LIESST, Quen, relax	84
[Fe(**L199**)(DAPP)](ClO$_4$)$_2$	[187,188]	HS and LS	Monomer	Abrupt, 10 K hysteresis	Mag, Möss	171/181
trans-[Fe(**L229**)$_2$(NCS)$_2$]	[736]	HS	Monomer	Abrupt	Mag, IR, EXAFS	231
trans-[Fe(**L200**)$_2$(NCS)$_2$]$_2$·*cis*-[Fe(**L200**)$_2$(NCS)$_2$]	[192]	HS	Monomer	Gradual (1/3, probably only one of the *trans* isomers)	Mag, Möss	180
[Fe(**L230**)$_2$(NCS)$_2$]·H$_2$O	[193]	HS and LS	Monomer	Gradual	Mag	269
[Fe(**H$_2$L231**)$_2$]A$_2$·H$_2$O (A = BF$_4^-$, ClO$_4^-$)	[195]	HS (NO$_3$·3H$_2$O)	Monomer	Not measured	Möss, Mag	Between 303 and 89 K
[Fe(**H$_2$L232**)$_2$]Cl$_2$·nH$_2$O (*n* = 3 and 0)	[195]	Ni analogue	Monomer	Not measured	Möss, Mag	Between 303 and 89 K for *n* = 3, >303 K for *n* = 0
[Fe(**HL233-HL235**)$_2$](ClO$_4$)$_2$·*n*H$_2$O	[737]		Monomer	Gradual also in solution (acetone)	Möss, Mag	RT
[Fe(**L236**)$_2$](ClO$_4$)$_2$·*n*H$_2$O (*n* = 1 or 2/3)	[738]	HS, 2 polymorphs *n* = 1 or 2/3	Monomer	Gradual (bulk)	Möss, Mag	265 (bulk)
[Fe$_2$(**L75**)$_2$(py)$_2$(NCBH$_3$)$_2$]	[197]		Dimer	2-Step	Mag	151 and 194
[Fe$_2$(**L237**)$_2$](BF$_4$)$_4$·DMF	[198]	HS and LS	Dimer	Abrupt, but only half SCO, remain HS-LS	Mag, Möss	224
[Fe$_2$(**L238**)$_5$(NCS)$_4$]$_2$[Fe(**L238**)$_2$(NCS)$_2$(H$_2$O)$_2$]	[199]	HS	Dimer + monomer	Abrupt (only dimers)	Mag, Möss	111
[Fe$_3$(**L193**)$_6$(H$_2$O)$_6$](CF$_3$SO$_3$)$_6$	[200,202]	HS and LS	Trimer	Gradual, 1/3 (central)	Mag, Möss	210
[Fe$_3$(**L211**)$_6$(H$_2$O)$_6$](p-tol)$_6$·4H$_2$O	[121]	HS (2MeOH·8H$_2$O)	Trimer	Gradual, 1/3 (central)	Mag, Möss	245
[Fe$_3$(**L250**)$_6$(H$_2$O)$_6$](p-tol)$_6$·2H$_2$O	[203]	HS	Trimer	Gradual, 1/3 (central)	Mag, Möss	242
[Fe$_3$(**L250**)$_6$(H$_2$O)$_6$](CF$_3$SO$_3$)$_6$	[203]		Trimer	Gradual, 1/3 (central)	Mag, Möss	187
[Fe$_3$(**L250**)$_6$(H$_2$O)$_6$](BF$_4$)$_6$·2H$_2$O	[739]	HS	Trimer	Gradual, 1/3 (central)	Mag	194
[Fe$_3$(**L250**)$_8$(H$_2$O)$_4$]I$_6$ + [Fe$_3$(**L250**)$_6$(H$_2$O)$_6$]I$_6$·8H$_2$O (mixture of 2 phases)	[739]	HS (both phases)	Trimer	Gradual, 1/3 (central)	Mag	195 (bulk mixture)

Table 4 (*Continued*)

Complex	Reference(s)	Structure	Nuclearity/ dimensionality	SCO type	Techniques used	$T_{1/2}$ (K)
$[Fe_3(\mathbf{HL82})_6(H_2O)_6](CF_3SO_3)_6$	[204]	HS and LS	Trimer	Gradual, 1/3 (central)	Mag, Möss	290
$[Fe_3(\mathbf{L251})_8(H_2O)_4](NO_3)_6$	[740]		Trimer	Gradual, 1/3 (central)	Mag, Cal	208
$[Fe_3(\mathbf{L239})_6(H_2O)_6](ReO_4)_6$	[205]	HS	Trimer	Gradual, 1/3 (central)	Mag	185
$[Fe(\mathbf{HL21})_2(\mathbf{L21})]BF_4$	[210–214]		1D	Abrupt, hysteresis up to 40 K	Mag, Cal, Möss, EXAFS, WAXS	385–345
$[Fe(\mathbf{L196}\text{-}\mathbf{L249})_3]A_2{\cdot}nH_2O$ ($A^- = BF_4^-$, ClO_4^-, $CF_3SO_3^-$, p-tol$^-$)	[741]		1D	Gradual to abrupt, including hysteresis of various widths	Mag, Vis, Cal	160–340
$[Fe(\mathbf{HL82})_3]A_2{\cdot}nH_2O$	[209,216,742]		1D	Gradual to abrupt, including hysteresis	Mag, Möss, Cal, Press	160–340
$[Fe(\mathbf{L31})_3]A{\cdot}nH_2O$	[743–749]		1D	Gradual to abrupt, including hysteresis	Mag, Möss, EXAFS, Cal	160–340
$[Fe(\mathbf{L252})_3]A_2{\cdot}nH_2O$ ($A^- = BF_4^-$, NO_3^-, $CF_3SO_3^-$, p-tol$^-$)	[750]		1D	Gradual to abrupt	Mag, Vis, Cal	225–325
$[Fe(\mathbf{L253}\text{-}\mathbf{L255})_3]A_2{\cdot}nH_2O$	[222]		1D	Abrupt	Mag, Möss, Cal	325–340
$[Fe(\mathbf{L40})_2(NCS)_2]_n{\cdot}nH_2O$	[229–237]	HS, LS, LIESST	2D	Abrupt, hysteresis 21 K	Mag, Möss, Cal, Dilution, LIESST, Relax, Vis, Press, EPR, muSR, NMR, Quen, Cell	144/123
$[Fe(\mathbf{L40})_2(NCSe)_2]_n{\cdot}nH_2O$	[232]	HS	2D	Abrupt, hysteresis 6 K	EPR, NMR	217/211
$[Fe(\mathbf{L256})_2]_n$	[238]	HS and LS	2D	Abrupt, hysteresis 5 K	Mag, Cal, Cell	273.4/278.8
$[Fe(\mathbf{L40})_3]_n(ClO_4)_{2n}$	[240,241]	HS, intermediate, LS	3D	Abrupt, 2-step, LT step has 3 K hysteresis	Mag, Cal, Möss	222, 185/182

a: Cal: calorimetric studies (DSC or adiabatic calorimetry); Cell: temperature variation of cell parameters; Dilution: studies of the effect of metal dilution on the SCO; EPR: variable-temperature Electron Paramagnetic Resonance of Mn(II) and/or Cu(II) dopes; EXAFS and XANES: X-ray absorption spectroscopy; IR: variable-temperature infrared spectroscopy; LIESST: light-induced trapping of HS phase; Mag: variable-temperature magnetisation/magnetic susceptibility; Möss: Mössbauer spectroscopy; muSR: muon relaxation/resonance; Press: magnetic susceptibility, diffuse reflectance or Mössbauer spectroscopy under applied pressure; Quen: thermal trapping of the HS phase by rapid cooling; Relax: studies of the thermally-activated relaxation of the thermally or light-induced metastable HS state at low temperatures; Vis: absorption spectroscopy or diffuse reflectance; WAXS: wide-angle X-ray scattering.

b: $T_{1/2}$ corresponds to the temperature at which half the Fe(II) centers presenting SCO have changed their spin state. When several values are given they correspond either to the presence of two steps in the SCO or to hysteretic behaviour, e.g. to the $T_{1/2}$ temperatures upon warming and cooling.

ture of SCO1 was solved. The solvent-free compound was later shown to crystallize as two polymorphs, either monoclinic (SCO3A) or triclinic (SCO3B) [174]. The selenium derivative (X = Se) was reported with no solvent lattice molecules (SCO4), although its crystal structure was not determined [173]. It can be noticed that the coordination compound with three chelating **L224** ligands, *i.e.* $[Fe(\mathbf{L224})_3](BF_4)_2$, does not show a SCO behaviour, like $[Fe(bpy)_3]^{2+}$ complexes. This absence of SCO can be explained by an increase of the LF strength caused by the replacement of the NCX^- donors by comparatively stronger aromatic N donors. Hence, the compound $[Fe(\mathbf{L224})_3](BF_4)_2$ exhibits a LS state over the whole studied temperature range [173].

In all the $[Fe(\mathbf{L224})_2(NCX)_2]$ series, the neutral complex core is comparable (Fig. 62), with two **L224** ligands coordinated at the equatorial positions and two NCX^- groups occupying the axial sites. The resulting *trans* coordination compound possesses a rather symmetric FeN_6 octahedral coordination environment, with Fe–N bond distances at 293 K of 2.217–2.193 Å (pyridine), 2.211–2.174 Å (triazole) and 2.107–2.113 Å (NCX^-). All these bond lengths are typical of an iron(II) center in the HS state. In SCO3A, for which the structure of the LS phase was also solved at 40 K, the FeN_6 octahedron decreases in volume from 13.1 to 10.1 $Å^3$ upon going from the HS to the LS state. Moreover, the coordination geometry is much closer to a regular octahedron, as commonly observed for SCO iron(II) com-

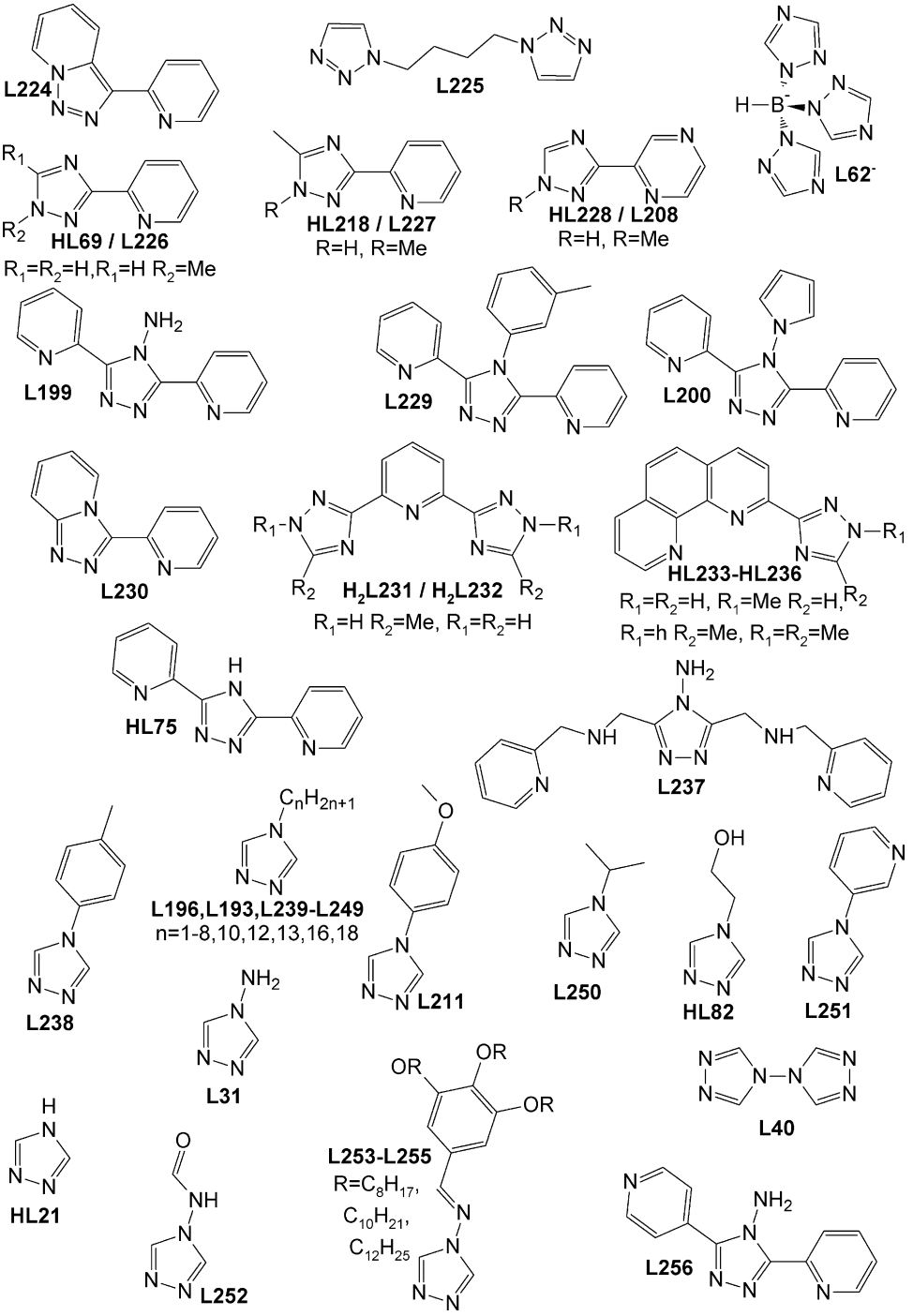

Fig. 61. List of the 1,2,3-triazole (**L224** and **L225**) and 1,2,4-triazole (**L62⁻-L256**) ligands involved in the coordination sphere of spin-crossover compounds.

Table 5
Tetrazole-containing SCO compounds.

Complex	Reference	Structure	Nuclearity/ Dimensionality	SCO type	Techniques used[a]	$T_{1/2}$ (K)[b]
$[Fe(\mathbf{L257})_6](BF_4)_2$	[245,253,254,256,258,751–753]	HS,50:50,LS	Monomer	Gradual 50%	IR, LIESST, Mag, Möss, Pos, Quen, T_1, Vis	75
$[Fe(\mathbf{L257})_6](ClO_4)_2$	[258,754]	HS	Monomer	Gradual 50%	LIESST, Möss	66
$[Fe(\mathbf{L257})_6](PF_6)_2$	[755]		Monomer	Gradual	Möss	207
$[Fe(\mathbf{L257})_6](CF_3SO_3)_2$	[756]		Monomer	Abrupt/hysteresis 12 K, 33%	Mag, Möss, Quen	178/166
$[Fe(\mathbf{L107})_6](BF_4)_2$	[253,256,257,754,757,758]	HS	Monomer	Gradual 66%	IR, LIESST, Mag, Möss, Pos, Press, T1, Vis	105
$[Fe(\mathbf{L258})_6](BF_4)_2$	[245,249–261]	3 HS + LS ordered	Monomer	Abrupt (hysteresis 7 K if slow cooling)	Brill, DFT, Dilution, EPR, INS, IR, LIESST, Mag, Möss, Pos, PXD, PND, Press, Raman, T_1, XAS	125 or 128–135
$[Fe(\mathbf{L258})_6](ClO_4)_2$	[252,258,759,760]	HS	Monomer	Gradual	Brill, Mag, Möss, muSR	150
$[Fe(\mathbf{L258})_6](PF_6)_2$	[761]	2 HS	Monomer	Abrupt	LIESST, Mag, Möss, Press, Vis	74
$[Fe(\mathbf{L258})_6](CF_3SO_3)_2{\cdot}2(\mathbf{L258})$	[753]		Monomer	Abrupt	Mag, Möss, Cal, Vis	178
$[Fe(\mathbf{L257}\text{-}\mathbf{L266})_6](BF_4)_2$	[257]		Monomer	Not shown	IR	Not specified
$[Fe(\mathbf{L259}\text{-}\mathbf{L262})_6](BF_4)_2$	[762]	HS (with **HL261**)	Monomer	Gradual	Mag, Möss	134 (**HL261**)
$[Fe(\mathbf{L260}\text{-}\mathbf{L264}\text{-}\mathbf{L265})_6](BF_4)_2$	[763]		Monomer	Gradual	IR, LIESST, Mag, Möss, Vis	148/120/153
$[Fe(\mathbf{L267})_6](BF_4)_2$	[764]		Monomer	Gradual, 2 step, 67%	IR, Mag, Möss	108,137
$[Fe(\mathbf{L267})_6](ClO_4)_2$	[764]		Monomer	Gradual	IR, Mag, Möss	130
$[Fe(\mathbf{L113})_6](BF_4)_2$	[764–767]	HS, LS (PXD)	Monomer	Gradual, 2 step	Mag, Möss, PXD, Vis	142/190 (powder) or 108/190 (crystal)
$[Fe(\mathbf{L113})_6](ClO_4)_2$	[768]	HS, LS (PXD)	Monomer	2 step, gradual and 13 K hysteresis first step (powder), gradual 50% (crystals)	IR, Möss, PXD, Vis	135(143/126)/178 or 178
$[Fe(\mathbf{L113})_6](PF_6)_2$	[767]		Monomer	Gradual 2 step	Mag, Möss, PXD, Vis	121/185
$[Fe(\mathbf{L268})_6](BF_4)_2$	[764,769]	HS, LS (PXD)	Monomer	Gradual	IR, Mag, Möss, PXD	166
$[Fe(\mathbf{L268})_6](ClO_4)_2$	[764]		Monomer	Gradual	IR, Mag, Möss, PXD	150
$[Fe(\mathbf{L269})_6](BF_4)_2$	[764,769]	HS, LS (PXD)	Monomer	Gradual	IR, Mag, Möss, PXD	205
$[Fe(\mathbf{L269})_6](ClO_4)_2$	[764]		Monomer	Gradual 2 step	IR, Mag, Möss, PXD	177
$[Fe(\mathbf{L270})_6](BF_4)_2$	[245,254]		Monomer	33%	IR, Mag, Möss	72
$[Fe(\mathbf{L271})_6](A)_2$ ($A = BF_4^-$, PF_6^-)	[248]	PF_6	Monomer	Gradual	Mag, Vis, Möss	
$[Fe(\mathbf{L272})_6](BF_4)_2$	[247]		Monomer	Gradual (70% res. HS)	Mag	80
$[Fe(\mathbf{L273})_6](BF_4)_2$	[247]		Monomer	Gradual (20% res. HS)	Vis, Mag, Cal, Möss	210
$[Fe(\mathbf{L274})_2]{\cdot}n$MeOH ($n = 0$, 1)	[262]	HS and LS ($n = 0$), HS ($n = 1$)	Monomer	Abrupt hysteresis 6 K ($n = 1$ LS, looses MeOH 350 K first heating then same as $n = 0$)	Mag, Cal	258, 252
$[Fe(\mathbf{L275})_2](ClO_4)_2{\cdot}CH_3OH$	[262]	LS	Monomer	Abrupt first up, then gradual	Mag	341 first up, then 310
$[Fe(\mathbf{L276})_2](A)_2{\cdot}H_2O$ ($A = ClO_4^-$, BF_4^-)	[262]	LS	Monomer	Gradual, 2step (BF_4)	Mag	350 (ClO_4), 350/290 (BF_4)
$[Fe(\mathbf{L277})_2](A)_2$ ($A = ClO_4^-$, BF_4^-)	[262]		Monomer	Gradual	Mag	375 (ClO_4)/377 (BF_4)
$[Fe(\mathbf{L278})_2](A)_2$ ($A = ClO_4^-$, BF_4^-)	[262]	LS (BF_4 only)	Monomer	Gradual (ClO_4), 2step first step abrupt hysteresis (BF_4)	Mag, Cal (BF_4)	365 (ClO_4), 300-268 (1st step)/210 (BF_4)
$[Fe(\mathbf{L279})_2](A)_2{\cdot}H_2O$ ($A = ClO_4^-$, BF_4^-)	[262]		Monomer	Abrupt (ClO_4), 2step abrupt and 10 K hsyt 2nd step (BF_4)	Mag, Cal	386 (ClO_4), 355/170–160 (BF_4)
$[Fe(\mathbf{L280})_2](A)_2{\cdot}H_2O$ ($A = ClO_4^-$, BF_4^-)	[262]		Monomer	Abrupt first up (350-360 K), then gradual incomplete	Mag, Cal	290 (ClO_4), 274 (BF_4)
$[Fe(\mathbf{L281})_2](A)_2{\cdot}H_2O$ ($A = ClO_4^-$, BF_4^-)	[262]		Monomer	Abrupt first up (350-375 K), then gradual incomplete	Mag, Cal	289 (ClO_4), 277 (BF_4)

Table 5 (*Continued*)

Complex	Reference	Structure	Nuclearity/ Dimensionality	SCO type	Techniques used[a]	$T_{1/2}$ (K)[b]
[Fe(**L282**)$_2$](A)$_2$·H$_2$O (A = ClO_4^-, BF_4^-)	[262]		Monomer	Abrupt first up (365–375 K), then gradual incomplete	Mag, Cal	276 (ClO_4), 274 (BF_4)
[Fe(**L283**)$_2$](A)$_2$·H$_2$O (A = ClO_4^-, BF_4^-)	[262]	HS and intermediate (ClO_4)	Monomer	2 step gradual (ClO_4), Abrupt first up (373 K), then gradual incomplete (BF4)	Mag, Cal	170/245 (ClO_4), 262 (BF_4)
[Fe(**L126**)$_3$]$_n$(BF_4)$_{2n}$	[264]	HS and LS	1D	Gradual	Mag, Möss, IR, Vis	140
[Fe(**L131**)$_3$]$_n$(ClO_4)$_{2n}$	[274,277]	HS	3D interlocked	Crystal: hysteresis 20 K, very incomplete (solvent loss) Powder: two step complete	Mag, Möss (only crystal), Cal (only crystal), Vis, LIESST	Crystal: 150/170 powder: 84–134
[Fe(**L131**)$_3$]$_n$(PF_6)$_{2n}$ xnsolv (solv = MeOH, x = 0.075 or EtOH, x = 0.25)	[275,277]	HS, LS	3D interlocked	MeOH: abrupt 2 step (plateau centered at 174 K), 4 K hysteresis in second step EtOH: shifted 7 K lower, no hysteresis	Mag, Möss, IR, cell, cal	180–168/172 (MeOH) 173-161 (EtOH)
[Fe(**L131**)$_3$]$_n$(BF_4)$_{2n}$	[276]	HS and partially HS	3D interlocked	50% complete rather abrupt, crystals from EtOH/H_2O 95/5 have 9 K hysteresis, from EtOH no hysteresis more gradual	Mag, Möss, Quen (EtOH/H_2O), LIESST, Vis	80/89 (EtOH/H_2O) 84 (EtOH)
[Fe(**L284**-**L287**)$_3$]$_n$(ClO_4)$_{2n}$	[265,277]		1D	Gradual	Mag, LIESST, Vis, IR	125–169
[Fe(**L284**-**L289**)$_3$]$_n$(BF_4)$_{2n}$	[265]		1D	Gradual	Mag, LIESST, Vis	131–164
[Fe(**L290**)$_3$]$_n$(ClO_4)$_{2n}$	[266]	HS and LS	1D	Gradual (20% res. HS)	Mag, Möss, EXAFS, LIESST	130
[Fe(**L128**)$_3$]$_n$(ClO_4)$_{2n}$	[267]	HS and LS	1D	Abrupt, 3 K hysteresis	Mag, Möss, Vis	133/136
[Fe(**L291**)$_3$]$_n$(PF_6)$_{2n}$·nMeOH	[27]	HS and LS	1D	Gradual (14% res. HS)	Mag, Möss	160
[Fe(**L291**)$_3$]$_n$(CF_3SO_3)$_{2n}$·nMeCN	[27]	2 HS phases, LS	1D	Gradual 1/2	Mag, Möss, LIESST	130
[Fe(**L291**)$_3$]$_n$(ClO_4)$_{2n}$·nMeCN	[27]		1D	Gradual very incomplete	Mag	ca. 90
[Fe(**HL176**)$_2$(MeCN)$_2$]$_n$(ClO_4)$_{2n}$	[243]	HS, 80% LS	1D	Gradual	Mag	110
[Fe(**L292**)$_2$]$_n$A$_{2n}$ (A = ClO_4^-, BF_4^-)	[269]	HS (ClO_4)	2D	Abrupt, 9 K hysteresis	Mag, Cal	176/167 (ClO_4) 168/157 (BF_4)
[Fe(**HL293**)$_{1.8}$(**L294**)$_{1.2}$]$_n$(BF_4)$_{0.8n}$·nMeOH·0.8nH$_2$O	[270]	HS	2D	Gradual	Mag, Vis, LIESST, relax	112
[Fe(**L295**)$_2$(MeCN)]$_n$(ClO_4)$_{2n}$	[242]	2 HS, 2 in the SCO, LS	2D	Gradual	Mag	128
[Fe(**L130**)$_3$]$_n$(ClO_4)$_{2n}$·2nEtOH	[244]	2 HS, LS	3D	Gradual (20% res. HS)	Mag	145
[(Fe$_3$O)Fe(**L183**)$_6$(H_2O)$_3$]$_n$(ClO_4)$_{2n}$(NO_3)$_n$·nEtOH·2nH$_2$O	[279]	HS, LS and 3 in the SCO	3D	Gradual	Mag, Möss, Press	Within 125–175 K

[a] Brill: Brillouin spectroscopy; Cal: calorimetric studies (DSC or adiabatic calorimetry); DFT; density functional calculations; Dilution: studies of the effect of metal dilution on the SCO; EPR: variable-temperature Electron Paramagnetic Resonance of Mn(II) and/or Cu(II) dopes; EXAFS, XANES or XAS: X-ray absorption spectroscopy; INS: inelastic neutron scattering; IR: variable-temperature infrared spectroscopy; LIESST: efficient light-induced trapping of HS phase; Mag: variable-temperature magnetisation/magnetic susceptibility; Möss: Mössbauer spectroscopy; muSR: muon relaxation/resonance; PND: polarised neutron diffraction; Pos: positronium anihiliation lifetime measurements; Press: magnetic susceptibility, diffuse reflectance or Mössbauer spectroscopy under applied pressure; PXD: high resolution powder diffraction; Quen: thermal trapping of the HS phase by rapid cooling;Raman: variable-temperature Raman spectroscopy; Relax: studies of the thermally-activated relaxation of the thermally or light-induced metastable HS state at low temperatures; T_1: variable-temperature solid-state NMR T_1 measurements; Vis: absorption spectroscopy or diffuse reflectance.

[b] $T_{1/2}$ corresponds to the temperature at which half the Fe(II) centers presenting SCO have changed their spin state. When several values are given they correspond either to the presence of two steps in the SCO or to hysteretic behaviour, e.g. to the $T_{1/2}$ temperatures upon warming and cooling.

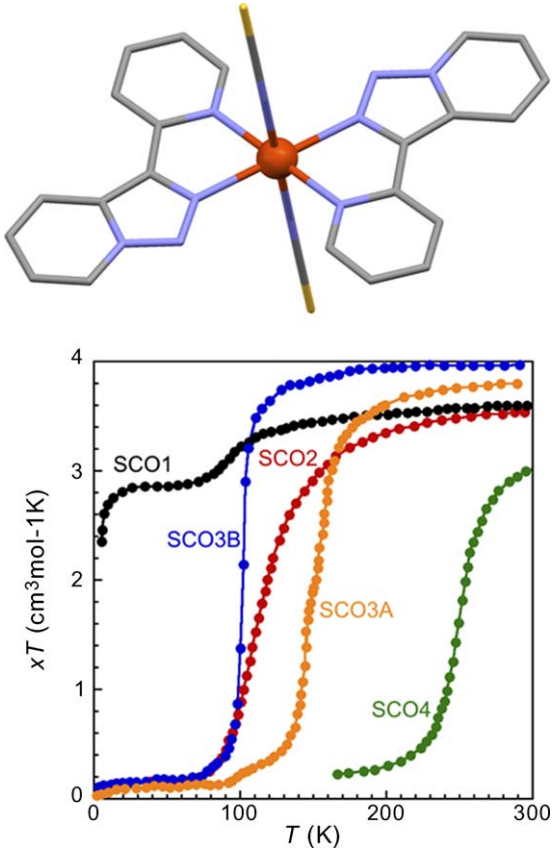

Fig. 62. (top) The neutral complex [Fe(**L224**)$_2$(NCS)$_2$] [173]. (bottom) χT versus T plot showing the SCO properties of the different [Fe(**L224**)$_2$(NCX)$_2$] phases studied (see text).

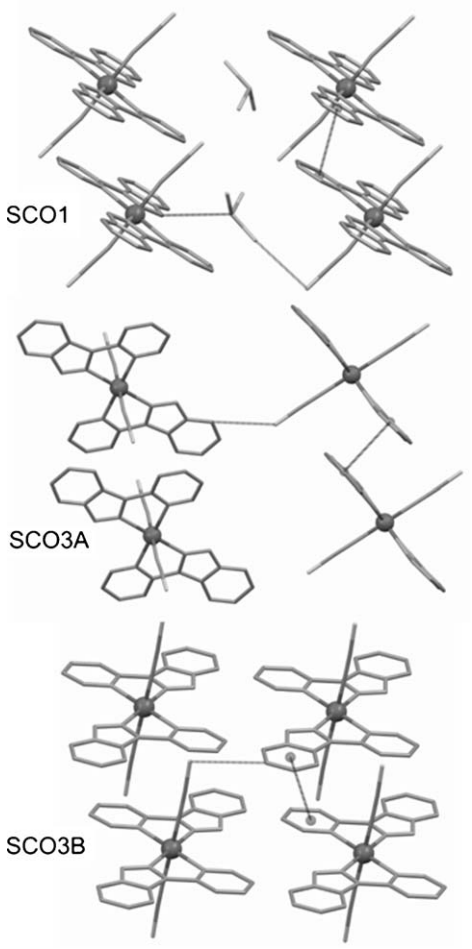

Fig. 63. Views of the crystal packing of [Fe(**L224**)$_2$(NCS)$_2$]·CHCl$_3$ (top) and the two polymorphs of [Fe(**L224**)$_2$(NCS)$_2$] [173], monoclinic (middle) and triclinic (bottom), evidencing the supramolecular interactions within layers of [Fe(**L224**)$_2$(NCX)$_2$] complexes and between these layers. π–π and S···H–C interactions are represented by thin lines (see text for distances).

plexes. π–π interactions between the **L224** ligands, present in all the series, result in the formation of layers, where all complexes are orientated in the same direction (same N_{thio}–Fe–N_{thio} axes) in the triclinic structures SCO1 and SCO3B, or in two alternating orientations (related by symmetry) in the monoclinic structure SCO3A (Fig. 63).

The π–π interactions are stronger in SCO3B (intercentroid distances of 3.364 and 3.257 Å) than in SCO3A (distances of 3.608 and 3.352 Å). The strongest inter-sheet interactions for SCO1 occur through the lattice chloroform molecules, with S···Cl and C–H···N contacts of 3.528 and 3.412 Å, respectively. The resulting inter-layer Fe···Fe distance is 11.69 Å. Both in SCO3A and SCO3B, the complexes are directly interacting through interlayer S···H–C contacts of 3.482 and 3.621 Å, respectively, generating inter-layer Fe···Fe distances of 12.375 and 9.343 Å (see Fig. 63).

These packing differences affect both the temperature of the SCO and its cooperative character and completeness (Fig. 62, bottom). The dramatic increase in $T_{1/2}$ between SCO3B and SCO4, of about 150 K, is much larger than expected from the sole influence on the ligand-field strength of the less electronegative $NCSe^-$ anion, for which shifts of only 20–50 K have been observed. Therefore, although the structure of the selenium derivative has not been reported, it appears that packing features participate as well in the observed increase of $T_{1/2}$. Indeed, small variations in the packing between very similar complexes can justify significant disparities in the SCO behaviour within a family of related compounds. The SCO curves for the solvent-free compound SCO3 are clearly more cooperative, as a result of direct inter-sheet interactions. In contrast, these interactions occur through the solvent molecule for the chloroform solvate SCO1, or the analogous hydrated compound. For the polymorph SCO3B, these interactions take place between identical layers, resulting in a much shorter interlayer Fe···Fe distance; in addition, it also exhibits the shortest π–π interactions within the sheets. These peculiarities can reasonably explain the particular SCO properties of SCO3B, which are the most cooperative of the series. The two-step SCO curve of the polymorph SCO3A is also ascribed to inter-sheet interactions. In fact, the existence of two types of sheets of differently oriented complexes creates a competition between short- and long-range interactions, which are known to potentially produce intermediate HS-LS states, and therefore two-step transitions [165]. Photomagnetic studies have been performed with both the chloroform solvate SCO1 [173] and the solvent-free compound SCO3A [174]. In both cases, the relaxation from the light-induced HS state was exponential, *i.e.* mostly non-cooperative. To avoid the effect of this relaxation, the crystal structure of the excited phase of SCO3A was solved through pump–probe experiments at 40 K [174]. The resulting structure was very similar to the HS one at 200 K.

4.1.2. Extended systems (2D)

The only other SCO compound containing a 1,2,3-triazole ligand reported so far, namely [Fe(**L225**)$_3$]$_n$(ClO$_4$)$_{2n}$ (Fig. 64), is a 2D coordination polymer built from the bridging ligand 1,4-di(1,2,3-triazol-1-yl)-butane (**L225**) [175]. In the $P\bar{3}$ structure, each 1,2,3-triazole ring coordinates the iron(II) ions in a monodentate fashion, generating regular octahedral Fe(triazole)$_6$ building blocks

that are connected to six neighbors (Fe···Fe distance of 11.719 Å) to produce 2D sheets (Fig. 64). The ligand is sitting on an inversion centre and has a *Gauche–Trans–Gauche* conformation; hence, the triazole rings of **L225** are *trans* and therefore allow the bridging of neighboring iron(II) ions. The resulting layers are arranged in a parallel manner along the *c* axis, leaving triangular channels in which the perchlorate anions are pillared. The layers interact through several C–H···O–Cl hydrogen bonds involving the perchlorate ions. The inter-layer Fe···Fe distance (7.804 Å) is shorter than the intra-layer one.

$[Fe(\mathbf{L225})_3]_n(ClO_4)_{2n}$ exhibits a complete SCO with a 8 K wide hysteresis $T_{1/2}^{up} = 109\ K$ and $T_{1/2}^{down} = 101\ K$. While the 2D sheet structure with the direct Fe–Fe links and the inter-sheet hydrogen bonding interactions may produce a cooperative SCO, it is unclear whether the hysteresis can be ascribed only to such cooperativity. Indeed, the branches of the hysteresis loop are not parallel to each other: the warming branch presents some asymmetry with a change of slope at $T > T_{1/2}^{up}$. This asymmetric character is confirmed by thermal measurements, the anomaly associated with the SCO in differential scanning calorimetry (DSC) upon warming being clearly associated to two peaks. Although the LS structure could not be solved, it appears that a structural phase transition is coupled to the SCO in $[Fe(\mathbf{L225})_3]_n(ClO_4)_{2n}$, which is probably at the origin of both the occurrence of hysteresis and the asymmetric SCO curves.

4.2. Complexes of 1,2,4-triazoles

Ligands containing a 1,2,4-triazole ring have been extensively used for the design and preparation of SCO materials. In particular, this ring has been combined with a wide range of other donors resulting in numerous molecular complexes of nuclearities ranging from 1, by far the most common, to 3. Although the 1,2,4-triazole ring itself has several coordination bridging modes, and many ligands with more than one 1,2,4-triazole groups have been used, the number of extended coordination networks with this donor exhibiting SCO properties is extremely limited, except for unidimensional systems formed through the $\mu_{1,2}$ bridging mode (Scheme 7). This is most likely due to the fact that monocoordinating 1,2,4-triazole ligands generate weak ligand fields and almost systematically yield HS coordination compounds. For all the few exceptions showing a SCO behaviour, the triazole ring is involved in some supramolecular interactions that compensate this effect through the modification of its donor strength. SCO triazole compounds have been partially reviewed in 2004 [170,171] and 2007 [172].

4.2.1. Monomers

Terminal 1,2,4-triazole ligands are weak donors; therefore, they stabilize the HS state of the corresponding mononuclear coordination compounds. A recent extensive review on mononuclear iron(II) complexes obtained from nitrogen-donor ligands[172] includes all triazole-containing mononuclear SCO complexes reported at the time. In the present section, an updated exhaustive list of such complexes is given together with relevant details and properties (Table 4). However, only a selected example per type of ligand/complex geometry/composition will be described.

4.2.1.1. Monodentate triazole. Similarly to the [Fe(hydrotris(pyrazol-1-yl)borate)$_2$] system, known to display an abrupt SCO in some cases above RT [176], the 1,2,4-triazole analogue $[Fe(\mathbf{L62})_2]$ consists of a mononuclear neutral complex, with an iron(II) center surrounded octahedrally by six N1-donating 1,2,4-triazole rings (Fig. 65). $[Fe(\mathbf{L62})_2]$ crystallizes as a hexahydrate LS compound, as indicated by the average Fe–N bond length of 1.99 Å at RT [177]. The anhydrous form, however, displays an abrupt and complete SCO at *ca.* 340 K [178]. The SCO was also shown to take place in solution. Dilution with zinc(II) of the crystalline material result in a drastic diminution of the cooperative character of the SCO [178]. This compound is the only monomeric iron(II) SCO complex from monodentate N1-1,2,4-triazole ligand(s). Nevertheless, it should be noted that the N2 nitrogen of the azole rings in $\mathbf{L62}^-$ is connected to a boron atom; therefore, the 1,2,4-triazole moiety in $\mathbf{L62}^-$ acts as a N1,N2-bridging ligand. This particular circumstance apparently allows the generation of a favorable environment for the SCO to occur.

4.2.1.2. Ligands with the 1,2,4-triazole ring pertaining to a di-imine coordination pocket. With di-imine triazole ligands, the SCO phenomenon has been observed either in $[Fe(\mathbf{L})_3]^{2+}$ complexes (**L = HL69, L226, HL218, L227, HL228, and L208**) with different anions and distinct degrees of hydration, or in $[Fe(\mathbf{L})_2(X)_2]$ complexes (**L = L199, L229, L200, and L230**) in which **L** is always a chelating ligand and X is a terminal cyanide-like donor such as

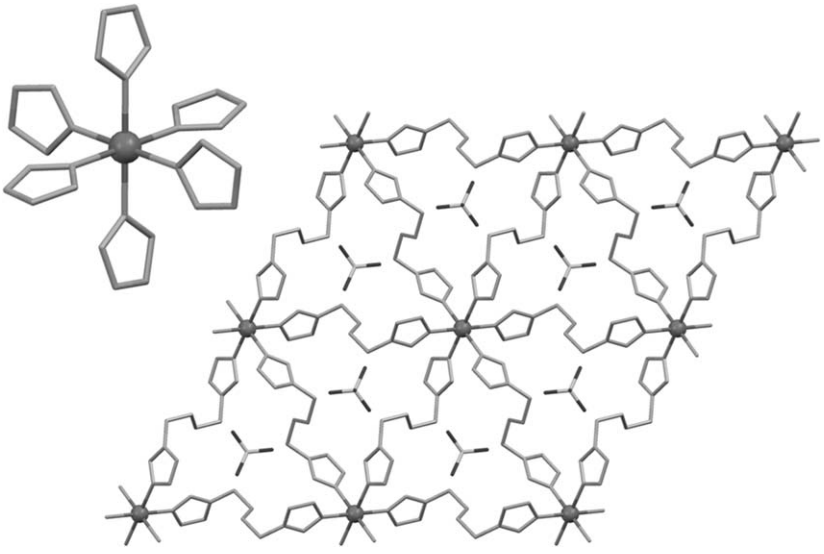

Fig. 64. (left) The Fe(1,2,3-triazole)$_6$ unit constructing the 2D framework of $[Fe(\mathbf{L225})_3]_n(ClO_4)_{2n}$ [175]. (right) A view along the *c* axis showing the planes in the structure of $[Fe(\mathbf{L225})_3]_n(ClO_4)_{2n}$ with triangular voids occupied by perchlorate ions.

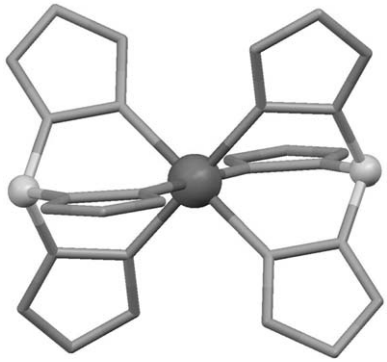

Fig. 65. A view of the only SCO complex with terminal mono-coordinating 1,2,4-triazole ring, [Fe(**L62**)$_2$] [177].

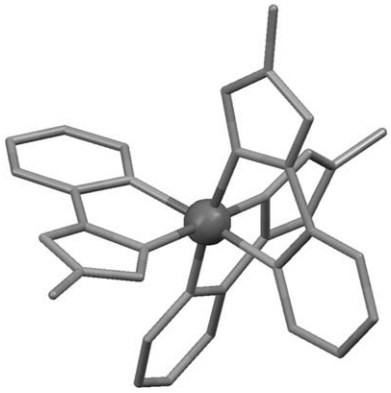

Fig. 67. The cationic complex in [Fe(**L208**)$_3$](ClO$_4$)$_2$·H$_2$O [101].

NCS^-, $NCSe^-$, $N(CN)_2^-$ or $TCNQ^-$ (see Table 4). The asymmetric nature of 2-pyridyl-1,2,4-triazole ligands may lead to the formation of $[Fe(\mathbf{L})_3]^{2+}$ complexes having a facial or a meridional geometry. In all crystal structures so far solved, the sole meridional geometry has been observed, which is common for iron(II) coordination compounds. Thus, *mer*-[Fe(**HL69**)$_3$](BF$_4$)$_2$·2H$_2$O (Fig. 66) displays a very gradual SCO centered at ca. 135 K, and presents a large residual HS fraction of ca. 30% [179]. Its crystal structure has been reported both in the HS state (295 K) and in the LS state (90 K). In addition to the usual HS-to-LS shortening of the Fe–N average bond length (ca. 0.15 Å), the chelate bite angle of the ligand increases and the FeN_6 octahedron is more regular in the (mostly) LS phase. The anion and solvent areas could not be resolved, with a strong rotational and positional disorder of the BF_4^- anions suggesting the absence of distinct intermolecular interactions. Detailed calorimetric as well as photomagnetic studies have been reported for this system [180]. The *fac* geometry with bis-N-donor chelates apparently favors the LS state [181,182].

A similar solid-state structure is observed with the ligand 1-methyl-3-(pyrazin-2-yl)-1,2,4-triazole (**L208**) in the hydrated complex [Fe(**L208**)$_3$](ClO$_4$)$_2$·H$_2$O (Fig. 67). This compound exhibits a LS state up to 296 K, with a regular octahedron and characteristic HS Fe–N bond lengths, both at 150 and 296 K [101]. The anhydrous compound does exhibit a SCO behaviour resembling that of [Fe(**HL69**)$_3$](BF$_4$)$_2$·2H$_2$O, with a gradual transition centered at ca. 175 K and a residual HS fraction of about 40%. Interestingly, the PF_6^- and BF_4^- complexes display pure LS populations at temperatures up to ca. 290 K, with their SCO being centered around 400 K. The crystal structures of these anhydrous complexes could not be solved.

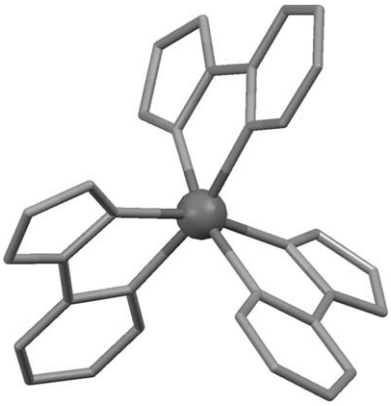

Fig. 66. The cationic complex in [Fe(**HL69**)$_3$](BF$_4$)$_2$·2H$_2$O showing the *mer* configuration adopted in this type of SCO complexes [179].

Such difficulties in obtaining good crystals and/or good quality crystal structures are very common for this type of systems [101,179,183–185]. In most reported structures, highly disordered areas, including the anions and/or unresolved solvent molecules, were detected. This almost systematic poor crystallinity/disorder most likely explains the residual HS fractions observed in bulk samples of these materials. In addition, the presence of such highly disordered areas results in isolated SCO complexes, hence justifying the gradual character of the transition curves observed invariably for these systems. The apparent absence of significant intermolecular interactions between the complexes in the solid state is quite surprising since most of the ligands used have at least one nitrogen atom (hydrogen bond acceptor) and in some cases an N–H moiety (hydrogen bond donor) that in principle should allow the formation of hydrogen-bonding contacts. Besides, the preparation of these compounds is often performed in water or alcoholic conditions (which should favour the generation of hydrogen-bonding networks).

Among the di-imine triazole ligands, the case of 3,5-bis(pyridin-2-yl)-1,2,4-triazoles (usually abbreviated as Rdpt, R being the substituent on the N4 of the triazole ring) is peculiar as this family of ligands contain two coordination pockets, and may thus form dinuclear compounds (see below). SCO compounds with these ligands have been reviewed recently [186a]. In monomers, the presence of the second pyridyl moiety may render the formation of a $[Fe(\mathbf{L})_3]^{2+}$ complex more difficult. Nevertheless both the *mer* and *fac* $[M(Rdpt)^3]^{2+}$ complexes have been reported with several first-row transition-metal ions [186a], and this arrangement of Rdpt ligands with iron(II) has recently been reported, although no SCO was observed [186b].

A synthetic strategy to obtain mononuclear complexes with this type of ligands is to combine in the same reaction Rdpt with other nitrogen donors. An interesting example is [Fe(**L199**)(DAPP)](ClO$_4$)$_2$ (Fig. 68), obtained from the tetradentate chelating ligand bis-(3-aminopropyl)(2-pyridylmethyl)amine (DAPP). This iron(II) compound shows an abrupt SCO with a 10 K wide hysteresis in the range 165–185 K (see Fig. 68, bottom) [187].

Structural investigations at 123 K (LS state) and at 183 and 293 K (HS state) revealed the importance of both, a network of intermolecular interactions and two order-disorder transitions involving the methylene carbon of the ligand DAPP and one of the two perchlorate ions for the occurrence of the cooperative SCO observed. Indeed, hydrogen-bonding contacts between the perchlorate ions, the amino group of **L199** and the methylene groups of DAPP result in the formation of layers of interacting complexes. These layers further interact through π–π stacking between pyridyl rings of **L199** ligands. Although it is unclear whether the order–disorder transitions are strongly coupled to the SCO phe-

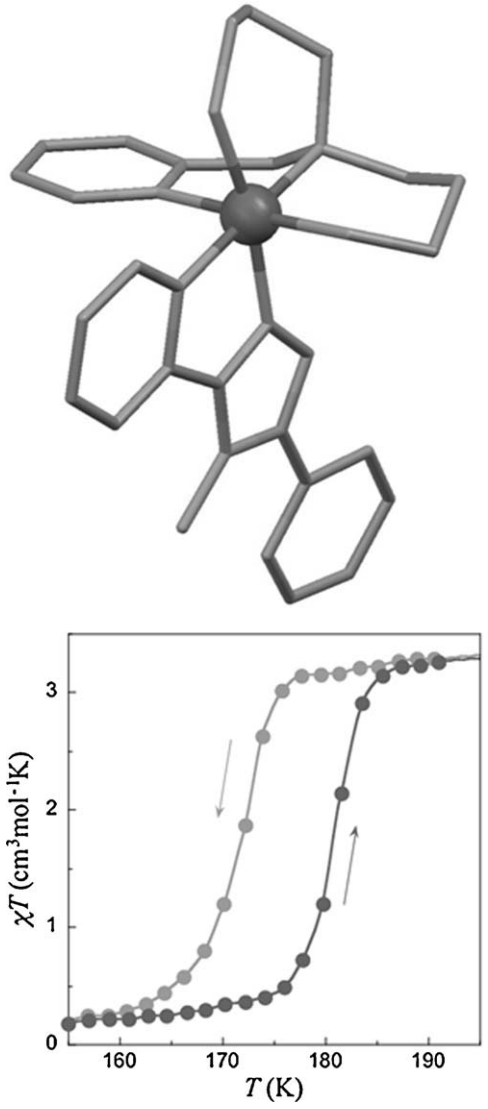

Fig. 68. The cationic complex (top) in [Fe(**L199**)(DAPP)](ClO$_4$)$_2$ and a representation of its cooperative SCO (bottom) with a portion of the χT versus T plot showing the observed 10 K wide hysteresis [187]. Light/dark grey dots correspond to data upon cooling/warming.

nomenon, an ordering of the DAPP ligands occurs in the range of the HS to LS transition, namely between 183 and 123 K, while the perchlorate ion is disordered at 183 K, just above the transition. Studies on the coupling between the order–disorder and the SCO in this compound using adiabatic calorimetry coupled to spectroscopic experiments and vibrational calculations were later reported, evidencing a self-grinding effect of the crystals upon cycling the transitions [188].

Another strategy to obtain mononuclear compounds with di-imine chelating ligands consists in combining them with cyanide-type coordinating anions. This approach is widely used to obtain mononuclear SCO complexes, also with triazole-based ligands. While almost only the thiocyanate and selenocyanate anions have been used, a large series with relative N-donor strength $NCO^- < NCS^- < NCSe^- < N(CN)_2^- < C(CN)_3^- < NCBH_3^- < NCCH_3^- < < CN^-$, offers a unique way to adjust the ligand field around the metal ion. The most commonly used anion is thiocyanate, and all corresponding complexes exhibiting SCO have a *trans* configuration, with four nitrogen donors from two di-imine ligands in the equatorial positions and two axial cyanide-type donors. An remarkable illustration of this type of materials is the neutral

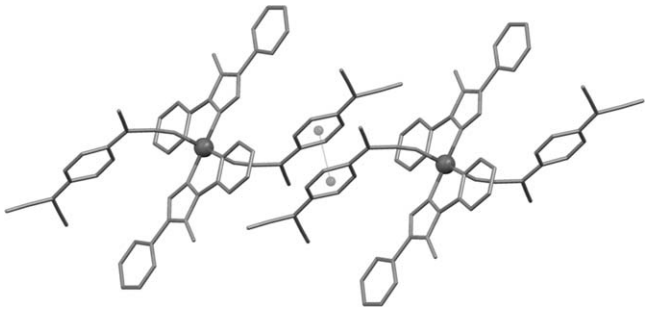

Fig. 69. π–π stacking of two TCNQ ions from neighboring neutral [Fe(**L199**)$_2$(TCNQ)$_2$] complexes [189], resulting in the formation of supramolecular chains.

complex [Fe(**L199**)$_2$(TCNQ)$_2$], obtained from **L199** and the radical anion TCNQ$^-$, which represents the first hybrid SCO compound [189]. Its SCO curve is complete and gradual, the spin change occurring over more than 100 K and being centered at ca. 280 K. Its structure was solved at 100 K (LS state) and 293 K (mostly HS state). The TCNQ radical anions are mono-coordinated through one of their nitrile group, the corresponding average Fe–N bond length exhibiting one of the largest reported LS-to-HS variation (+0.23 Å). This change of distance was ascribed to the extended π system of TCNQ, which favours back-bonding in the LS state, and thus shorter Fe–N bond lengths. The TCNQ moieties of neighboring complexes are strongly π-stacked (centroid-to-centroid distances of 3.265/3.321 Å in the LS/HS states, respectively), forming 1D supramolecular chains (see Fig. 69). The stacked radical dimers are thus strongly antiferromagnetically coupled and are therefore diamagnetic over the whole temperature range studied. This is common with coordinated TCNQ. As in most related compounds, the HS-to-LS transition induces an increase of the di-imine bite angle, and a comparatively more regular octahedral environment.

A number of similar 1:2 complexes with other terminal anionic donors or Rdpt ligands have also been isolated (see Table 4) and reviewed recently [186a]. Since then, two new polymorphs (C and D) of *trans*-[Fe(**L199**)$_2$(NCS)$_2$] have been reported that exhibit SCO properties for only half of the iron(II) centers [190]. While in the original polymorph A [191] there is only one type of complex arranged in π-stacked layers, in polymorphs C and D there are two types of such layers, with different orientations, corresponding to two crystallographic iron sites. Similarly to the family of *trans*-[Fe(**L224**)$_2$(NCX)$_2$] complexes, structural analysis indicates that the varying SCO properties within the different polymorphs of this compound (see Fig. 70 bottom) are mostly dominated by the relative strength of the π–π interactions between **L199** planes in the stacked layers, as well as by inter-sheet interactions through the thiocyanate ions (Fig. 70, top). The planarity of the **L199** ligand is one of the parameters which differ among the different polymorphs of this compound. The HS state of this system has been trapped thermally and through light-irradiation, allowing the observation of both incommensurate and commensurate modulated structures in two different polymorphs [174,190]. Very recently, a novel compound has been reported that contains co-crystallized *cis* and *trans* isomers of [Fe(**L200**)$_2$(NCS)$_2$] in a 2:1 ratio. A partial SCO of ca. 1/3 of the iron(II) ions around 180 K in the unsolvated compound is observed that is ascribed to the *trans* isomer [192]. Strikingly, the pure *trans* isomer does not show a SCO behaviour, thus indicating an important role played by the packing in the *cis-trans* co-crystal.

4.2.1.3. Ligands with a fused 1,2,4-triazole ring. With a fused 1,2,4-triazole ring, the only SCO complex reported so far has been isolated recently using the same synthetic procedure as above, with NCS$^-$ anions [193]. The triclinic neutral complex [Fe(**L230**)$_2$(NCS)$_2$] has

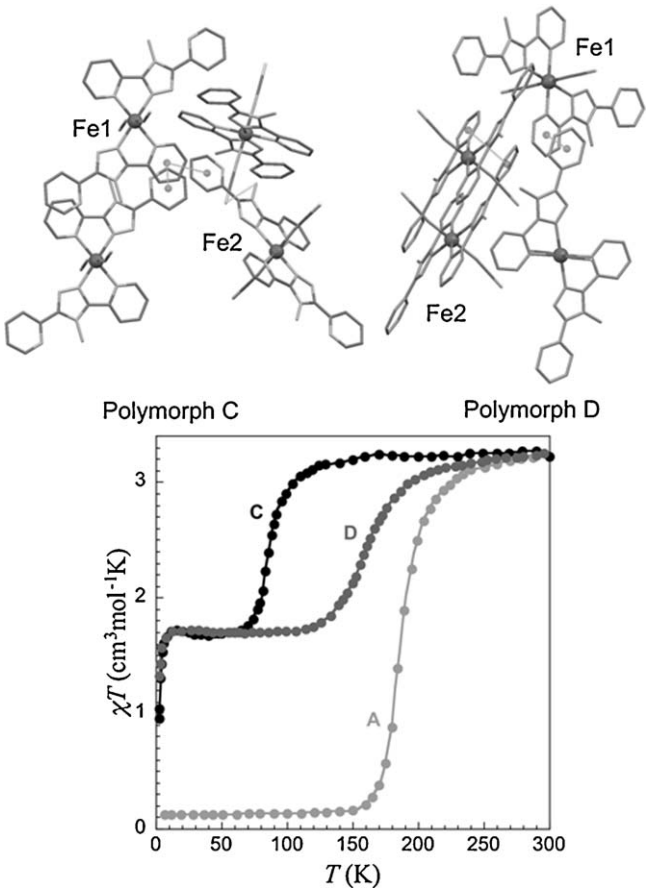

Fig. 70. Top: Views of the packing in the structures of polymorphs C and D of *trans*-[Fe(**L199**)$_2$(NCS)$_2$] showing the π–π stacking interactions (thin lines) within the layers of complexes and between these layers [190]. Bottom: χT versus T plot showing the SCO properties of the different polymorphs of *trans*-[Fe(**L199**)$_2$(NCS)$_2$]. Polymorph B (not shown) is a HS compound at ambient pressure but shows SCO when pressure is applied (see Table 4).

a *trans* configuration (Fig. 71) and strongly resembles its 1,2,3-triazole analogue with **L224** (SCO3A), which exhibits π-staked layers with alternating orientations (see Fig. 62, top). The main structural differences are the tighter bite angle of the 1,2,3-triazole analogue, and the absence of solvent molecules in the structure of [Fe(**L230**)$_2$(NCS)$_2$].

In addition, [Fe(**L230**)$_2$(NCS)$_2$] exhibits π-stacking interactions between neighboring complexes forming layers between shifted planes, therefore leading to weaker interactions. Although similar S···H–C interlayer interactions (3.490 Å) are observed, the differences most likely justify the comparatively more gradual (more than 100 K wide) SCO observed for [Fe(**L230**)$_2$(NCS)$_2$], centered at ca. 270 K. Quite remarkably, $T_{1/2}$ shows an increase of ca. 150 K with respect to the 1,2,3-triazole analogue.

4.2.1.4. Ligands with 1,2,4-triazole pertaining to a tris-imine coordination pocket. Chelating tris-imine ligands bearing either one or two 1,2,4-triazole ring(s) have also been used to prepare mononuclear iron(II) SCO complexes, isolated as hydrated [Fe(**L**)$_2$]$^{2+}$ salts with various anions (see Table 4). These complexes have a similar FeN_6 octahedron formed by two η^3 chelating ligands whose planes are roughly perpendicular (see Figs. 72 and 73). With the symmetric di-(1,2,4-triazol-3-yl)-pyridine ligands **H$_2$L231** and **H$_2$L232**, the complex core is very similar to that of the pyrazole analogues, which have been widely investigated due to the very cooperative SCO displayed by their anhydrous forms [194]. In the case of 1,2,4-triazoles, all hydrates, e.g. those that could be structurally

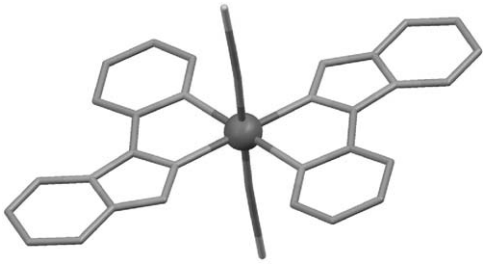

Fig. 71. The neutral complex [Fe(**L230**)$_2$(NCS)$_2$] [193], the only SCO compound isolated with a fused 1,2,4-triazole ligand.

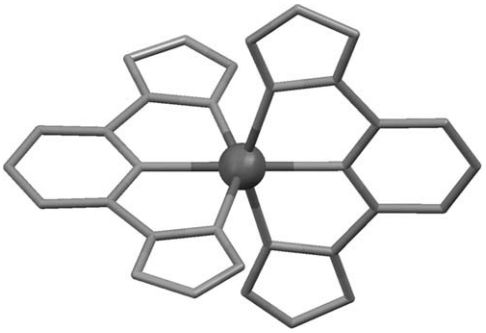

Fig. 72. A view of the di-ter-imine iron(II) complex in [Fe(**H$_2$L231**)$_2$](NO$_3$)$_2$·2H$_2$O [172].

characterized such as [Fe(**H$_2$L231**)$_2$](NO$_3$)$_2$·2H$_2$O (Fig. 72), were HS compounds [172]. The anhydrous chloride salt was LS, while the anhydrous BF_4^- and ClO_4^- salts did show a gradual SCO [195]. Unfortunately, these anhydrous compounds could not be structurally characterized. This is reminiscent of the pyrazole systems, whose hydrates have gradual SCO and could be structurally characterized, while the anhydrous forms with cooperative SCO properties at higher temperatures could not. This sensitivity to water has been proposed to be used in sensors for moisture detection [196].

Several hydrated complexes obtained from 2-(1,2,4-triazol-3-yl)-1,10-phenantroline, substituted or not with one or two methyl group(s) show SCO properties and have been structurally characterized [737–738]. For instance, the monohydrate compound

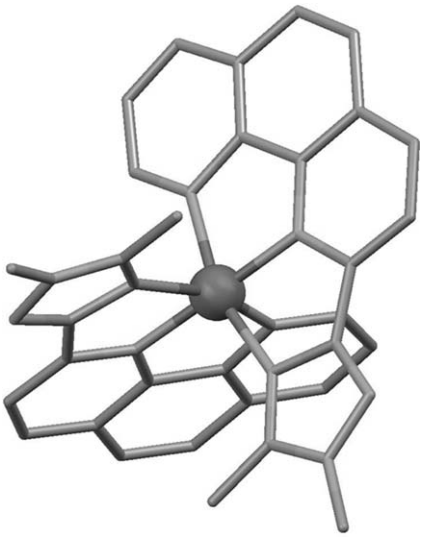

Fig. 73. The cationic complex in [Fe(**L236**)$_2$](ClO$_4$)$_2$·H$_2$O [738], with the almost perpendicular ter-imine ligands **L236**.

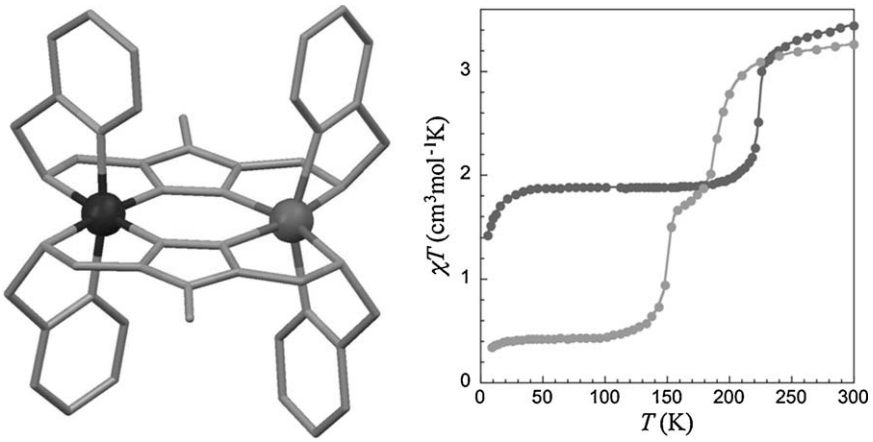

Fig. 74. Left: The cationic complex in the low-temperature LS:HS structure of $[Fe_2(\mathbf{L237})_2](BF_4)_4$·DMF showing the constrained environment of the iron(II) sites [198]. The iron(II) site in the LS state is highlighted in darker grey. Right: χT versus T plot showing the SCO properties of the two SCO dimers with Rdtp ligands, $[Fe_2(\mathbf{L75})_2(NCBH_3)_2py_2]$ (light grey) and $[Fe_2(\mathbf{L237})_2](BF_4)_4$·DMF (dark grey).

$[Fe(\mathbf{L236})_2](ClO_4)_2{\cdot}H_2O$, whose cation is shown in Fig. 73, exhibits a very gradual but complete, 200 K wide, SCO centered at ca. 265 K. The structure shows positional disorder of the perchlorate anions, and although the water molecule forms a hydrogen bond with one of these perchlorate groups, the cation does not participate in any intermolecular network, thus justifying the very gradual character of the SCO for this compound.

4.2.2. Dimers

The $\mu_{1,2}$ bridging coordination mode is quite common for 1,2,4-triazoles, as seen in section 3. Nevertheless, it is often complemented by an additional bridging moiety such as a halide, and the effect of such weak donors on the ligand-field strength usually results in a HS ground state for the iron(II) center of dimeric species. There are only three exceptions reported so far. The first one belongs to the family of the dinuclear compounds $[Fe_2(\mathbf{L75})_2X_2(solv.)_2]$ [68,186], in which each pocket of the $\mathbf{L75}^-$ ligand chelates an iron(II) ion. The two deprotonated **L75**-ligands in *trans* configuration generate a double planar 1,2-triazolate bridge, the axial positions of the coordination sphere of the iron(II) ions being completed by coordinated anions, *i.e.* NCS^-, $NCSe^-$, $NCBH_3^-$ and Cl^-, and either methanol or pyridine solvent molecules. Though, a SCO behaviour has only been observed for $[Fe_2(\mathbf{L75})_2(NCBH_3)_2py_2]$ [197]. Quite interestingly, this compound displays a complete SCO with two distinct steps, and a small plateau in the range 155–185 K (see Fig. 74 right), suggesting that the complex may exist in three different states, namely the [HS–HS], [HS–LS] and [LS–LS] states. Unfortunately, no crystal structure was reported for this specific compound, therefore impeding to discard the possibility of a 1:1 [HS–HS]:[LS–LS] mixture.

A similar dinuclear complex, namely $[Fe_2(\mathbf{L237})_2](BF_4)_4$·DMF, is formed with the ligand 3,5-bis-(2-pyridylmethyl-methylamino)-4-amino-1,2,4-triazole (**L237** or PMAT), a bis-terdentate ligand containing two chelating N,N pockets formed by the N1 and N2 donors of a central triazole ring, two secondary amine nitrogens, and two pyridyl arms [198a]. The latter N-donors occupy the axial positions of both iron(II) ions, while the equatorial positions are occupied by two double coplanar 1,2-triazole bridges and the secondary amine donors. Due to the rigidity of the ligand, a rather tightly constrained complex is obtained (Fig. 74, left). This compound exhibits an abrupt SCO involving only one of the two iron ions. Its crystal structure determined in the low-temperature phase, *i.e.* at 123 K, clearly demonstrates that the complex is trapped in the intermediate localized [LS–HS] state. Mössbauer studies later confirmed this mixed-spin state [198b], and the effect of applied pressure and irradiation were also investigated [198c]. The occurrence of the mixed [LS–HS] spin pair is most likely due to constraints inherent to the complex. This unique result highlights the potential of suitably designed macrocyclic or acyclic polydentate ligands implementing a central bridging moiety, such as a 1,2,4-triazole ring, to generate cooperative polymetallic SCO molecules.

Besides these two peculiar compounds, SCO complexes bearing N1,N2 bridging triazoles involve triple-triazole bridges. The stability of the resulting conformation in these triple-triazole bridges results in a tendency to extend the coordination into 1D systems. Consequently, the isolation of oligomeric systems showing SCO properties and based on these triple triazole bridges is quite difficult and has been limited to only trimers (see following section), and one sole dimer [199]. The two iron(II) ions of the dimer are bridged solely by three 4-(p-tolyl)-1,2,4-triazoles (**L238**), through their N1,N2 pairs. The coordination sphere of the iron(II) centers is completed by two thiocyanate anions and one terminal **L238** ligand. The neutral dimer $[Fe_2(\mathbf{L238})_5(NCS)_4]$ co-crystallizes in a 2:1 ratio with a neutral monomer of formula $[Fe(NCS)_2(\mathbf{L238})_2(H_2O)_2]$, thus forming a pentanuclear supramolecular assembly through strong H-bonds between the free N2 atom of the terminal **L238** of the dimers and the coordinated water molecules (see Fig. 75). The dimeric coordination unit in $[Fe_2(\mathbf{L238})_5(NCS)_4][Fe(NCS)_2(\mathbf{L238})_2(H_2O)_2]$ exhibits *cis* thiocyanate ions whereas in similar complexes with other metal(II) ions (see Section 3), these anions are in *trans* conformation. The *cis* coordination of the NCS^- ions is forced by the hydrogen bond formed

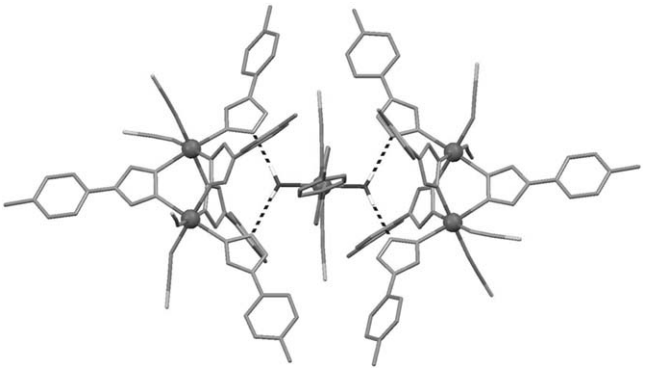

Fig. 75. A view of the pentanuclear assembly in $[Fe_2(\mathbf{L238})_5(NCS)_4]_2[Fe(NCS)_2(\mathbf{L238})_2(H_2O)_2]$ [199]. Hydrogen bonds connecting the two SCO dinuclear units to the central HS monomer are shown as dashed lines.

between the terminal **L238** ligand and the central iron(II) unit. Similarly to [Fe(**L62**)$_2$] where the N1-donating triazole rings have their N2 atom linked to a boron atom, these hydrogen bonds probably induce a modification of the donor strength of the terminal N1-donating atom of the **L238** ligand. Indeed, while the iron(II) ions bearing monocoordinated 1,2,4-triazole are usually HS, such as the central metal ion of [Fe$_2$(**L238**)$_5$(NCS)$_4$]$_2$[Fe(NCS)$_2$(**L238**)$_2$(H$_2$O)$_2$], the iron(II) ions in the dinuclear unit exhibit a complete, 40 K wide SCO, centered at 111 K.

4.2.3. Trimers

As mentioned above, polynuclear linear-chain products can be formed through successive triple $\mu_{1,2}$ triazole bridges that connect the transition-metal ions. The iron(II) compounds are among the most interesting and widely studied SCO compounds, and will be described in the next section. Nevertheless, so far no crystal structure of such coordination polymers could be obtained, and they therefore remain ill-defined polymeric materials, for which smaller iron(II) oligomeric well-defined systems can serve as models. In this respect, trinuclear complexes seem to be for geometric reasons the most stable models of 1D repeated triple triazole bridges. A number of such compounds exhibiting SCO properties, with formulae [Fe$_3$(4-R-1,2,4-triazole)$_6$(H$_2$O)$_6$](A)$_6$·nH$_2$O or [Fe$_3$(4-R-1,2,4-triazole)$_8$(H$_2$O)$_4$](A)$_6$·nH$_2$O, have been isolated. The disparities between theses systems result from the different substituents R on the 4-position of the 1,2,4-triazole ligand, the anion A and the degree of hydration n (see Table 4).

The first trinuclear compound of the series was reported in 1983 with the ligand **L193** [200], soon after the first reports on 1D polymers, by the same research group at Leiden University [201]. The structures, solved at 300 and 105 K (corresponding to a HS and a LS state for the central iron(II) ion, respectively) [202], show a linear trinuclear unit formed through the bridging of the three iron(II) ions by two successive groups of three N1,N2-donating triazole ligands. The triazole units are shifted from one bridge to the other resulting in a propeller arrangement (Fig. 76, top). Hence, the central iron(II) ion is octahedrally surrounded by six triazole N-donors, a favorable feature for the occurrence of SCO. Actually, the main structural variations upon cooling are the decrease of about 0.14 Å of the central Fe–N bond lengths, associated with the SCO of this ion, and the slight reorientations of the triazole rings induced by the volume reduction of the coordination sphere of the central iron(II). The octahedral environment of each outer iron(II) ion is completed by three water molecules, that form hydrogen bonds with the lattice triflate anions.

The structures of the other members [121,203–205,739,740] of this family of compounds are very similar. The most important variation in this series is the replacement of one of the water molecules coordinated to the outer iron(II) ions by a terminal triazole ligand, for instance in [Fe$_3$(**L250**)$_8$(H$_2$O)$_4$](BF$_4$)$_6$ and [Fe$_3$(**L251**)$_8$(H$_2$O)$_4$](NO$_3$)$_6$. In the former compound, the three iron(II) ions remain HS, while the central iron(II) ion displays a gradual SCO phenomenon in all other cases (the external iron(II) centers remaining in HS state). The most cooperative SCO transition is observed for the compound with the ligand **L193**, whereas the other ones present similar albeit more gradual transitions, at temperatures ranging from 185 to 290 K. Even the compound obtained from the ligand 4-hydroxyethyl-1,2,4-triazole (**HL82**) [204], in an attempt to favor hydrogen-bonding interactions and thus intermolecular contacts, exhibits a gradual transition. Although the environment of the central iron(II) is analogous in this series of compounds, both the substituent on the triazole ligand and the anion have an obvious impact on the transition temperature (see Table 4 and Fig. 76, bottom).

It can be noticed that two linear trinuclear complexes have been very recently reported with the ligands 4-isopropyl-3,5-di-(pyrid-2-yl)-1,2,4-triazole and 4-phenyl-3,5-di-(pyrid-2-yl)-1,2,4-triazole in combination with terminal thiocyanate anions [206]. In these complexes, the bidentate pockets from two Rdpt ligands bridge the iron(II) ions, while two other Rdpt molecules act as chelating ligands to bind the external iron(II) ions. The octahedral FeN$_6$ environment of the three iron(II) ions is completed by two *trans* NCS$^-$ anions, thus resulting in a coordination sphere closely related to that of mononuclear SCO complexes with dpt-type ligands. Although these complexes do not exhibit SCO properties, this similarity and the fact that they have differing spin states, respectively [LS–HS–LS] and [HS–HS–HS], is appealing since slight modifications of the electron-donating ability of the 4-substituent on the central triazole ring may yield new SCO trinuclear complexes.

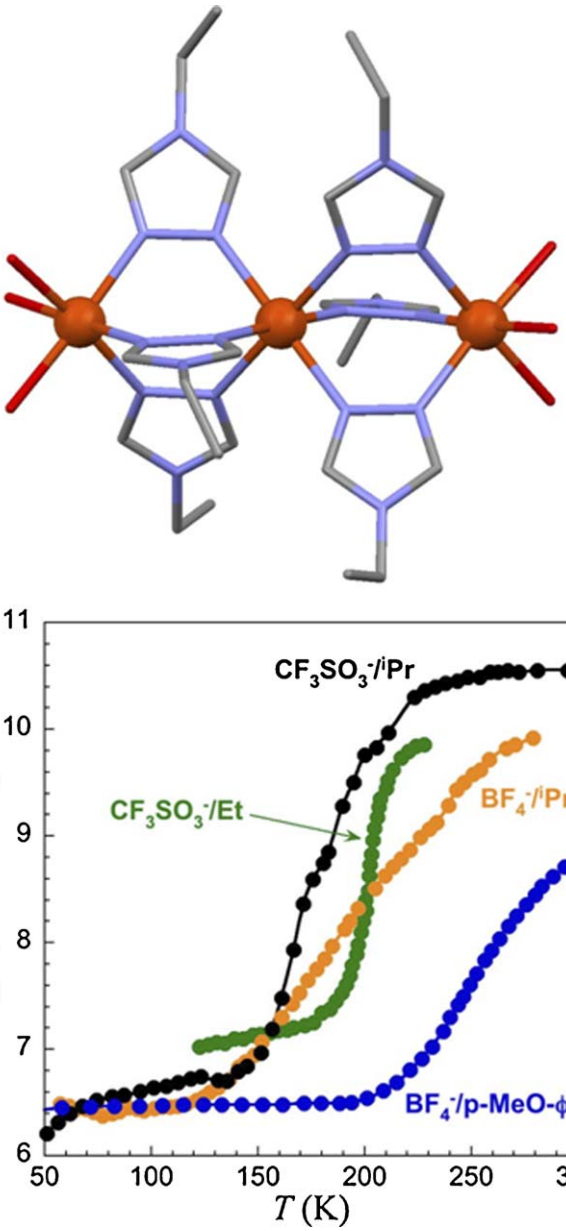

Fig. 76. (top) The cationic complex in the first reported trinuclear SCO compound, [Fe$_3$(**L193**)$_6$(H$_2$O)$_6$](CF$_3$SO$_3$)$_6$ [202]. Only the central iron(II) exhibits a SCO behaviour. (bottom) χT versus T plot showing the SCO properties of four similar trinuclear compounds, differing in the substituent on the 4-position of the 1,2,4-triazole and in the anion used.

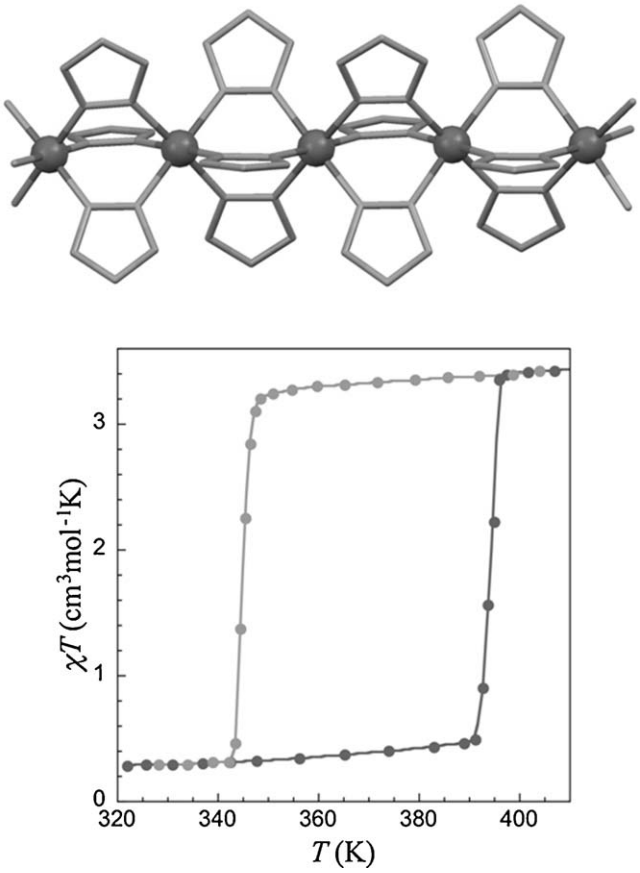

Fig. 77. (top) schematics of the linear chains formed by triple N1,N2 triazole bridges. (bottom) χT versus T plot showing the extremely cooperative SCO properties with a 40 K wide hysteresis in [Fe(**HL21**)$_2$(**L21**)]$_n$(BF$_4$)$_n$ [213,214]. Light/dark grey dots correspond to data upon cooling/warming.

4.2.4. 1D compounds

The triple $\mu_{1,2}$ 1,2,4-triazole bridges between iron(II) ions present in linear trinuclear complexes tend to extend into longer linear assemblies, such as those found in structurally characterized copper(II) analogues [207–209], at least for 1,2,4-triazoles bearing 4-substituents that do not impede such assembly due to bulkiness, as would do for instance substituents at the 3 and 5 positions. The resulting iron(II) coordination polymers all exhibit SCO properties, in general with abrupt transitions apparently induced by an efficient propagation along the chains through direct covalent connections of the local modifications due to the SCO. Unfortunately, such materials are isolated as fine microcrystalline powders at best, and so far no single-crystal structure could be determined. Nevertheless, a combination of EXAFS and WAXS experiments, as well as comparisons with structurally characterized copper(II) analogues (when available) have allowed a satisfactory (structural) description of these materials [209–212]. It appears that these compounds contain finite linear chains of iron(II) ions triply bridged by triazole rings (through the N1 and N2 donor atoms) and separated by a distance of 3.6–3.7 Å, depending on the spin state (Fig. 77, top). All the iron(II) ions within the chain thus have an octahedral FeN$_6$ environment comparable to that observed for the central iron(II) ion in linear trinuclear assemblies. Consequently, these iron(II) centers hold the coordination characteristics that favor SCO properties. The coordination sphere of the terminal iron(II) ions is believed to be completed by solvent molecules, *i.e.* either water or alcohols, or N1-monodonating triazoles. The anions are expected to be located in between the linear chains, possibly interacting through hydrogen bonds with either the substituent on the triazole ligands or directly with the triazole ring. This is particularly true for the model compound [Fe(**HL21**)$_2$(**L21**)]$_n$(BF$_4$)$_n$ whose extended network of hydrogen bonds between the tetrafluoroborate anions and the C–H groups of protonated triazoles has been singled out as the origin of its unusually abrupt transitions and large hysteresis of 40 K above room temperature (Fig. 77, bottom) [213,214]. These unique cooperative properties at useful temperatures, coupled to a pronounced thermochromism (often observed for iron(II) SCO materials), and the synthetic ability to tune the material properties without losing most of its interesting features, have attracted much interest because this system appears to be ideal for potential technological applications of SCO [166].

The SCO properties of these polymeric materials can be fine tuned through variations of (i) the substituent at the N4 position of the triazole ring, (ii) the non-coordinating anions or (iii) the solvent conditions and/or solvent content. Families of compounds formulated as [Fe(4-R-1,2,4-triazole)$_3$]$_n$(A)$_{2n}$·nH$_2$O have thus been reported by several groups worldwide, a selection of relevant ones being gathered in Table 4. The donor strength of the R substituent at the N4 position can be modified, with a direct consequence on the ligand field around the iron(II) ion, and thus on $T_{1/2}$. For example, the adjustment of the composition of a mixed-ligand system, *i.e.* [Fe(**HL21**)$_{3-3x}$(**L31**)$_{3x}$]$_n$(ClO$_4$)$_{2n}$·nH$_2$O, has allowed the preparation of a material with an abrupt transition and a large hysteresis centered at 25 °C [215], which is one of the pre-requisites for a possible application in optical devices [166]. The 4-substituent can also have a strong influence on the size of the oligomeric coordination chains as well as on the cooperative character of the SCO [741]. The nature of the anion A has even a stronger effect on $T_{1/2}$. For instance, a linear correlation has been found between this temperature and the volume of spherical anions with **HL82** [216], showing that the SCO transition temperature can be fine-tuned through this simple synthetic parameter. Anions including a sulfonate group, such as p-tolylsulfonate or naphtalenesulfonate, usually yield materials that are LS at room temperature and exhibit abrupt SCO above RT [217,218]. These features have been ascribed to the formation of bridging hydrogen bonds with C–H groups from neighboring triazole rings [219]. Most interestingly, in some of these sulfonate compounds, lattice water molecules are lost irreversibly by the initial LS compound at temperatures in the range 320–340 K. The resulting dehydrated materials then exhibit SCO properties at much lower temperatures. While the stabilization effect of the LS state by lattice water molecules is well documented, the abruptness of the irreversible LS-to-HS change and the large difference of the transition temperatures between the hydrated and dehydrated materials has led to a proposed application as temperature threshold sensor [216,218].

A number of recent works on this system have indeed been devoted to the design of materials with improved potentiality for applications. Plastic composites were obtained by simple blending with polymethylmetacrylate or introducing a polymerizable function on the N4 position of the triazole [220,221]. Typical substituents of organic liquid crystals were successfully used to isolate 1D polymeric materials exhibiting SCO properties as well as a thermotropic liquid crystal phases [222]. Using long alkyl-chain substituents, it was also shown that these materials can be transferred into soft matter phases such as Langmuir–Blodgett films [223,224], and physical gels [219,225,226] without loss of their SCO properties. Along the same line, dispersable nanoparticles of these materials were also prepared [227,228], and shown to present similar properties to those of the original compound, down to a certain size. All these studies thus allow implementing additional physical properties, to access formulation tools widely used in soft-matter science, thus reducing greatly the amount of SCO material necessary to eventually build a device.

4.2.5. 2D compounds

Although 1,2,4-triazole-based ligands have allowed the isolation of an increasing number of extended coordination networks (see Section 2 of this review), the number of such compounds exhibiting SCO remains extremely limited. As mentioned before, this is due to the fact that the monodentate coordination mode of the 1,2,4-triazole ring, both through the N1 atom for 4-substituted ligands, or through the N4 for 1-substituted ones, provides a too weak ligand field and thus produces HS species. Exceptions are found when a complementary stronger donor group and/or the participation of the triazole ring in supramolecular interactions (H-bonds) result in the correct adjustment of the overall ligand-field strength around the iron(II) ion. The sole exception reported so far that has a bidimensional structure is $[Fe(\mathbf{L40})_2(NCS)_2]_n{\cdot}nH_2O$, which exhibits an abrupt transition with a symmetric 21 K wide hysteresis ($T_{1/2}^{down} = 123\ K$ and $T_{1/2}^{up} = 144\ K$, see Fig. 78) [229]. Despite its highly cooperative SCO behaviour, thus associated with a first-order transition, the compound remains in the monoclinic *C*2/*c* space group over the whole temperature range, as shown by several detailed structural studies [230,231]. The selenocyanate analogue has also been isolated [232], and presents a SCO with a narrower 6 K wide hysteresis at higher temperatures $T_{1/2}^{down} = 208\ K$ and $T_{1/2}^{up} = 220\ K$, as expected from the relatively stronger donor character of $NCSe^-$. The bidimensional structure arises from N1,N1′-bridges in the *bc* plane, connecting to each other the equatorial positions of the distorted FeN_6 octahedra. Two *trans* thiocyanate ligands complete the coordination sphere of the iron(II) ion (Fig. 78). These are directed away from the layers, providing inter-sheet connections through van der Waals interactions and weak hydrogen bonds with the lattice water molecules sitting in the voids that are perpendicular to the *bc* plane. Most importantly, each water molecule forms two hydrogen bonds (O–H···N distances of 3.1 and 3.7 Å) with the free N2 and N2′ atoms of the **L40** ligands, thus affecting the donor strength of the N1-donating 1,2,4-triazole ligands. The absence of these interactions in the dehydrated compound, while not strongly altering the structure, results in the disappearance of the SCO [229], therefore indicating a weaker LF strength. The major structural modifications observed upon the SCO, besides the usual shortening of the Fe–N bond lengths (−0.175 Å and −0.213 Å for the Fe–NCS and Fe–N_{L40} bonds, respectively) lies in a reorientation of the NCS^- groups, which results in a more linear Fe–N–C–S geometry and a lower distortion in the LS state. The HS → LS transition also reduces the O–H···N contacts [230]. Clearly, both the direct rigid **L40** bridges between the spin-changing iron(II) ions and the hydrogen-bonding network provide the structural frame with a highly efficient propagation of the local modification of the iron(II) coordination sphere, and thus with the observed highly cooperative SCO behaviour.

Indeed, $[Fe(\mathbf{L40})_2(NCS)_2]_n{\cdot}nH_2O$ is considered to be the prime example of highly cooperative SCO compounds. Hence, the system has been the subject of numerous studies, as well as the basis for original studies and discoveries. The hysteresis loop has thus been detected with NMR spectroscopy [232], EPR spectroscopy through Mn- and Cu-doping experiments [232], or muon relaxation studies [233]. The effect of metal dilution on the SCO properties was analyzed in Fe–M (M = Co, Ni, Zn) mixed systems [234,235]. These investigations revealed that the metal dilution smoothes the transition curve and, depending on the doping metal, shifts the transition temperatures. Light-induced trapping and relaxation of the metastable HS state were studied [236], in particular through a detailed structural analysis of the different accessible states, including the thermally trapped metastable HS state [231,237]. These studies showed that the thermally and light-induced trapped HS states were virtually identical, and that the thermal SCO and the LIESST result in identical structural variations [230]. The effect of a permanent irradiation in SCO compounds, with the observation of a Light-Induced Thermal Hysteresis, was first studied and modeled on this remarkable system [236].

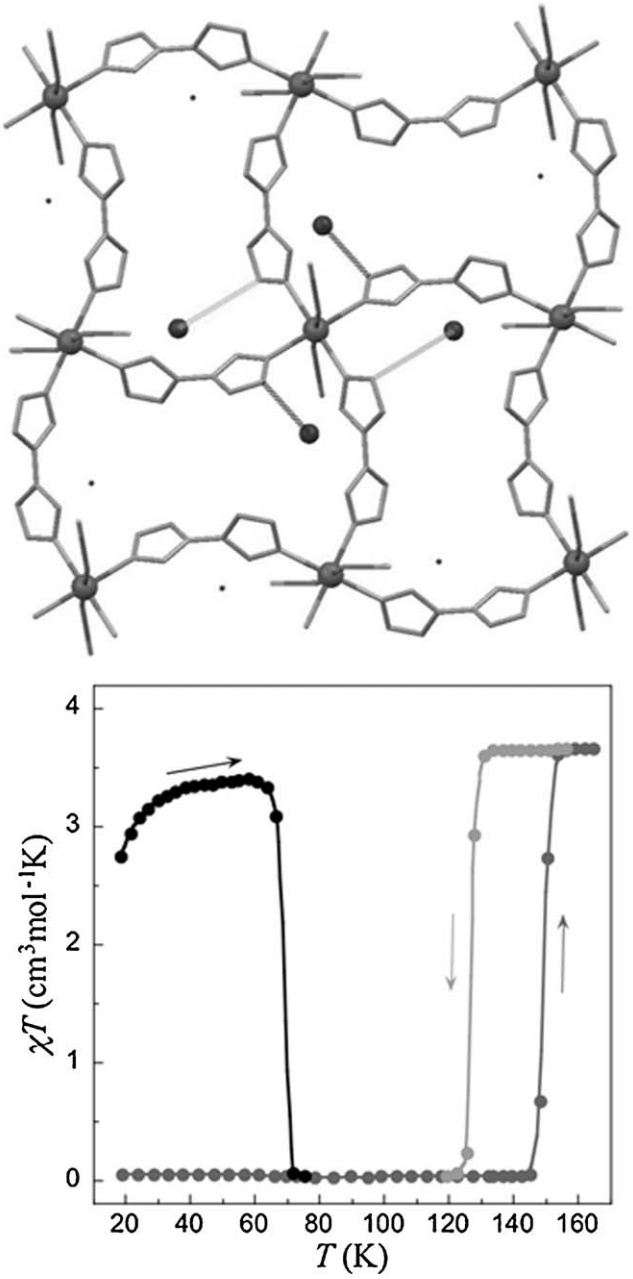

Fig. 78. (top) A view of the structure of $[Fe(\mathbf{L40})_2(NCS)_2]_n{\cdot}nH_2O$ along the *a* axis, showing the 2D grid formed by N1,N1′ **L40** bridges [229]. The two types of hydrogen bonds formed by the lattice water molecule with the free N2 atom of the monocoordinated triazole rings are shown as thin dashed lines. (bottom) χT versus *T* plot showing the SCO properties of $[Fe(\mathbf{L40})_2(NCS)_2]_n{\cdot}nH_2O$ as well as the thermal relaxation to the LS state after thermal or light-induced trapping of the metastable HS state at low temperatures (black dots and line). Light/dark grey dots correspond to data upon cooling/warming.

Another strategy to create iron(II)-based extended networks exhibiting SCO properties has been introduced very recently [238], simply by replacing one of the 2-pyridyl group of **L189** by a 4-pyridyl moiety. The resulting ligand **L256** still displays one pyridyl-triazole chelating pocket, and thus affords a potential coordination environment which is similar to that of the mononuclear SCO compounds described above. In addition, the remaining 4-pyridine donor group can participate in the gener-

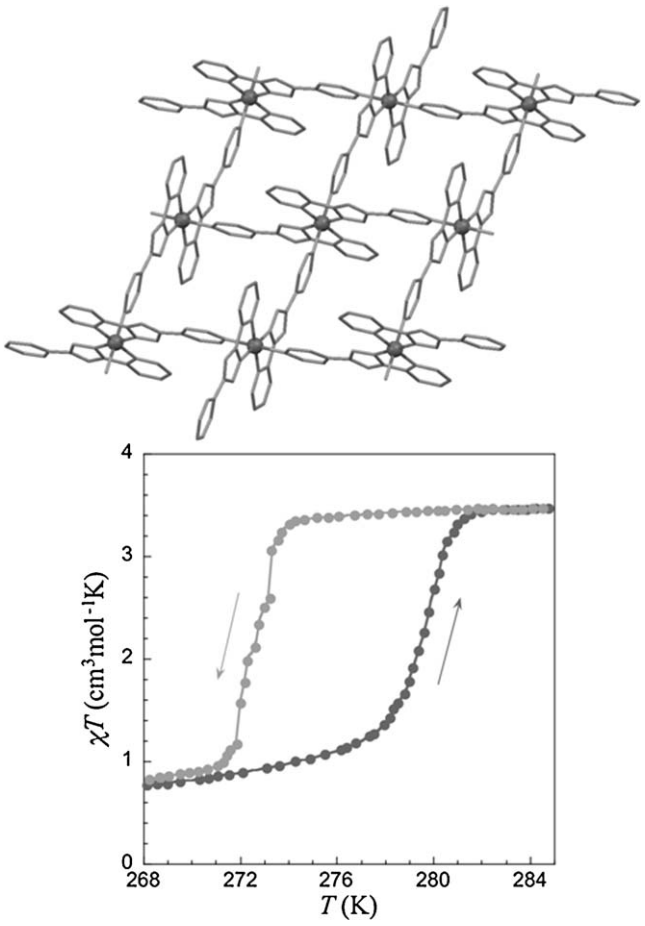

Fig. 79. (top) A view of the 2D connections through the 4-pyridyl group of **L256** in the structure of $[Fe(\mathbf{L256})_2]_n$. (bottom) χT versus T plot showing the SCO properties of $[Fe(\mathbf{L256})_2]_n$ [238]. Light/dark grey dots correspond to data upon cooling/warming.

ation of an extended network. So far, only one SCO compound has been produced applying this strategy. Its 2D structure is built from $[Fe(\mathbf{L256})_2]$ building blocks, whose four equatorial sites are occupied by two *trans* 3-(pyrid-2-yl)-1,2,4-triazolate chelating pockets, and the axial positions are occupied by 4-pyridyl N-donor units from two neighboring building blocks (Fig. 79). Each metal ion is thus connected to four neighbors, giving rise to square-grid layers. The layers are organized in a staggered manner and interact strongly through π–π stacking (ca. 3.4 Å) and hydrogen bonds involving the charged triazolate ring (C–H···N distances of 3.1–3.8 Å). As for $[Fe(\mathbf{L40})_2(NCS)_2]_n \cdot nH_2O$, the result of these interactions together with the rather rigid network is a cooperative SCO behaviour, with a 5.4 K hysteresis at temperatures close to 0 °C ($T_{1/2}^{down} = 273.4\ K$ and $T_{1/2}^{up} = 278.8\ K$). Similar compounds with the exact same formulation or including solvent guests have been isolated under very similar solvothermal conditions, although they all present LS iron(II) ions up to 100 °C. The difference between these compounds and $[Fe(\mathbf{L256})_2]_n$ lies in a rotation of the axial 3-pyridine donor, which allows the formation of very different frameworks, e.g. 3D and interpenetrated 3D structures. This synthetic approach is appealing since it may be applied to most chelating ligands, including those reviewed here that have been shown to favour SCO behaviour. In addition, thanks to the negatively charged triazolate ligand, the 2D network $[Fe(\mathbf{L256})_2]_n$ is neutral, and therefore does not rely on the counter anion for its formation.

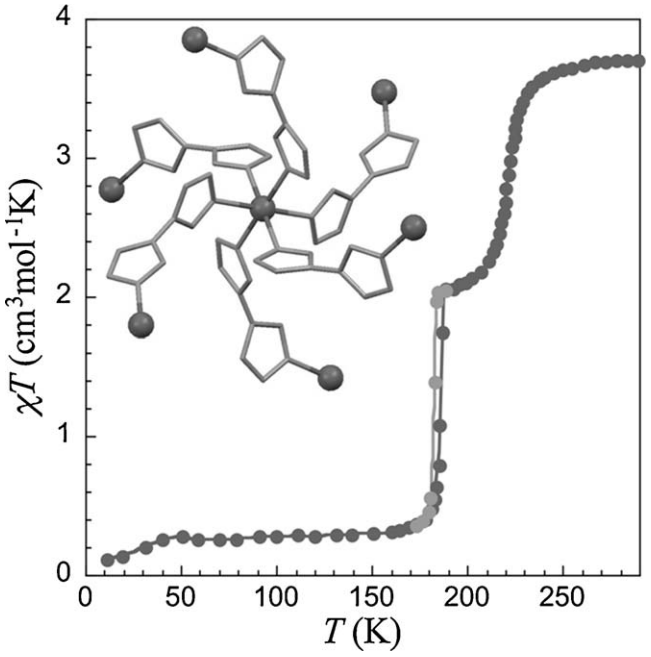

Fig. 80. χT versus T plot showing the SCO properties of $[Fe(\mathbf{L40})_3]_n(ClO_4)_{2n}$ (see text) [240]. Light/dark grey dots correspond to data upon cooling/warming. The inset shows how **L40** connects each iron(II) to six neighbors through N1,N1′ coordination, resulting in a 3D structure.

4.2.6. 3D compounds

As mentioned previously, **L40** is able to bridge iron(II) ions through its N1 and N1′ donor atoms. In the absence of terminal coordinating anions such as NCS^-, a 3D coordination polymer formulated as $[Fe(\mathbf{L40})_3]_n(A)_{2n}$ can be obtained (with $A = ClO_4^-$ or $CF_3SO_3^-$). Although the $CF_3SO_3^-$ compound is a HS system [239], the ClO_4^- one exhibits a complete SCO with two steps at 222 K and 184 K and a plateau corresponding to an intermediate 50% HS population in the range 210–185 K [240]. While the high-temperature transition is about 30 K wide, the low-temperature one is extremely abrupt and presents a hysteresis with a width of about 3 K (Fig. 80). Calorimetric and Mössbauer spectroscopic studies confirmed these observations, and the structure of the compound was solved in the HS, LS and intermediate states [240]. Despite the observation of a very abrupt SCO, indicative of a first-order transition, no change in space group was observed. It was nevertheless shown recently that the SCO in this compound proceeds through nucleation and formation of domains coupled to crystallographic modifications [241].

The structure of this compound exhibits two Fe crystallographic sites, which are both surrounded by six N1-donating triazole rings and are thus connected through bridging N1,N1′-**L40** to six neighbors (see inset in Fig. 80). This arrangement results in a 3D architecture with channels along the *b* axis that are occupied by two crystallographically independent perchlorate ions (Fig. 81, left). These perchlorate ions form several hydrogen bonds with the C–H groups of the ligand **L40**, giving rise to two types of electronic interactions with the iron(II) ions, either through a Fe–N–CH···O–Cl moiety or a longer Fe–N–N–CH···O–Cl pathway. The former interaction only concerns the Fe2 site, while both interactions are present for the Fe1 site. The reason is that the C–H group of **L40** which is the closest to the Fe2 site is involved in an N···H–C hydrogen bond with the uncoordinated N2 atom of a neighboring triazole ring coordinated to a Fe2 site (see Fig. 81, right). The resulting difference in donor strength most likely induces the two-step character of the SCO in $[Fe(\mathbf{L40})_3]_n(ClO_4)_{2n}$, the Fe2 site being LS in the intermediate phase. It should be noted that although the 1,2,4-triazole

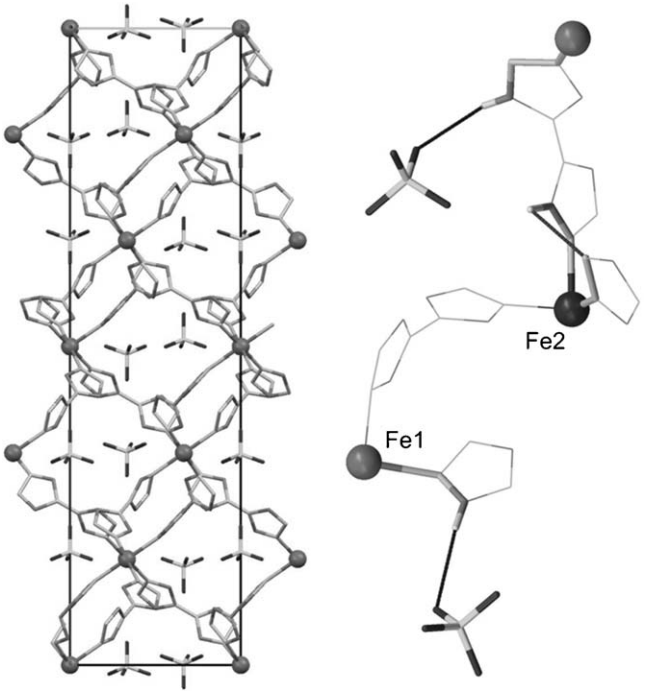

Fig. 81. (left) projection of the structure of $[Fe(\mathbf{L40})_3]_n(ClO_4)_{2n}$ in the *ac* plane [240]. (right) The three types of hydrogen bonds (thin lines) in the structure $[Fe(\mathbf{L40})_3]_n(ClO_4)_{2n}$ at the origin of the two-step SCO behaviour (see text).

rings in $[Fe(\mathbf{L40})_3]_n(ClO_4)_{2n}$ are N1-monodentate, they all participate to several hydrogen-bonding interactions. Without these hydrogen bonds, which evidently affect the donor strength of the N1-monodentate 1,2,4-triazole, the conditions would not favour the occurrence of SCO, as is actually observed in most compounds with terminal N1-donating 1,2,4-triazole ligands. For instance, the fact that the triflate analogue is a HS compound may be ascribed to the absence of such hydrogen-bonding contacts in the crystal lattice [239]. The very abrupt low-temperature transition can also be explained by structural modifications; indeed, while the cell-volume decrease is similar to that observed for the high-temperature step (ca. 3%, mostly along the *c* axis), the dihedral angle between the two triazole moieties of the ligand **L40** suffers a dramatic increase to a value close to 90°, as observed for the free ligand. Such reorientation of the triazole ring is obviously efficiently propagated through the network of hydrogen bonds involving the perchlorate ions, thus resulting in a very cooperative SCO for the Fe1 site.

4.3. Tetrazole compounds

Of the three azole rings considered in the present review, the mono-donating tetrazole (Fig. 82) is probably the weakest donor; indeed, SCO properties in complexes containing tetrazole ligands have been observed mostly in the 60–200 K range. Although tetrazole has many bridging coordination modes (see Scheme 7), in all reported SCO compounds it acts as a monodentate ligand through its N4 donor atom. The most common type of tetrazole ligands are 1-substituted tetrazoles, although several recent reports [242–244] have shown that 2-substituted tetrazole ligands may be used as well to prepare SCO compounds. Apart from the later compounds, all tetrazole-based SCO compounds contain a common [Fe(tetrazole)$_6$] octahedral moiety. As demonstrated in section 2, ligands bearing two tetrazole rings separated by a linker are potential candidates for the design of extended coordination networks with SCO properties. Indeed, and in contrast to 1,2,4-triazoles, most extended systems with this azole do show SCO properties, and ditetrazoles ligands are the source of the widest family of 1D, 2D and 3D SCO compounds. SCO tetrazole compounds have been partially reviewed in 2004 [170,171] and 2007 [172], but many new systems have been reported since then, in particular with the first use of 2-tetrazolyl ligands in SCO chemistry.

4.3.1. Monomers

Since the first report by Franke in 1979 [245], many homoleptic hexatetrazole iron(II) compounds with a range of anions have been synthesized, mostly with 1-alkyltetrazoles or 1-halogenoalkyltetrazoles. They all possess SCO properties and basically exhibit the same complex core with six monodentate tetrazole N-donors forming an octahedral coordination sphere. A complete list of all materials of this type known to date is given in Table 5. Surprisingly, the simplest analogue complex with 1H-tetrazole (**HL103**) has not been reported so far. Although, the complexes themselves are similar, the SCO properties in this class of compounds may be of almost any type. Thermal transitions ranging from gradual to abrupt, with hysteresis, complete, involving only a fraction of the iron(II) centers or occurring in two steps (with similar or different abruptness) can be found. This wide spectrum of properties is strongly related to crystal-structure features, including crystallographic transitions, packing aspects as well as thermal history. The transition temperatures are influenced by both the anion and the tetrazole substituent. These temperatures remain quite low overall; for instance, the family with 1-alkyltetrazoles has a $T_{1/2}$ lying in the range 69–207 K. This family of compounds has been extensively investigated, in part as the basis of many innovative studies related to light-induced effects in SCO compounds, as well as theoretical modeling of the SCO phenomenon. Several reviews cover these specific aspects in detail [164,246]. In addition, a recent review on mononuclear SCO compounds with N-donor ligands includes most of these compounds and discusses in detail those with peculiar structural or physical features [172]. Since then, there has been only one new very similar SCO system reported, using as ligand 1-cycloalkyltetrazoles (**L271**–**L273**) [247,248]. Therefore, only one illustrative example, *i.e.* $[Fe(\mathbf{L258})_6](BF_4)_2$, will be described in detail, and the reader is referred to the complete list shown in Table 5, and to previous reviews [171,172,249].

The high-spin crystalline form of $[Fe(\mathbf{L258})_6](BF_4)_2$ crystallizes in the rhombohedric space group *R*-3. Its solid-state structure is shown in Fig. 83; the complex is centered on a special position with 1/3 occupancy, all ligands being thus identical. The tetrafluoroborate ions are lying on the threefold axis and form together with the complexes layers that are perpendicular to the *c* axis and are separated by a distance of ca. 11 Å. Each complex is thus surrounded by six BF_4^- anions involved in C–H···F hydrogen bonding interactions (3.129 Å) with the tetrazole rings of three neighboring complexes. Consequently, all complexes within the layers are connected. If the crystals are cooled sufficiently fast, a reversible abrupt SCO without hysteresis is detected ($T_{1/2}$ = 125 K), and the structure of the LS phase is comparable to that of the HS phase, with no lowering of symmetry or superstructure. In fact, the main differences are the typical decrease of the Fe–N bond lengths with averages from 2.2 to 2.0 Å. If the crystals are cooled slowly (typically over a period of 30 min) to a temperature below 135 K, no such quenching of the HS phase occurs, and a crystallographic phase transition takes place together with the SCO, accompanied by a small hysteresis with $T_{1/2}^{down} = 128\ K$ and $T_{1/2}^{up} = 135\ K$. Upon cooling, a broadening and splitting of the single-crystal diffraction peaks occur simultaneously with the SCO. Although this event has been interpreted as a structural transition, the LS phase obtained by slow cooling is better described as a disordered phase with poor

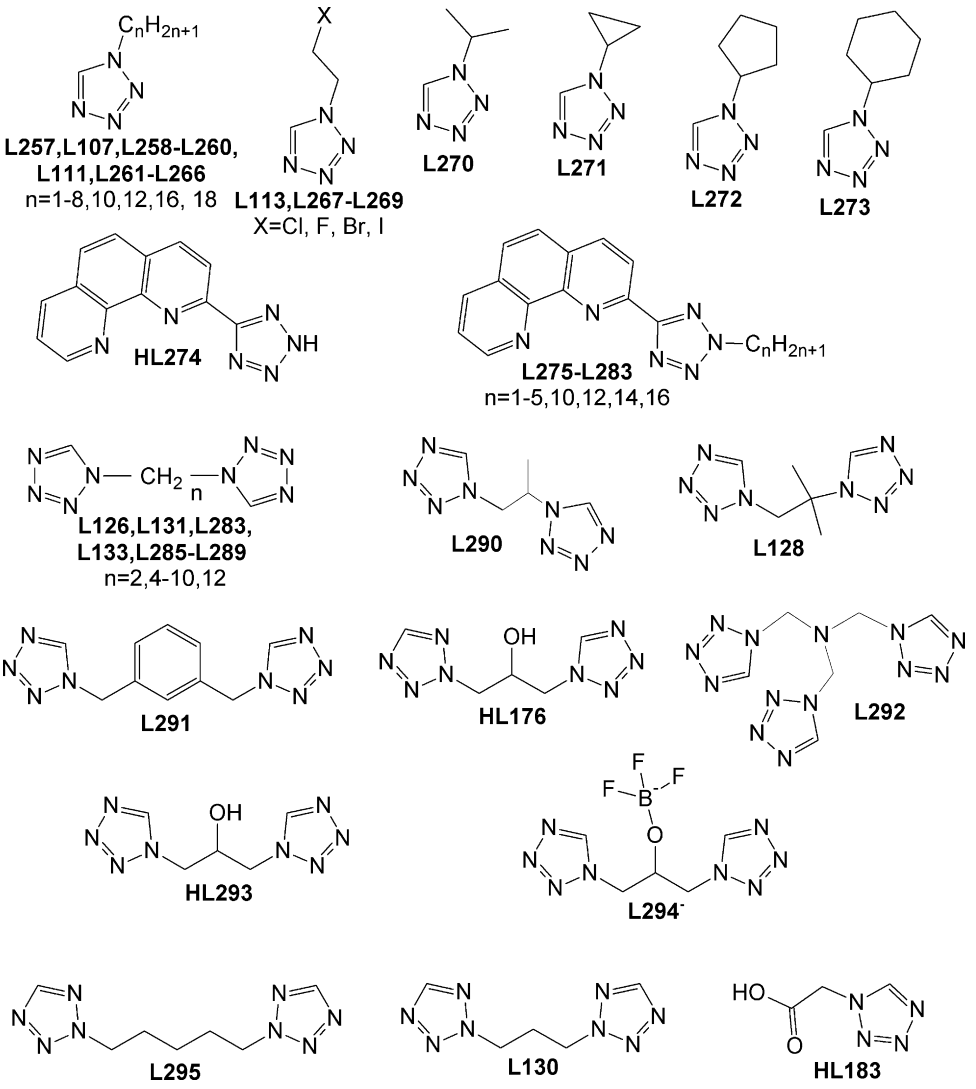

Fig. 82. List of tetrazole ligands involved in the coordination sphere of spin-crossover compounds.

crystallinity. Interestingly, upon warming above 135 K, the HS crystalline phase is restored, the whole process being fully reversible, and the crystals are apparently not damaged. The spin transition in [Fe(**L258**)$_6$](BF$_4$)$_2$ is thus not triggered by the structural phase change, but rather induces it if the compound is maintained in the SCO temperature range long enough. This is further confirmed by the fact that the *R*-3 LS phase can be converted to the "disorder" LS phase by annealing above 120 K. The abruptness of the SCO is reasonably ascribed to the network of hydrogen bonds connecting the spin-changing centers within layers perpendicular to the *c* axis. Doping studies with zinc(II) showed that the diluted compounds present a similar behaviour down to an iron(II) content of 44%. Below this concentration, the transition only takes place in the ordered phase, and becomes more gradual (see Fig. 83, bottom).

Despite its intricate behaviour, [Fe(**L258**)$_6$](BF$_4$)$_2$ is one of the most studied and better characterized SCO compounds [245,249–259], in part because it has served as an model SCO material in the discovery and the physical interpretation of spin-state trapping (LIESST and reverse-LIESST effects), and their relaxation [164,246]. It has also often been used to develop new physical techniques for the detection of the SCO phenomenon (see Table 5). More recently, the first spin-density map of a SCO compound was obtained using this compound, by single-crystal polarized neutron diffraction [260], and an optical hysteresis in the rates of laser-induced interconversion of HS and LS states was demonstrated [261].

All these (now) classical SCO complexes are based on tetrazole ligands substituted on the nitrogen N1 atom. Lately, a series of tetrazole ligands substituted on their carbon atom by a 1,10-phenantroline and alkylated on their N2 atom, namely the ligands **HL274-L283**, were used as asymmetric terdentate ligands to produce a series of complexes with iron(II) tetrafluoroborate and perchlorate [262]. These compounds exhibit structural features analogous to those of complexes obtained from 2-(1,2,4-triazol-3-yl)-1,10-phenanthroline ligands (**HL233-L236**). A view of the neutral complex obtained with the non-alkylated and deprotonated ligand **L274**$^-$ is depicted in Fig. 84. This coordination compound displays a *mer* conformation, as all complexes of this series. This complex presents an abrupt SCO with a 4 K wide hysteresis, characterized by $T_{1/2}^{down} = 252\ K$ and $T_{1/2}^{up} = 256\ K$.

The whole series of compounds, including various solvates (S = H$_2$O or MeOH), exhibit SCO properties at relatively high temperatures, as a result of the stronger donor character of 1,10-phenanthroline. Details on the specific SCO features of structurally characterized compounds, ranging from abrupt to gradual (and in some cases with two-step transitions), are collected in Table 5. For instance, the hydrated BF$_4^-$ salt of the complex with a pentyl substituent on the tetrazole ring (**L279**) has a very abrupt and reversible

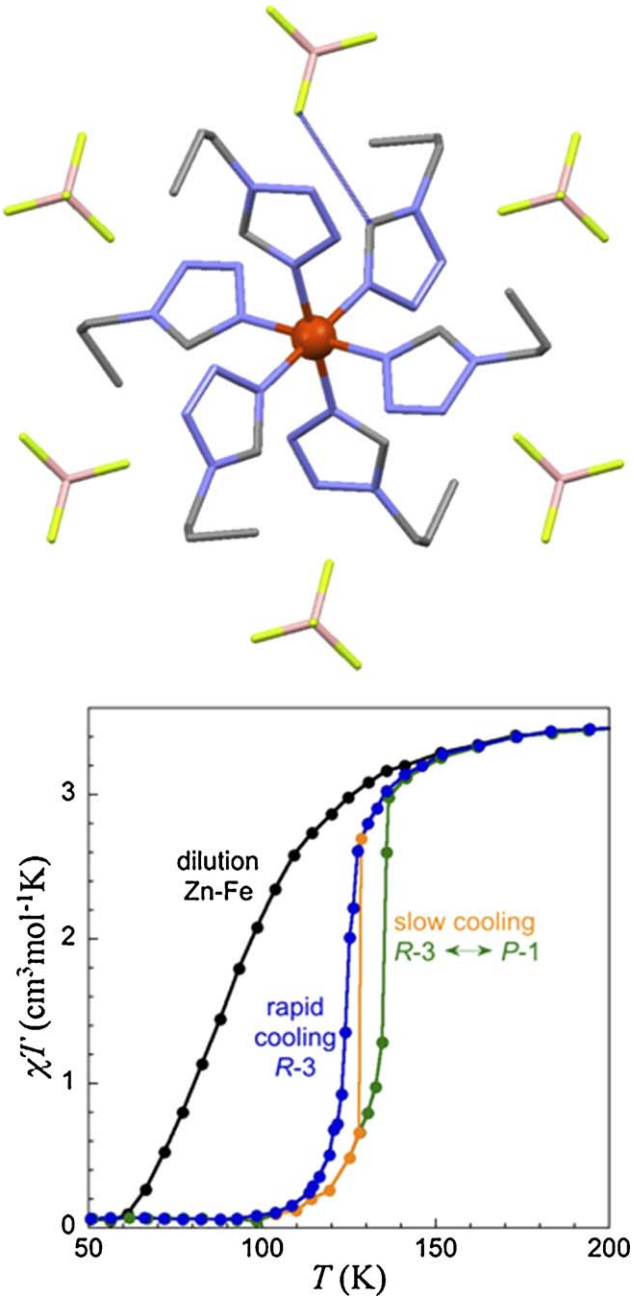

Fig. 83. (top) The complex cation in $[Fe(\mathbf{L258})_6](BF_4)_2$ with its six nearest BF_4^- anions forming C–H···F hydrogen bonds (3.129 Å) [245,249–259]. Only one hydrogen bond is shown (blue line) for clarity. (bottom) χT versus T plot showing the SCO properties of $[Fe(\mathbf{L258})_6](BF_4)_2$ and their dependence on dilution with diamagnetic zinc(II) ions and a crystallographic phase transition triggered by the SCO (see text). Green/orange dots correspond to data upon slow warming/cooling.

SCO at $T_{1/2}$ = 386 K. Amazingly, with an hexadecyl substituent (**L283**), the situation is significantly different. The ClO_4^- and BF_4^- complexes, whose cation is shown in Fig. 85, present strikingly distinct behaviours. Indeed, the SCO curve of the perchlorate salt presents two similar gradual steps, with $T^1_{1/2} = 170\ \ K$ and $T^2_{1/2} = 245\ \ K$ and a plateau in the 180–220 K, while the tetrafluoroborate salt exhibits an abrupt LS-to-HS transition upon the first warming at $T^{1st\,up}_{1/2} = 373\ \ K$, and then a reproducible gradual SCO centered at ca. 262 K. The observation of such SCO disparities in closely related compounds has been ascribed to different intermolecular interactions and molecular-packing arrangements in the corresponding solid-state structures. The most influential factor is likely to be the

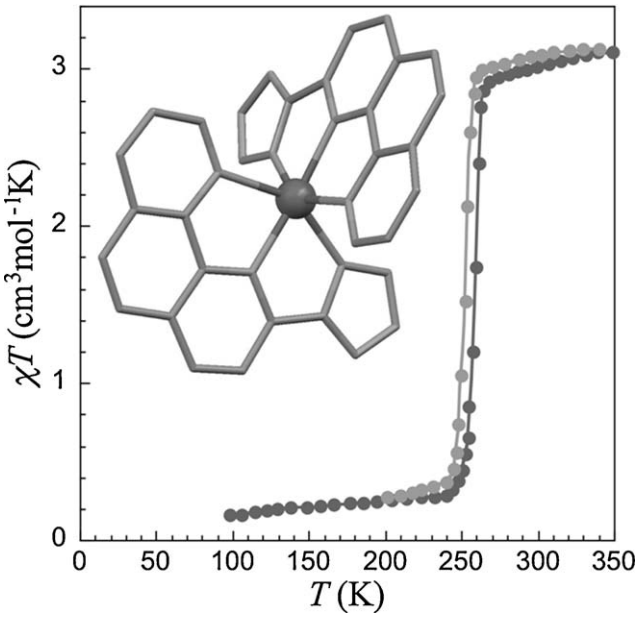

Fig. 84. χT versus T plot showing the abrupt SCO properties of $[Fe(\mathbf{L274})_2]$ [262]. Light/dark grey dots correspond to data upon cooling/warming. The inset shows the cationic complex with the two terdentate planar $\mathbf{L274}^-$ anionic ligands almost perpendicular.

interaction between the nearly planar chelating aromatic rings of neighboring complexes. These rings are nearly perpendicular to each other within each complex; however, the different embrace motifs proposed by Dance[263] to describe such π–π interactions are observed in the present series of complexes, with offset face-to-face, edge-to-face and/or parallel four-fold aryl embrace modes (see Fig. 85 for an example). With longer alkyl tails on the tetrazole ring, the packing of these chains becomes a second dominating

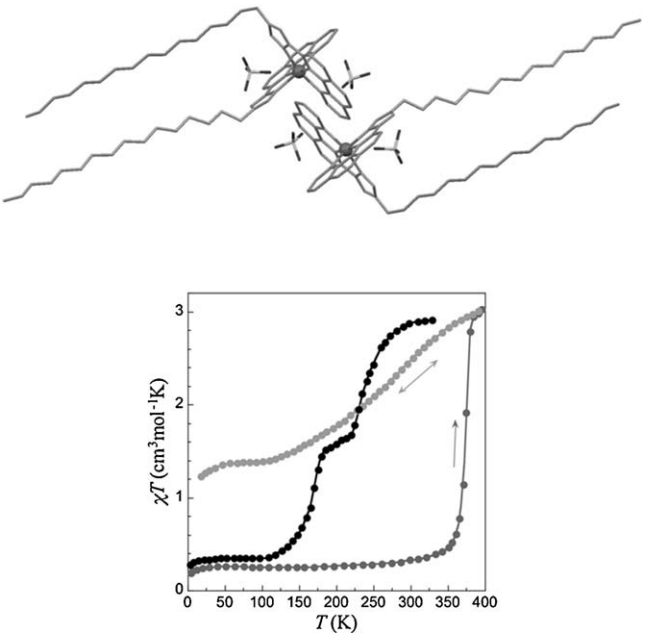

Fig. 85. (top) A view of an embrace motif among the complexes in $[Fe(\mathbf{L283})_2](ClO_4)_2$ resulting from intermolecular π–π interactions [262]. The hexadecyl chains are parallel to each other and point outwards the embrace motif separating the layers in the structure. (bottom) χT versus T plot showing the two-step SCO properties of $[Fe(\mathbf{L283})_2](ClO_4)_2$ (black dots) and the gradual SCO of $[Fe(\mathbf{L283})_2](BF_4)_2$ (light grey) after a first abrupt LS to HS change upon the first warming (dark grey).

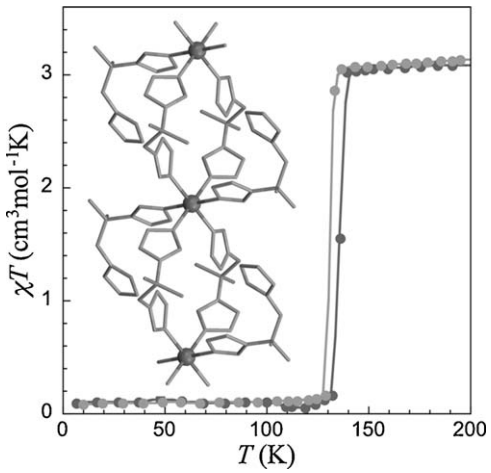

Fig. 86. χT versus T plot showing the abrupt SCO properties of [Fe($\mu_{4,4'}$-**L128**)$_2$(**L128**)]$_n$(ClO$_4$)$_{2n}$ [267]. Light/dark grey dots correspond to data upon cooling/warming. The inset shows a view of the chain with double **L128** bridges and pendant monocoordinated **L128** ligands.

parameter: the two alkyl chains within each complex are forced to be almost parallel to each other (see Fig. 85) to interdigitate with adjacent chains pointing in the opposite direction. This spatial arrangement yields alternatively arranged layers separated by a distance of ca. 26 Å. Such systems are particularly relevant to obtain SCO liquid-crystalline materials. The highly interesting properties of this series of compounds, described in one sole dense report [262], deserve further studies.

4.3.2. 1D compounds

A number of di(tetrazol-1-yl)alkane ligands as well as a similar ligand with a xylylene spacer (**L126**–**L291**, see Fig. 82) have been used in conjunction with simple iron(II) salts to form extended networks (most of them showing SCO properties), which are listed in Table 5. The largest group in this family of compounds is that made of linear chains formed through the bridging of iron(II) ions by three di-tetrazol-1-yl ligands, coordinated through their N4,N4′ donor atoms. The anions are located in the hollow spaces generated by the packing of the chains. Indeed, except with 1,4-di(tetrazol-1-yl)butane (**L131**) that forms interlocked 3D structures (see below), all α,ω-di(tetrazol-1-yl)alkane ligands used so far (with BF_4^- and ClO_4^- salts) have yielded such 1D compounds, although only the crystal structure of [Fe(**L126**)$_3$]$_n$(BF$_4$)$_{2n}$ has been reported [264]. All these compounds exhibit a gradual SCO with $T_{1/2}$ in the range 125–170 K. A recent paper compiles information on these systems, discussing the influence of the spacer length and the anion on the SCO characteristics [265]. A similar 1D compound was obtained from 1,2-di(tetrazol-1-yl)propane (**L290**) and ClO_4^-. This material also showed a gradual SCO centered at 190 K. This compound was in fact the first structurally characterized SCO iron(II) chain compound [266]. The absence of cooperativity in the SCO properties of these compounds, in which the iron(II) centers are connected covalently, has been ascribed to the flexible character of the spacer, able to absorb the local changes induced by the transition, instead of propagating them. In this respect, the use of a bulkier spacer in 1,2-di(tetrazol-1-yl)-2-methyl-propane (**L128**) has resulted in a drastic effect. The structure of [Fe(μ-**L128**)$_2$(**L128**)]$_n$(ClO$_4$)$_{2n}$ also presents 1D coordination chains, but the neighboring iron(II) ions are bridged by only two **L128** ligands, the remaining coordination position being occupied by terminal monocoordinating *trans*-**L128** ligands (Fig. 86) [267]. With respect to the triply-bridged systems, the Fe···Fe separation is shortened by 1 Å. Moreover, the perchlorate anions are involved in anion–π interactions with the tetrazole rings in [Fe(μ-**L128**)$_2$(**L128**)]$_n$(ClO$_4$)$_{2n}$, probably thanks to the relatively longer inter-chain separations. These perchlorate ions are disordered at high temperature (HS state), and the "opening" of the tetrazole rings upon the SCO, e.g. the increase of the centroid–N–Fe angle, induces an ordering of the perchlorate, probably as a result of the strengthening of the anion–π interactions. These structural modifications are most likely involved in the observation of an abrupt SCO with a 3 K wide hysteresis (with $T_{1/2}^{down}$ = 133 K and $T_{1/2}^{up}$ = 136 K) for this compound (Fig. 86). This behaviour is indeed unique among the 1D tetrazole-based compounds reported so far, and indicates that the use of other spacers in di-(tetrazol-1-yl) ligands, for example chosen among those developed for MOFs (see Section 2), should provide new and potentially interesting materials.

This is the case for the recently reported 1D SCO system with the comparatively more rigid *m*-xylylen-di(tetrazole-N1) bridging ligand, **L291** [27]. Three similar compounds with formula [Fe(**L291**)$_3$]$_n$A$_{2n}$·solvent have been isolated, with A = PF_6^- in methanol, and with A = $CF_3SO_3^-$ and ClO_4^- in acetonitrile. The structures, determined for the PF_6^- and $CF_3SO_3^-$ derivatives, exhibit coordination chains resulting from the bridging of octahedrally surrounded iron(II) ions through three **L291** ligands. The bent conformation of the three xylylene spacers results in the formation of cages along the chain, that are occupied by methanol or acetonitrile molecules for the PF_6^- and $CF_3SO_3^-$ compounds, respectively (Fig. 87). In the former, the PF_6^- anions are lying in the space between the chains in the same plane as the crystallographically unique Fe atom, and interact through anion–π contacts with three different chains. The compound displays a rather gradual SCO centered at 150 K (Fig. 87 bottom), which induces insignificant structural modifications of the *P*63/m arrangement, except the usual Fe–N bond length variations. The structure of the $CF_3SO_3^-$ compound is similar at high temperatures; however, at 170 K it experiences a transition to the trigonal *P*-3 space group that generates two different chains having C_3 and S_6 symmetry, respec-

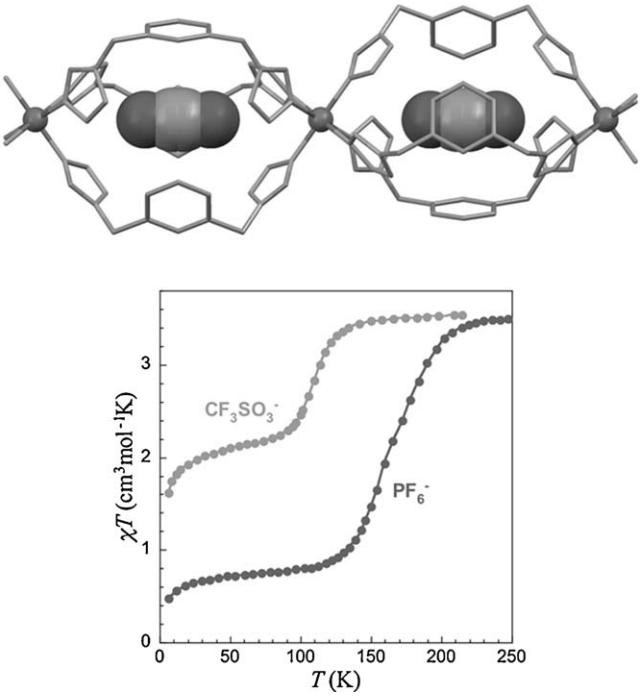

Fig. 87. Top: A view of the chains constructed through triple *m*-xylylene bridges in the structure of [Fe(**L291**)$_3$]$_n$(PF$_6$)$_{2n}$·*n*MeOH [27]. The MeOH molecule is disordered over two positions within the cages formed by three xylylen groups and is shown in space filling. Bottom: χT versus T plot showing the SCO properties of [Fe(**L291**)$_3$]$_n$(PF$_6$)$_{2n}$·*n*MeOH and [Fe(**L291**)$_3$]$_n$(CF$_3$SO$_3$)$_{2n}$·*n*MeCN.

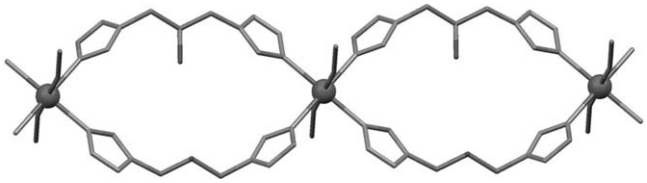

Fig. 88. A representation of the coordination chains in $[Fe(\mathbf{HL176})_2(MeCN)_2]_n(ClO_4)_n{\cdot}2n$MeCN constructed through double **HL176** bridges [243]. Note the asymmetric nature of **HL176** ligand, with one 1-substituted tetrazole and one 2-substituted tetrazole, as well as the original $(N_{tetrazole})_4(N_{acetonitrile})_2$ coordination sphere of the iron(II) ions.

tively, each containing two crystallographic Fe sites. The compound exhibits a gradual SCO at $T_{1/2}$ = 110 K, corresponding to only half of the iron(II) ions (Fig. 87 bottom). Indeed, the low-temperature structure indicates that within each type of chain, only one of the two Fe sites has Fe–N bond lengths characteristic of a LS state. It is thus the first SCO chain exhibiting the alternating ···HS-LS-HS··· pattern. The ClO_4^- compound has a very partial SCO at even lower temperatures, but since its crystal structure could not be determined, these differences could not be rationalized. However, on basis of the $[Fe(\mathbf{L291})_3]_n(CF_3SO_3)_{2n}{\cdot}n$MeCN system, the authors were able to discuss for the first time the effect of the anion on the SCO properties of 1D tetrazole-based compounds [27].

The recent design and use of a ditopic ligand bearing two different tetrazole units, *i.e.* 2-hydroxy-1-(tetrazol-1-yl)-3-(tetrazol-2-yl)propane, with iron(II), yield an even more interesting material. In the single-crystal X-ray structure of the resulting compound, $[Fe(\mathbf{HL176})_2(MeCN)_2]_n(ClO_4)_n{\cdot}2n$MeCN, both tetrazole rings of the **HL176** ligand are coordinated to an iron(II) ion through their N4 atom. These double connections along the *c* axis to two neighboring iron(II) ions generates a 1D chain compound (Fig. 88) [243]. The coordination sphere of the iron(II) ions is completed by two *trans* acetonitrile molecules. The perchlorate ions are involved in hydrogen-bonding interactions with the alcohol groups of **HL176**. A gradual SCO, centered at *ca.* 110 K, is detected for this compound, hence making it the first tetrazole-based iron(II) SCO compound whose iron(II) coordination environment is *not* composed of six tetrazole rings. $[Fe(\mathbf{HL176})_2(MeCN)_2]_n(ClO_4)_n{\cdot}2n$MeCN is also the first SCO compound from a tetrazole ligand substituted at the N2 position, in contrast to the widely-used 1-substituted tetrazoles. The present system together with the recently reported [268] compounds obtained from *N*-(ω-bromoalkyl)tetrazoles, α-(pyridylazoly)-ω-(tetrazolyl)alkanes, α-(tetrazolyl)-ω-(1,2,3-triazolyl)alkanes and α-(tetrazol-1-yl)-ω-(tetrazol-2-yl)alkanes are particularly appealing, and a great future can safely be predicted for tetrazole-based SCO research.

4.3.3. 2D compounds

The first 2D extended network based on a tetrazole ligand that exhibits SCO properties is $[Fe(\mathbf{L292})_2]_n(A)_{2n}$ (with A = BF_4^- and ClO_4^-). The iron(II) ions of this compound are bridged through the tri-connecting tri(2-(tetrazol-1-yl)ethyl)amine ligand **L292**, producing a 2D grid. The compounds have a complete and abrupt SCO with a 9 K wide hysteresis ($T_{1/2}{}^{down}$ = 167 and 157 K and $T_{1/2}{}^{up}$ = 176 and 168 K, respectively). These complexes were first reported in a conference proceedings [269], and so far no further studies on this interesting system have been described in the literature.

With di-(tetrazol-yl) ligands, one 2D SCO compound has been isolated to date, namely $[Fe(\mathbf{HL293})_{1.8}(\mathbf{L294})_{1.2}]_n(BF_4)_{0.8n}{\cdot}n$MeOH·0.8$nH_2$O [270]. The formation of the 2D structure appears to arise from an *in situ* reaction between **HL293** and tetrafluoroborate ions, yielding the

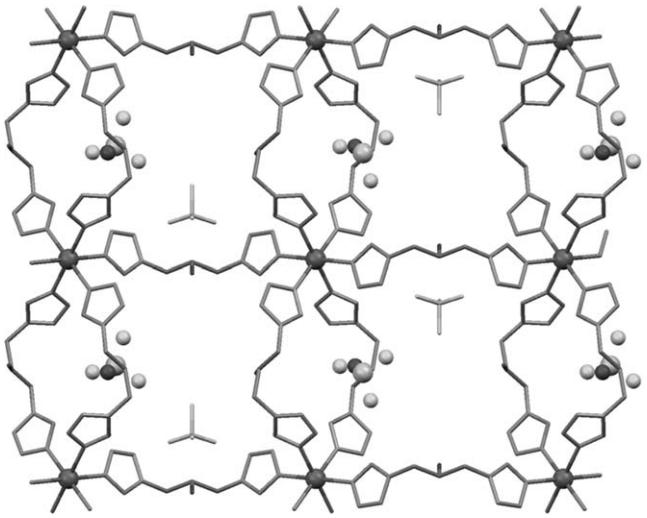

Fig. 89. A view of the 2D grid perpendicular to the *a* axis in the structure of $[Fe(\mathbf{HL293})_{1.8}(\mathbf{L294})_{1.2}]_n(BF_4)_{0.8n}{\cdot}n$MeOH·0.8$nH_2$O [270]. The $[BF_3O]$ moiety pertaining to the negatively charged $\mathbf{L294}^-$ ligand, formed in-situ by reaction of the alcohol group of a **HL293** molecule with a BF_4^- ion, are shown in ball and stick mode for clarity.

charged ligand $\mathbf{L294}^-$. The iron(II) ions are connected by double disordered **HL293**/$\mathbf{L294}^-$ bridges in the *c* direction, and by only one **HL293** bridge in the *b* direction, thus creating grids that are perpendicular to the *a* axis (Fig. 89). The remaining BF_4^- anions as well as the lattice solvent molecules occupy the voids along this axis. Despite its striking structure, this compound presents a gradual SCO, centered at 112 K. As for most SCO tetrazole-based compounds, the LIESST effect is operative here, and studies of the HS → LS relaxation revealed an exponential behaviour, typical for non-cooperative SCO systems [270].

Subsequently to previous reports on copper(II) and zinc(II) extended coordination networks with di-(tetrazol-2-yl) ligands [271–273], two 2D iron(II) compounds were very recently obtained by reaction of 1,6-di(tetrazol-2-yl)hexane (**L295**) with $Fe(ClO_4)_2$ in either acetonitrile or ethanol. The resulting compounds $[Fe(\mathbf{L295})_2(MeCN)_2]_n(ClO_4)_{2n}$ and $[Fe(\mathbf{L295})_2(EtOH)_2]_n(ClO_4)_{2n}$ are isostructural and present 2D grids of iron(II) centers connected to four neighbors by single **L295** N4,N4' bridges [242]. Similarly to $[Fe(\mathbf{HL176})_2(MeCN)_2]_n(ClO_4)_n{\cdot}2n$MeCN, the coordination sphere of the iron(II) ions is completed by two *trans* acetonitrile or ethanol molecules (Fig. 90). The perchlorate ions are disordered and are located between the layers where they weakly interact

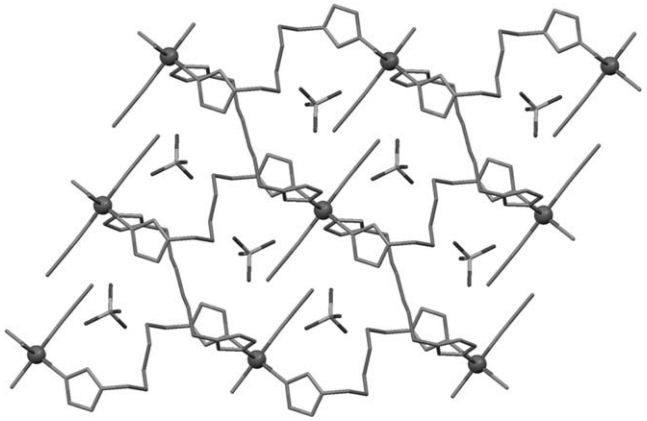

Fig. 90. A view of the 2D grids of iron(II) ions in $[Fe(\mathbf{L295})_2(MeCN)_2]_n(ClO_4)_{2n}$, the first SCO compound containing only 2-substituted tetrazoles [242].

with C–H groups of **L295**. As expected from the presence of weak alcoholic donor ligands, $[Fe(\mathbf{L295})_2(EtOH)_2]_n(ClO_4)_{2n}$ remains HS. In contrast, the acetonitrile analogue does exhibit a rather abrupt SCO at $T_{1/2}$ = 128 K. This compound represents the second example of SCO system based on 2-substituted tetrazole ligands, therefore confirming that such ligands are suitable for the preparation of SCO materials.

4.3.4. 3D compounds

Among the α,ω-di-(tetrazol-1-yl)alkane ligands, 1,4-di-(tetrazole-1-yl)butane (**L131**) appears to possess the ideal combination of length and spacer flexibility to favor the formation of 3D structures instead of the 1D structures usually generated with these ligands (see above). Indeed, although the anions could not be located, $[Fe(\mathbf{L131})_3]_n(ClO_4)_{2n}$ represents the first SCO compound with a catenane structure consisting of three interlocked 3D networks [274]. The PF_6^- and BF_4^- analogue compounds were later reported and the interlocked 3D structures confirmed (see Fig. 91) [275,276]. By comparison with the 1D systems, it appears that the ability of **L131** to adopt an *anti* conformation (rather than the bent *syn* one) is responsible for the formation of a 3D network. Indeed, in the PF_6^- derivative, the highly symmetric structure exhibits identical *anti* **L131** bridges [275]. The PF_6^- anion, whose size matches the cavities of the 3D network, seems to be an additional favorable factor through its probable role as a template. In contrast, in the BF_4^- derivative, the symmetry is highly reduced, with three different butylene spacers, *i.e.* one *trans*, one *syn* and one disordered over two positions [276]. The corresponding contraction of two of the butylene chains is ascribed to the smaller size of the BF_4^- anion. Besides this difference, the two compounds have very similar structural characteristics, with small voids arranged along the *c* axis and containing small amounts of disordered solvent molecules (at most half a MeOH molecule in the PF_6^- compound). As often with SCO compounds, this small solvent content, in particular its nature, has a drastic effect on the SCO properties of these materials (see Fig. 91, bottom).

The SCO behaviour of the ClO_4^- compound was first measured on dried microcrystals grown from an ethanolic solution. An abrupt SCO with a 20 K wide hysteresis was observed ($T_{1/2}{}^{down}$ = 150 K and $T_{1/2}{}^{up}$ = 170 K) [274]. However, this cooperative transition corresponds only to about 16% of the iron centers. Subsequent measurements on a dried powder revealed a two-step SCO with $T_{1/2}{}^1$ = 134 K and $T_{1/2}{}^2$ = 84 K [277]. The PF_6^- compound, if obtained without methanol or in a methanol/chloroform mixture, exhibits a SCO with two abrupt steps, the low-temperature one presenting a hysteresis of 4 K ($T_{1/2}{}^1$ = 180 K, $T_{1/2}{}^{2down}$ = 168 K and $T_{1/2}{}^{2up}$ = 172 K). When isolated from ethanol, the SCO is similar but is shifted towards a lower temperature by 7 K. Moreover, it does not display a hysteretic behaviour anymore in the low-temperature step ($T_{1/2}{}^1$ = 173 K, $T_{1/2}{}^2$ = 161 K) [278]. The solvent contents of the respective polycrystalline materials have been evaluated to 0.075 and 0.25 molecules per Fe ion, respectively for MeOH and EtOH [278]. Similarly, the BF_4^- derivative can be obtained from a pure ethanol solution or from a 95:5 ethanol:water mixture. Although both samples present a SCO of only 50% of the iron content, the former has a gradual SCO curve centered at 84 K, while the latter presents abrupt transitions with an asymmetric hysteresis with a width of 9 K ($T_{1/2}{}^{down}$ = 80 K, $T_{1/2}{}^{up}$ = 89 K) [276]. Such sensitivity to even tiny amounts of lattice solvent molecules is apparently enhanced in the present systems through their involvement in intricate interlocked structure.

As already demonstrated with 1D and 2D SCO compounds, tetrazol-2-yl ligands favour the conditions to generate SCO materials. In the case of $[Fe(\mathbf{L130})_3]_n(ClO_4)_{2n}$, which is obtained from 1,3-di(tetrazol-2-yl)propane (**L130**) either as the di-ethanol solvate or the unsolvated product, the coordination sphere of the iron(II) centers is solely built from N4-donating tetrazole ligands [244], contrary to the 1D and 2D compounds that included two coordinated acetonitrile molecules. The **L130** ligands thus connect each iron(II) ion, through its N4,N4′ donor atoms, to six neighbors generating a regular non-interpenetrated 3D network. The perchlorate ions as well as the ethanol lattice molecules located in the voids of the structure only weakly interact with the tetrazole rings. While the unsolvated compound remains HS, the ethanol solvate exhibits a gradual SCO centered at 145 K. The observed residual HS fraction of ca. 20% has been tentatively ascribed to a partial loss of solvent and/or partial oxidation. $[Fe(\mathbf{L130})_3]_n(ClO_4)_{2n}$ is the first 3D compound based on tetrazol-2-yl donor groups. Considering the similarity of this *R*3 structure with its zinc(II) analogue [272], one can reasonably expect that new iron(II) compounds with related ligands will be pro-

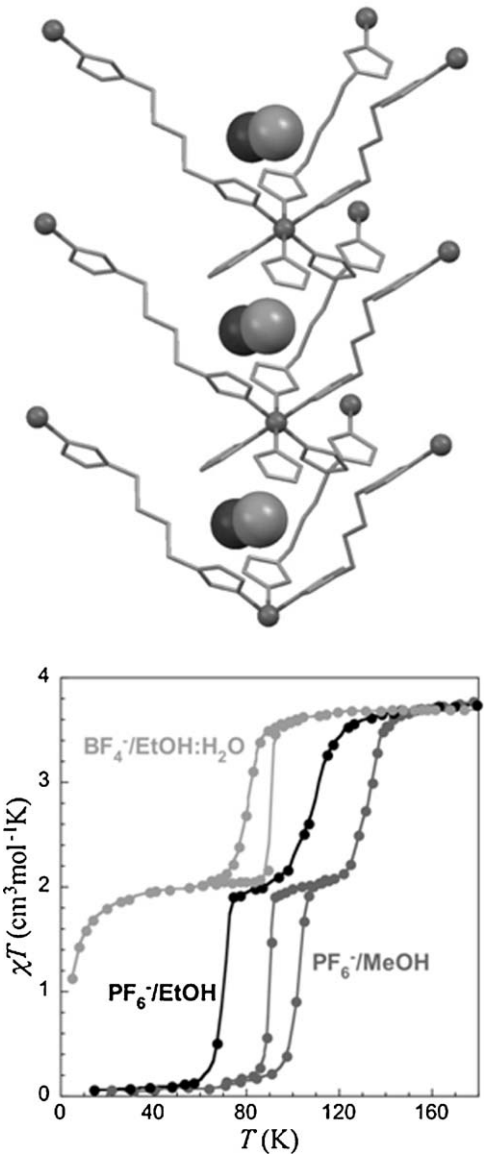

Fig. 91. (top) A view of the interlocked 3D structure in $[Fe(\mathbf{L131})_3]_n(PF_6)_{2n}\cdot x n$solv. Only one vertex of the three interlocked cubic networks is shown for clarity. The trace amount of disordered solvent (here methanol) are represented in space filling to highlight their location, in a void surrounded by six tetrazole rings. (bottom) χT versus T plot showing the SCO properties of the three reported $[Fe(\mathbf{L131})_3]_n(A)_{2n}\cdot x n$solv phases evidencing the significant effect of the solvent content/synthetic conditions (see text) [275,276].

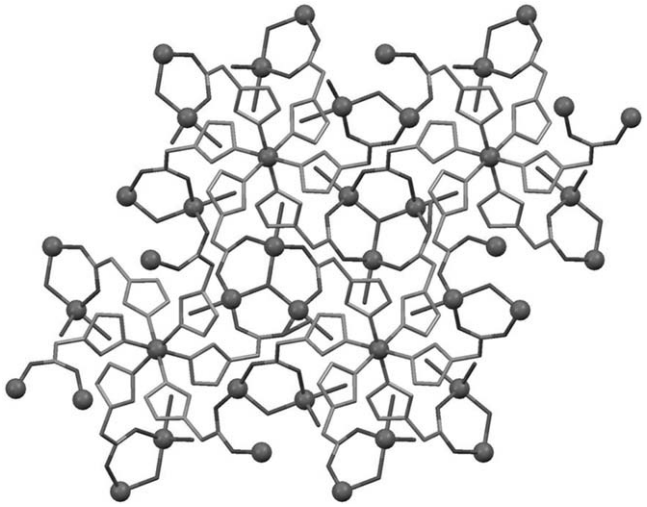

Fig. 92. A projection of the structure of $[(Fe_3O)Fe(\mathbf{L183})_6(H_2O)_3]_n(ClO_4)_{2n}(NO_3)_n$ in the *ab* plane showing the [Fe(tetrazole)]$_6$ and [Fe$_3$] units and their connection through $\mathbf{L183}^-$ [279].

duced, on the basis of known zinc(II) or copper(II) compounds [271–273].

Another potential source of new SCO materials may arise from the use of mixed ligands, such as **HL183** which possesses a carboxylic group connected to a tetrazol-1-yl ring by means of a methylene spacer. Such ligand may form Fe(tetrazole)$_6$ coordination units with SCO properties, and at the same time coordinate other metals through its carboxylic moiety.

This has now been demonstrated in $[(Fe_3O)Fe(\mathbf{HL183})_6(H_2O)_3]_n(ClO_4)_{2n}(NO_3)_n$ [279], whose octahedral FeN_6 part and prismatic oxo-centered [Fe$_3$] unit are connected through the ligand $\mathbf{L183}^-$ to build a 3D NiAs-type framework (Fig. 92). The iron(II) site surrounded by six tetrazole N4-donors clearly exhibits a SCO behaviour, with the Fe–N bond lengths shortening from the HS (ca. 2.20 Å at 330 K) to the LS state (ca. 2.01 Å at 90 K). The analysis of the spin transition by magnetic measurements is difficult due to the presence of antiferromagnetic interactions within the [Fe$_3$] moiety. However, it can be described as gradual and occurring between 125 and 175 K. The application of pressure to the system results in shifts of the SCO, up to 330 K for the highest pressure. This last example, based on a ditopic bridging ligand typically found in MOF chemistry, clearly leaves much room for further development of SCO chemistry.

5. Conclusions

The high versatility of the 1,2,3-triazole, 1,2,4-triazole and tetrazole rings for the design and construction of remarkable coordination materials with attractive physicochemical properties has been clearly demonstrated in the present review. The straightforward preparation of such azole-containing ligands together with their synthetic flexibility has allowed the creation of a myriad of outstanding systems. We have restricted our review to the utilization of these azoles for the preparation of coordination polymers and MOFs, metal complexes, and coordination compounds with spin-crossover properties. These areas of chemistry research indeed represent current hot topics of investigation. However, these N-donor ligands have found applications in many other fields of applied coordination chemistry, such as biological chemistry, nanomaterials, anion recognition, and nonlinear optics. Thus, many research groups are engaged in the design, preparation and study of the coordination chemistry of 1,2,3-triazole-1,2,4-triazole- and tetrazole-based ligands. For instance, (poly)metallic complexes derived from these heteroarenes are reported weekly in the literature. The facile access to this family of ligands actually stimulates the imagination and creativity of research scientists who are building up beautiful and increasingly intricate azole-based molecules. With the present review, we hope that we will encourage even more researchers to use these fascinating small aromatic rings to generate great new metal-organic architectures with original properties.

Acknowledgements

PG acknowledges the COST program Action D35/0011 for financial support and ICREA (Institució Catalana de Recerca i Estudis Avançats). GA and LA acknowledge the Spanish Ministry of Science (CTQ2009-06959) for financial support and the Generalitat de Catalunya for the prize *ICREA Academia 2008* for excellence in university research.

Appendix A. Supplementary data

Supplementary data associated with this article can be found, in the online version, at doi:10.1016/j.ccr.2010.10.038.

References

[1] A. Werner, E. Stiasny, Berichte 32 (1899) 3256–3282.
[2] R.F. Wilson, L.E. Wilson, J. Am. Chem. Soc. 77 (1955) 6204–6205.
[3] J. Meunier-Piret, P. Piret, J.P. Putzeys, M. Van Meerssche, Acta Crystallogr. B 32 (1976) 714–717.
[4] K.T. Potts, Chem. Rev. 61 (1961) 87–127.
[5] J.A. Bladin, Berichte 18 (1885) 1544–1551.
[6] J.G. Haasnoot, Coord. Chem. Rev. 200 (2000) 131–185.
[7] J.A.J. Jarvis, Acta Crystallogr. 15 (1962) 964–966.
[8] J.A. Bladin, Berichte 19 (1886) 2598–2605.
[9] E. Oliveri-Mandala, B. Alagna, Gazz. Chim. Ital. 40 (1910) 441–444.
[10] W.P. Fehlhamm, L.F. Dahl, J. Am. Chem. Soc. 94 (1972) 3370–3377, and references therein.
[11] C. Temple Jr., The Chemistry of Heterocyclic Compounds, Wiley, New York, 1981.
[12] H. Struthers, T.L. Mindt, R. Schibli, Dalton Trans. 39 (2010) 675–696.
[13] F. Amblard, J.H. Cho, R.F. Schinazi, Chem. Rev. 109 (2009) 4207–4220.
[14] M. Meldal, C.W. Tornoe, Chem. Rev. 108 (2008) 2952–3015.
[15] R. Huisgen, Proc. Chem. Soc., Lond. (1961) 357–369.
[16] V.V. Rostovtsev, L.G. Green, V.V. Fokin, K.B. Sharpless, Angew. Chem. Int. Ed. 41 (2002) 2596–2599.
[17] C.W. Tornoe, C. Christensen, M. Meldal, J. Org. Chem. 67 (2002) 3057–3064.
[18] H.C. Kolb, M.G. Finn, K.B. Sharpless, Angew. Chem. Int. Ed. 40 (2001) 2004–2021.
[19] W.H. Binder, R. Sachsenhofer, Macromol. Rapid Commun. 29 (2008) 952–981.
[20] G.C. Tron, T. Pirali, R.A. Billington, P.L. Canonico, G. Sorba, A.A. Genazzani, Med. Res. Rev. 28 (2008) 278–308.
[21] H. Nandivada, X.W. Jiang, J. Lahann, Adv. Mater. 19 (2007) 2197–2208.
[22] J.E. Moses, A.D. Moorhouse, Chem. Soc. Rev. 36 (2007) 1249–1262.
[23] A. Einhorn, E. Bischkopff, B. Szelinski, G. Schupp, E. Sprömgerts, C. Ladisch, T. Mauermayer, Justus Liebigs Annln. Chem. 343 (1905) 207–305.
[24] (a) G. Pellizzari, Gazz. Chim. Ital. 41 (1911) 20;
(b) US Patent 3,821,376, June 28, 1974, H.O. Bayer, R.S. Cook, W.C. von Meyer.
[25] M.R. Atkinson, J.B. Polya, J. Chem. Soc. (1954) 141–145.
[26] Y.I. Lin, S.A. Lang, M.F. Lovell, N.A. Perkinson, J. Org. Chem. 44 (1979) 4160–4164.
[27] M. Quesada, F. Prins, E. Bill, H. Kooijman, P. Gamez, O. Roubeau, A.L. Spek, J.G. Haasnoot, J. Reedijk, Chem. Eur. J. 14 (2008) 8486–8499.
[28] W.K. Su, Z. Hong, W.G. Shan, X.X. Zhang, Eur. J. Org. Chem. (2006) 2723–2726.
[29] B. Moulton, M.J. Zaworotko, Chem. Rev. 101 (2001) 1629–1658.
[30] S. Natarajan, P. Mahata, Chem. Soc. Rev. 38 (2009) 2304–2318.
[31] A.Y. Robin, K.M. Fromm, Coord. Chem. Rev. 250 (2006) 2127–2157.
[32] O.M. Yaghi, G.M. Li, H.L. Li, Nature 378 (1995) 703–706.
[33] D.J. Tranchemontagne, J.L. Mendoza-Cortes, M. O'Keeffe, O.M. Yaghi, Chem. Soc. Rev. 38 (2009) 1257–1283.
[34] T. Loiseau, C. Serre, C. Huguenard, G. Fink, F. Taulelle, M. Henry, T. Bataille, G. Ferey, Chem. Eur. J. 10 (2004) 1373–1382.
[35] S.R. Venna, M.A. Carreon, J. Am. Chem. Soc. 132 (2010) 76–78.
[36] A. Phan, C.J. Doonan, F.J. Uribe-Romo, C.B. Knobler, M. O'Keeffe, O.M. Yaghi, Acc. Chem. Res. 43 (2010) 58–67.
[37] Z. Lu, C.B. Knobler, H. Furukawa, B. Wang, G.N. Liu, O.M. Yaghi, J. Am. Chem. Soc. 131 (2009) 12532–12533.
[38] K.S. Park, Z. Ni, A.P. Cote, J.Y. Choi, R.D. Huang, F.J. Uribe-Romo, H.K. Chae, M. O'Keeffe, O.M. Yaghi, Proc. Natl. Acad. Sci. U. S. A. 103 (2006) 10186–10191.

[39] F.H. Allen, Acta Crystallogr. B 58 (2002) 380–388.
[40] I. Sotofte, K. Nielsen, Acta Chem. Scand. 35 (1981) 739–745.
[41] J. Lu, K. Zhao, Q.R. Fang, J.Q. Xu, J.H. Yu, X. Zhang, H.Y. Bie, T.G. Wang, Cryst. Growth Des. 5 (2005) 1091–1098.
[42] P. Børsting, P.J. Steel, Eur. J. Inorg. Chem. (2004) 376–380.
[43] X.-M. Zhang, Z.-M. Hao, W.-X. Zhang, X.-M. Chen, Angew. Chem. Int. Ed. 46 (2007) 3456–3459.
[44] D.W. Engelfriet, W. Den Brinker, G.C. Verschoor, S. Gorter, Acta Crystallogr. B 35 (1979) 2922–2927.
[45] W. Ouellette, M.H. Yu, C.J. O'Connor, D. Hagrman, J. Zubieta, Angew. Chem. Int. Ed. 45 (2006) 3497–3500.
[46] O.A. Bondar, L.V. Lukashuk, A.B. Lysenko, H. Krautscheid, E.B. Rusanov, A.N. Chernega, K.V. Domasevitch, CrystEngComm 10 (2008) 1216–1226.
[47] P. Gamez, T.J. Mooibroek, S.J. Teat, J. Reedijk, Acc. Chem. Res. 40 (2007) 435–444.
[48] T.J. Mooibroek, C.A. Black, P. Gamez, J. Reedijk, Cryst. Growth Des. 8 (2008) 1082–1093.
[49] Y. Wang, P. Cheng, Y. Song, D.Z. Liao, S.P. Yanl, Chem. Eur. J. 13 (2007) 8131–8138.
[50] M.A. Pierce-butler, Acta Crystallogr. B 38 (1982) 2681–2683.
[51] L. Carlucci, G. Ciani, D.M. Proserpio, Angew. Chem. Int. Ed. 38 (1999) 3488–3492.
[52] M. Dinca, A.F. Yu, J.R. Long, J. Am. Chem. Soc. 128 (2006) 8904–8913.
[53] F. Nouar, J.F. Eubank, T. Bousquet, L. Wojtas, M.J. Zaworotko, M. Eddaoudi, J. Am. Chem. Soc. 130 (2008) 1833–1835.
[54] C. Richardson, P.J. Steel, Dalton Trans. (2003) 992–1000.
[55] G. Vos, A.J. Dekok, G.C. Verschoor, Z. Naturforsch. (B) 36 (1981) 809–813.
[56] H.S. Yoo, J.H. Lim, J.S. Kang, E.K. Koh, C.S. Hong, Polyhedron 26 (2007) 4383–4388.
[57] G. Vos, J.G. Haasnoot, G.C. Verschoor, J. Reedijk, Inorg. Chim. Acta 102 (1985) 187–198.
[58] D.W. Engelfriet, G.C. Verschoor, W. Den Brinker, Acta Crystallogr. B 36 (1980) 1554–1560.
[59] D.W. Engelfriet, G.C. Verschoor, W.J. Vermin, Acta Crystallogr. B 35 (1979) 2927–2931.
[60] U. Beckmann, S. Brooker, Coord. Chem. Rev. 245 (2003) 17–29.
[61] E. Aznar, S. Ferrer, J. Borras, F. Lloret, M. Liu-Gonzalez, H. Rodriguez-Prieto, S. Garcia-Granda, Eur. J. Inorg. Chem. (2006) 5115–5125.
[62] P. Ren, B. Ding, W. Shi, Y. Wang, T.B. Lu, P. Cheng, Inorg. Chim. Acta 359 (2006) 3824–3830.
[63] J.H. Zhou, R.M. Cheng, Y. Song, Y.Z. Li, Z. Yu, X.T. Chen, X.Z. You, Polyhedron 25 (2006) 2426–2432.
[64] U. Beckmann, J.D. Ewing, S. Brooker, Chem. Commun. (2003) 1690–1691.
[65] C.V. Depree, U. Beckmann, K. Heslop, S. Brooker, Dalton Trans. (2003) 3071–3081.
[66] U. Beckmann, S. Brooker, C.V. Depree, J.D. Ewing, B. Moubaraki, K.S. Murray, Dalton Trans. (2003) 1308–1313.
[67] L. Shen, Y.J. Zhang, G.D. Sheng, Acta Crystallogr. E 62 (2006) M3098–M3100.
[68] M.H. Klingele, S. Brooker, Coord. Chem. Rev. 241 (2003) 119–132.
[69] L. Cheng, W.X. Zhang, B.H. Ye, J.B. Lin, X.M. Chen, Inorg. Chem. 46 (2007) 1135–1143.
[70] J. Zhou, J. Yang, L. Qi, X. Shen, D.R. Zhu, Y. Xu, Y. Song, Transit. Met. Chem. 32 (2007) 711–715.
[71] M.L. Tong, C.G. Hong, L.L. Zheng, M.X. Peng, A. Gaita-Arino, J.M.C. Juan, Eur. J. Inorg. Chem. (2007) 3710–3717.
[72] F.S. Keij, R.A.G. De Graaff, J.G. Haasnoot, J. Reedijk, J. Chem. Soc. -Dalton Trans. (1984) 2093–2097.
[73] R. Prins, P. Birker, J.G. Haasnoot, G.C. Verschoor, J. Reedijk, Inorg. Chem. 24 (1985) 4128–4133.
[74] M.H. Klingele, P.D.W. Boyd, B. Moubaraki, K.S. Murray, S. Brooker, Eur. J. Inorg. Chem. (2006) 573–589.
[75] J.A. Kitchen, A. Noble, C.D. Brandt, B. Moubaraki, K.S. Murray, S. Brooker, Inorg. Chem. 47 (2008) 9450–9458.
[76] M.H. Klingele, P.D.W. Boyd, B. Moubaraki, K.S. Murray, S. Brooker, Eur. J. Inorg. Chem. (2005) 910–918.
[77] P.J. Van Koningsbruggen, J.G. Haasnoot, R.A.G. De Graaff, J. Reedijk, S. Slingerland, Acta Crystallogr. C 48 (1992) 1923–1926.
[78] W.M.E. Koomenvanoudenniel, R.A.G. De Graaff, J.G. Haasnoot, R. Prins, J. Reedijk, Inorg. Chem. 28 (1989) 1128–1133.
[79] S. Ferrer, P.J. Van Koningsbruggen, J.G. Haasnoot, J. Reedijk, H. Kooijman, A.L. Spek, L. Lezama, A.M. Arif, J.S. Miller, J. Chem. Soc. -Dalton Trans. (1999) 4269–4276.
[80] P.M. Slangen, P.J. Van Koningsbruggen, J.G. Haasnoot, J. Jansen, S. Gorter, J. Reedijk, H. Kooijman, W.J.J. Smeets, A.L. Spek, Inorg. Chim. Acta 212 (1993) 289–301.
[81] P.M. Slangen, P.J. Van Koningsbruggen, K. Goubitz, J.G. Haasnoot, J. Reedijk, Inorg. Chem. 33 (1994) 1121–1126.
[82] P.J. Van Koningsbruggen, M.W. Gluth, V. Ksenofontov, D. Walcher, D. Schollmeyer, G. Levchenko, P. Gütlich, Inorg. Chim. Acta 273 (1998) 54–61.
[83] S. Tardito, O. Bussolati, M. Maffini, M. Tegoni, M. Giannetto, V. Dall'Asta, R. Franchi-Gazzola, M. Lanfranchi, M.A. Pellinghelli, C. Mucchino, G. Mori, L. Marchio, J. Med. Chem. 50 (2007) 1916–1924.
[84] Z.X. Wang, C.Y. Liu, X.M. Zhang, X.N. Gong, Acta Crystallogr. E 65 (2009), M22-U320.
[85] Y.J. Zhang, X. Fang, M.L. Cao, H.Y. Yu, J.D. Wang, Acta Crystallogr. E 63 (2007), M2630-U1825.
[86] S.F. Palopoli, S.J. Geib, A.L. Rheingold, T.B. Brill, Inorg. Chem. 27 (1988) 2963–2971.
[87] Z.H. Shao, J. Luo, R.F. Cai, X.G. Zhou, L.H. Weng, Z.X. Chen, Acta Crystallogr. E 60 (2004) M225–M227.
[88] Y. Gong, J.H. Li, Y.C. Zhou, J.B. Qin, X.X. Wu, Acta Crystallogr. E 65 (2009), M791-U962.
[89] K. Drabent, Z. Ciunik, P.J. Chmielewski, Eur. J. Inorg. Chem. (2003) 1548–1554.
[90] O. Castillo, U. Garcia-Couceiro, A. Luque, J.P. Garcia-Teran, P. Roman, Acta Crystallogr. E 60 (2004) M9–M11.
[91] X.G. Zhou, Z.E. Huang, R.F. Cai, L.X. Zhang, X.F. Hou, X.J. Feng, X.Y. Huang, J. Organomet. Chem. 563 (1998) 101–112.
[92] P.J. Van Koningsbruggen, D. Gatteschi, R.A.G. De Graaff, J.G. Haasnoot, J. Reedijk, C. Zanchini, Inorg. Chem. 34 (1995) 5175–5182.
[93] V. Lozan, S.V. Voitekhovich, P.N. Gaponik, O.A. Ivashkevich, B. Kersting, Z. Naturforsch. (B) 63 (2008) 496–502.
[94] K. Skorda, T.C. Stamatatos, A.P. Vafiadis, A.T. Lithoxoidu, A. Terzis, S.P. Perlepes, J. Mrozinski, C.P. Raptopoulou, J.C. Plakatouras, E.G. Bakalbassis, Inorg. Chim. Acta 358 (2005) 565–582.
[95] K. Skorda, E.G. Bakalbassis, J. Mrozinski, S.P. Perlepes, C.P. Raptopoulou, A. Terzis, J. Chem. Soc. -Dalton Trans. (1995) 2317–2319.
[96] I. Sotofte, K. Nielsen, Acta Chem. Scand. 35 (1981) 733–738.
[97] Z.X. Wang, I.N. Gong, C.Y. Liu, X.M. Zhang, Acta Crystallogr. E 65 (2009), M157-U423.
[98] M.B. Cingi, A.M.M. Lanfredi, A. Tiripicchio, J.G. Haasnoot, J. Reedijk, Inorg. Chim. Acta 72 (1983) 81–88.
[99] J.A.R. Navarro, M.A. Romero, J.M. Salas, M. Quiros, E.R.T. Tiekink, Inorg. Chem. 36 (1997) 4988–4991.
[100] J.G. Haasnoot, W.L. Driessen, J. Reedijk, Inorg. Chem. 23 (1984) 2803–2807.
[101] F.E. Bradford, L.P. Connor, C.A. Kilner, M.A. Halcrow, Polyhedron 23 (2004) 2141–2151.
[102] P.C. Andrews, T. Beck, B.H. Fraser, P.C. Junk, M. Massi, Polyhedron 26 (2007) 5406–5413.
[103] E. Escriva, J. ServerCarrio, L. Lezama, J.V. Folgado, J.L. Pizarro, R. Ballesteros, B. Abarca, J. Chem. Soc. -Dalton Trans. (1997) 2033–2038.
[104] Y.Q. Lan, S.L. Li, K.Z. Shao, X.L. Wang, X.R. Hao, Z.M. Su, Dalton Trans. (2009) 940–947.
[105] H.M.J. Hendriks, P. Birker, G.C. Verschoor, J. Reedijk, J. Chem. Soc. -Dalton Trans. (1982) 623–631.
[106] E.V. Tretyakov, S.V. Fokin, G.V. Romanenko, V.I. Ovcharenko, Polyhedron 22 (2003) 1965–1972.
[107] L.M. Field, P.M. Lahti, Inorg. Chem. 42 (2003) 7447–7454.
[108] C.W. Reimann, M. Zocchi, Chem. Commun. (1968) 272.
[109] B. Liu, L. Xu, G.C. Guo, J.S. Huang, J. Mol. Struct. 825 (2006) 79–86.
[110] B. Ding, L. Yi, W.Z. Shen, P. Cheng, D.Z. Liao, S.P. Yan, Z.H. Jiang, J. Mol. Struct. 784 (2006) 138–143.
[111] L. Antolini, A.C. Fabretti, D. Gatteschi, A. Giusti, R. Sessoli, Inorg. Chem. 29 (1990) 143–145.
[112] I. Sotofte, K. Nielsen, Acta Chem. Scand. 35 (1981) 747–752.
[113] L.R. Groeneveld, R.A. Lefebre, R.A.G. De Graaff, J.G. Haasnoot, G. Vos, J. Reedijk, Inorg. Chim. Acta 102 (1985) 69–82.
[114] W. Vreugdenhil, J.G. Haasnoot, M.F.J. Schoondergang, J. Reedijk, Inorg. Chim. Acta 130 (1987) 235–242.
[115] B. Ding, E.C. Yang, X.J. Zhao, X.G. Wang, J. Coord. Chem. 61 (2008) 3793–3799.
[116] L. Antolini, A.C. Fabretti, D. Gatteschi, A. Giusti, R. Sessoli, Inorg. Chem. 30 (1991) 4858–4860.
[117] G. Vos, J.G. Haasnoot, G.C. Verschoor, J. Reedijk, P.E.L. Schaminee, Inorg. Chim. Acta 105 (1985) 31–39.
[118] O.G. Shakirova, A.V. Virovets, D.Y. Naumov, Y.G. Shvedenkov, V.N. Elokhina, L.G. Lavrenova, Inorg. Chem. Commun. 5 (2002) 690–693.
[119] J.C. Liu, D.G. Fu, J.Z. Zhuang, C.Y. Duan, X.Z. You, J. Chem. Soc. -Dalton Trans. (1999) 2337–2342.
[120] J.C. Liu, G.C. Guo, J.S. Huang, X.Z. You, Inorg. Chem. 42 (2003) 235–243.
[121] M. Thomann, O. Kahn, J. Guilhem, F. Varret, Inorg. Chem. 33 (1994) 6029–6037.
[122] P.J. Van Koningsbruggen, J.W. Vanhal, R.A.G. De Graaff, J.G. Haasnoot, J. Reedijk, J. Chem. Soc. -Dalton Trans. (1993) 2163–2167.
[123] R.D. Willet, D. Gatteschi, O. Kahn (Eds.), Magneto-Strucutral Correlations in Exchange-Coupled Systems, Reidel, Dordrecht, 1984.
[124] F.J. Rietmeijer, G.A. Van Albada, R.A.G. De Graaff, J.G. Haasnoot, J. Reedijk, Inorg. Chem. 24 (1985) 3597–3601.
[125] G.A. Van Albada, R.A.G. De Graaff, J.G. Haasnoot, J. Reedijk, Inorg. Chem. 23 (1984) 1404–1408.
[126] Q.H. Zhao, H.F. Li, Z.D. Chen, R.B. Fang, Inorg. Chim. Acta 336 (2002) 142–146.
[127] M. Bichay, J.W. Fronabarger, R. Gilardi, R.J. Butcher, W.B. Sanborn, M.E. Sitzmann, M.D. Williams, Tetrahedron Lett. 47 (2006) 6663–6666.
[128] S. Ferrer, J.G. Haasnoot, J. Reedijk, E. Muller, M.B. Cingi, M. Lanfranchi, A.M.M. Lanfredi, J. Ribas, Inorg. Chem. 39 (2000) 1859–1867.
[129] S. Ferrer, F. Lloret, I. Bertomeu, G. Alzuet, J. Borras, S. Garcia-Granda, M. Liu-Gonzalez, J.G. Haasnoot, Inorg. Chem. 41 (2002) 5821–5830.
[130] J.H. Zhou, R.M. Cheng, Y. Song, Y.Z. Li, Z. Yu, X.T. Chen, Z.L. Xue, X.Z. You, Inorg. Chem. 44 (2005) 8011–8022.
[131] C. Stadler, J. Daub, J. Kohler, R.W. Saalfrank, V. Coropceanu, V. Schunemann, C. Ober, A.X. Trautwein, S.F. Parker, M. Poyraz, T. Inomata, R.D. Cannon, J. Chem. Soc. -Dalton Trans. (2001) 3373–3383.

[132] J.B. Vincent, H.R. Chang, K. Folting, J.C. Huffman, G. Christou, D.N. Hendrickson, J. Am. Chem. Soc. 109 (1987) 5703–5711.
[133] L.F. Jones, G. Rajaraman, J. Brockman, M. Murugesu, E.C. Sañudo, J. Raftery, S.J. Teat, W. Wernsdorfer, G. Christou, E.K. Brechin, D. Collison, Chem. Eur. J. 10 (2004) 5180–5194.
[134] A.S. Lyakhov, P.N. Gaponik, M.M. Degtyarik, L.S. Ivashkevich, Acta Crystallogr. C 60 (2004) M399–M401.
[135] R. Prins, R.A.G. De Graaff, J.G. Haasnoot, C. Vader, J. Reedijk, J. Chem. Soc. -Chem. Commun. (1986) 1430–1431.
[136] J.P. Zhang, Y.Y. Lin, X.C. Huang, X.M. Chen, J. Am. Chem. Soc. 127 (2005) 5495–5506.
[137] J.P. Zhang, Y.Y. Lin, X.C. Huang, X.M. Chen, Chem. Commun. (2005) 1258–1260.
[138] A. Ray, S. Mitra, G.M. Rosair, Inorg. Chem. Commun. 11 (2008) 1256–1259.
[139] B. Abarca, R. Ballesteros, M. Chadlaoui, C. Ramirez de Arellano, J.A. Real, Eur. J. Inorg. Chem. (2007) 4574–4578.
[140] D. Li, R.Z. Li, Z.Y. Qi, X.L. Feng, J.W. Cai, X.H. Shi, Inorg. Chem. Commun. 4 (2001) 483–485.
[141] M.G.B. Drew, P.C. Yates, J. Trochagrimshaw, K.P. McKillop, S.M. Nelson, J. Chem. Soc. -Chem. Commun. (1985) 262–263.
[142] V.L. Himes, A.D. Mighell, A.R. Siedle, J. Am. Chem. Soc. 103 (1981) 211–212.
[143] Y.L. Bai, J. Tao, R.B. Huang, L.S. Zheng, Angew. Chem. Int. Ed. 47 (2008) 5344–5347.
[144] J. Handley, D. Collison, C.D. Garner, M. Helliwell, R. Docherty, J.R. Lawson, P.A. Tasker, Angew. Chem. Int. Ed. Engl. 32 (1993) 1036–1038.
[145] M. Murrie, D. Collison, C.D. Garner, M. Helliwell, P.A. Tasker, S.S. Turner, Polyhedron 17 (1998) 3031–3043.
[146] E.G. Bakalbassis, E. Diamantopoulou, S.P. Perlepes, C.P. Raptopoulou, V. Tangoulis, A. Terzis, T.F. Zafiropoulos, J. Chem. Soc. -Chem. Commun. (1995) 1347–1348.
[147] V. Tangoulis, C.P. Raptopoulou, A. Terzis, E.G. Bakalbassis, E. Diamantopoulou, S.P. Perlepes, Inorg. Chem. 37 (1998) 3142–3153.
[148] Y.X. Yuan, P.J. Wei, W. Qin, Y. Zhang, J.L. Yao, R.A. Gu, Eur. J. Inorg. Chem. (2007) 4980–4987.
[149] J. Tabernor, L.F. Jones, S.L. Heath, C. Muryn, G. Aromi, J. Ribas, E.K. Brechin, D. Collison, Dalton Trans. (2004) 975–976.
[150] E.V. Lider, E.V. Peresypkina, A.I. Smolentsev, V.N. Elokhina, T.I. Yaroshenko, A.V. Virovets, V.N. Ikorskii, L.G. Lavrenova, Polyhedron 26 (2007) 1612–1618.
[151] E. Diamantopoulou, C.P. Raptopoulou, A. Terzis, V. Tangoulis, S.P. Perlepes, Polyhedron 21 (2002) 2117–2126.
[152] M. Dinca, T.D. Harris, A.T. Iavarone, J.R. Long, J. Mol. Struct. 890 (2008) 139–143.
[153] R. Shaw, F. Tuna, W. Wernsdorfer, A.L. Barra, D. Collison, E.J.L. McInnes, Chem. Commun. (2007) 5161–5163.
[154] S. Salameh, M. Abul-Haj, M. Quiros, J.M. Salas, Eur. J. Inorg. Chem. (2005) 2779–2782.
[155] L.F. Jones, E.K. Brechin, D. Collison, A. Harrison, S.J. Teat, W. Wernsdorfer, Chem. Commun. (2002) 2974–2975.
[156] L.F. Jones, E.K. Brechin, D. Collison, J. Raftery, S.J. Teat, Inorg. Chem. 42 (2003) 6971–6973.
[157] D.M. Low, L.F. Jones, A. Bell, E.K. Brechin, T. Mallah, E. Riviere, S.J. Teat, E.J.L. McInnes, Angew. Chem. Int. Ed. 42 (2003) 3781–3784.
[158] M. Evangelisti, E.K. Brechin, Dalton Trans. 39 (2010) 4672–4676.
[159] R. Shaw, R.H. Laye, L.F. Jones, D.M. Low, C. Talbot-Eeckelaers, Q. Wei, C.J. Milios, S. Teat, M. Helliwell, J. Raftery, M. Evangelisti, M. Affronte, D. Collison, E.K. Brechin, E.J.L. McInnes, Inorg. Chem. 46 (2007) 4968–4978.
[160] R.H. Laye, Q.A. Wei, P.V. Mason, M. Shanmugam, S.J. Teat, E.K. Brechin, D. Collison, E.J.L. McInnes, J. Am. Chem. Soc. 128 (2006) 9020–9021.
[161] C. Papatriantafyllpoulou, E. Diamantopoulou, A. Terzis, N. Lalioti, V. Tangoulis, S.P. Perlepes, Inorg. Chem. Commun. 11 (2008) 454–460.
[162] G.S. Papaefstathiou, S.P. Perlepes, A. Escuer, R. Vicente, M. Font-Bardia, X. Solans, Angew. Chem. Int. Ed. 40 (2001) 884–886.
[163] A. Hauser, J. Jeftic, H. Romsted, R. Hinek, H. Spiering, Coord. Chem. Rev. 192 (1999) 471–491.
[164] H. Spiering, Elastic interaction in spin crossover compounds, in: Spin Crossover, in: Transition Metal Compounds III, Springer-Verlag Berlin, Berlin, 2004, pp. 171–195.
[165] H. Spiering, T. Kohlhaas, N. Romstedt, A. Hauser, C. Bruns-Yilmaz, J. Kusz, P. Gütlich, Coord. Chem. Rev. 192 (1999) 629–647.
[166] O. Kahn, C.J. Martinez, Science 279 (1998) 44–48.
[167] A. Hauser, Light-induced spin crossover and the high-spin → low-spin relaxation, in: Spin Crossover in Transition Metal Compounds II, Springer-Verlag, Berlin, 2004, pp. 155–198.
[168] P. Gütlich, A. Hauser, H. Spiering, Angew. Chem. Int. Ed. Engl. 33 (1994) 2024–2054.
[169] H.A. Goodwin, P. Gütlich, Spin Crossover in Transition Metal Compounds I–III, Springer-Verlag Berlin, Berlin, 2004.
[170] Y. Garcia, V. Niel, M.C. Muñoz, J.A. Real, Spin crossover in 1D, 2D and 3D polymeric Fe(II) networks, in: Spin Crossover in Transition Metal Compounds I, Springer-Verlag Berlin, Berlin, 2004, pp. 229–257.
[171] P.J. Van Koningsbruggen, Special classes of iron(II) azole spin crossover compounds, in: Spin Crossover in Transition Metal Compounds I, Springer-Verlag Berlin, Berlin, 2004, pp. 123–149.
[172] M.A. Halcrow, Polyhedron 26 (2007) 3523–3576.
[173] V. Niel, A.B. Gaspar, M.C. Muñoz, B. Abarca, R. Ballesteros, J.A. Real, Inorg. Chem. 42 (2003) 4782–4788.
[174] C.F. Sheu, K. Chen, S.M. Chen, Y.S. Wen, G.H. Lee, J.M. Chen, J.F. Lee, B.M. Cheng, H.S. Sheu, N. Yasuda, Y. Ozawa, K. Toriumi, Y. Wang, Chem. Eur. J. 15 (2009) 2384–2393.
[175] R. Bronisz, Inorg. Chem. 44 (2005) 4463–4465.
[176] G.J. Long, F. Grandjean, D.L. Reger, Spin Crossover in Pyrazolylborate and Pyrazolylmethane Complexes, in: Spin Crossover in Transition Metal Compounds II, Springer-Verlag Berlin, Berlin, 2004, pp. 91–122.
[177] C. Janiak, J. Chem. Soc. -Chem. Commun. (1994) 545–547.
[178] C. Janiak, T.G. Scharmann, T. Brauniger, J. Holubova, M. Nadvornik, Z. Anorg. Allg. Chem. 624 (1998) 769–774.
[179] A.F. Stassen, M. de Vos, P.J. Van Koningsbruggen, F. Renz, J. Ensling, H. Kooijman, A.L. Spek, J.G. Haasnoot, P. Gütlich, J. Reedijk, Eur. J. Inorg. Chem. (2000) 2231–2237.
[180] O. Roubeau, M. deVos, A.F. Stassen, R. Burriel, J.G. Haasnoot, J. Reedijk, J. Phys. Chem. Solids 64 (2003) 1003–1013.
[181] A.M. Greenaway, E. Sinn, J. Am. Chem. Soc. 100 (1978) 8080–8085.
[182] B.A. Katz, C.E. Strouse, Inorg. Chem. 19 (1980) 658–665.
[183] P. Stupik, W.M. Reiff, R. Hage, J. Jacobs, J.G. Haasnoot, J. Reedijk, Hyperfine Interact. 40 (1988) 343–345.
[184] P. Stupik, J.H. Zhang, M. Kwiecien, W.M. Reiff, J.G. Haasnoot, R. Hage, J. Reedijk, Hyperfine Interact. 28 (1986) 725–727.
[185] K.H. Sugiyarto, D.C. Craig, A.D. Rae, H.A. Goodwin, Aust. J. Chem. 48 (1995) 35–54.
[186] (a) J.A. Kitchen, S. Brooker, Coord. Chem. Rev. 252 (2008) 2072–2092;
(b) J.A. Kitchen, N.G. White, M. Boyd, B. Moubaraki, K.S. Murray, P.D.W. Boyd, S. Brooker, Inorg. Chem. 48 (2009) 6670–6679.
[187] G.S. Matouzenko, A. Bousseksou, S.A. Borshch, M. Perrin, S. Zein, L. Salmon, G. Molnar, S. Lecocq, Inorg. Chem. 43 (2004) 227–236.
[188] Y. Miyazaki, T. Nakamoto, S. Ikeuchi, K. Saito, A. Inaba, M. Sorai, T. Tojo, T. Atake, G.S. Matouzenko, S. Zein, S.A. Borshch, J. Phys. Chem. B 111 (2007) 12508–12517.
[189] P.J. Kunkeler, P.J. Van Koningsbruggen, J.P. Cornelissen, A.N. Van der Horst, A.M. Van der Kraan, A.L. Spek, J.G. Haasnoot, J. Reedijk, J. Am. Chem. Soc. 118 (1996) 2190–2197.
[190] C.F. Sheu, S.M. Chen, S.C. Wang, G.H. Lee, Y.H. Liu, Y. Wang, Chem. Commun. (2009) 7512–7514.
[191] N. Moliner, M.C. Muñoz, S. Létard, J.F. Létard, X. Solans, R. Burriel, M. Castro, O. Kahn, J.A. Real, Inorg. Chim. Acta 291 (1999) 279–288.
[192] J.A. Kitchen, G.N.L. Jameson, J.L. Tallon, S. Brooker, Chem. Commun. 46 (2010) 3200–3202.
[193] J. Klingele, D. Kaase, J. Hilgert, G. Steinfeld, M.H. Klingele, J. Lach, Dalton Trans. 39 (2010) 4495–4507.
[194] H.A. Goodwin, Spin crossover in iron(II) tris(diimine) and bis(terimine) systems, in: Spin Crossover in Transition Metal Compounds I, Springer-Verlag Berlin, Berlin, 2004, pp. 59–90.
[195] K.H. Sugiyarto, D.C. Craig, A.D. Rae, H.A. Goodwin, Aust. J. Chem. 46 (1993) 1269–1290.
[196] F. Renz, P.A. De Souza, G. Klingelhofer, H.A. Goodwin, Hyperfine Interact. 139 (2002) 699–704.
[197] C.J. Schneider, J.D. Cashion, B. Moubaraki, S.M. Neville, S.R. Batten, D.R. Turner, K.S. Murray, Polyhedron 26 (2007) 1764–1772.
[198] (a) M.H. Klingele, B. Moubaraki, J.D. Cashion, K.S. Murray, S. Brooker, Chem. Commun. (2005) 987–989;
(b) C.M. Grunert, S. Reiman, H. Spiering, J.A. kitchen, S. Brooker, P. Gütlich, Angew. Chem. Int. Ed. 47 (2008) 2997–2999;
(c) A. Bhattacharjee, V. Ksenovontov, J.A. Kitchen, N.G. White, S. Brooker, P. Gütlich, Appl. Phys. Lett. 92 (2008) 174104.
[199] J.J.A. Kolnaar, M.I. de Heer, H. Kooijman, A.L. Spek, G. Schmitt, V. Ksenofontov, P. Gütlich, J.G. Haasnoot, J. Reedijk, Eur. J. Inorg. Chem. (1999) 881–886.
[200] G. Vos, R.A. Lefebre, R.A.G. De Graaff, J.G. Haasnoot, J. Reedijk, J. Am. Chem. Soc. 105 (1983) 1682–1683.
[201] J.G. Haasnoot, G. Vos, W.L. Groeneveld, Z. Naturforsch. (B) 32 (1977) 1421–1430.
[202] G. Vos, R.A.G. De Graaff, J.G. Haasnoot, A.M. Van der Kraan, P. De Vaal, J. Reedijk, Inorg. Chem. 23 (1984) 2905–2910.
[203] J.J.A. Kolnaar, G. Van Dijk, H. Kooijman, A.L. Spek, V.G. Ksenofontov, P. Gütlich, J.G. Haasnoot, J. Reedijk, Inorg. Chem. 36 (1997) 2433–2440.
[204] Y. Garcia, P. Guionneau, G. Bravic, D. Chasseau, J.A.K. Howard, O. Kahn, V. Ksenofontov, S. Reiman, P. Gütlich, Eur. J. Inorg. Chem. (2000) 1531–1538.
[205] M.B. Bushuev, L.G. Lavrenova, Y.G. Shvedenkov, A.V. Virovets, L.A. Sheludyakova, S.V. Larionov, Russ. J. Inorg. Chem. 52 (2007) 46–51.
[206] J.A. Kitchen, G.N.L. Jameson, V.A. Milway, J.L. Tallon, S. Brooker, Dalton Trans. 39 (2010) 7637–7639.
[207] Y. Garcia, P.J. Van Koningsbruggen, G. Bravic, D. Chasseau, O. Kahn, Eur. J. Inorg. Chem. (2003) 356–362.
[208] K. Drabent, Z. Ciunik, Chem. Commun. (2001) 1254–1255.
[209] Y. Garcia, P.J. Van Koningsbruggen, G. Bravic, P. Guionneau, D. Chasseau, G.L. Cascarano, J. Moscovici, K. Lambert, A. Michalowicz, O. Kahn, Inorg. Chem. 36 (1997) 6357–6365.
[210] A. Michalowicz, J. Moscovici, B. Ducourant, D. Cracco, O. Kahn, Chem. Mater. 7 (1995) 1833–1842.
[211] A. Michalowicz, J. Moscovici, O. Kahn, J. Phys. IV 7 (1997) 633–635.
[212] M. Verelst, L. Sommier, P. Lecante, A. Mosset, O. Kahn, Chem. Mater. 10 (1998) 980–985.

[213] J. Kröber, J.P. Audière, R. Claude, E. Codjovi, O. Kahn, J.G. Haasnoot, F. Grolière, C. Jay, A. Bousseksou, J. Linarès, F. Varret, A. Gonthiervassal, Chem. Mater. 6 (1994) 1404–1412.
[214] K.H. Sugiyarto, H.A. Goodwin, Aust. J. Chem. 47 (1994) 263–277.
[215] J. Kröber, E. Codjovi, O. Kahn, F. Grolière, C. Jay, J. Am. Chem. Soc. 115 (1993) 9810–9811.
[216] Y. Garcia, P.J. Van Koningsbruggen, R. Lapouyade, L. Fournès, L. Rabardel, O. Kahn, V. Ksenofontov, G. Levchenko, P. Gütlich, Chem. Mater. 10 (1998) 2426–2433.
[217] E. Codjovi, L. Sommier, O. Kahn, C. Jay, New J. Chem. 20 (1996) 503–505.
[218] P.J. Van Koningsbruggen, Y. Garcia, E. Codjovi, R. Lapouyade, O. Kahn, L. Fournès, L. Rabardel, J. Mater. Chem. 7 (1997) 2069–2075.
[219] T. Fujigaya, D.L. Jiang, T. Aida, Chem. -Asian J. 2 (2007) 106–113.
[220] S.W. Lee, J.W. Lee, S.H. Jeong, I.W. Park, Y.M. Kim, J.I. Jin, Synth. Met. 142 (2004) 243–249.
[221] G. Schwarzenbacher, M.S. Gangl, M. Goriup, M. Winter, M. Grunert, F. Renz, W. Linert, R. Saf, Mon. Chem. 132 (2001) 519–529.
[222] M. Seredyuk, A.B. Gaspar, V. Ksenofontov, S. Reiman, Y. Galyametdinov, W. Haase, E. Rentschler, P. Gütlich, Chem. Mater. 18 (2006) 2513–2519.
[223] O. Roubeau, B. Agricole, R. Clérac, S. Ravaine, J. Phys. Chem. B 108 (2004) 15110–15116.
[224] O. Roubeau, E. Natividad, B. Agricole, S. Ravaine, Langmuir 23 (2007) 3110–3117.
[225] P. Grondin, O. Roubeau, M. Castro, H. Saadaoui, A. Colin, R. Clérac, Langmuir 26 (2010) 5184–5195.
[226] O. Roubeau, V. Colin, W. Schmitt, R. Clérac, Angew. Chem. Int. Ed. 43 (2004) 3283–3286.
[227] (a) E. Coronado, J.R. Galan-Mascaros, M. Monrabal-Capilla, J. Garcia-Martinez, P. Pardo-Ibanez, Adv. Mater. 19 (2007) 1359–1361;
(b) J.-F. Létard, O. Nguyen, N. Daro, PCT Int. Appl., CODEN: PIXXD2 WO 2007065996 A1 20070614, 2007.
[228] T. Forestier, S. Mornet, N. Daro, T. Nishihara, S. Mouri, K. Tanaka, O. Fouche, E. Freysz, J.F. Létard, Chem. Commun. (2008) 4327–4329.
[229] W. Vreugdenhil, J.H. Van Diemen, R.A.G. De Graaff, J.G. Haasnoot, J. Reedijk, A.M. Van der Kraan, O. Kahn, J. Zarembowitch, Polyhedron 9 (1990) 2971–2979.
[230] V. Legrand, S. Pillet, C. Carbonera, M. Souhassou, J.F. Létard, P. Guionneau, C. Lecomte, Eur. J. Inorg. Chem. (2007) 5693–5706.
[231] S. Pillet, J. Hubsch, C. Lecomte, Eur. Phys. J. B 38 (2004) 541–552.
[232] A. Ozarowski, S.Z. Yu, B.R. McGarvey, A. Mislankar, J.E. Drake, Inorg. Chem. 30 (1991) 3167–3174.
[233] O. Roubeau, P.C.M. Gubbens, D. Visser, M. Blaauw, P.D. de Reotier, A. Yaouanc, J.G. Haasnoot, J. Reedijk, S. Sakarya, U.A. Jayasooriya, S.P. Cottrell, P.J.C. King, Chem. Phys. Lett. 395 (2004) 177–181.
[234] J.P. Martin, J. Zarembowitch, A. Bousseksou, A. Dworkin, J.G. Haasnoot, F. Varret, Inorg. Chem. 33 (1994) 6325–6333.
[235] J.P. Martin, J. Zarembowitch, A. Dworkin, J.G. Haasnoot, E. Codjovi, Inorg. Chem. 33 (1994) 2617–2623.
[236] A. Desaix, O. Roubeau, J. Jeftic, J.G. Haasnoot, K. Boukheddaden, E. Codjovi, J. Linarès, M. Noguès, F. Varret, Eur. Phys. J. B 6 (1998) 183–193.
[237] S. Pillet, V. Legrand, M. Souhassou, C. Lecomte, Phys. Rev. B 74 (2006) 140101.
[238] X. Bao, J.D. Leng, Z.S. Meng, Z.J. Lin, M.L. Tong, M. Nihei, H. Oshio, Chem. Eur. J. 16 (2010) 6169–6174.
[239] W. Vreugdenhil, Ph.D Thesis, Leiden University, 1987, pp. 164.
[240] Y. Garcia, O. Kahn, L. Rabardel, B. Chansou, L. Salmon, J.P. Tuchagues, Inorg. Chem. 38 (1999) 4663–4670.
[241] I. Krivokapic, C. Enachescu, R. Bronisz, A. Hauser, Inorg. Chim. Acta 361 (2008) 3616–3622.
[242] A. Bialonska, R. Bronisz, Inorg. Chem. 49 (2010) 4534–4542.
[243] A. Bialonska, R. Bronisz, M. Weselski, Inorg. Chem. 47 (2008) 4436–4438.
[244] R. Bronisz, Inorg. Chem. 46 (2007) 6733–6739.
[245] P.L. Franke, J.G. Haasnoot, A.P. Zuur, Inorg. Chim. Acta 59 (1982) 5–9.
[246] A. Hauser, Light-induced spin crossover and the high-spin → low-spin relaxation, in: Spin Crossover in Transition Metal Compounds II, Springer-Verlag Berlin, Berlin, 2004, pp. 155–198.
[247] N. Hassan, P. Weinberger, F. Kubel, G. Molnar, A. Bousseksou, L. Dlhan, R. Boca, W. Linert, Inorg. Chim. Acta 362 (2009) 3629–3636.
[248] A.A. Soliman, M.M. Khattab, M. Reissner, P. Weinberger, F. Werner, W. Linert, Inorg. Chim. Acta 360 (2007) 3987–3996.
[249] J. Kusz, P. Gütlich, H. Spiering, Structural investigations of tetrazole complexes of iron(II), in: Spin Crossover in Transition Metal Compounds II, Springer-Verlag Berlin, Berlin, 2004, pp. 129–153.
[250] S. Decurtins, P. Gütlich, K.M. Hasselbach, A. Hauser, H. Spiering, Inorg. Chem. 24 (1985) 2174–2178.
[251] A. Hauser, Chem. Phys. Lett. 124 (1986) 543–548.
[252] J. Jung, F. Bruchhauser, R. Feile, H. Spiering, P. Gütlich, Z. Phys. B-Condens. Mater. 100 (1996) 517–522.
[253] T. Marek, M. Bokor, K. Tompa, A. Vertes, K. Suvegh, Z. Nemes-Vetessy, K. Burger, Struct. Chem. 14 (2003) 349–368.
[254] E.W. Muller, J. Ensling, H. Spiering, P. Gütlich, Inorg. Chem. 22 (1983) 2074–2078.
[255] A. Ozarowski, B.R. McGarvey, Inorg. Chem. 28 (1989) 2262–2266.
[256] A. Vertes, M. Bokor, K. Suvegh, T. Marek, Z. Nemes-Vetessy, I. Labadi, K. Burger, J. Phys. Chem. Solids 59 (1998) 1235–1239.
[257] P. Weinberger, M. Grunert, Vib. Spectrosc. 34 (2004) 175–186.
[258] L. Wiehl, Acta Crystallogr. B 49 (1993) 289–303.
[259] L. Wiehl, H. Spiering, P. Gütlich, K. Knorr, J. Appl. Crystallogr. 23 (1990) 151–160.
[260] A. Goujon, B. Gillon, A. Gukasov, J. Jeftic, Q. Nau, E. Codjovi, F. Varret, Phys. Rev. B 67 (2003).
[261] X.J. Liu, Y. Moritomo, T. Kawamoto, A. Nakamoto, N. Kojima, Phys. Rev. B 67 (2003) 012102.
[262] W. Zhang, F. Zhao, T. Liu, M. Yuan, Z.M. Wang, S. Gao, Inorg. Chem. 46 (2007) 2541–2555.
[263] V. Russell, M. Scudder, I. Dance, J. Chem. Soc. -Dalton Trans. (2001) 789–799.
[264] J. Schweifer, P. Weinberger, K. Mereiter, M. Boca, C. Reichl, G. Wiesinger, G. Hilscher, P.J. Van Koningsbruggen, H. Kooijinan, M. Grunert, W. Linert, Inorg. Chim. Acta 339 (2002) 297–306.
[265] A. Absmeier, M. Bartel, C. Carbonera, G.N.L. Jameson, F. Werner, M. Reissner, A. Caneschi, J.F. Létard, W. Linert, Eur. J. Inorg. Chem. (2007) 3047–3054.
[266] P.J. Van Koningsbruggen, Y. Garcia, O. Kahn, L. Fournès, H. Kooijman, A.L. Spek, J.G. Haasnoot, J. Moscovici, K. Provost, A. Michalowicz, F. Renz, P. Gütlich, Inorg. Chem. 39 (2000) 1891–1900.
[267] M. Quesada, H. Kooijman, P. Gamez, J.S. Costa, P.J. Van Koningsbruggen, P. Weinberger, M. Reissner, A.L. Spek, J.G. Haasnoot, J. Reedijk, Dalton Trans. (2007) 5434–5440.
[268] A. Bialonska, R. Bronisz, Tetrahedron 64 (2008) 9771–9779.
[269] R. Bronisz, Z. Ciunik, K. Drabent, M.F. Rudolf, in: I.P. Society) (Ed.), ICAME-95, Editrice Compositori, Rimini, Italy, 1996, pp. 15–18.
[270] M. Quesada, F. Prins, O. Roubeau, P. Gamez, S.J. Teat, P.J. Van Koningsbruggen, J.G. Haasnoot, J. Reedijk, Inorg. Chim. Acta 360 (2007) 3787–3796.
[271] R. Bronisz, Inorg. Chim. Acta 340 (2002) 215–220.
[272] R. Bronisz, Eur. J. Inorg. Chem. (2004) 3688–3695.
[273] R. Bronisz, Inorg. Chim. Acta 357 (2004) 396–404.
[274] P.J. Van Koningsbruggen, Y. Garcia, H. Kooijman, A.L. Spek, J.G. Haasnoot, O. Kahn, J. Linarès, E. Codjovi, F. Varret, J. Chem. Soc. -Dalton Trans. (2001) 466–471.
[275] C.M. Grunert, J. Schweifer, P. Weinberger, W. Linert, K. Mereiter, G. Hilscher, M. Muller, G. Wiesinger, P.J. Van Koningsbruggen, Inorg. Chem. 43 (2004) 155–165.
[276] G.N.L. Jameson, F. Werner, M. Bartel, A. Absmeier, M. Reissner, J.A. Kitchen, S. Brooker, A. Caneschi, C. Carbonera, J.F. Létard, W. Linert, Eur. J. Inorg. Chem. (2009) 3948–3959.
[277] A. Absmeier, M. Bartel, C. Carbonera, G.N.L. Jameson, P. Weinberger, A. Caneschi, K. Mereiter, J.F. Létard, W. Linert, Chem. Eur. J. 12 (2006) 2235–2243.
[278] M. Bartel, A. Absmeier, G.N.L. Jameson, F. Werner, K. Kato, M. Takata, R. Boca, M. Hasegawa, K. Mereiter, A. Caneschi, W. Linert, Inorg. Chem. 46 (2007) 4220–4229.
[279] Y.L. Bai, J. Tao, R.B. Huang, L.S. Zheng, S.L. Zheng, K. Oshida, Y. Einaga, Chem. Commun. (2008) 1753–1755.
[280] K. Nomiya, K. Tsuda, N.C. Kasuga, J. Chem. Soc. -Dalton Trans. (1998) 1653–1659.
[281] J. Chuang, W. Ouellette, J. Zubieta, Inorg. Chim. Acta 361 (2008) 2357–2364.
[282] T. Wu, M. Li, D. Li, X.C. Huang, Cryst. Growth Des. 8 (2008) 568–574.
[283] R.F. Hu, J. Zhang, Y. Kang, Y.G. Yao, Inorg. Chem. Commun. 8 (2005) 828–830.
[284] Z. An, H. Sun, R.S. Wang, Acta Crystallogr. E 61 (2005) M2157–M2159.
[285] E.C. Yang, H.K. Zhao, B. Ding, X.G. Wang, X.J. Zhao, Cryst. Growth Des. 7 (2007) 2009–2015.
[286] Y.C. Shen, Z.J. Li, J.K. Cheng, Y.Y. Qin, Y.G. Yao, Inorg. Chem. Commun. 10 (2007) 888–890.
[287] Y.Y. Qin, J. Zhang, Z.J. Li, L. Zhang, X.Y. Cao, Y.G. Yao, Chem. Commun. (2008) 2532–2534.
[288] K.Z. Shao, Y.H. Zhao, Y. Xing, Y.Q. Lan, X.L. Wang, Z.M. Su, R.S. Wang, Cryst. Growth Des. 8 (2008) 2986–2989.
[289] K.Z. Shao, Y.H. Zhao, X.L. Wang, Y.Q. Lan, D.J. Wang, Z.M. Su, R.S. Wang, Inorg. Chem. 48 (2009) 10–12.
[290] L.P. Xu, Acta Crystallogr. E 65 (2009), M884-U592.
[291] I. Sotofte, K. Nielsen, Acta Chem. Scand. 38 (1984) 257–260.
[292] X.L. Wang, C. Qin, Y.Q. Lan, K.Z. Shao, Z.M. Su, E.B. Wang, Chem. Commun. (2009) 410–412.
[293] G.S. Papaefstathiou, R. Vicente, C.P. Raptopoulou, A. Terzis, A. Escuer, S.P. Perlepes, Eur. J. Inorg. Chem. (2002) 2488–2493.
[294] I. Sotofte, K. Nielsen, Acta Chem. Scand. 38 (1984) 253–255.
[295] K. Muller-Buschbaum, Y. Mokaddem, Eur. J. Inorg. Chem. (2006) 2000–2010.
[296] Z.-H. Shao, J. Luo, R.-F. Cai, X.-G. Zhou, L.-H. Weng, Z.-X. Chen, Acta Crystallogr. C 60 (2004) m250–m253.
[297] J. Luo, B.S. Liu, X.G. Zhou, L.H. Weng, Y.R. Li, R.F. Cai, Acta Crystallogr. E 60 (2004) M1391–M1393.
[298] V.C. Sharma, U. Lal, T. Singh, D. Chopra, T.N.G. Row, Acta Crystallogr. E 61 (2005) M1108–M1110.
[299] M. Rajeswaran, T.N. Blanton, D.J. Giesen, D.R. Whitcomb, N. Zumbulyadis, B.J. Antalek, M.M. Neumann, S.T. Misture, J. Solid State Chem. 179 (2006) 1053–1059.
[300] C. Lambert, F. Hampel, P.V. Schleyer, J. Organomet. Chem. 455 (1993) 29–35.
[301] K. Muller-Buschbaum, Y. Mokaddem, Z. Anorg. Allg. Chem. 633 (2007) 521–523.
[302] K. Muller-Buschbaum, Y. Mokaddem, Z. Anorg. Allg. Chem. 634 (2008) 2360–2366.
[303] L.F. Jones, L. O'Dea, D.A. Offermann, P. Jensen, B. Moubaraki, K.S. Murray, Polyhedron 25 (2006) 360–372.
[304] E.A. Goreshnik, D. Schollmeyer, M.G. Mys'kiv, Z. Anorg. Allg. Chem. 631 (2005) 835–837.

[305] E.A. Goreshnik, Pol. J. Chem. 73 (1999) 1253–1258.
[306] E.A. Goreshnik, M.G. Mys'kiv, Russ. J. Coord. Chem. 31 (2005) 341–346.
[307] C.S. Liu, L.M. Zhou, L.Q. Guo, S.T. Ma, S.M. Fang, Acta Crystallogr. C 64 (2008) M394–M397.
[308] J. Wang, M.H. Huang, P. Liu, W. Cheng, J. Mol. Struct. 875 (2008) 22–26.
[309] C.-S. Liu, G.-H. Sun, M. Li, L.-Q. Guo, L.-M. Zhou, S.-M. Fang, Open Crystallogr. J. 1 (2008) 24–30.
[310] J. Zhou, X. Liu, Y. Zhang, B. Li, Y. Zhang, J. Mol. Struct. 788 (2006) 194–199.
[311] J.H. Zhou, X.G. Liu, Y.P. Zhang, B.L. Li, Y. Zhang, Inorg. Chem. Commun. 9 (2006) 216–219.
[312] J. Zhou, Y. Peng, Y. Zhang, B. Li, Y. Zhang, Inorg. Chem. Commun. 7 (2004) 1181–1183.
[313] P. Borsting, P.J. Steel, Eur. J. Inorg. Chem. (2004) 376–380.
[314] X.R. Meng, Y.L. Song, H.W. Hou, Y.T. Fan, G. Li, Y. Zhu, Inorg. Chem. 42 (2003) 1306–1315.
[315] X. Meng, J. Li, H. Hou, Y. Song, Y. Fan, Y. Zhu, J. Mol. Struct. 891 (2008) 305–311.
[316] H. Hou, X. Meng, Y. Song, Y. Fan, Y. Zhu, H. Lu, C. Du, W. Shao, Inorg. Chem. 41 (2002) 4068–4075.
[317] X.L. Zhou, X.R. Meng, W. Cheng, H.W. Hou, M.S. Tang, Y.T. Fan, Inorg. Chim. Acta 360 (2007) 3467–3474.
[318] G.F. Zhang, Y.L. Dou, J.B. She, M.H. Yin, J. Chem. Crystallogr. 37 (2007) 63–67.
[319] C.M. Thomas, A. Neels, H. Stoeckli-Evans, G. Suss-Fink, Inorg. Chem. Commun. 5 (2002) 264–266.
[320] H. Ohi, M. Shimizu, M. Obata, T. Funabiki, S. Yano, Acta Crystallogr. E 64 (2008), M1256-U1396.
[321] W. Shi, X.Y. Chen, N. Xu, H.B. Song, B. Zhao, P. Cheng, D.Z. Liao, S.P. Yan, Eur. J. Inorg. Chem. (2006) 4931–4937.
[322] Y.F. Yue, J. Liang, E.O. Gao, C.J. Fang, Z.G. Yan, C.H. Yan, Inorg. Chem. 47 (2008) 6115–6117.
[323] W.X. Zhang, W. Xue, J.B. Lin, Y.Z. Zheng, X.M. Chen, CrystEngComm 10 (2008) 1770–1776.
[324] G.F. Liu, Z.G. Ren, Y. Chen, D. Liu, H.X. Li, Y. Zhang, J.P. Lang, Inorg. Chem. Commun. 11 (2008) 225–229.
[325] W.Q. Zou, M.S. Wang, Y. Li, A.Q. Wu, F.K. Zheng, Q.Y. Chen, G.C. Guo, J.S. Huang, Inorg. Chem. 46 (2007) 6852–6854.
[326] X. Han, C. An, Z. Zhang, Appl. Organomet. Chem. 22 (2008) 565–572.
[327] X.L. Han, C.X. An, Z.H. Zhang, Appl. Organomet. Chem. 22 (2008) 565–572.
[328] X.P. Li, J.Y. Zhang, M. Pan, S.R. Zheng, Y. Liu, C.Y. Su, Inorg. Chem. 46 (2007) 4617–4625.
[329] J.G. Haasnoot, G.C.M. Dekeyzer, G.C. Verschoor, Acta Crystallogr. C 39 (1983) 1207–1209.
[330] W. Ouellette, B.S. Hudson, J. Zubieta, Inorg. Chem. 46 (2007) 4887–4904.
[331] Y.C. Lu, X.R. Li, Z.H. Zhang, M. Du, Chin. J. Struct. Chem. 26 (2007) 15–20.
[332] Q.G. Zhai, C.Z. Lu, X.Y. Wu, S.R. Batten, Cryst. Growth Des. 7 (2007) 2332–2342.
[333] J.M. Ellsworth, K.L. Seward, M.D. Smith, H.C. zur Loye, Solid State Sci. 10 (2008) 267–282.
[334] E.C. Yang, Q.Q. Liang, X.G. Wang, X.J. Zhao, Aust. J. Chem. 61 (2008) 813–820.
[335] Q.G. Zhai, C.Z. Lu, S.M. Chen, X.J. Xu, W.B. Yang, Cryst. Growth Des. 6 (2006) 1393–1398.
[336] D.J. Chesnut, A. Kusnetzow, R. Birge, J. Zubieta, Inorg. Chem. 38 (1999) 5484–5494.
[337] W. Ouellette, A.V. Prosvirin, V. Chieffo, K.R. Dunbar, B. Hudson, J. Zubieta, Inorg. Chem. 45 (2006) 9346–9366.
[338] J.R. Li, Q. Yu, E.C. Sañudo, Y. Tao, X.H. Bu, Chem. Commun. (2007) 2602–2604.
[339] X. He, C.Z. Lu, C.D. Wu, L.J. Chen, Eur. J. Inorg. Chem. (2006) 2491–2503.
[340] Y.X. Gao, L.B. Wang, Y.L. Niu, Acta Crystallogr. E 63 (2007), M2366-U1086.
[341] A.B. Lysenko, E.V. Govor, H. Krautscheid, K.V. Domasevitch, Dalton Trans. (2006) 3772–3776.
[342] B. Ding, L. Yi, P. Cheng, D.Z. Liao, S.P. Yan, Inorg. Chem. 45 (2006) 5799–5803.
[343] X.C. Huang, W. Luo, Y.F. Shen, X.J. Lin, D. Li, Chem. Commun. (2008) 3995–3997.
[344] K. Muller-Buschbaum, Y. Mokaddem, Chem. Commun. (2006) 2060–2062.
[345] A.A. Soudi, A. Morsali, S. Moazzenchi, Inorg. Chem. Commun. 9 (2006) 1259–1262.
[346] W. Ouellette, J.R. Galan-Mascaros, K.R. Dunbar, J. Zubieta, Inorg. Chem. 45 (2006) 1909–1911.
[347] D.W. Engelfriet, W. Den Brinker, G.C. Verschoor, S. Gorter, Acta Crystallogr. B 35 (1979) 2922–2927.
[348] X.L. Qi, Acta Crystallogr. E 65 (2009), M47-U542.
[349] X.L. Qi, Acta Crystallogr. E 65 (2009), M134-U222.
[350] P.J. Hagrman, R.L. LaDuca, H.J. Koo, R. Rarig, R.C. Haushalter, M.H. Whangbo, J. Zubieta, Inorg. Chem. 39 (2000) 4311–4317.
[351] Z. Liu, J.H. Zhou, Y.Z. Li, Y. Song, X.T. Chen, Chin. J. Inorg. Chem. 21 (2005) 1601–1604.
[352] Z.H. Weng, Z.L. Chen, F.P. Liang, Acta Crystallogr. C 64 (2008) M64–M66.
[353] Y.X. Gao, L.B. Wang, X.R. Hao, Acta Crystallogr. E 63 (2007), M2142-U1044.
[354] W. Ouellette, A.V. Prosvirin, J. Valeich, K.R. Dunbar, J. Zubieta, Inorg. Chem. 46 (2007) 9067–9082.
[355] G. Mahmoudi, A. Morsali, L.G. Zhu, Z. Anorg. Allg. Chem. 633 (2007) 539–541.
[356] Q.G. Zhai, X.Y. Wu, S.M. Chen, L.J. Chen, C.Z. Lu, Inorg. Chim. Acta 360 (2007) 3484–3492.
[357] Y.X. Gao, L.B. Wang, X.R. Hao, Acta Crystallogr. E 63 (2007), M2232-U1860.
[358] Y.X. Gao, L.B. Wang, X.R. Hao, Acta Crystallogr. E 63 (2007), M1800-U1297.
[359] E. Barea, A. Rodriguez-Dieguez, J.A.R. Navarro, G. D'Alfonso, A. Sironi, Dalton Trans. (2008) 1825–1827.
[360] K. Muller-Buschbaum, Y. Mokaddem, C.J. Holler, Z. Anorg. Allg. Chem. 634 (2008) 2973–2977.
[361] J.P. Zhang, S.L. Zheng, X.C. Huang, X.M. Chen, Angew. Chem. Int. Ed. 43 (2004) 206–209.
[362] J.P. Zhang, Y.Y. Lin, X.C. Huang, X.M. Chen, Dalton Trans. (2005) 3681–3685.
[363] X.H. Huang, T.L. Sheng, S.C. Xiang, R.B. Fu, S.M. Hu, Y.M. Li, X.T. Wu, Inorg. Chem. 46 (2007) 497–500.
[364] Y.L. Fu, H. Lu, J. Mol. Struct. 892 (2008) 205–209.
[365] L. Yi, B. Ding, B. Zhao, P. Cheng, D.Z. Liao, S.P. Yan, Z.H. Jiang, Inorg. Chem. 43 (2004) 33–43.
[366] Q.G. Zhai, X.Y. Wu, S.M. Chen, C.Z. Lu, W.B. Yang, Cryst. Growth Des. 6 (2006) 2126–2135.
[367] Q.G. Zhai, C.Z. Lu, Q.Z. Zhang, X.Y. Wu, X.J. Xu, S.M. Chen, L.J. Chen, Inorg. Chim. Acta 359 (2006) 3875–3887.
[368] P. Nockemann, I. Pantenburg, G. Meyer, Z. Anorg. Allg. Chem. 634 (2008) 228–230.
[369] Q.G. Zhai, M.C. Hu, S.N. Li, Y.C. Jiang, Inorg. Chim. Acta 362 (2009) 1355–1357.
[370] J.P. Zhang, X.M. Chen, J. Am. Chem. Soc. 130 (2008) 6010–6017.
[371] G. Yang, R.G. Raptis, Chem. Commun. (2004) 2058–2059.
[372] C. Yang, X.P. Wang, M.A. Omary, J. Am. Chem. Soc. 129 (2007) 15454–15455.
[373] K.L. Zhang, N. Qiao, H.Y. Gao, F. Zhou, M. Zhang, Polyhedron 26 (2007) 2461–2469.
[374] H. Park, G. Krigsfeld, S.J. Teat, J.B. Parise, Cryst. Growth Des. 7 (2007) 1343–1349.
[375] Q. Wang, M.J. Wu, X.G. Wang, X.J. Zhao, Acta Crystallogr. E 62 (2006) M2496–M2498.
[376] Z.Q. Zheng, C.W. Liu, B. Lin, Acta Crystallogr. E 63 (2007) M1252–M1253.
[377] S. Sun, S.P. Chen, S.L. Gao, J. Coord. Chem. 61 (2008) 2068–2078.
[378] Y.Y. Lin, Y.B. Zhang, J.P. Zhang, X.M. Chen, Cryst. Growth Des. 8 (2008) 3673–3679.
[379] Z.L. Chen, X.L. Li, F.P. Liang, J. Solid State Chem. 181 (2008) 2078–2086.
[380] Q.G. Zhai, M.C. Hu, S.N. Li, Y.C. Jiang, Inorg. Chem. Commun. 11 (2008) 1147–1150.
[381] S.P. Chen, S. Sun, S.L. Gao, J. Solid State Chem. 181 (2008) 3308–3316.
[382] W. Li, H.P. Jia, Z.F. Ju, J. Zhang, Cryst. Growth Des. 6 (2006) 2136–2140.
[383] B. Liu, X.C. Zhang, Inorg. Chem. Commun. 11 (2008) 1162–1165.
[384] R. Patel, M.T. Weller, D.J. Price, Dalton Trans. (2007) 4034–4039.
[385] B. Liu, Y.H. Chen, X.C. Zhang, Inorg. Chem. Commun. 11 (2008) 965–968.
[386] W.W. Zhou, L. Bing, W.T. Chen, F.K. Zheng, J.T. Chen, G.C. Guo, J.S. Huang, Chin. J. Struct. Chem. 26 (2007) 703–706.
[387] C.Y. Su, A.M. Goforth, M.D. Smith, P.J. Pellechia, H.C. zur Loye, J. Am. Chem. Soc. 126 (2004) 3576–3586.
[388] H.O. Desseyn, A.C. Fabretti, W. Malavasi, J. Crystallogr. Spectrosc. Res. 20 (1990) 355–362.
[389] G.F. Zhang, S.M. Zhao, J.B. She, S.W. Ng, Acta Crystallogr. E 62 (2006) M2148–M2150.
[390] R.B. Zhang, Z.J. Li, Y.Y. Qin, J.K. Cheng, J. Zhang, Y.G. Yao, Inorg. Chem. 47 (2008) 4861–4876.
[391] A.C. Fabretti, A. Giusti, R. Sessoli, Inorg. Chim. Acta 205 (1993) 53–57.
[392] J.P. Zhang, Y.Y. Lin, W.X. Zhang, X.M. Chen, J. Am. Chem. Soc. 127 (2005) 14162–14163.
[393] Q.G. Zhai, C.Z. Lu, S.M. Chen, X.J. Xu, W.B. Yang, Inorg. Chem. Commun. 9 (2006) 819–822.
[394] R.B. Zhang, J. Zhang, Z.J. Li, J.K. Cheng, Y.Y. Qin, Y.G. Yao, Cryst. Growth Des. 8 (2008) 3735–3744.
[395] B. Ding, Y.Q. Huang, Y.Y. Liu, W. Shi, P. Cheng, Inorg. Chem. Commun. 10 (2007) 7–10.
[396] G.V. Romanenko, Z.A. Savelieva, N.V. Podberezskaya, S.V. Larionov, J. Struct. Chem. 38 (1997) 171–176.
[397] U. Garcia-Couceiro, O. Castillo, A. Luque, J.P. Garcia-Teran, G. Beobide, P. Roman, Eur. J. Inorg. Chem. (2005) 4280–4290.
[398] M.A.M. Abu-Youssef, A. Escuer, R. Vicente, F.A. Mautner, L. Ohrstrom, M.A.S. Goher, Polyhedron 24 (2005) 557–562.
[399] U. Garcia-Couceiro, D. Olea, O. Castillo, A. Luque, P. Roman, P.J. de Pablo, J. Gomez-Herrero, F. Zamora, Inorg. Chem. 44 (2005) 8343–8348.
[400] P. Nockemann, G. Meyer, Z. Anorg. Allg. Chem. 633 (2007) 2238–2241.
[401] Y. Wang, P. Cheng, Struct. Chem. 18 (2007) 677–682.
[402] J.J. Liu, X. He, M. Shao, M.X. Li, J. Mol. Struct. 919 (2009) 189–195.
[403] L.R. Groeneveld, G. Vos, G.C. Verschoor, J. Reedijk, J. Chem. Soc. -Chem. Commun. (1982) 620–621.
[404] A.L. Spek, J. Kolnaar, J. Reedijk, Private Commun. (2004).
[405] Y. Guo, H. Cai, J.G. Li, G.B. Wan, Acta Crystallogr. E 64 (2008), M784-U480.
[406] K. Drabent, Z. Ciunik, A. Ozarowski, Inorg. Chem. 47 (2008) 3358–3365.
[407] E.V. Govor, A.B. Lysenko, K.V. Domasevitch, Acta Crystallogr. C 64 (2008) M201–M204.
[408] E.V. Govor, A.B. Lysenko, K.V. Domasevitch, E.B. Rusanov, A.N. Chernega, Acta Crystallogr. C 64 (2008) M117–M120.
[409] Y.Q. Huang, X.Q. Zhao, W. Shi, W.Y. Liu, Z.L. Chen, P. Cheng, D.Z. Liao, S.P. Yan, Cryst. Growth Des. 8 (2008) 3652–3660.
[410] S. Pillet, C. Lecomte, Acta Crystallogr. C 63 (2007) M184–M186.
[411] W. Vreugdenhil, J.G. Haasnoot, R.A.G. De Graaff, H.A. Nieuwenhuis, D. Reefman, J. Reedijk, Acta Crystallogr. C 43 (1987) 1527–1530.
[412] X.Y. Wang, L. Wang, Z.M. Wang, G. Su, S. Gao, Chem. Mater. 17 (2005) 6369–6380.
[413] Y.Q. Huang, P. Cheng, Inorg. Chem. Commun. 11 (2008) 66–68.

[414] M. Biaginicingi, A.M. Manottilanfredi, F. Ugozzoli, J.G. Haasnoot, J. Reedijk, Gazz. Chim. Ital. 124 (1994) 509–513.
[415] W. Vreugdenhil, S. Gorter, J.G. Haasnoot, J. Reedijk, Polyhedron 4 (1985) 1769–1775.
[416] A.B. Lysenko, E.V. Govor, K.V. Domasevitch, Inorg. Chim. Acta 360 (2007) 55–60.
[417] X.C. Zhang, Y.H. Chen, B. Liu, Inorg. Chem. Commun. 11 (2008) 446–449.
[418] F. Guedira, M.S. Idrissi, H. Krautscheid, L. El Ammari, Acta Crystallogr. C 59 (2003) M530–M532.
[419] W.W. Zhou, J.T. Chen, G. Xu, M.S. Wang, J.P. Zou, X.F. Long, G.J. Wang, G.C. Guo, J.S. Huang, Chem. Commun. (2008) 2762–2764.
[420] R.B. Zhang, J. Zhang, Z.J. Li, Y.Y. Qin, J.K. Cheng, Y.G. Yao, Chem. Commun. (2008) 4159–4161.
[421] L. Zhang, Y. Ling, J. Li, H. Gao, Struct. Chem. 19 (2008) 911–916.
[422] W. Dong, Y. Ouyang, L.N. Zhu, D.Z. Liao, Z.H. Jiang, S.P. Yan, P. Cheng, W. Dong, Transit. Met. Chem. 31 (2006) 801–804.
[423] Effendy, F. Marchetti, C. Pettinari, R. Pettinari, M. Ricciutelli, B.W. Skelton, A.H. White, Inorg. Chem. 43 (2004) 2157–2165.
[424] Effendy, F. Marchetti, C. Pettinari, R. Pettinari, B.W. Skelton, A.H. White, Inorg. Chem. 42 (2003) 112–117.
[425] X.Y. Chen, P. Cheng, S.P. Yan, D.Z. Liao, Z.H. Jiang, Z. Anorg. Allg. Chem. 631 (2005) 3104–3107.
[426] L.F. Tang, Z.H. Wang, J.F. Chai, W.L. Jia, Y.M. Xu, J.T. Wang, Polyhedron 19 (2000) 1949–1954.
[427] W. Dong, Q.L. Wang, Z.Q. Liu, D.Z. Liao, Z.H. Jiang, S.P. Yan, P. Cheng, Polyhedron 22 (2003) 3315–3319.
[428] Y. Garcia, G. Bravic, C. Gieck, D. Chasseau, W. Tremel, P. Gütlich, Inorg. Chem. 44 (2005) 9723–9730.
[429] Y. Carcia, P.J. Van Koningsbruggen, H. Kooijman, A.L. Spek, J.G. Haasnoot, O. Kahn, Eur. J. Inorg. Chem. (2000) 307–314.
[430] H.A. Habib, A. Hoffmann, H.A. Hoppe, G. Steinfeld, C. Janiak, Inorg. Chem. 48 (2009) 2166–2180.
[431] L. Yi, X. Yang, T.B. Lu, P. Cheng, Cryst. Growth Des. 5 (2005) 1215–1219.
[432] H.A. Habib, A. Hoffmann, H.A. Hoppe, C. Janiak, Dalton Trans. (2009) 1742–1751.
[433] H.A. Habib, J. Sanchiz, C. Janiak, Dalton Trans. (2008) 1734–1744.
[434] X. Zhu, Y.M. Zhang, B.L. Li, Y. Zhang, J. Coord. Chem. 59 (2006) 513–522.
[435] B. Ding, E.C. Yang, X.J. Zhao, X.G. Wang, J. Coord. Chem. 62 (2009) 287–293.
[436] B.L. Li, B.Z. Li, X. Zhu, L.M. Zhu, Y. Zhang, Acta Crystallogr. C 59 (2003) M350–M351.
[437] B.L. Li, B.Z. Li, X. Zhu, X.H. Lu, Y. Zhang, J. Coord. Chem. 57 (2004) 1361–1367.
[438] X. Zhu, B.Z. Li, J.H. Zhou, B.L. Li, Y. Zhang, Acta Crystallogr. C 60 (2004) M191–M193.
[439] B.L. Li, X. Zhu, J.H. Zhou, Y. Zhang, J. Coord. Chem. 58 (2005) 271–278.
[440] B.L. Li, Z. Xu, Z.B. Cao, L.M. Zhu, K.B. Yu, Transit. Met. Chem. 24 (1999) 622–627.
[441] J.G. Ding, H.Y. Ge, Y.M. Zhang, B.L. Li, Y. Zhang, J. Mol. Struct. 782 (2006) 143–149.
[442] S.W. Wang, Y. Yang, B.L. Li, Y. Zhang, Chin. J. Struct. Chem. 26 (2007) 763–766.
[443] B.L. Li, X. Zhu, J.H. Zhou, Y.F. Peng, Y. Zhang, Polyhedron 23 (2004) 3133–3141.
[444] X. Zhu, H.Y. Ge, Y.M. Zhang, B.L. Li, Y. Zhang, Polyhedron 25 (2006) 1875–1883.
[445] L. Shen, M.X. Luo, J. Chem. Crystallogr. 38 (2008) 163–167.
[446] B.L. Li, X.Y. Wang, X. Zhu, S. Gao, Y. Zhang, Polyhedron 26 (2007) 5219–5224.
[447] X.Y. Wang, B.L. Li, X. Zhu, S. Gao, Eur. J. Inorg. Chem. (2005) 3277–3286.
[448] J.H. Zhou, X. Zhu, Y.N. Zhang, Y. Zhang, B.L. Li, Inorg. Chem. Commun. 7 (2004) 949–952.
[449] A.X. Tian, J. Ying, J. Peng, J.Q. Sha, H.J. Pang, P.P. Zhang, Y. Chen, M. Zhu, Z.M. Su, Cryst. Growth Des. 8 (2008) 3717–3724.
[450] A.X. Tian, J. Ying, J. Peng, J.Q. Sha, H.J. Pang, P.P. Zhang, Y. Chen, M. Zhu, Z.M. Su, Inorg. Chem. 48 (2009) 100–110.
[451] G.A. Van Albada, R.C. Guijt, J.G. Haasnoot, M. Lutz, A.L. Spek, J. Reedijk, Eur. J. Inorg. Chem. (2000) 121–126.
[452] Q.H. Zhao, H.F. Li, X.F. Wang, Z.D. Chen, New J. Chem. 26 (2002) 1709–1710.
[453] G. Yin, Y.P. Zhang, B.L. Li, Y. Zhang, J. Mol. Struct. 837 (2007) 263–268.
[454] Z.G. Gu, Y.F. Xu, X.H. Zhou, J.L. Zuo, X.Z. You, Cryst. Growth Des. 8 (2008) 1306–1312.
[455] A.X. Tian, J. Ying, J. Peng, J.Q. Sha, Z.G. Han, J.F. Ma, Z.M. Su, N.H. Hu, H.Q. Jia, Inorg. Chem. 47 (2008) 3274–3283.
[456] X.G. Liu, H.Y. Ge, Y.M. Zhang, L. Hu, B.L. Li, Y. Zhang, J. Mol. Struct. 796 (2006) 129–138.
[457] L. Shen, Acta Crystallogr. E 63 (2007), M3045-U1677.
[458] X.L. Wang, C. Qin, E.B. Wang, Z.M. Su, Chem. Eur. J. 12 (2006) 2680–2691.
[459] X.G. Liu, K. Liu, Y. Yang, B.L. Li, Inorg. Chem. Commun. 11 (2008) 1273–1275.
[460] B.Z. Li, X.G. Liu, Z.H. Wang, B.L. Li, Y. Zhang, Acta Crystallogr. C 62 (2006) M10–M12.
[461] J.G. Ding, X.G. Liu, B.L. Li, L.Y. Wang, Y. Zhang, Inorg. Chem. Commun. 11 (2008) 1079–1081.
[462] L.Y. Wang, Y. Yang, K. Liu, B.L. Li, Y. Zhang, Cryst. Growth Des. 8 (2008) 3902–3904.
[463] A.X. Tian, J. Ying, J. Peng, J.Q. Sha, D.X. Zhu, H.J. Pang, P.P. Zhang, Y. Chen, M. Zhu, Inorg. Chem. Commun. 11 (2008) 1132–1135.
[464] Y.Y. Liu, L. Yi, B. Ding, Y.Q. Huang, P. Cheng, Inorg. Chem. Commun. 10 (2007) 517–519.
[465] Y.Y. Liu, B. Ding, Y.Q. Huang, H.S. Wang, P. Cheng, Chin. J. Inorg. Chem. 22 (2006) 1495–1498.
[466] W.B. Wang, L.Y. Wang, B.L. Li, Y. Zhang, Acta Crystallogr. E 63 (2007), M2416-U1535.
[467] L.Y. Wang, Y.F. Peng, Y.P. Zhang, B.L. Li, Y. Zhang, Acta Crystallogr. C 63 (2007) M297–M299.
[468] X.R. Meng, Y.L. Song, H.W. Hou, H.Y. Han, B. Xiao, Y.T. Fan, Y. Zhu, Inorg. Chem. 43 (2004) 3528–3536.
[469] X. Wang, L.K. Li, H.W. Hou, J. Wu, Y.T. Fan, Eur. J. Inorg. Chem. (2007) 5234–5245.
[470] B.Z. Li, X.G. Liu, Y.F. Peng, B.L. Li, Y. Zhang, Acta Crystallogr. C 62 (2006) M41–M44.
[471] B.L. Li, Y.F. Peng, B.Z. Li, Y. Zhang, Chem. Commun. (2005) 2333–2335.
[472] Y.Y. Niu, H.L. Zhang, H.W. Hou, S.W. Ng, Acta Crystallogr. E 61 (2005) M2536–M2537.
[473] Y.F. Peng, H.Y. Ge, B.Z. Li, B.L. Li, Y. Zhang, Cryst. Growth Des. 6 (2006) 994–998.
[474] B.Z. Li, Y.F. Peng, Y.P. Zhang, B.L. Li, Y. Zhang, Acta Crystallogr. C 60 (2004) M560–M562.
[475] X.P. Shen, H. Zhou, Acta Crystallogr. E 62 (2006) M3548–M3550.
[476] J. Lin, G.Y. Dong, Acta Crystallogr. E 63 (2007), M1944-U1416.
[477] Y.F. Peng, X.G. Liu, B.Z. Li, B.L. Li, Y. Zhang, Acta Crystallogr. C 61 (2005) M333–M336.
[478] Y. Zhang, Y.M. Zhang, X.G. Liu, B.L. Li, Chin. J. Struct. Chem. 24 (2005) 1129–1132.
[479] B.Z. Li, Y.F. Peng, X.G. Liu, B.L. Li, Y. Zhang, J. Mol. Struct. 741 (2005) 235–240.
[480] Y.F. Peng, T.B. Liu, X.H. Yang, B.L. Li, Chin. J. Struct. Chem. 25 (2006) 793–796.
[481] J.M. Salas, M.A. Romero, A. Rahmani, M. Quiros, An. Quim. 92 (1996) 249–254.
[482] J.L. Du, T.L. Hu, S.M. Zhang, Y.F. Zeng, X.H. Bu, CrystEngComm 10 (2008) 1866–1874.
[483] X.R. Meng, Y.R. Liu, Y.L. Song, H.W. Hou, Y.T. Fan, Y. Zhu, Inorg. Chim. Acta 358 (2005) 3024–3032.
[484] C. Qin, X.L. Wang, E.B. Wang, Z.M. Su, Inorg. Chem. 47 (2008) 5555–5557.
[485] C. Qin, X.L. Wang, L. Yuan, E.B. Wang, Cryst. Growth Des. 8 (2008) 2093–2095.
[486] H.Y. Ge, K. Liu, Y. Yang, B.L. Li, Y. Zhang, Inorg. Chem. Commun. 11 (2008) 260–264.
[487] H.Y. Ge, L.Y. Wang, Y. Yang, B.L. Li, Y. Zhang, J. Mol. Struct. 876 (2008) 288–293.
[488] H.Y. Ge, Y.M. Zhang, B.L. Li, Y. Zhang, Acta Crystallogr. C 62 (2006) M501–M503.
[489] W. He, B. Wang, X. Bai, Transit. Met. Chem. 33 (2008) 399–403.
[490] D.Z. Wang, C.S. Liu, J.R. Li, L. Li, Y.F. Zeng, X.H. Bu, CrystEngComm 9 (2007) 289–297.
[491] X.L. Wang, C. Qin, E.B. Wang, Z.M. Su, Chem. Commun. (2007) 4245–4247.
[492] H.P. Zhou, P. Wang, F.Y. Hao, H.P. Ye, Q. Zhao, R.L. Zhang, Y.P. Tian, J.Y. Wu, X.T. Tao, M.H. Jiang, J. Mol. Struct. 892 (2008) 316–319.
[493] Y. Gao, B. Twamley, J.M. Shreeve, Organometallics 25 (2006) 3364–3369.
[494] X.L. Zhou, X.R. Meng, H.W. Hou, Acta Crystallogr. E 63 (2007), M1717-U1257.
[495] C. He, B.G. Zhang, L.X. Xie, Y. Liu, C.Y. Duan, CrystEngComm 10 (2008) 759–764.
[496] G.A. Senchyk, A.B. Lysenko, H. Krautscheid, J. Sieler, K.V. Domasevitch, Acta Crystallogr. C 64 (2008) M246–M249.
[497] K.T. Youm, S. Huh, Y. Kim, S. Park, M.J. Jun, Bull. Korean Chem. Soc. 27 (2006) 1521–1522.
[498] G.G. Lobbia, M. Pellei, C. Pettinari, C. Santini, B.W. Skelton, A.H. White, Polyhedron 24 (2005) 181–187.
[499] G.G. Lobbia, M. Pellei, C. Pettinari, C. Santini, B.W. Skelton, A.H. White, Inorg. Chim. Acta 358 (2005) 1162–1170.
[500] C. Janiak, T.G. Scharmann, H. Hemling, D. Lentz, J. Pickardt, Chem. Ber. 128 (1995) 235–244.
[501] K.T. Youm, M.G. Kim, J. Ko, M.J. Jun, Polyhedron 26 (2007) 929–932.
[502] K.T. Youm, M.G. Kim, J. Ko, M.J. Jun, Angew. Chem. Int. Ed. 45 (2006) 4003–4007.
[503] C. Janiak, H. Hemling, J. Chem. Soc. -Dalton Trans. (1994) 2947–2952.
[504] C. Janiak, T.G. Scharmann, W. Gunther, W. Hinrichs, D. Lentz, Chem. Berichte 129 (1996) 991–995.
[505] C. Janiak, T.G. Scharmann, P. Albrecht, F. Marlow, R. Macdonald, J. Am. Chem. Soc. 118 (1996) 6307–6308.
[506] C. Janiak, S. Temizdemir, T.G. Scharmann, A. Schmalstieg, J. Demtschuk, Z. Anorg. Allg. Chem. 626 (2000) 2053–2062.
[507] C. Janiak, T.G. Scharmann, W. Gunther, F. Girgsdies, H. Hemling, W. Hinrichs, D. Lentz, Chem. Eur. J. 1 (1995) 637–644.
[508] Y. Wang, B. Ding, P. Cheng, D.Z. Liao, S.P. Yan, Inorg. Chem. 46 (2007) 2002–2010.
[509] B. Ding, L. Yi, Y. Wang, P. Cheng, D.Z. Liao, S.P. Yan, Z.H. Jiang, H.B. Song, H.G. Wang, Dalton Trans. (2006) 665–675.
[510] Z.N. Yang, T.T. Sun, Acta Crystallogr. E 64 (2008), M1327-U3021.
[511] S.W. Liang, M.X. Li, M. Shao, X. He, J. Mol. Struct. 875 (2008) 17–21.
[512] Y. Wang, L. Yi, X. Yang, B. Ding, P. Cheng, D.Z. Liao, S.P. Yan, Inorg. Chem. 45 (2006) 5822–5829.
[513] H. Li, L.M. Xie, Acta Crystallogr. E 65 (2009), M935-U1058.
[514] P. de Fremont, N.M. Scott, E.D. Stevens, T. Ramnial, O.C. Lightbody, C.L.B. Macdonald, J.A.C. Clyburne, C.D. Abernethy, S.P. Nolan, Organometallics 24 (2005) 6301–6309.
[515] X.C. Zhang, Y.H. Chen, B. Liu, Inorg. Chem. Commun. 11 (2008) 876–878.
[516] B. Liu, G.C. Guo, J.S. Huang, J. Solid State Chem. 179 (2006) 3136–3144.
[517] X.D. Sun, X.H. He, W. Wang, D.H. Miao, Q.Z. Sun, Acta Crystallogr. E 65 (2009), M518-U535.
[518] L. Cheng, W.X. Zhang, B.H. Ye, J.B. Lin, X.M. Chen, Eur. J. Inorg. Chem. (2007) 2668–2676.
[519] S. Hu, S.H. Zhang, M.H. Zeng, Acta Crystallogr. E 63 (2007), M2543-U2964.
[520] Y.W. Zhang, G. Zhang, Y.Y. Sun, L. Cheng, Acta Crystallogr. E 64 (2008), M1073-U1924.

[521] J.C. Chen, A.J. Zhou, S. Hu, M.L. Tong, Y.X. Tong, J. Mol. Struct. 794 (2006) 225–229.
[522] G. Yucesan, M.H. Yu, W. Ouellette, C.J. O'Connor, J. Zubieta, CrystEngComm 7 (2005) 480–490.
[523] J.P. Zhang, Y.Y. Lin, X.C. Huang, X.M. Chen, Cryst. Growth Des. 6 (2006) 519–523.
[524] X.F. Xie, S.P. Chen, Z.Q. Xia, S.L. Gao, Polyhedron 28 (2009) 679–688.
[525] X.M. Jin, Q.F. Xu, Q.X. Zhou, J.M. Lu, L.H. Wang, Y. Zhang, Chin. J. Inorg. Chem. 25 (2009) 539–543.
[526] M.X. Peng, C.J. Li, M.L. Tong, Inorg. Chem. Commun. 11 (2008) 707–710.
[527] Y.B. Dong, H.Y. Wang, J.P. Ma, R.Q. Huang, Cryst. Growth Des. 5 (2005) 789–800.
[528] J.J. Liu, X. He, M. Shao, M.X. Li, J. Mol. Struct. 891 (2008) 50–57.
[529] M.H. Klingele, S. Brooker, Inorg. Chim. Acta 357 (2004) 3413–3417.
[530] Y. Garcia, J. Moscovici, A. Michalowicz, V. Ksenofontov, G. Levchenko, G. Bravic, D. Chasseau, P. Gütlich, Chem. Eur. J. 8 (2002) 4992–5000.
[531] Z.G. Zhao, J. Zhang, X.Y. Wu, Q.G. Zhai, L.J. Chen, S.M. Chen, Y.M. Xie, C.Z. Lu, CrystEngComm 10 (2008) 273–275.
[532] B. Ding, E.C. Yang, J.H. Guo, X.J. Zhao, X.G. Wang, Inorg. Chem. Commun. 11 (2008) 1481–1483.
[533] B. Ding, Y.Y. Liu, X.J. Zhao, E.C. Yang, X.G. Wang, J. Mol. Struct. 920 (2009) 248–251.
[534] T.L. Hu, W.P. Du, B.W. Hu, J.R. Li, X.H. Bu, R. Cao, CrystEngComm 10 (2008) 1037–1043.
[535] D.G. Ding, H. Xu, Y.T. Fan, H.W. Hou, Inorg. Chem. Commun. 11 (2008) 1280–1283.
[536] X.Y. Zhou, Y.Q. Huang, W.Y. Sun, Chin. J. Inorg. Chem. 24 (2008) 1733–1737.
[537] X.X. Zhao, J.P. Ma, Y.B. Dong, R.Q. Huang, Cryst. Growth Des. 7 (2007) 1058–1068.
[538] D.G. Ding, B.L. Wu, Y.T. Fan, H.W. Hou, Cryst. Growth Des. 9 (2009) 508–516.
[539] P.J. Van Koningsbruggen, J.W. Vanhal, E. Muller, R.A.G. De Graaff, J.G. Haasnoot, J. Reedijk, J. Chem. Soc. -Dalton Trans. (1993) 1371–1375.
[540] Y.Y. Liu, Acta Crystallogr. E 63 (2007), M1605-U1419.
[541] Y.Y. Sun, Y.W. Zhang, G. Zhang, L. Cheng, Acta Crystallogr. E 64 (2008), M1113-U1159.
[542] R.X. Yuan, R.G. Xiong, B.F. Abrahams, G.H. Lee, S.M. Peng, C.M. Che, X.Z. You, J. Chem. Soc. -Dalton Trans. (2001) 2071–2073.
[543] J.S. Bradshaw, C.W. McDaniel, B.D. Skidmore, R.B. Nielsen, B.E. Wilson, N.K. Dalley, R.M. Izatt, J. Heterocycl. Chem. 24 (1987) 1085–1092.
[544] S.W. Liang, M.X. Li, M. Shao, H.J. Liu, Inorg. Chem. Commun. 10 (2007) 1347–1350.
[545] Y.Y. Liu, Y.Q. Huang, W. Shi, P. Cheng, D.Z. Liao, S.P. Yan, Cryst. Growth Des. 7 (2007) 1483–1489.
[546] Y.Q. Huang, B. Ding, H.B. Song, B. Zhao, P. Ren, P. Cheng, H.G. Wang, D.Z. Liao, S.P. Yan, Chem. Commun. (2006) 4906–4908.
[547] W. Li, M.X. Li, M. Shao, Z.X. Wang, H.J. Liu, Inorg. Chem. Commun. 11 (2008) 954–957.
[548] S.W. Liang, X. He, M. Shao, M.X. Li, J. Coord. Chem. 61 (2008) 2999–3007.
[549] S.J. Hong, J.Y. Ryu, J.Y. Lee, C. Kim, S.J. Kim, Y. Kim, Dalton Trans. (2004) 2697–2701.
[550] K.T. Youm, H.C. Kang, G.B. Lee, H.K. Woo, Y.J. Park, N.K. Lee, J. Ko, M.J. Jun, Polyhedron 25 (2006) 2318–2324.
[551] S.K. Yoo, J.Y. Ryu, J.Y. Lee, C. Kim, S.J. Kim, Y. Kim, Dalton Trans. (2003) 1454–1456.
[552] S.J. Hong, J.S. Seo, J.Y. Ryu, J.H. Lee, C. Kim, S.J. Kim, Y. Kim, A.J. Lough, J. Mol. Struct. 751 (2005) 22–28.
[553] K.T. Youm, J. Ko, M.J. Jun, Polyhedron 25 (2006) 2717–2720.
[554] J.Y. Ryu, J.Y. Lee, S.H. Choi, S.J. Hong, C. Kim, Y. Kim, S.J. Kim, Inorg. Chim. Acta 358 (2005) 3398–3406.
[555] J.Y. Ryu, J.Y. Lee, S.J. Hong, H.W. Yang, C. Kim, Y. Kim, S. Kim, A.J. Lough, Appl. Organomet. Chem. 18 (2004) 497–498.
[556] Y.M. Kim, S.J. Kim, A.J. Lough, Polyhedron 20 (2001) 3073–3078.
[557] J.Y. Ryu, J.Y. Lee, J.S. Seo, C. Kim, Y. Kim, Appl. Organomet. Chem. 17 (2003) 805–806.
[558] J.Y. Ryu, J.H. Han, J.Y. Lee, S.J. Hong, S.H. Choi, C. Kim, S.J. Kim, Y. Kim, Inorg. Chim. Acta 358 (2005) 3659–3670.
[559] J.L. Du, T.L. Hu, J.R. Li, S.M. Zhang, X.H. Bu, Eur. J. Inorg. Chem. (2008) 1059–1066.
[560] M.H. Klingele, S. Brooker, Inorg. Chim. Acta 357 (2004) 1598–1602.
[561] M. Du, Z.H. Zhang, L.F. Tang, X.G. Wang, X.J. Zhao, S.R. Batten, Chem. Eur. J. 13 (2007) 2578–2586.
[562] H.B. Zhu, C.H. Huang, W. Huang, S.H. Gou, Inorg. Chem. Commun. 7 (2004) 1095–1099.
[563] Z.L. Chu, H.B. Zhu, D.H. Hu, W. Huang, S.H. Gou, Cryst. Growth Des. 8 (2008) 1599–1604.
[564] Z.L. Chu, W. Huang, H.B. Zhu, S.H. Gou, J. Mol. Struct. 874 (2008) 1–13.
[565] Z.L. Chu, Acta Crystallogr. E 65 (2009), M288-U583.
[566] Z.L. Chu, G. Xu, W. Huang, S.H. Gou, Acta Crystallogr. E 63 (2007), M2155-U1170.
[567] H.B. Zhu, Z.L. Chu, D.H. Hu, W. Huang, S.H. Gou, Inorg. Chem. Commun. 10 (2007) 362–366.
[568] L. Zhang, Y. Ling, F. Peng, M. Du, J. Mol. Struct. 829 (2007) 161–167.
[569] X.J. Zhao, Q. Wang, M. Du, Inorg. Chim. Acta 360 (2007) 1970–1976.
[570] H. Han, Y.L. Song, H.W. Hou, Y.T. Fan, Y. Zhu, Dalton Trans. (2006) 1972–1980.
[571] Y. Ling, L. Zhang, Acta Crystallogr. E 63 (2007) M4–M6.
[572] Y. Gong, C.W. Hu, Z.N. Xia, J. Mol. Struct. 837 (2007) 48–57.
[573] Y. Gong, C.W. Hu, Z.N. Xia, Acta Crystallogr. E 62 (2006) M2997–M2999.
[574] Y. Gong, J.Z. Liu, C.W. Hu, W.L. Gao, Inorg. Chem. Commun. 10 (2007) 575–579.
[575] H.Y. Han, S.J. Zhang, H.W. Hou, Y.T. Fan, Y. Zhu, Eur. J. Inorg. Chem. (2006) 1594–1600.
[576] E.P. Zhang, H.W. Hou, H.Y. Han, Y.T. Fan, J. Organomet. Chem. 693 (2008) 1927–1937.
[577] L. Zhang, Y. Ling, M. Du, Inorg. Chim. Acta 360 (2007) 3182–3188.
[578] Y. Gong, T.F. Liu, W. Tang, F.J. Wu, W.L. Gao, C.W. Hua, J. Solid State Chem. 180 (2007) 1476–1488.
[579] S.L. Li, Y.Q. Lan, J.F. Ma, J. Yang, X.H. Wang, Z.M. Su, Inorg. Chem. 46 (2007) 8283–8290.
[580] Y.Q. Lan, S.L. Li, K.Z. Shao, X.L. Wang, Z.M. Su, Dalton Trans. (2008) 3824–3835.
[581] Y.Q. Lan, S.L. Li, Y.G. Li, Z.M. Su, K.Z. Shao, X.L. Wang, CrystEngComm 10 (2008) 1129–1131.
[582] S.L. Li, Y.Q. Lan, J.F. Ma, J. Yang, J. Liu, Y.M. Fu, Z.M. Su, Dalton Trans. (2008) 2015–2025.
[583] K. Nomiya, R. Noguchi, M. Oda, Inorg. Chim. Acta 298 (2000) 24–32.
[584] X.M. Zhang, Y.T. Zhao, W.X. Zhang, X.M. Chen, Adv. Mater. 19 (2007) 2843–2845.
[585] X.M. Zhang, Y.F. Zhao, H.S. Wu, S.R. Battenb, S.W. Ng, Dalton Trans. (2006) 3170–3178.
[586] X. He, C.D. Wu, M.X. Li, S.R. Batten, Inorg. Chem. Commun. 11 (2008) 1378–1381.
[587] X. He, C.Z. Lu, D.Q. Yuan, Inorg. Chem. 45 (2006) 5760–5766.
[588] X.S. Wang, Y.Z. Tang, X.F. Huang, Z.R. Qu, C.M. Che, P.W.H. Chan, R.G. Xiong, Inorg. Chem. 44 (2005) 5278–5285.
[589] T. Wu, M. Chen, D. Li, Eur. J. Inorg. Chem. (2006) 2132–2135.
[590] T. Wu, B.H. Yi, D. Li, Inorg. Chem. 44 (2005) 4130–4132.
[591] J.J. Hou, Z.M. Hao, X.M. Zhang, Inorg. Chim. Acta 360 (2007) 14–20.
[592] M. Li, Z. Li, D. Li, Chem. Commun. (2008) 3390–3392.
[593] Z. Li, M. Li, S.Z. Zhan, X.C. Huang, S.W. Ng, D. Li, CrystEngComm 10 (2008) 978–980.
[594] T. Wu, R. Zhou, D. Li, Inorg. Chem. Commun. 9 (2006) 341–345.
[595] H. Deng, Y.C. Qiu, Y.H. Li, Z.H. Liu, R.H. Zeng, M. Zeller, S.R. Batten, Chem. Commun. (2008) 2239–2241.
[596] Y.B. Ding, Y. Cheng, Z.L. Zhang, J. Zhang, Y.G. Yin, W.H. Gao, Inorg. Chem. Commun. 12 (2009) 45–47.
[597] Y. Chen, Y. Song, Y. Zhang, J.P. Lang, Inorg. Chem. Commun. 11 (2008) 572–575.
[598] P.N. Gaponik, M.M. Degtyarik, A.S. Lyakhov, V.E. Matulis, O.A. Ivashkevich, M. Quesada, J. Reedijk, Inorg. Chim. Acta 358 (2005) 3949–3957.
[599] L.S. Ivashkevich, A.S. Lyakhov, M.M. Degtyarik, P.N. Gaponik, Acta Crystallogr. E 61 (2005) M394–M396.
[600] L.S. Ivashkevich, A.S. Lyakhov, D.O. Ivashkevich, M.M. Degtyarik, P.N. Gaponik, Russ. J. Inorg. Chem. 50 (2005) 78–82.
[601] X.L. Zhang, Y. Qiu, S.W. Ng, Acta Crystallogr. E 62 (2006) M3301–M3302.
[602] Y. Shvedenkov, M. Bushuev, G. Romanenko, L. Lavrenova, V. Ikorskii, P. Gaponik, S. Larionov, Eur. J. Inorg. Chem. (2005) 1678–1682.
[603] A.S. Lyakhov, P.N. Gaponik, M.M. Degtyarik, L.S. Ivashkevich, Acta Crystallogr. C 59 (2003) M204–M206.
[604] A.V. Virovets, G.A. Bikzhanova, N.V. Podberezskaya, L.G. Lavrenova, J. Struct. Chem. 38 (1997) 103–109.
[605] A.S. Lyakhov, M.M. Degtyarik, L.S. Ivashkevich, P.N. Gaponik, Acta Crystallogr. C 61 (2005) M158–M160.
[606] A.S. Lyakhov, P.N. Gaponik, M.M. Degtyarik, V.E. Matulis, V.E. Matulis, L.S. Ivashkevich, Acta Crystallogr. C 59 (2003) M90–M92.
[607] Y.G. Shvedenkov, A.V. Virovets, L.G. Lavrenova, Russ. Chem. Bull. 52 (2003) 1353–1357.
[608] X.L. Tong, H. Liu, Q. Yu, J.R. Li, Acta Crystallogr. E 64 (2008), M132-U1276.
[609] A.S. Lyakhov, P.N. Gaponik, M.M. Degtyarik, L.S. Ivashkevich, Acta Crystallogr. E 59 (2003) M38–M40.
[610] A.F. Stassen, H. Kooijman, A.L. Spek, L.J. de Jongh, J.G. Haasnoot, J. Reedijk, Inorg. Chem. 41 (2002) 6468–6473.
[611] A.F. Stassen, M. Grunert, A.M. Mills, A.L. Spek, J.G. Haasnoot, J. Reedijk, W. Linert, Dalton Trans. (2003) 3628–3633.
[612] L.S. Ivashkevich, A.S. Lyakhov, A.P. Mosalkova, P.N. Gaponik, O.A. Ivashkevich, Acta Crystallogr. E 65 (2009), M236-U1092.
[613] Q. Ye, Y.H. Li, Y.M. Song, X.F. Huang, R.G. Xiong, Z.L. Xue, Inorg. Chem. 44 (2005) 3618–3625.
[614] X.L. Zhang, Y. Qiu, S.W. Ng, Acta Crystallogr. E 62 (2006) M3539–M3540.
[615] Y. Chen, Z.G. Ren, H.X. Li, X.Y. Tang, W.H. Zhang, Y. Zhang, J.P. Lang, J. Mol. Struct. 875 (2008) 339–345.
[616] M.S. Hill, P.B. Hitchcock, N. Smith, Polyhedron 23 (2004) 801–807.
[617] D.O. Ivashkevich, A.S. Lyakhov, M.M. Degtyarik, P.N. Gaponik, Acta Crystallogr. E 59 (2003) M14–M16.
[618] J. Xiao, Y.Y. Zhao, W.X. Wang, H. Zhao, Chin. J. Inorg. Chem. 24 (2008) 1347–1351.
[619] G.F. Han, G.X. Wang, C.J. Zhu, Y. Cai, R.G. Xiong, Inorg. Chem. Commun. 11 (2008) 652–654.
[620] X.G. Jin, M.C. Shao, H.C. Huang, J.M. Wang, Y. Zhu, Chem. Bull. (1982) 336.
[621] V.I. Sokol, V.V. Davydov, N.Y. Merkuréva, M.A. Ryabov, V.S. Sergienko, S.A. Pervushina, Y.V. Shklyaev, Russ. J. Inorg. Chem. 48 (2003) 791–795.
[622] M.A.S. Goher, B. Sodin, B. Bitschnau, E.C. Fuchs, F.A. Mautner, Polyhedron 27 (2008) 1423–1431.

[623] L.Z. Wang, X.S. Wang, Y.H. Li, Z.P. Bai, R.G. Xiong, M. Xiong, G.W. Li, Chin. J. Inorg. Chem. 18 (2002) 1191–1194.
[624] P.P. Liu, A.L. Cheng, N. Liu, W.W. Sun, E.Q. Gao, Chem. Mater. 19 (2007) 2724–2726.
[625] P.P. Liu, Y.Q. Wang, C.Y. Tian, H.Q. Peng, E.Q. Gao, J. Mol. Struct. 920 (2009) 459–465.
[626] J.H. Yu, K. Mereiter, N. Hassan, C. Feldgitscher, W. Linert, Cryst. Growth Des. 8 (2008) 1535–1540.
[627] P.P. Liu, A.L. Cheng, N. Liu, W.W. Sun, E.Q. Gao, Cryst. Growth Des. 8 (2008) 1668–1674.
[628] R.Y. Li, X.Y. Wang, T. Liu, H.B. Xu, F. Zhao, Z.M. Wang, S. Gao, Inorg. Chem. 47 (2008) 8134–8142.
[629] E.Q. Gao, P.P. Liu, Y.Q. Wang, Q. Yue, Q.L. Wang, Chem. Eur. J. 15 (2009) 1217–1226.
[630] X. Xue, B.F. Abrahams, R.G. Xiong, X.Z. You, Aust. J. Chem. 55 (2002) 495–497.
[631] X.W. Wang, J.Z. Chen, J.H. Liu, Cryst. Growth Des. 7 (2007) 1227–1229.
[632] D.O. Ivashkevich, A.S. Lyakhov, D.S. Pytleva, S.V. Voitekhovich, P.N. Gaponik, Acta Crystallogr. C 59 (2003) M221–M223.
[633] D.O. Ivashkevich, M.M. Degtyarik, P.N. Gaponik, A.S. Lyakhov, Acta Crystallogr. C 58 (2002) m288–m289.
[634] S. Bhandari, M.F. Mahon, K.C. Molloy, J.S. Palmer, S.F. Sayers, J. Chem. Soc. -Dalton Trans. 7 (2000) 1053–1060.
[635] M. Hill, M.F. Mahon, K.C. Molloy, J. Chem. Soc. -Dalton Trans. (1996) 1857–1865.
[636] A. Goodger, M. Hill, M.F. Mahon, J. McGinley, K.C. Molloy, J. Chem. Soc. -Dalton Trans. (1996) 847–852.
[637] M. Hill, M.F. Mahon, J. McGinley, K.C. Molloy, J. Chem. Soc. -Dalton Trans. (1996) 835–845.
[638] C. Jiang, Z.P. Yu, C. Jiao, S.J. Wang, J.M. Li, Z.Y. Wang, Y. Cui, Eur. J. Inorg. Chem. (2004) 4669–4674.
[639] L.S. Ivashkevich, A.S. Lyakhov, P.N. Gaponik, M.M. Degtyarik, O.A. Ivashkevich, S.I. Tiutiunnikov, V.V. Efimov, Acta Crystallogr. C 62 (2006) M607–M609.
[640] J. Tao, Z.J. Ma, R.B. Huang, L.S. Zheng, Inorg. Chem. 43 (2004) 6133–6135.
[641] J.R. Li, Y. Tao, Q. Yu, X.H. Bu, Chem. Commun. (2007) 1527–1529.
[642] Z.Q. Liu, W. Dong, S.W. Ng, Acta Crystallogr. E 63 (2007), M2943-U2780.
[643] L.L. Zheng, H.X. Li, J.D. Leng, J. Wang, M.L. Tong, Eur. J. Inorg. Chem. (2008) 213–217.
[644] N. Liu, Q. Yue, Y.Q. Wang, A.L. Cheng, E.Q. Gao, Dalton Trans. (2008) 4621–4629.
[645] T. Jiang, X.M. Zhang, Cryst. Growth Des. 8 (2008) 3077–3083.
[646] M. Friedrich, J.C. Galvez-Ruiz, T.M. Klapotke, P. Mayer, B. Weber, J.J. Weigand, Inorg. Chem. 44 (2005) 8044–8052.
[647] J.M. Lin, B.S. Huang, Y.F. Guan, Z.Q. Liu, D.Y. Wang, W. Dong, CrystEngComm 11 (2009) 329–336.
[648] E.Q. Gao, N. Liu, A.L. Cheng, S. Gao, Chem. Commun. (2007) 2470–2472.
[649] Y.B. Lu, M.S. Wang, W.W. Zhou, G. Xu, G.C. Guo, J.S. Huang, Inorg. Chem. 47 (2008) 8935–8942.
[650] J.M. Lin, Y.F. Guan, D.Y. Wang, W. Dong, X.T. Wang, S. Gao, Dalton Trans. (2008) 6165–6169.
[651] K. Karaghiosoff, T.M. Klapotke, C.M. Sabate, Eur. J. Inorg. Chem. (2009) 238–250.
[652] B.J. Jiao, S.P. Chen, F.Q. Zhao, R.Z. Hu, S.L. Gao, J. Hazard. Mater. 142 (2007) 550–554.
[653] A.S. Lyakhov, T.V. Serebryanskaya, P.N. Gaponik, S.V. Voitekhovich, L.S. Ivashkevich, Acta Crystallogr. C 62 (2006) M223–M226.
[654] R.W. Saalfrank, R. Harbig, J. Nachtrab, W. Bauer, K.P. Zeller, D. Stalk, M. Teichert, Chem. Eur. J. 2 (1996) 1363–1367.
[655] M. Dinca, A. Dailly, Y. Liu, C.M. Brown, D.A. Neumann, J.R. Long, J. Am. Chem. Soc. 128 (2006) 16876–16883.
[656] M. Dinca, A. Dailly, C. Tsay, J.R. Long, Inorg. Chem. 47 (2008) 11–13.
[657] M. Dinca, A. Dailly, J.R. Long, Chem. Eur. J. 14 (2008) 10280–10285.
[658] C. Jiang, Z.P. Yu, S.J. Wang, C. Jiao, J.M. Li, Z.Y. Wang, Y. Cui, Eur. J. Inorg. Chem. (2004) 3662–3667.
[659] K. Karaghiosoff, T.M. Klapotke, C.M. Sabate, Chem. Eur. J. 15 (2009) 1164–1176.
[660] P.N. Gaponik, S.V. Voitekhovich, A.S. Lyakhov, V.E. Matulis, O.A. Ivashkevich, M. Quesada, J. Reedijk, Inorg. Chim. Acta 358 (2005) 2549–2557.
[661] S.N. Semenov, A.Y. Rogachev, S.V. Eliseeva, Y.A. Belousov, A.A. Drozdov, S.I. Troyanov, Polyhedron 26 (2007) 4899–4907.
[662] T.M. Klapotke, J. Stierstorfer, K.R. Tarantik, I.D. Thoma, Z. Anorg. Allg. Chem. 634 (2008) 2777–2784.
[663] G. Geisberger, T.M. Kapotke, J. Stierstorfer, Eur. J. Inorg. Chem. (2007) 4743–4750.
[664] T.M. Klapotke, J. Stierstorfer, A.U. Wallek, Chem. Mater. 20 (2008) 4519–4530.
[665] E.J. Graeber, B. Morosin, Acta Crystallogr. C 39 (1983) 567–570.
[666] X.H. Huang, T.L. Sheng, S.C. Xiang, R.B. Fu, S.M. Hu, Y.M. Li, X.T. Wu, Inorg. Chem. Commun. 9 (2006) 1304–1307.
[667] Y.C. Wang, H. Zhao, Y.M. Song, X.S. Wang, R.G. Xiong, Appl. Organomet. Chem. 18 (2004) 494–495.
[668] X.C. Wen, Acta Crystallogr. E 64 (2008), M1033-U1586.
[669] Y. Zou, S. Hong, M. Park, H. Chun, M.S. Lah, Chem. Commun. (2007) 5182–5184.
[670] C. Zhang, H.Q. Ai, S.W. Ng, Acta Crystallogr. E 62 (2006) M2908–M2909.
[671] J.T. Liu, S.D. Fan, S.W. Ng, Acta Crystallogr. E 63 (2007), M1652-U1729.
[672] X.S. Wang, Y.Z. Tang, R.G. Xiong, Chin. J. Inorg. Chem. 21 (2005) 1025–1029.
[673] R.G. Xiong, X. Xue, H. Zhao, X.Z. You, B.F. Abrahams, Z.L. Xue, Angew. Chem. Int. Ed. 41 (2002) 3800–3803.
[674] Y.Z. Tang, G.X. Wang, Q. Ye, R.G. Xiong, R.X. Yuan, Cryst. Growth Des. 7 (2007) 2382–2386.
[675] L.Z. Wang, Z.R. Qu, H. Zhao, X.S. Wang, R.G. Xiong, Z.L. Xue, Inorg. Chem. 42 (2003) 3969–3971.
[676] R.Y. Li, S. Gao, Chin. J. Inorg. Chem. 24 (2008) 1229–1236.
[677] T.T. Luo, H.L. Tsai, S.L. Yang, Y.H. Liu, R.D. Yaday, C.C. Su, C.H. Ueng, L.G. Lin, K.L. Lu, Angew. Chem. Int. Ed. 44 (2005) 6063–6067.
[678] G.W. Yang, Q.Y. Li, J. Wang, R.X. Yuan, J.M. Xie, Chin. J. Inorg. Chem. 23 (2007) 1887–1894.
[679] C.K. Wang, X.Y. Li, Acta Crystallogr. E 65 (2009), M363-U243.
[680] X.A. Xue, X.S. Wang, L.Z. Wang, R.G. Xiong, B.F. Abrahams, X.Z. You, Z.L. Xue, C.M. Che, Inorg. Chem. 41 (2002) 6544–6546.
[681] S. Bhandari, C.G. Frost, C.E. Hague, M.F. Mahon, K.C. Molloy, J. Chem. Soc. -Dalton Trans. (2000) 663–669.
[682] G.X. Wang, B. Li, R.G. Xiong, Chin. J. Inorg. Chem. 23 (2007) 1997–1998.
[683] X.L. Zhang, C.L. Zhang, Y.E. Qiu, N. An, Acta Crystallogr. E 63 (2007), M2423-U1591.
[684] J.T. Liu, S.D. Fan, Acta Crystallogr. E 63 (2007), M1632-U1558.
[685] A. Rodriguez-Dieguez, M.A. Palacios, A. Sironi, E. Colacio, Dalton Trans. (2008) 2887–2893.
[686] A. Rodriguez, R. Kivekas, E. Colacio, Chem. Commun. (2005) 5228–5230.
[687] A. Rodriguez-Dieguez, A. Salinas-Castillo, S. Galli, N. Masciocchi, J.M. Gutierrez-Zorrilla, P. Vitoria, E. Colacio, Dalton Trans. (2007) 1821–1828.
[688] J.Y. Zhang, A.L. Cheng, Q. Yue, W.W. Sun, E.Q. Gao, Chem. Commun. (2008) 847–849.
[689] J.Y. Zhang, Q. Yue, Q.X. Jia, A.L. Cheng, E.Q. Gao, CrystEngComm 10 (2008) 1443–1449.
[690] A. Rodriguez-Dieguez, E. Colacio, Chem. Commun. (2006) 4140–4142.
[691] J.R. Li, Q. Yu, E.C. Sañudo, Y. Tao, W.C. Son, X.H. Bu, Chem. Mater. 20 (2008) 1218–1220.
[692] Z. Li, M. Li, X.P. Zhou, T. Wu, D. Li, S.W. Ng, Cryst. Growth Des. 7 (2007) 1992–1998.
[693] Y. Tao, J.R. Li, Q. Yu, W.C. Song, X.L. Tong, X.H. Bu, CrystEngComm 10 (2008) 699–705.
[694] R.Y. Huang, K. Zhu, H. Chen, G.X. Liu, X.M. Ren, Chin. J. Inorg. Chem. 25 (2009) 162–165.
[695] D.W. Fu, H. Zhao, Chin. J. Inorg. Chem. 23 (2007) 122–123.
[696] D.W. Fu, H. Zhao, Chin. J. Inorg. Chem. 23 (2007) 281–282.
[697] Z.R. Qu, Chin. J. Inorg. Chem. 23 (2007) 1117–1120.
[698] D.O. Ivashkevich, A.S. Lyakhov, P.N. Gaponik, A.N. Bogatikov, A.A. Govorova, Acta Crystallogr. E 57 (2001) M335–M337.
[699] V.P. Sinditskii, M.D. Dutov, A.E. Fogelzang, T.Y. Vernidub, V.I. Sokol, M.A. Poraikoshits, Inorg. Chim. Acta 189 (1991) 259–266.
[700] R.W. Saalfrank, R. Harbig, O. Struck, E.M. Peters, K. Peters, H.G. von Schnering, Z. Naturforsch. (B) 51 (1996) 399–408.
[701] F. Chen, H.Y. Ye, Acta Crystallogr. E 64 (2008), M1060-U1802.
[702] G.X. Wang, H.Y. Ye, Acta Crystallogr. E 64 (2008), M1006-U1334.
[703] D.W. Fu, W. Zhang, R.G. Xiong, Cryst. Growth Des. 8 (2008) 3461–3464.
[704] Q. Ye, Y.Z. Tang, X.S. Wang, R.G. Xiong, Dalton Trans. (2005) 1570–1573.
[705] R.W. Saalfrank, K. Schobert, S. Trummer, A. Wolski, Z. Naturforsch. (B) 50 (1995) 642–648.
[706] H. Gallardo, E. Meyer, A.J. Bortoluzzi, F. Molin, A.S. Mangrich, Inorg. Chim. Acta 357 (2004) 505–512.
[707] L. Li, T.L. Hu, X.H. Bu, Acta Crystallogr. E 63 (2007) M1393–M1394.
[708] H. Zhao, Q. Ye, Q. Wu, Y.M. Song, Y.J. Liu, R.G. Xiong, Z. Anorg. Allg. Chem. 630 (2004) 1367–1370.
[709] H.R. Li, Y. Tao, Q. Yu, X.H. Bu, H. Sakamoto, S. Kitagawa, Chem. Eur. J. 14 (2008) 2771–2776.
[710] Q.X. Jia, Y.Q. Wang, Q. Yue, Q.L. Wang, E.Q. Gao, Chem. Commun. (2008) 4894–4896.
[711] G.W. Yang, Q.Y. Li, Y. Zhou, P. Sha, Y.S. Ma, R.X. Yuan, Inorg. Chem. Commun. 11 (2008) 723–726.
[712] Q. Yu, X.P. Zhang, H.D. Bian, H. Liang, B. Zhao, S.P. Yan, D.Z. Liao, Cryst. Growth Des. 8 (2008) 1140–1146.
[713] W.W. Dong, J. Zhao, L. Xu, J. Solid State Chem. 181 (2008) 1149–1154.
[714] W.W. Dong, J. Zhao, L. Xu, Cryst. Growth Des. 8 (2008) 2882–2886.
[715] X.Z. Li, Z.R. Qu, Acta Crystallogr. E 64 (2008), M808-U698.
[716] X.H. Huang, T.L. Sheng, S.C. Xiang, R.B. Fu, S.M. Hu, Y.M. Li, X.T. Wu, Chin. J. Struct. Chem. 26 (2007) 333–337.
[717] X.Z. Li, B.Z. Wu, Z.R. Qu, Acta Crystallogr. E 64 (2008), M1008-U1355.
[718] J.T. Li, J. Tao, R.B. Huang, L.S. Zhang, Acta Crystallogr. E 61 (2005) M984–M985.
[719] X.S. Wang, X.F. Huang, R.G. Xiong, Chin. J. Inorg. Chem. 21 (2005) 1020–1024.
[720] T. Jiang, Y.F. Zhao, X.M. Zhang, Inorg. Chem. Commun. 10 (2007) 1194–1197.
[721] J.Y. Zhang, Y.Q. Wang, H.Q. Peng, A.L. Cheng, E.Q. Gao, Struct. Chem. 19 (2008) 535–539.
[722] Y. Li, G. Xu, W.O. Zou, N.S. Wang, F.K. Zheng, M.F. Wu, H.Y. Zeng, G.C. Guo, J.S. Huang, Inorg. Chem. 47 (2008) 7945–7947.
[723] Z.P. Yu, Y. Xie, S.J. Wang, G.P. Yong, Z.Y. Wang, Inorg. Chem. Commun. 11 (2008) 372–376.
[724] Z.P. Yu, S.S. Xiong, G.P. Yong, Z.Y. Wang, J. Coord. Chem. 62 (2009) 242–248.
[725] Z.R. Qu, Z. Xing, B.Z. Wu, X.Z. Li, G.F. Han, Z. Anorg. Allg. Chem. 635 (2009) 39–42.
[726] Q.Y. Li, G.W. Yang, R.X. Yuan, J.P. Wang, P.F. Cui, Acta Crystallogr. C 64 (2008) M26–M29.
[727] Q.Y. Li, G.W. Yang, Y.S. Ma, M.J. Li, Y. Zhou, Inorg. Chem. Commun. 11 (2008) 795–798.

[728] G.W. Yang, Q.Y. Li, Y. Zhou, G.Q. Gu, Y.S. Ma, R.X. Yuan, Inorg. Chem. Commun. 11 (2008) 1239–1242.
[729] Z.R. Qu, H. Zhao, X.S. Wang, Y.H. Li, Y.M. Song, Y.J. Liu, Q.O. Ye, R.G. Xiong, B.F. Abrahams, Z.L. Xue, X.Z. You, Inorg. Chem. 42 (2003) 7710–7712.
[730] Q. Ye, Y.M. Song, G.X. Wang, K. Chen, D.W. Fu, P.W.H. Chan, J.S. Zhu, S.D. Huang, R.G. Xiong, J. Am. Chem. Soc. 128 (2006) 6554–6555.
[731] G.W. Yang, Q.Y. Li, Y. Zhou, G.Q. Gu, Y.S. Ma, R.X. Yuan, Inorg. Chim. Acta 362 (2009) 1234–1238.
[732] R.W. Saalfrank, P. Harbig, O. Struck, F. Hampel, E.M. Peters, K. Peters, H.G. von Schnering, Z. Naturforsch. (B) 52 (1997) 125–134.
[733] A.B. Gaspar, M.C. Muñoz, N. Moliner, V. Ksenofontov, G. Levchenko, P. Gütlich, J.A. Real, Mon. Chem. 134 (2003) 285–294.
[734] N. Moliner, M.C. Muñoz, P.J. Van Koningsbruggen, J.A. Real, Inorg. Chim. Acta 274 (1998) 1–6.
[735] N. Moliner, A.B. Gaspar, M.C. Muñoz, V. Niel, J. Cano, J.A. Real, Inorg. Chem. 40 (2001) 3986–3991.
[736] D.R. Zhu, Y. Xu, Z. Yu, Z.J. Guo, H. Sang, T. Liu, X.Z. You, Chem. Mater. 14 (2002) 838–843.
[737] K.H. Sugiyarto, D.C. Craig, A.D. Rae, H.A. Goodwin, Aust. J. Chem. 49 (1996) 505–515.
[738] K.H. Sugiyarto, D.C. Craig, H.A. Goodwin, Aust. J. Chem. 49 (1996) 497–504.
[739] J.J.A. Kolnaar, Ph.D Thesis, Leiden University, 1998.
[740] O.G. Shakirova, L.G. Lavrenova, Y.G. Shvedenkov, G.A. Berezovskii, D.Y. Naumov, L.A. Sheludyakova, G.V. Dolgushin, S.V. Larionov, Russ. J. Coord. Chem. 30 (2004) 473–479.
[741] O. Roubeau, J.M.A. Gomez, E. Balskus, J.J.A. Kolnaar, J.G. Haasnoot, J. Reedijk, New J. Chem. 25 (2001) 144–150.
[742] Y. Garcia, P.J. Van Koningsbruggen, R. Lapouyade, L. Rabardel, O. Kahn, M. Wieczorek, R. Bronisz, Z. Ciunik, M.F. Rudolf, C. R. Acad. Sci. Ser. II C 1 (1998) 523–532.
[743] G.A. Berezovskii, O.G. Shakirova, Y.G. Shvedenkov, L.G. Lavrenova, Russ. J. Phys. Chem. 77 (2003) 1054–1058.
[744] V.A. Varnek, L.G. Lavrenova, J. Struct. Chem. 36 (1995) 104–111.
[745] V.A. Varnek, L.G. Lavrenova, J. Struct. Chem. 35 (1994) 509–516.
[746] L.G. Lavrenova, V.N. Ikorski, V.A. Varnek, I.M. Oglezneva, S.V. Larionov, J. Struct. Chem. 34 (1993) 960–965.
[747] L.G. Lavrenova, V.N. Ikorski, V.A. Varnek, I.M. Oglezneva, S.V. Larionov, Koord. Khim. 16 (1990) 654–661.
[748] M.M. Dirtu, C. Neuhausen, A.D. Naik, A. Rotaru, L. Spinu, Y. Garcia, Inorg. Chem. 49 (2010) 5723–5736.
[749] M.M. Dirtu, A. Rotaru, D. Gillard, J. Linarès, E. Codjovi, B. TInant, Y. Garcia, Inorg. Chem. 48 (2009) 7838–7852.
[750] O. Roubeau, J.G. Haasnoot, E. Codjovi, F. Varret, J. Reedijk, Chem. Mater. 14 (2002) 2559–2566.
[751] R. Hinek, P. Gütlich, A. Hauser, Inorg. Chem. 33 (1994) 567–572.
[752] J. Kusz, H. Spiering, P. Gütlich, J. Appl. Crystallogr. 34 (2001) 229–238.
[753] O. Roubeau, A.F. Stassen, I.F. Gramage, E. Codjovi, J. Linarès, F. Varret, J.G. Haasnoot, J. Reedijk, Polyhedron 20 (2001) 1709–1716.
[754] P. Poganiuch, P. Gütlich, Hyperfine Interact. 40 (1988) 331–334.
[755] P. Adler, P. Poganiuch, H. Spiering, Hyperfine Interact. 52 (1989) 47–63.
[756] (a) P. Poganiuch, S. Decurtins, P. Gütlich, J. Am. Chem. Soc. 112 (1990) 3270–3278;
(b) A.F. Stassen, O. Roubeau, I. Ferrero Gramage, J. Linarès, F. Varret, I. Mutikainen, U. Turpeinen, J.G. Haasnoot, J. Reedijk, Polyhedron 20 (2001) 1699–1707.
[757] R. Hinek, H. Spiering, P. Gütlich, A. Hauser, Chem. Eur. J. 2 (1996) 1435–1439.
[758] R. Hinek, H. Spiering, D. Schollmeyer, P. Gütlich, A. Hauser, Chem. Eur. J. 2 (1996) 1427–1434.
[759] T. Buchen, D. Schollmeyer, P. Gütlich, Inorg. Chem. 35 (1996) 155–161.
[760] S.J. Campbell, V. Ksenofontov, Y. Garcia, J.S. Lord, Y. Boland, P. Gütlich, J. Phys. Chem. B 107 (2003) 14289–14295.
[761] J. Jeftic, R. Hinek, S.C. Capelli, A. Hauser, Inorg. Chem. 36 (1997) 3080–3087.
[762] N. Hassan, P. Weinberger, K. Mereiter, F. Werner, G. Molnar, A. Bousseksou, M. Valtiner, W. Linert, Inorg. Chim. Acta 361 (2008) 1291–1297.
[763] T. Buchen, P. Gütlich, Chem. Phys. Lett. 220 (1994) 262–266.
[764] A.F. Stassen, M. Grunert, E. Dova, M. Muller, P. Weinberger, G. Wiesinger, H. Schenk, W. Linert, J.G. Haasnoot, J. Reedijk, Eur. J. Inorg. Chem. (2003) 2273–2282.
[765] E. Dova, R. Peschar, M. Takata, E. Nishibori, H. Schenk, A.F. Stassen, J.G. Haasnoot, Chem. Eur. J. 11 (2005) 5855–5865.
[766] E. Dova, A.F. Stassen, R.A.J. Driessen, E. Sonneveld, K. Goubitz, R. Peschar, J.G. Haasnoot, J. Reedijk, H. Schenk, Acta Crystallogr. B 57 (2001) 531–538.
[767] A.F. Stassen, E. Dova, R. Ensling, H. Schenk, P. Gütlich, J.G. Haasnoot, J. Reedijk, Inorg. Chim. Acta 335 (2002) 61–68.
[768] E. Dova, R. Peschar, M. Sakata, K. Kato, H. Schenk, Chem. Eur. J. 12 (2006) 5043–5052.
[769] E. Dova, R. Peschar, M. Sakata, K. Kato, A.F. Stassen, H. Schenk, J.G. Haasnoot, Acta Crystallogr. B 60 (2004) 528–538.
[770] J.M. Wang, L.J. Li, G.S. Zhang, Chin. J. Org. Chem. 29 (2009) 13–19.